



**BEHAVIOUR OF BOLTED CONNECTION SYSTEM IN
PULTRUDED GFRP STRUCTURES**

A Thesis submitted by

Mohammad Hizam Shah Rusmi, M Eng

For the award of

Doctor of Philosophy

2018

Abstract

The pultruded GFRP hollow sections, in particular, have received growing interest from the engineering community due to better torsional rigidity, effective resistance of out-of-plane forces, high load transfer and improved strength and stiffness of the minor axis. However, one of the significant issues that hinders the widespread use of pultruded GFRP hollow sections is the inadequacy or unpredictability of its connection system. In this study, the behaviour of pultruded GFRP truss structure using through-bolt connection system was investigated based on the current industrial practice in Australia. The through-bolt connection system is incorporated with an FRP mechanical insert as a filled-type connection element and currently, there is no scientific research focusing on joint behaviour of pultruded GFRP hollow profiles with mechanical inserts. This has been the key motivation for this research whereby the suitability and joint strength adequacy of bolted connection with insert for pultruded FRP, in particular, tubular profiles were examined. Therefore, the study ultimately investigated this particular jointing technique on pultruded GFRP trusses and aimed to understand how the loads are resisted, transferred, and distributed to each FRP component. The experimental data and theoretical predictions developed in this study are critical to produce a safe, reliable and adequate connection system for pultruded GFRP hollow sections.

This thesis is presented as a compilation of technical papers. In the first paper, effects of threaded bolt with varying end distance to bolt diameter, laminate thickness, clamping pressure and laminate orientations (longitudinal and transverse) on the joint strength behaviour, joint efficiency and mode of failure were evaluated using a double lap joint test set-up configuration. The test results obtained from the effects of using threaded bolt were compared to that of plain bolt in order to assess the differences in joint behaviour and possible reduction in joint capacity. In this experiment, the joint was designed to promote bearing failure as it is preferable in composite joint due to its progressive nature of failure. From this study, approximately 30-40% reduction in joint strength was observed for specimens with longitudinal laminate orientation caused by laminate tearing of the bolt. In addition, under scanning electron microscope (SEM) imaging, this damaging effect was further observed to better understand its mechanism and how it affects the resulting mode of failures.

In the second paper, the joint behaviour of pultruded GFRP hollow sections with a single all-threaded bolt and mechanical insert connection system was investigated under elevated in-service temperature. A comparison of different bolted joint configurations of pultruded GFRP hollow sections, namely joint without mechanical insert (N), joint with mechanical insert with tight-fit attachment (I) and joint with mechanical insert bonded with epoxy adhesive (G) was conducted and the effects on the joint strength and failure mechanism were evaluated. The results of this experimental work have demonstrated that the bolted joint with adhesively bonded mechanical insert sustained the highest load-carrying capacity across the elevated temperatures compared to other configurations. Also, the proposed joint strength prediction equation, which incorporates the strength reduction and modification factors based on different joint configurations involving mechanical insert, produced reasonable outcomes against experimental failure load. These results suggest that, the use of mechanical inserts to strengthen bolted connections system can be adopted in pultruded GFRP hollow sections and the joint performance of this configuration at a structural level was discussed in the next paper.

In the third paper, the joint behaviour of through-bolt connection with mechanical insert under eccentric loading was investigated. The joint configuration was adopted in pultruded GFRP T-joints using both single and double bottom chords, with the former imbalanced configuration intended to impart load eccentricity. This eccentric condition can be found in composite truss bridges. The experimental results showed that, the presence of mechanical inserts in both single and double bottom chords of the T-joints had improved the joint strength and fixture stiffness when compared to their insert-less counterparts. It was found that the mechanical insert has prevented bolt flexure and contributed to the improvement in bending resistance when subjected to a couple moment developed due to eccentricity.

In the last paper, the structural behaviour of double-chorded pultruded GFRP trusses connected using through-bolt with mechanical inserts under different load cases were investigated. The structural performance of the trusses was described in terms of load-midspan deflection response, force distribution of internal members and mode of failure. The results of this study indicate that the adopted through-bolt with mechanical insert connection system possess high joint load-carrying capacity and demonstrated effective transmission of internal forces to other truss members. The

theoretical strength limits of pultruded GFRP truss members in tension, compression and flexural according to ASCE pre-standard were in close agreement with the experimental results. Meanwhile, the prediction equation proposed in the second paper was used here to evaluate the joint load-carrying capacity of the pultruded GFRP trusses. A two-dimensional numerical model to simulate the behaviour of the pultruded GFRP trusses was constructed using Strand7 finite element analysis software. Satisfactory comparisons against experimental results were achieved and this demonstrates the validity of the Strand7 simplified numerical model.

From this overall research program, it can be concluded that the combination of through-bolt and mechanical insert is a promising connection system for pultruded GFRP in truss application. The proposed factors and theoretical joint strength equations developed in this research can be important tools for practitioners to perform strength analysis of through-bolt with mechanical insert connection system, encouraging its acceptance and utilisation, especially in truss application.

Certification of Thesis

This Thesis is the work of Mohammad Hizam Shah Rusmi except where otherwise acknowledged, with the majority of the authorship of the papers presented as a Thesis by Publication undertaken by the Student. The work is original and has not previously been submitted for any other award, except where acknowledged.

Principal Supervisor: Prof. Karu Karunasena

Associate Supervisor: Associate Prof. Allan Manalo

Student and supervisors signatures of endorsement are held at the University.

Statement of Contribution

The following detail is the agreed share of contribution for candidate and co-authors in the presented publications in this thesis:

- **Article I: Hizam, R. M.,** Manalo, A. C., Karunasena, W., and Bai, Y. (2018). Effect of bolt threads on the double lap joint strength of pultruded fibre reinforced polymer composite materials. *Journal of Construction and Building Materials*. Vol.181, pp. 185-198. (IF: 3.485, SNIP: 2.309)

The overall contribution of *Hizam, R.M.* was 60% to the concept development, design of experiments, experimental works, analysis and interpretation of data, drafting and revising the final submission; *Manalo, A.C., Karunansena. W. and Bai, Y.* contributed to concept development, design of experiments, analysis, editing and providing important technical inputs by 20%, 15% and 5%, respectively.

- **Article II: Hizam, R. M.,** Manalo, A. C., Karunasena, W., and Bai, Y. (CCENG-2555, under review for publication). Joint strength of single-bolted pultruded GFRP square hollow sections (SHS) with mechanical inserts under elevated temperatures. *Journal of Composites for Construction*. (IF: 2.648, SNIP: 1.762)

The overall contribution of *Hizam, R.M.* was 65% to the concept development, design of experiments, experimental works, analysis and interpretation of data, drafting and revising the final submission; *Manalo, A.C., Karunansena. W. and Bai, Y.* contributed to concept development, design of experiments, analysis, editing and providing important technical inputs by 20%, 10% and 5%, respectively.

- **Article III: Hizam, R. M.,** Manalo, A. C., Karunasena, W., and Bai, Y. (COST_2018_2111, under review for publication). Behaviour of through-bolt connection for pultruded GFRP T-joint under eccentric loading. *Journal Composite Structures*. (IF: 4.101, SNIP: 1.939)

The overall contribution of **Hizam, R.M.** was 60% to the concept development, design of experiments, experimental works, analysis and interpretation of data, drafting and revising the final submission; **Manalo, A.C., Karunansena. W. and Bai, Y.** contributed to concept development, design of experiments, analysis, editing and providing important technical inputs by 20%, 15% and 5%, respectively.

- **Article IV: Hizam, R. M.,** Manalo, A. C., Karunasena, W., and Bai, Y. (JCOMB_2018_2512, under review for publication). Behaviour of pultruded GFRP truss system connected using through-bolt with mechanical insert. Journal Composite Part B: Engineering. (IF: 4.920, SNIP: 2.104)

The overall contribution of **Hizam, R.M.** was 60% to the concept development, design of experiments, experimental works, analysis and interpretation of data, drafting and revising the final submission; **Manalo, A.C., Karunansena. W. and Bai, Y.** contributed to concept development, design of experiments, analysis, editing and providing important technical inputs by 25%, 10% and 5%, respectively.

Acknowledgement

I would like to express *my deepest gratitude* to,

- ***Prof. Warna (Karu) Karunasena***, my principal supervisor, for giving me the opportunity to fulfil my PhD. I am indebted to him for his encouragement and advice all throughout these years. I am very grateful to have a supervisor that believe in my work and always provide me with guidance and valuable suggestions towards completing this thesis.
- ***Associate Prof. Allan Manalo***, my associate supervisor, for actively coaching me with his sound knowledge in regards to the experimental and analytical work. His expert technical suggestions and practical assistance were indispensable in improving the quality of this research work.
- ***Prof. Yu Bai***, my external advisor, indebted for his thoughtful guidance, constructive comments and valuable technical expertise.
- ***Dr. Noor Azwa Zulkarnain***, my external editor, for her valuable editorial advices and proofreading throughout the whole thesis.
- The ***Faculty of Health, Engineering and Science (HES)*** and ***the Centre of Future Materials (CFM)*** for the academic, financial, testing facilities and technical support that made this research possible.
- ***Mr. Wayne Crowell, Mr. Mohan Trada, Mr. Martin Geach, all the postgraduate students at CFM*** and other colleagues at USQ for their technical and administrative assistance during experimental works and for their support and friendship.
- ***Australian Commonwealth Government*** contribution through Research Training Program (RTP) Fees Offset scheme during my research and ***Wagners Composites Fibres Technologies (WCFT)*** for the valued test materials and technical support.
- ***My lovely wife***, for her never-ending support and countless sacrifices in achieving this success. I have been extremely lucky to have her by my side throughout all my academic achievements.
- ***My children, Kimi, Hafi and Aydin*** for their patience and support during Abah's PhD studies. You are the source of my motivation, the pride and joy of my life.

- *My parents, Abah and Mama*, for your love and encouragement throughout my life and during this study. *My parents in laws, my siblings* for their continued support and endless prayers that help me get to this point.
- Last but not least, the *Almighty Allah SWT*, for giving me good health, courage, knowledge and strength.

Table of Contents

Abstract.....	i
Certification of Thesis.....	iv
Statement of Contribution.....	v
Acknowledgement	vii
Table of Contents	ix
List of Figures.....	xii
List of Tables	xii
1. Introduction.....	1
1.1. Research background and motivation	1
1.2. Research questions.....	6
1.3. Research Objectives	7
1.4. Scope and limitations	8
1.5. Thesis organisation	10
2.0 REVIEW OF RELATED LITERATURE.....	15
2.1. General.....	15
2.2. Fibre reinforced polymer (FRP) composite material	15
2.2.1. Development in civil engineering applications	15
2.2.2. Pultruded FRP.....	16
2.2.3. Advantages and limitations of pultruded GFRP.....	18
2.2.4. Pultruded glass FRP (GFRP) hollow sections	21
2.3. FRP connection system	23
2.3.1. Mechanically fastened joint and its parameters.....	24

2.3.2.	Adhesively bonded joint and its parameters.....	27
2.3.3.	Joint development of pultruded FRP hollow section	29
2.3.4.	Effect of bolt threads.....	31
2.4.	FRP truss system	32
2.4.1.	Truss systems and its joint concepts.....	32
2.4.2.	Effects of eccentric loading.....	35
2.4.3.	Behaviour under in-service elevated temperature	37
2.5.	Summary	38
3.	Study on the use of threaded bolt	41
3.1.	Article I: Effect of bolt threads on the double lap joint strength of pultruded fibre reinforced polymer composite materials.....	41
4.	Study on the use of mechanical inserts.....	79
4.1.	Article II: Joint strength of single-bolted pultruded GFRP SHS sections with mechanical inserts under elevated temperatures.....	79
5.	Study on the effect of eccentric loading.....	117
5.1.	Article III: Behaviour of through-bolt connection for pultruded GFRP T-joint.....	117
6.	Study on pultruded GFRP truss connection system	147
6.1.	Article IV: Behaviour of pultruded GFRP truss system connected using through-bolt with mechanical insert.....	147
7.0	CONCLUSION.....	186
7.1.	Effect of bolt threads in GFRP bolted connection	186
7.2.	Behaviour of through-bolt with mechanical insert	188
7.3.	Behaviour of GFRP T-joint under eccentric loading.....	189
7.4.	Structural and joint behaviour of GFRP truss.....	190
7.5.	Contributions of the study	192

7.6.	Areas for further study	193
8.	References	195
Appendix A: Additional study		205
A.1	Material characterisation	205
A.2	Preliminary study on double lap single-bolted (DSLJ) coupon testing 209	
Appendix B: Supporting Information		211
B.1	Article I	211
B.2	Article II.....	225
B.3	Article III	227
B.4	Article IV.....	229
Appendix C: Conferences.....		230
C.1	Conference I.....	230
C.2	Conference II	231
C.3	Conference III.....	232
C.4	Conference IV.....	233
C.5	Conference V	234
C.6	Conference VI.....	235

List of Figures

Figure 1.1 The development of the FRP from the early 1970 (Hollaway 2010)	1
Figure 1.2 Various shapes and dimensions of Pultruded FRP	2
Figure 1.3 Space trusses (steel) in telecommunication tower	3
Figure 1.4 Example of frame bolted connections (<i>www.strongwell.com/literature</i>)... 4	
Figure 1.5. Number of journals articles published on the behaviour of bolted joint of pultruded fibre reinforced polymer (<i>Source: www.sciencedirect.com; keywords: pultruded, FRP, bolted, joint</i>)	5
Figure 2.1. Basic schematic diagram of Pultrusion process (<i>WCFT Product Guide</i>)	17
Figure 2.2. Typical pultruded layer (<i>www.creativepultrusions.com</i>).....	18
Figure 2.3. Glimpse of pultruded FRP advantages and disadvantages	19
Figure 2.4. Lightweight pultruded FRP beam structures (<i>www.strongwell.com/literature</i>)	20
Figure 2.5. Example of open and closed section.....	22
Figure 2.6. Geometric parameters for multi-bolt joint connection	25
Figure 2.7. Typical FRP bonded joints failure	28
Figure 2.8. Bolt threads effect on composite laminate.....	31
Figure 2.9. Snap joint concept by Goldsworthy & Hiel (1998)	33
Figure 2.10. The all FRP composite Pontresina bridge (Keller et al. 2007)	33
Figure 2.11. Cantilever trussed beam (Pfeil et al. , 2009).....	34
Figure 2.12. Pultruded GFRP novel connector for space truss (Bai and Yang, 2013)	35

List of Tables

Table 2.1.Common failures modes in FRP bolting joint.....	26
---	----

1. Introduction

1.1. Research background and motivation

Fibre reinforced polymer (FRP) composites is a material which is formed by the combination of fibres and its binding matrix. Also known as advanced polymer composites (APC), this material has many advantageous properties and attractive attributes, for instances, high strength-to-weight and stiffness-to-weight ratios, corrosion resistance, light weight and tailorable design characteristic (Maji et al., 1997; Bank, 2006). However, it took 30 years for this material to breakthrough into the construction of civil structures. Figure 1.1 presents the different applications of FRP material in civil engineering.

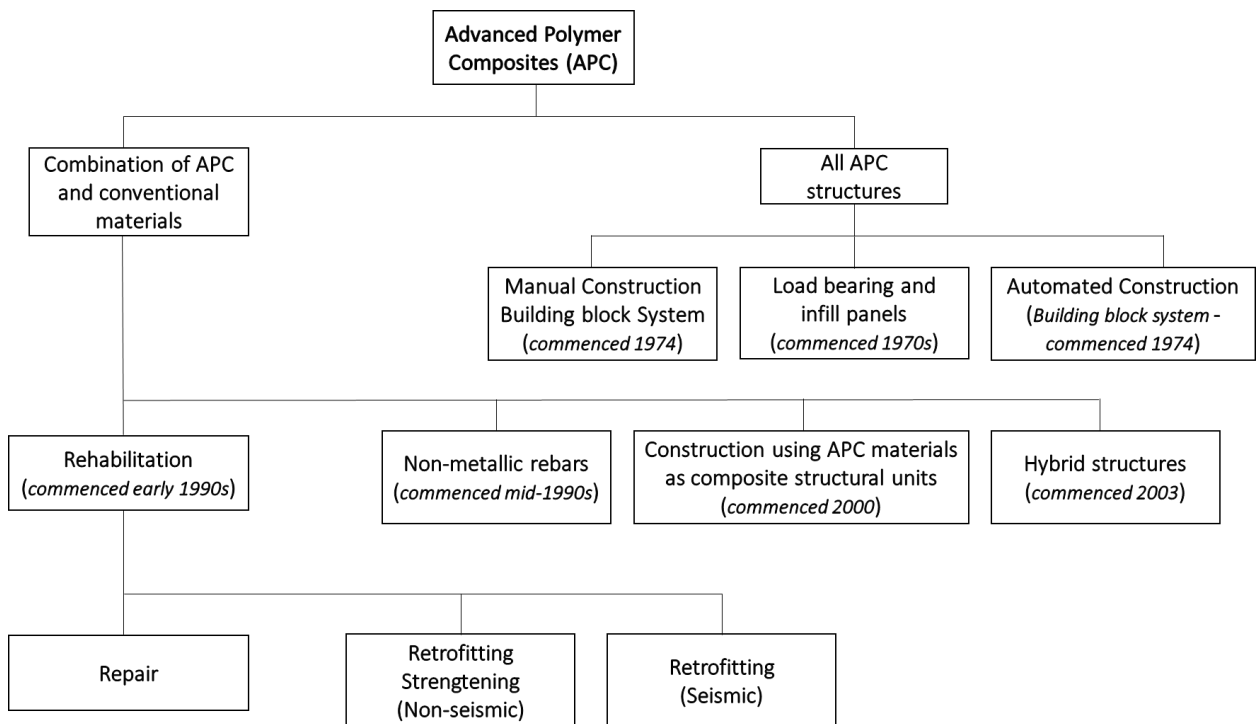


Figure 1.1 The development of the FRP from the early 1970 (Hollaway 2010)

The most economical and preferred manufacturing method of FRP in civil construction is pultrusion (Maji et al., 1997). The word pultrusion is a combination of *pull* and *extrusion*. It is one of the automated methods available that provides uniformity of member cross-section similar to steel (Figure 1.2) where the fibres are oriented predominantly uniaxial. Pultruded FRP exhibits high resistance to aggressive

environment which contributes to lower life cycle cost, produce more lightweight structure (1/6 of steel) and quick installation time (Keller, 2001).

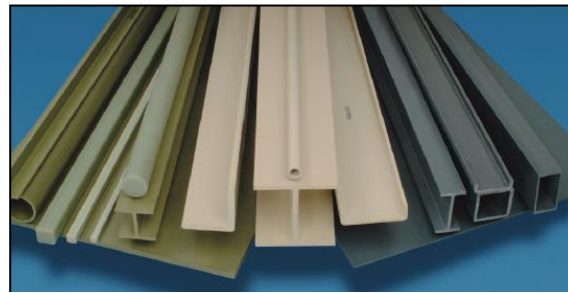


Figure 1.2 Various shapes and dimensions of Pultruded FRP

Pultruded glass FRP (GFRP) hollow section, in particular, have received growing interest from the engineering community due to better torsional rigidity, effective resistance of out-of-plane forces, high load transfer and improved strength and stiffness of the minor axis (Smith et al., 1998; DG9, 2004). These attractive features have marketed pultruded FRP sections as structural members in cooling towers, transmission towers, building construction (roof trusses), highway bridge decks and bridge girders (Gand et al., 2013). Trusses are structural frames formed from one or more triangles. Each straight slender member of a truss, which theoretically carries only axial tension or axial compression, is connected at the joints. The joints are assumed to be frictionless hinges or pins that allow the ends of the members to rotate slightly thus, creating a stable shape or configuration (Royslance, 2000). Trusses offer many advantages over solid web members especially on material and weight ratio which make trusses one of the prominent structural forms in the 19th century. It can also provide stiffness to a structure (balance the pultruded low material stiffness), support heavy loads over long spans and fast installation (Bai and Yang, 2012). Trusses are commonly used for bridges, towers, roofing in houses and have been acknowledged as one of the important types of load bearing component in civil infrastructure. An example of a truss system in telecommunication tower is shown in Figure 1.3. These areas of construction are suitable for FRP material as the low material usage in their production address the cost disparities between traditional and fibre composite structures (Einde et al., 2003; Uddin and Abro, 2008; Meiarashi et al., 2002). Also, high axial strength also contributes to low material usage in the truss production, offsetting the high material cost of FRPs compared to steel or timber

(Plastics, 2002). In turn, the role of FRP composites in civil engineering industry has expanding, primarily in the hostile environment (Hollaway, 2010).



Figure 1.3 Space trusses (steel) in telecommunication tower

However, despite these advantageous characteristics, there are a few concerns on pultruded FRP profiles for construction which apparently limit its application in civil engineering. Examples include the inability of GFRP materials to provide satisfactory structural deformations while in service (Bank, 2013), the highly sensitive change in behaviour at elevated temperatures hindering applications in hot outdoor climate (Manalo et al., 2017b; Feng et al., 2016; Turvey and Sana, 2016), and the orthotropic material characteristics causing various mode of failures which invalidates existing steel-profile design formulas (Wu et al., 2015b). On the mechanical properties aspect, despite having high strength and lightweight features, the pultruded FRP materials are associated with low material stiffness and lower strength (tensile and compressive) in the transverse direction when comparing to steel (Bai and Yang, 2012). Nevertheless, the design of reliable and durable jointing system is still recognized by many researchers as the major challenge in the development of pultruded FRP structures (Mottram, 2009; Manalo and Mutsuyoshi, 2011; Bai and Yang, 2013).

Generally, there are three common techniques used to connect FRP structural members i.e. bolted joint (Figure 1.4), adhesively bonded and a combination of both (Hizam et al., 2012). Early works conducted on investigating suitable connection methods for pultruded components were based around bolted joints due to its low cost,

ease of installation and removal, and design familiarity (Turvey, 2000; Bank, 2006; Mottram, 2009; Mosallam, 2011). While other methods, such as single-plate or welded connection are still impractical for pultruded GFRP sections. In addition, FRP fasteners are adopted in rocks and soil engineering applications since they are ideal for non-corrosive or low-conductivity conditions. Although the FRP fasteners can be engineered according to different connection modes, they possess linear elasticity and high brittleness which make them ineffective for connecting advanced composite materials.



Figure 1.4 Example of frame bolted connections (www.strongwell.com/literature)

Figure 1.5 shows the number of articles published on the behaviour of bolted joint of pultruded fibre reinforced polymer (FRP) over the past 10 years. Although the increment is unsteady, the figure roughly indicates increased interest of researchers on this topic. This continuous interest from researchers shows the importance of reliable jointing system as a vital element for transmitting loads in FRP structures and the importance of improving the gaps in this related area which lead a promising future of the FRP material in civil engineering industry.

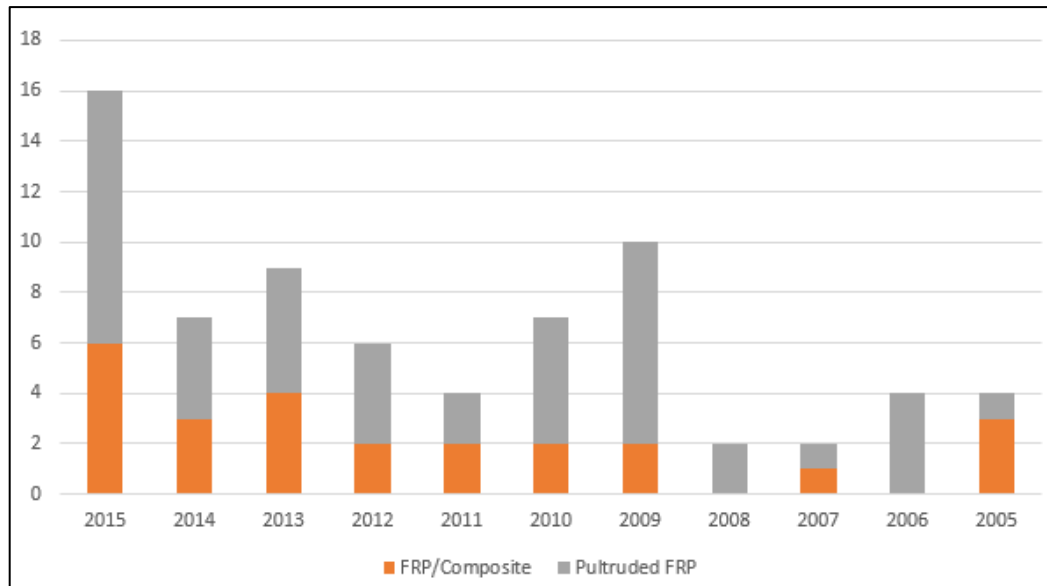


Figure 1.5. Number of journals articles published on the behaviour of bolted joint of pultruded fibre reinforced polymer (Source: www.sciencedirect.com; keywords: *pultruded, FRP, bolted, joint*)

Presently, extensive research in understanding the behaviour of pultruded GFRP with different connection techniques at components (coupons) level have been carried out (Boyd et al., 2004; Lau et al., 2012; Hashim and Nisar, 2013; Coelho and Mottram, 2015). However, the authors have found only a handful of literatures focussing on the interaction of pultruded GFRP connection system at a structural level. Taking advantage of pultruded FRP's high strength in unidirectional, investigation on structural truss system is considered for this study.

In this study, the behaviour of pultruded FRP truss system with bolted joints was investigated. As the design and construction of pultruded FRP trusses are influenced by the types and cross sections of the FRP materials used as well as the truss configuration, the jointing technique employed in this study was based on the current industrial practice in Australia. It focused on the pultruded GFRP profiles manufactured by Wagners Composite Fibre Technologies (WCFT) in Toowoomba, Australia. This WCFT composite material consists of high volume, symmetrical layers of fibres, in long continuous uni-direction (0°), contributing to the material's high tensile strength and elastic modulus. Meanwhile, the reinforcement from stitch fabrics ($\pm 45^\circ$) has improved its transverse strength. Overall, the material is efficient in term of stiffness and is suitable for load bearing applications. Different parameters that

affect the joint behaviour of bolted connection such as loading conditions, FRP material mechanical properties (stacking sequence, volume fraction), the influence of joint geometry, the influence of lateral restraint, the influence of pultrusion direction, and the influence of fastener parameters (plain bolt and threaded bolt) were evaluated. To date, studies on eccentrically compressed pultruded GFRP tubular members are limited and as such, their structural behaviour are not fully understood. This has been supported by Gand et al. (2013) on their comprehensive review focusing on the developments of FRP closed sections as well as studied by Mottram (2009) on the research gaps for connection design guidance, whereby the authors had outlined the behaviour of FRP tubular members under eccentric loading as one of the areas that need further research investigation. In the context of the filled-type connection element, to the best of the authors' knowledge, there is no scientific research on the mechanical insert filled the pultruded GFRP hollow profile, and this is one of the key motivations in this study to explore this innovative joint system in a truss structure.

The primary focus was on the connection system behaviour of pultruded FRP trusses and understanding on how the loads are resisted, transferred, and distributed to each FRP component with bolted joints. The results of this study provided designers and engineers with a better understanding of the potential of pultruded FRP composites trusses and advance its application in other civil engineering applications. Moreover, the experimental data and theoretical predictions developed in this study are critical to produce a safe and reliable connections for pultruded GFRP sections.

1.2. Research questions

The main research questions that were addressed through the course of this research study are the following:

1. What are the effects of bolt threads on the bolted lap joint geometric parameters (end distance to bolt diameter (e/d_b), laminate thickness), pin-bearing strength, laminate orientations, and clamping pressure on the joint behaviour and its load-carrying capacity in pultruded GFRP?

2. What are the effects of mechanical insert with and without adhesive on the joint strength of through-bolt pultruded GFRP hollow section under elevated temperatures?
3. How the through-bolt (all thread) joints with the presence of mechanical insert of pultruded GFRP behave under eccentricity loading?
4. How the through-bolt with mechanical inserts adopted in pultruded GFRP truss system behave under different load conditions?
5. Are the existing design codes such as ASCE pre-standard applicable to assess the effect of bolt threads and mechanical insert in pultruded FRP bolted connection?

1.3. Research Objectives

This thesis aimed at evaluating the behaviour of bolted connection system of pultruded glass fibre reinforced polymer (GFRP) structures through experimental and analytical investigations. The specific objectives of this study were:

1. To investigate the effects of bolt threads with varying end distance to bolt diameter, laminate thickness, clamping pressure, and laminate orientations on the joint load-carrying capacity of mechanically fastened pultruded GFRP under tensile loading. Also, to determine the pin-bearing strength of pultruded GFRP using the threaded bolts and investigate its joint behaviour under scanning electron microscope (SEM) imaging to understand the failure mechanism.
2. To investigate the effect of mechanical insert with and without adhesive on the joint strength of through-bolt pultruded GFRP hollow section under elevated temperatures.
3. To examine the behaviour of through-bolt connection of pultruded GFRP hollow section under eccentric loading with and without the presence of mechanical inserts.
4. To investigate the structural behaviour of 1-meter span pultruded GFRP truss structures and its joint behaviour under different loading conditions. The tubular pultruded GFRP is employed as a truss member and is connected using through-bolt connection system.

5. To evaluate the applicability of existing design codes in determining the joint strength of through-bolt connection system of pultruded FRP hollow section and, if not, to develop a resistance factor of unity (one) or less on the existing equations to take account on the presence of threads and mechanical insert.

1.4. Scope and limitations

This thesis investigated the structural performance of pultruded GFRP truss which were constructed by assembling pultruded FRP hollow sections into a double chord truss configuration using through-bolt with insert connection system. A single-bolt of through-bolt connection system was employed to assemble the pultruded FRP truss structure and it was thoroughly investigated in this study. The overall system behaviour as well as the local behaviour of its connections were investigated using experimental and theoretical approaches. The theoretical approaches of strength limits according to existing design code and analytical truss model using finite element analysis software were evaluated to analyse the effectiveness of the proposed connection system at the structural level.

As for the configuration, a double chord truss system was used in this study due to the constraint in joint design provided by the pultruded GFRP hollow sections. This type of configuration has previously been used for steel and concrete trusses. Early finite element study on planar tabular steel trusses consisting of rectangular hollow sections showed that double chord trusses outperform their single chord counterparts, unless stiffening plates were utilised to provide comparable end moments of members (Mirza et al., 1982; Shehata et al., 1987). Additionally, for the similar material, Korol (1986) concluded that double-chord arrangement for both K and T-joints have higher joint strength and stiffness than the single-chord arrangement. The spacing apart of the double chords also provides lateral stability, reducing the need for bracing. This improvement in joint performance of double-chord configuration was also investigated on a preliminary study performed on T-joints of pultruded GRFP rectangular hollow sections. It was found that the joint resistance of T-joint with one chord was only a third that of T-joint with double chords as a result of a couple moment developed from the eccentric loading.

The pultruded GFRP tubular members were connected through a jointing system that consists of through-bolts and adhesive bonded mechanical inserts which were installed in the vicinity of every joint in the truss structure. However, due to commercial sensitivity, information on the process of epoxy adhesive injection and mechanical insert installation in the vicinity of SHS cannot be divulged. The main connection components are the 20 mm diameter (M20) through-bolts which are made of stainless steel (SS). These are high strength all-thread structural bolts suitable for pultruded GFRP box section as in accordance to Australian standard AS 1252:1996 (AS/NZS1252:1996, 1996b) and AS 1110:1995 (AS/NZS1110:1995, 1995). The Steel Construction Institute (SCI and BCSA, 2002) indicated that M20 x 60 mm long grade 8.8 all threaded bolts are used for 90% of the connections in a typical multi-storey steel frame. For practical use, this specific type and diameter of bolt was employed throughout this study. By standardising the size and the grade of all thread bolts, it will lead into simple connection fabrications which eventually reduce the workmanship costs. Furthermore, these bolts meet the requirement of a minimum yield strength of 372 MPa (54 ksi) to give an adequate margin of safety against slippage of the connected parts when sufficiently tightened as stated in Guide to Design Criteria for Bolted and Riveted Joints (AISC, 2001). Additionally, to deal with those deficiencies in hollow joint, the introduction of mechanical inserts is anticipated to further improve the compressive strength at the bearing connection. The advancement in knowledge on effective connection method is a critical issue here especially under elevated temperatures. Thus, a total of sixty (60) square pultruded GFRPs with a single all threaded bolt connection was tested up to failure at room temperature, 40°C, 60°C, and 80°C were carried out to study on the effect of mechanical insert on the joint strength behaviour of through-bolt pultruded GFRP. Its failure behaviours are thoroughly investigated and the strength reduction factor, k and modification factor, m which incorporates the increasing temperatures and the designed joint configurations were proposed.

To assess the influence of bolt threads in FRP bolted design, an experimental investigation on the influence of M20 all threaded bolt and clamping pressure on double lap, single bolted joints of pultruded FRP materials prepared from 6.5 mm and 5 mm thick hollow section structural shapes were evaluated. All the 150 pultruded specimens with varied geometric ratio of e/d_b were prepared according to ASCE pre-

standard, were loaded parallel to the direction of pultrusion axis and a tight fitting 20 mm diameter mechanical fastener was used. The pin-bearing strength of the pultruded FRP used in this study was evaluated following the test procedure suggested by Keller et al. (2015) (Keller et al., 2015). Their paper has addressed a few limitations with existing standards ASTM D953-02 (2010) (ASTMD953, 2010) and EN 13706-2:2002 (EN13706-2, 2002) and has called for an alternative test arrangement. Thus, the pin-bearing test was executed adopting the set-up used by the Warwick University (Mottram and Zafari, 2011a) test setup, with a few adjustments on the bolt configuration and the test specimen's dimension. The test setup used steel bolts with a nominal diameter of 20 mm and a ratio of end distance to bolt diameter (e/d_b) up to 4. In this case, thread bolt was also included. It is the aim of this thesis to provide a better level of understanding associated to the influence of bolt threads with the recognised joining parameters and to advice a reduction factor that account the bolt threads effect in the preliminary FRP bolted design. The obtained mode of failures and its failure mechanism were revealed under imaging microscopic scale using Scanning Electron Microscope (SEM) to refine the understanding on the affected bolted joint strength behaviour.

1.5. Thesis organisation

This dissertation is comprised of an introduction that presents the research theme, an extensive review of related literature, four (4) major studies which address the main objectives of this research, a conclusion that summarises the general findings and contribution of this research, and some recommendations for future works. The main results from the four major studies are/will be presented in high quality international journals and the related journal manuscripts are highlighted as following:

- **Article I: Hizam, R. M.,** Manalo, A. C., Karunasena, W., and Bai, Y. (2018). Effect of bolt threads on the double lap joint strength of pultruded fibre reinforced polymer composite materials. *Journal of Construction and Building Materials*. Vol.181, pp. 185-198. (IF: 3.485, SNIP: 2.309)
- **Article II: Hizam, R. M.,** Manalo, A. C., Karunasena, W., and Bai, Y. (CCENG-2555, under review for publication). Joint strength of single-bolted

pultruded GFRP square hollow sections (SHS) with mechanical inserts under elevated temperatures. *Journal of Composites for Construction*. (IF: 2.648, SNIP: 1.762)

- **Article III: Hizam, R. M.,** Manalo, A. C., Karunasena, W., and Bai, Y. (COST_2018_2111, under review for publication). Behaviour of through-bolt connection for pultruded GFRP T-joint under eccentric loading. *Journal Composite Structures*. (IF: 4.101, SNIP: 1.939)
- **Article IV: Hizam, R. M.,** Manalo, A. C., Karunasena, W., and Bai, Y. (JCOMB_2018_2512, under review for publication). Behaviour of pultruded GFRP truss system connected using through-bolt with mechanical insert. *Journal Composite Part B: Engineering*. (IF: 4.920, SNIP: 2.104)

In addition, the significant findings from this research were presented in related national and international conferences, which are summarised in Appendix C.

The **first objective** was successfully addressed and the results were presented in **Article I**. This paper presents the extensive experimental program that gives an overview of joint behaviour of double lap, single bolt joint (DLSJ) pultruded GFRP using both plain bolt and threaded bolt under tensile loading. The effects of threaded bolt with varying end distance to bolt diameter, laminate thickness, clamping pressure and laminate orientations (longitudinal and transverse) on the joint strength behaviour, joint efficiency and mode of failure were evaluated. Then, the test results obtained from the effects of threaded bolt were compared to that of the plain bolt to assess the differences in joint behaviour and possible reduction in joint capacity. In this experiment, the joint was designed to promote bearing failure as it is preferable in composite joint due to its progressive nature. **Article I** also present the importance of finding the correct pin-bearing strength which accounts for all detrimental effects in calculating the bearing resistance of pultruded FRP bolted joint. In this case, both plain and thread bolt were included in the pin-bearing test arrangement used by the Warwick University (Mottram and Zafari, 2011a). From the result of this study, about 30%-40% reduction in joint strength was observed in longitudinal direction due to the bolt threads tearing through the laminates. Under scanning electron microscope (SEM), it revealed the failure development of softened zone at micro-level which resulted in a lower connection strength due to the presence of thread embedment. These findings

provided a better level of understanding associated to the influence of threaded bolt with the recognised joining parameters. This could resolve the joint adaptability (large-scale construction) and awareness issues among practitioners in regards to the application of threaded bolts in joining the pultruded FRP components which were investigated to address the key objectives of the study.

The **second specific objective** on the joint behaviour of through-bolt pultruded GFRP hollow section under elevated in-service temperatures, is covered in **Article II**. In this study, the mechanical inserts with and without adhesive are introduced at the vicinity of the joint area as the filled-type connection element and its effects on the joint strength and failure mechanism were evaluated. Additionally, a comparison of different bolted joint configurations of pultruded GFRP hollow section namely joint without mechanical insert, joint with mechanical insert with tight-fit attachment and joint with mechanical insert bonded with epoxy adhesive was conducted. The results of this experimental work have demonstrated that the bolted joint with adhesively bonded mechanical insert sustained the highest load-carrying capacity across the elevated temperatures compared to other configurations. These results suggest that, the use of mechanical inserts to strengthen bolted connections system can be adopted in pultruded GFRP hollow section and its joint performance in structural level will be investigated as per fourth and fifth objectives.

Article III addressed the **third objective** of the study whereby it investigates the behaviour of through-bolt connection with mechanical insert under eccentric loading. The joint configuration was adopted in pultruded GFRP T-joint single and double bottom chords, with the former imbalanced configuration intended to impart load eccentricity, which can be found in composite truss bridges. A comparison is made against the pultruded GFRP T-joint single and double bottom chords but without the presence of mechanical inserts at the vicinity of joint area. Then, the behaviour of pultruded GFRP T-joint was described in terms of load-displacement response, initial fixture stiffness and mode of failure. The experimental results showed that, the presence of mechanical inserts in both single and double bottom chords of the T-joints had improved the joint strength and fixture stiffness when compared to their insert-less counterparts. It was found that the mechanical insert has prevented the bolt flexure and contributed to the improvement in bending resistance when subjected to a couple

moment developed due to eccentricity. The effectiveness of double chord pultruded T-joint with mechanical insert was then investigated to address another objective of the study.

Article IV addressed the **fourth specific objective** of the study. The structural behaviour of double-chorded pultruded GFRP truss structures connected using through-bolt with mechanical inserts under different load cases were investigated. The structural performance of pultruded GFRP truss structure was described in terms of load-midspan deflection response, internal members' forces distribution and mode of failure. Also, a bolted connection system using through-bolt with mechanical inserts was examined. A comparison between the numerical models using finite element software and experimental results was evaluated. From the results in this study, it indicates that the adopted through-bolt with mechanical insert connection system are capable of sustaining higher joint load-carrying capacity and effectively transmitted the internal forces to other truss members. This experimental program focussing on the interaction of pultruded GFRP connection system at a structural level had addressed the main objective of this study.

The **fifth specific objective** was successfully addressed in each paper. The failure modes of bolted connection of pultruded FRP and its joint load-carrying capacity were examined using the current existing design codes for instance 'ASCE Pre-standard for Load Resistance Factor Design (LRFD)'(ASCE, 2010) and 'Guide for the Design and Construction of Structures made of FRP Pultruded Elements' (CNR, 2008). In **Article I**, a reduction factor is proposed in preliminary FRP bolted connection design, where all threaded bolt is anticipated in pultruded joints. In **Article II**, the joint strength prediction equation is proposed which incorporates the strength reduction factor and modification factors based on the joint configuration involving the mechanical inserts. In **Article III**, the theoretical equations of combined axial compression and bending stress with a modification factor are considered to determine the pultruded GFRP T-joint resistance against eccentric loading. In **Article IV**, the pultruded GFRP truss members were examined based on the theoretical strength limits according to ASCE pre-standard LRFD, while, the joint load-carrying capacity was evaluated using the prediction equation proposed in **Article II**. In addition, the simplified numerical model developed using finite element software shows a

favourable comparison with the experimental results. This result validated the numerical model which modified its node connection rigidity to incorporate the influence of bonded mechanical insert.

2.0 REVIEW OF RELATED LITERATURE

2.1. General

This chapter presents an overview of the recent developments and challenges on fibre reinforced polymer (FRP) as truss structure, which has been evolving and has become a viable construction system especially in civil infrastructure area. The chapter also discusses the state-of-the-art composite jointing systems for FRP components and FRP trusses. The studies on different parameters that affect the integrity of connections are also highlighted.

2.2. Fibre reinforced polymer (FRP) composite material

2.2.1. Development in civil engineering applications

The interest in a composite material made of a polymer matrix reinforced with fibres, has increased dramatically due to their key advantages, for instances, high strength-to-weight and stiffness-to-weight ratios, corrosion resistance, light weight and tailorable design characteristic (Maji et al., 1997; Bank, 2006). At the beginning, FRPs have been used for the advancement of aerospace and automotive industries where their high strength profile, high durability and weight savings are the crucial aspects. Commonly, FRP is known for its expensive manufacturing cost compared to the conventional materials such as wood and steel. However, in recent years, reduced material demand in the high priced defence industry, expansion of a highly competitive market in the sporting goods industry and prospects for large volume use in the civil sector have led to new low cost materials manufacturing (Einde et al., 2003; Uddin and Abro, 2008; Meiarashi et al., 2002). In turn, the role of FRP composites in civil engineering industry has expanding, primarily in hostile environment (Hollaway, 2010).

Recent developments in the fibre reinforced polymer techniques have led to a renewed interest in using FRP as structural members in civil engineering applications. Techniques such as pultrusion, resin transfer moulding (RTM), filament winding and semi-automated manufacturing of large components have led to advances in low cost FRP production. For structural applications, pultrusion is an increasingly important FRP manufacturing process which offers a relatively inexpensive alternative method for making high-quality prismatic members resemble of steel with high longitudinal

properties (Bank et al., 2000; Gand et al., 2013). In the following section describes more about the pultrusion manufacturing process, its fibre architectures and characterisation and the future of pultruded FRP as an alternative material in construction industry.

2.2.2. Pultruded FRP

Pultrusion manufacturing is one of the most industrialized and attractive choice for the building of large beam as it imposes the fewer restrictions on the designer when developing structural FRP shapes (Maji et al., 1997). Besides, pultrusion offers an almost constant cross section and can be pulled continuously up to a product length which limited only as to what practical to transport. However, the pultrusion process has developed slowly compared to other composite fabrication processes such as molding or filament winding. The initial pultrusion patent in the United States was issued in 1951 (Plastics, 2002). In the early 1950s, pultrusion machines for the production of simple solid rod stock were in operation at several plants. Most of these machines were the intermittent pull type. In the mid-1950s, the first continuous pull machine was invented by the father of pultrusion, Brandt Goldsworthy (Plastics, 2002). Starting in 1970, there has been a dramatic increase in market acceptance, technology development, and pultrusion industry sophistication. High quality of composite structural materials can be fabricated by pultrusion because of uniformity of cross-section, resin dispersion, fibre distribution and alignment (Jones and Ellis, 1986).

The most common composites are those made with strong fibres held together in a binder. The fibres offer good features to the material in term of stiffness and strength and the matrix material holds the fibres together, thus transferring the load between fibres and between the composite and the supports (Manalo et al., 2017a). The matrix also works as a protection to the fibres from the environment and mechanical abrasion and carries some of the loads, particularly transverse stress and interlaminar shear stress (Liao et al. , 1999). Some properties of the composite, such as transverse stiffness and strength are matrix dominated. They affect the matrix selection more that fibre dominated properties. Furthermore, matrix dominated

properties depend strongly on the operation temperature. Ceramic, metal and polymer are matrices in advance composite materials; however, the most widely used is polymer. Polymer is a matrix of choice as it provides vital advantages to composite material such as low capital investment and ease of fabrication of very complex parts (Berg et al., 1973; Hollaway, 2003). There are two types of polymer matrices which are thermoset and thermoplastic. Polyester, vinyl ester, epoxy, and phenolic are example of popular thermoset and widely used because of their ease in processing and low cost. Low viscosity feature of thermosets can provide excellent impregnation of the fibre reinforcement and high processing speeds (Hollaway, 2003). On the other hand, thermoplastic has higher viscosity resulting in poor fibre impregnation. However, with recent technology, thermoplastic has become competitive in the composite industry as it provides post-process formability and recyclability (Bourban et al., 1998; van Rijswijk and Bersee, 2007)

The basic pultrusion process (refer Figure 2.1) usually begins when reinforcing fibres are pulled from a series of creels. The fibres proceed through a bath, where they are impregnated with formulated resin. The resin-impregnated fibres are preformed to the shape of the profile to be produced. This composite material is then passed through a heated steel die that has been machined precisely to the final shape of the part to be manufactured. Heat initiates an exothermic reaction thus curing the thermosetting resin matrix. The profile is continuously pulled and exits the mould as a hot, constant cross-sectional member. The profile cools in ambient or forced air or assisted by water. The product emerges from the puller mechanism and is cut to the desired length by an automatic, flying cut-off saw (Carlone et al. , 2006).

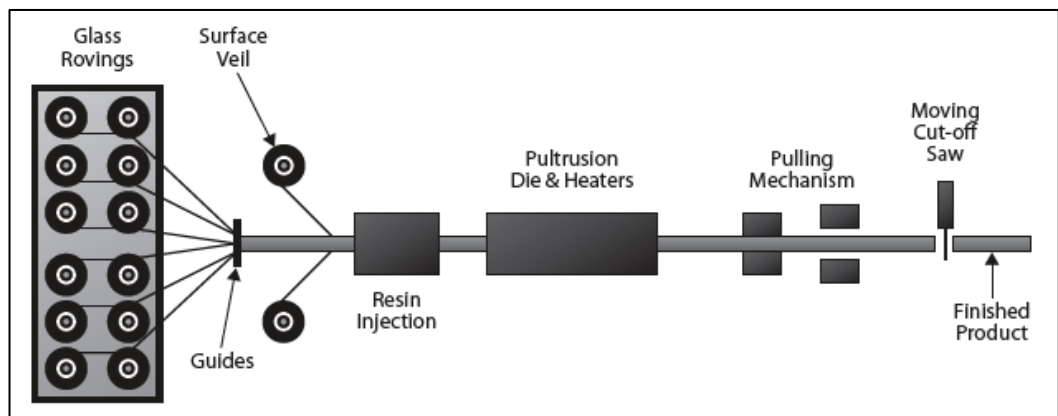


Figure 2.1. Basic schematic diagram of Pultrusion process (*WCFT Product Guide*)

There are four (4) type of layers (Figure 2.2) in a typical pultruded section as following (Davalos et al., 1996):

- a) A resin rich layer of randomly oriented chopped fibres (nexus veil). This thin layer is noticeable on the surface of the composite.
- b) Different weights of continuous strand mats (CSM). It consists of continuous randomly oriented fibres
- c) Stitched fabrics (SF) with different angle orientations
- d) Continuous unidirectional fibre bundles or known as roving layer.

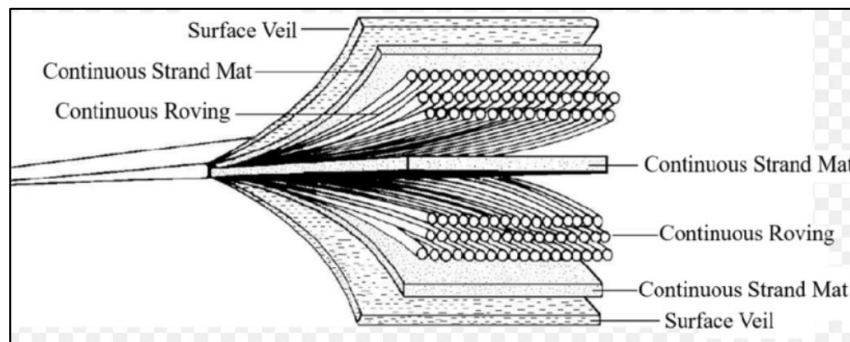


Figure 2.2. Typical pultruded layer (www.creativepultrusions.com)

The advancement of pultrusion technology resulted in the manufacturing of structural profiles composed of unidirectional and $\pm 45^\circ$ fibres become a viable construction material in civil infrastructure. The pultruded material has extraordinary mechanical and important in-service properties which looks promising for civil applications if they are employed innovatively. However, there are limitations that restrain the growth of this material which requires further investigation.

2.2.3. Advantages and limitations of pultruded GFRP

Figure 2.3 presents the pultrusion's vital advantages which are low cost and marketable operational part, light weight (sometimes a bit problematic in wind resistance design) and high strength-to-weight ratios. Superior performance and high durability in corrosive environment make this product appealing to be embraced by the practitioner. This could be one of the solutions for many large, non-civil structures that have been used in harsh environments for decades (Plastics, 2002). The major cost of the process is in equipment, the chrome plated dies, and the design and tune-up of the guiding system. For these reasons, pultrusion is ideally suited for high volume

applications (Bank, 2006). In particular, glass fibres dominates the market and are preferred over carbon, aramid and basalt due to its lower cost (Uddin and Abro, 2008; Manalo et al., 2017a). For polymer, thermoset type is common for structural uses rather than thermoplastic resin. There are variety of resins available in the market such as polyester, vinyl ester, polyurethane and epoxy, however polyester is the lowest cost of resin accessible and it is easy to use. Therefore, majority of pultruded FRP composites are produced from glass fibre reinforced polyesters (Karbhari et al. , 2007). Nevertheless, manufacturer can tailor its FRP performances based on the need and its field operation. For example, with polyester resin, low cost FRP profile can be obtained however it provides moderate mechanical properties and susceptible to ultraviolet (UV) degradation (Azwa and Yousif, 2017). Depending on the applications, manufacturer could choose vinyl ester instead, especially for industry use in very hostile environment (Karbhari et al., 2007). Considering its lightweight feature (Figure 2.4), some structures for instance bridge girders, can be pre-assembled into section or modular and then rapidly assemble the sections at designated site to complete the whole bridge (Foster et al., 2004). It considerably eases the installation work duration that the conventional materials for example steel and reinforced concrete.

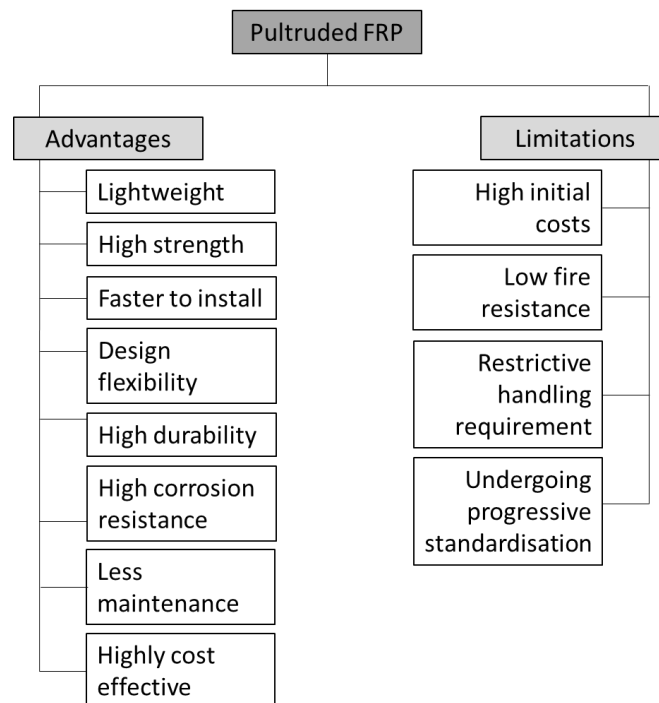


Figure 2.3. Glimpse of pultruded FRP advantages and disadvantages

Another critical advantage is potentially high durability. FRP decks are expected to provide a long service life with little maintenance. While definitive estimates of the service life of an FRP deck cannot be made at this time, it is not unreasonable to expect the service life of the FRP deck to be as long as the bridge (Einde et al. , 2003; Keller et al., 2007b). In November 2010, American Society of Civil Engineers (ASCE) had made a huge step in publishing a Pre-standard for load and resistance factor design (LRFD) of pultruded FRP structure (ASCE, 2010). The published ASCE pre-standard paves a promising future in FRP application and intended to provide design guidelines for practical engineer. This consequently will result in wider acceptance of pultruded FRP in civil and structure industry.



Figure 2.4. Lightweight pultruded FRP beam structures (www.strongwell.com/literature)

However, despite these advantageous characteristics, there seems to be some reluctance in the widespread use of pultruded GFRP among civil engineering practitioners due to several limitations as highlighted in Figure 2.3. In designing civil structures, stiffness-to-density ratio proves to be more important property than strength-to-density ratio for pultruded materials. Evaluation by Maji et al. (1997), showed that the conventional materials are superior than pultruded FRP in terms of stiffness (elastic modulus) or damping characteristic. In this case, the investigation had been done to observe the bending behaviour of GFRP tubes and the results showed that the bending stiffness of GFRP tubes is low compared to that of steel section of the same shape. This occurred due to relatively low modulus of elasticity of the glass fibres as compared to steel and the low shear modulus of resin (Mottram, 1992; Davalos and Qiao, 1997; Kumar et al., 2001). Also, Bai and Yang (2013) have addressed the same concern of low material stiffness and the lack of material ductility of pultruded GFRP composite for civil construction. The elastic modulus of pultruded glass FRP is about 10% that of conventional material (steel). However, this drawback can be minimised

in the structural stage whereby satisfactory stiffness can be achieved through redundant structural systems and flexible adhesive joints (Bai and Zhang, 2012). Further examples include, the inability of GFRP materials to provide satisfactory structural deformations while in service (Bank, 2013), the highly sensitive change in behaviour at elevated temperatures hindering applications in hot outdoor climate (Manalo et al., 2017b; Feng et al., 2016; Turvey and Sana, 2016), and the orthotropic material characteristics causing various mode of failures which invalidates existing steel-profile design formulas (Wu et al., 2015b).

Apart from this, another major issue is pertaining the inadequacy or unpredictability of the connection system of structures made from pultruded GFRP members (Mottram, 2009; Mosallam, 2011; Turvey, 2000). Connection is very important to ensure that the overall structure made from pultruded FRP retains its integrity through their working lives in a reliable and safe manner. Mottram (2009) had mentioned that designing the structural joints for pultruded FRP components are very demanding and challenging. The lack of a ductile response, several distinct failure modes and reliable prediction of strength are the primary reasons contributing to the complexity in designing bolted connection for FRP structures (Coelho and Mottram, 2015; Hai and Mutsuyoshi, 2012; Ibrahim and Pettit, 2005). In civil engineering applications, there is still limited knowledge in designing effective jointing system where thicker pultruded FRP profile are generally used and there are only a few studies on this context that have been conducted especially when used in truss structures. In the next section, recent developments on the application of hollow section of pultruded FRP are presented.

2.2.4. Pultruded glass FRP (GFRP) hollow sections

As a structural material, pultruded GFRP has been widely accepted as alternatives to steel and timber, as advancements have been achieved through many research studies (Turvey and Wang, 2007; Hollaway, 2010) and the pultruded GFRP hollow section, specifically, has excellent properties with regard to loading in compression, torsion and bending in all directions. The hollow (internal void) can be engineered in many ways such as for heating or ventilation system, fire protection and to improve the bearing resistance by filling with concrete (Chen and Wang, 2015). There are three (3) preferred hollow structural section (HSS) in civil engineering application which are,

circular hollow sections (CHS), rectangular hollow sections (RHS) and square hollow sections (SHS). The rectangular hollow section was introduced by Stewarts and Lloyds in 1952 (Wardenier et al., 2010) has enable the connections to be made by straight end cuttings and it had eliminated some connection problems from circular hollow sections.

Further research on pultruded GFRP of open (I-Beam) and closed (rectangular shapes) profiles as shown in Figure 2.5 were experimentally investigated by Smith et al. (1998). These pultruded GFRP members were tested in framed structures (beam-to-column) and a nonlinear behaviour arises by the moment and forces transferred between members was evaluated. In this study, side plates which are stronger and stiffer than the web clips were used as reinforcement for the box sections. They found out that the closed section (rectangular shapes) are generally better than open section (I-shapes) for any material because of improved local flange buckling characteristics, improved torsional rigidity, and improved weak axis strength and stiffness. The experimental results clearly showed that the standard box sections produced 14% increase in joint stiffness of entire frame compare to that of standard I-Beam. It is noteworthy that ultimate strength of the closed section was about 280% of the strength of the open section (Smith et al. 1998). It was suggested that closed section should be considered for temporary bridges as inappropriate selection of open section composite had caused undesirable local effects and damages (Keller et al. , 2007a).

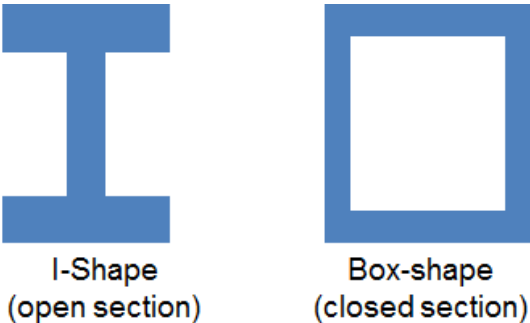


Figure 2.5. Example of open and closed section

Aiming to take advantage of those properties especially high axial resistance, hollow section of pultruded FRP can be adopted as truss components (such as bottom and top chord members) in all-composite bridge systems. Despite their advantageous characteristics, however, the joint performance associated with pultruded hollow

section was poor in term of localised load application (McCormick, 1999) and will be further discussed in this chapter. In steel construction, conversely, there are many alternative ways to connect the material with closed profile such as single-plate or welded connection to name a few. Due to sound knowledge in steel design practice, below are the common joint configurations that can be found in experimental studies used for pultruded FRP framed structures (Coelho and Mottram, 2015):

- Bolted web angles
- Top and seat angles bolted to the column and beam
- Top and seat bolted angles and bolted web angles

However, as in the case of pultruded GFRP structural frame applications, bolted joint designs based on steel practice may not be applicable due to lack of optimisation concerning its joint strength and stiffness. Thus, the following paragraphs discuss the commonly used jointing system for fibre composites and some development work on the joint design focussing on pultruded FRP hollow section.

2.3. FRP connection system

The ability to provide joint versatility for FRP material in civil structures industry is crucial for its application demands. Many earlier studies on connection of pultruded components were done based on the concepts widely used in steel industry (Bank, 2006; Mottram, 2009; Mosallam, 2011) and the three common techniques used are mechanically fastened (bolting), adhesively bonded and a combination of both (Hizam et al., 2012). These methods have been extensively used as structural joints in pultruded FRP for civil infrastructures and it continues to draw the attention of researchers due to the many possibilities of failure modes, the complexity of stress relieving mechanism and the complex nature of the stress fields in the vicinity of the joint (Khashaba et al. , 2006). The following sections discuss the advantages and disadvantages of commonly used jointing system for FRP materials. In addition, discussion on selected innovative concepts for connecting GFRP composite developed to fully benefit the improved strength and stiffness provided by the pultruded FRP hollow section are presented.

2.3.1. Mechanically fastened joint and its parameters

Bolting connection is a common jointing method to provide continuity between members and it is preferable due to low cost, ease of performing maintenance and inspection checks, and design familiarity to the practitioners (Ramakrishna et al. , 1995). This type of connection is relatively easy to assemble and is capable of transferring the high loads. However, for FRP material, Zhou and Keller (2006) have stressed that the holes for bolting should be drilled using diamond tipped bits to minimise the breaking of glass fibres and to avoid local stress concentration at the bolt-hole region. Also, the continuous fibres are affected by the holes in bolted connections which compromise the members' strength at the joint (Manalo and Mutsuyoshi, 2011). Extensive research on bolted connections in FRP has been conducted by many researchers, focusing on the evaluation of joint performance as well as its failure modes and failure mechanism (SCI and BCSA, 2002; C.Cooper and G.J.Turvey, 1995; K.Hassan et al., 1996; Bank et al., 1994; Xiao and Ishikawa, 2005a; Khashaba et al., 2006; Keller et al., 2007a; Ascione et al., 2010; Bai and Yang, 2013; Lau et al., 2012; Luo et al., 2016b; Russo, 2016; Mottram and Turvey, 2003).

This also has been well recognised in the recent design guidelines, i.e. 'Pre-Standard for Load Resistance Factor Design (LRFD) of Pultruded FRP structures' and 'Guide for the Design and Construction of Structures made of FRP Pultruded Elements (CNR-DT 205/2007)' wherein the detailed parameters and design requirements for joining composite materials are presented in Chapter 8 (ASCE, 2010) and Chapter 5 (CNR, 2008), respectively. Recently, 'Prospect of a new guidance in the design of FRP' (Ascione et al., 2016) has been prepared for the development of future European guidelines for design and verification of FRP composite structures. In Chapter 8, this guideline presents the design criteria for FRP connections consists of bolted joints and adhesive bonded joints. As recommended by the above-mentioned guidelines, fastening parameters such as joint geometry (Figure 2.6), material thickness, clamping pressure, bolt hole tolerance, and loading conditions need to be carefully considered when designing FRP bolted connections. Further research on improving the FRP connection design parameters have been expanded in comprehensive studies by Kumar et al. (2017), Machado et al. (2018) and Nerilli and Vairo (2017). These provide

essential input that have potential to be included in a newer version of the design guidelines and codes of practices.

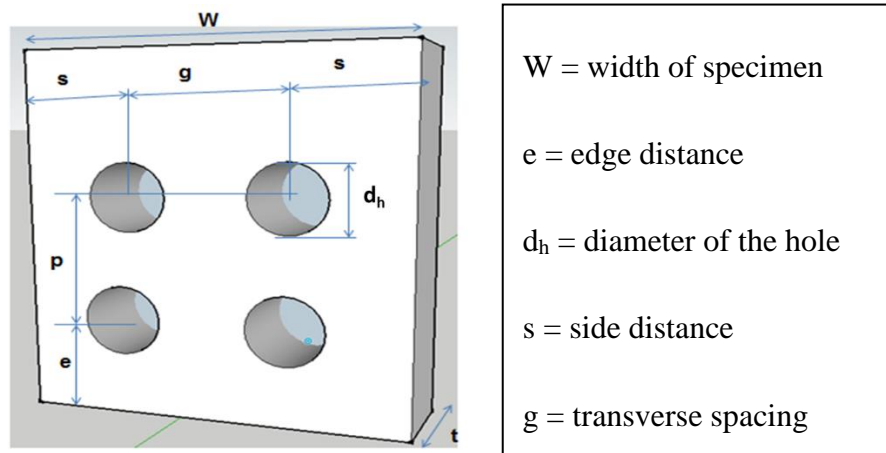
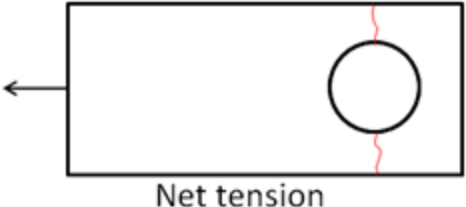
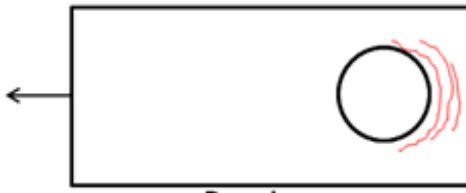
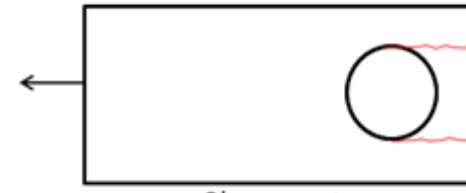
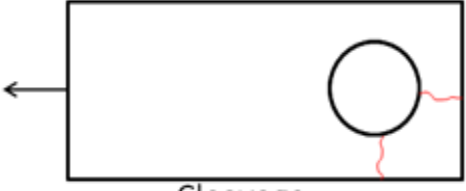


Figure 2.6. Geometric parameters for multi-bolt joint connection

These parameters significantly influence the failure modes (Table 2.1) for instance bearing, shear-out, net tension and combinations of these which eventually dictate the strength of the joint connection. Meanwhile, recent review papers by Coelho and Mottram (2015) and Correia et al. (2015) provide a comprehensive list of published contributions covering bolted FRP joint behaviour and its mechanical response against various range of joint parameters and environment exposure conditions. Bearing failure which is known as a process of compressive damage accumulation is the most desired form of failure. Bearing is the limiting factor for strength of a FRP connection (Xiao and Ishikawa, 2005a; Mottram and Zafari, 2011a). Stacking sequence is found to have influenced on joint strength as the bearing strength increased when 90° layer was placed at the surface. The bearing strength in carbon fibre reinforced polymer (CFRP) increased when plies of $\pm 45^\circ$ until approximately 75% of the total laminate thickness are added to a 0° or 90° plies. It was concluded that the laminates produced lower bearing strengths when less homogeneous stacking sequence is presented (Park, 2001). The effects of tension relative to pultrusion direction on single-bolt tension joint tests were investigated by Turvey (1998). He observed that the cracks propagated across the plate width once the off-axis angle exceeds 30° . The load capacity of the joint increases as the off-axis angle decreases and both end distance ratio and width ratio increases (Turvey 1998b). For the fabricated glass fibre reinforced epoxy (GFRE) laminates, the maximum bearing strength can be

achieved with bolted joint with 18 mm washer size and 15 Nm tightening torque as it provides optimum lateral constrained area and contact pressure (Khashaba et al. , 2006).

Table 2.1.Common failures modes in FRP bolting joint.

Failure modes	Description
<p>Net-Tension</p>  <p>Net tension</p>	<p>-Failure occurs for small coupon widths -Develop for large widths if laminates is deficient in the longitudinal reinforcement (Vangrimde & Boukhili 2003)</p>
<p>Bearing</p>  <p>Bearing</p>	<p>-Develop predominantly for combinations of large widths, large end distance and near quasi-isotropic lay-ups (Vangrimde & Boukhili 2003). -Failure leads to an elongation of the hole (Camanho & Matthews 1996).</p>
<p>Shear-out</p>  <p>Shear out</p>	<p>-Failure occurs for coupon with small end distance. - Deficient in off-axis reinforcement leads the failure to occur in large end distance (Vangrimde & Boukhili 2003).</p>
<p>Cleavage</p>  <p>Cleavage</p>	<p>-Failure occurs for coupon with inadequate end distance (Camanho & Matthews 1996) -Develop for laminates that have low off-axis reinforcement content (Vangrimde & Boukhili 2003)</p>

One of the interesting findings from finite element analysis done by Turvey and Wang (2008) highlighted the uncertainty on the validity of the simplified method for joint design given in the EUROCOMP. They found that friction between the bolt

shank and the hole and the small hole clearance are the principal factors of increasing tension and caused significant changes in the stress distributions at critical locations. In multi-bolts FRP connection, the finite element analysis verified the uneven distribution of shear forces among the bolts when compared to steel connections of similar geometry (Nahla et al. , 1996). Recent findings show that the distribution coefficient of shear forces are equal to 36% for the external rows and to 28% for central row (Ascione 2010).

Other than metallic fasteners, FRP fasteners (solid rod or bar) are adopted in rocks and soil engineering application as anchorage or strengthening strips (Terrasi et al., 2011). These FRP fasteners have the potential to be used in a variety of applications whereby its strength and stiffness properties are engineered according to different connection modes. It is ideal for applications that require fasteners to be non-corrosive, low in conductivity or no electromagnetic waves (Schmidt et al., 2012). FRP threaded rods are made by machining a thread on an FRP solid rod which can be used with metal hex nuts if the threads formed are a direct match and fit. Generally, however, the forming of thread has caused defects on the screw connections which resulted in a lower connection strength, about 20%-40% of the strength of the FRP solid bar itself (Min, 2008). Moreover, unlike steel fasteners, FRP threaded rods possesses linear elasticity and brittleness with anisotropic properties, making them ineffective as a joining component for advanced composites.

2.3.2. Adhesively bonded joint and its parameters

Bonded connection provides excellent sealing effect and there is no stress concentration presence due to the operation of bolt holes that damage the fibres. It is a common jointing technique which is widely applied in aerospace and aircraft industry, however adhesive bonding connection was introduced for connecting fibre reinforced polymer in nineties. It establishes more uniform load transfer between structure components and leading to an efficient jointing method (Machado et al., 2018; Hunter-Alarcon et al., 2018). On the other hand, this type of connection requires high quality control and workmanship for instance during the adhesive curing time for excellent bonding process. It also has high material cost and heavily affected by environmental conditions (Stazi et al., 2015). The failure mode of adhesive bonded FRP connection (Figure 2.7) always occurs in the adherends and never in the adhesives or in the

interface (Keller & Herbert 2004). Under quasi-static axial tensile loading, the adhesively double bonded stepped joint exhibited fibre tear-off failure mode which occurred in a brittle and sudden mechanism.

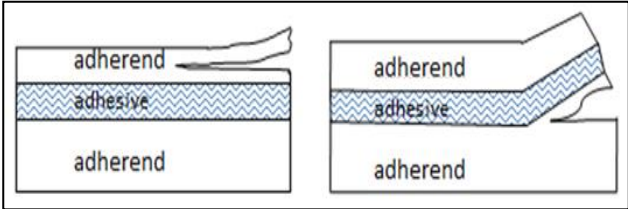


Figure 2.7. Typical FRP bonded joints failure

Unstable crack propagation occurred at crack lengths smaller than 20% of the overlap length (Zhang and Keller, 2008). There is only a small influence of adhesive layer thickness on the stress distribution while joint efficiency is constant with increasing overlap length (Keller and Vallée, 2005). Lee et al. (2009) conducted an experimental investigation to characterize the joint strengths, peel stresses and failure modes in adhesively bonded double-strap and supported single-lap GFRP joints. The bonded joint strength was almost autonomous and increased with overlap length (50% increase of joint strength was observed with overlap length of 100 mm in comparison with 50 mm length). An approximate adhesive layer thickness between 0.2 and 0.5 mm was found to maximize the joint strength of a GFRP double-strap. Manalo and Mutsuyoshi (2012) studied the behaviour of hybrid FRP girder with joints at midspan connected with bolts alone and combination of bolts and epoxy adhesives. They found out that the beam connected using bolts and epoxy exhibited the same strength and stiffness as the beam without joints while using bolts alone resulted to a beam with only 65% of the stiffness of those without joints. More recent studies on the combination of adhesive-bolted joints in pursuit of viable connection forms have been conducted by Qiu et al. (2018) and Biscaia and Chastre (2018). Hai and Mutsuyoshi (2012) investigated the use of V-notched splice plates and adhesive bonded as one of the alternative ways to join the hybrid FRP (HFRP) beam. The rough surface of V-notched splice plates had contributed to excellent bonding strength. They observed that V-notched splice plates and adhesive bonded had improved the joint stiffness. In 2008, a comparison study between plasticized adhesives and brittle adhesives was conducted by de Castro and Keller (2008). They observed that the joint strength of ductile joints with plasticized adhesive increases almost proportionally with increasing

overlap length. In addition, the introduction of adherend coating with low viscosity epoxy resin which produced high adhesion outer adherend. This method led to 39% significant strength improvement (Hashim, 2009).

On fatigue performance test, FRP bonded connection did not fail after 10 million fatigue cycles. Furthermore increased of stress ratio, has significantly increased the fatigue crack growth (FCG) and the fatigue threshold curve (Shahverdi et al. , 2011). While adhesive bonding is capable in providing a strong joint, the durability and its integrity is still a major concern. Keller et al. (2007) in their 8 years of observation (1997-2005) on all composite bridges had noticed that there was a significant increased in the deflection, about 16.3% of bonded span. Another recent work focusing on the durability of adhesively bonded double-lap shear joints made of steel and FRP was conducted by Heshmati et al. (2017), whereby 192 specimens were aged for up to three years in various environments. In general, it was found that under immersion at 45°C, the material and joint specimens had experienced significant strength and stiffness reduction.

The authors had addressed a few factors that might have resulted to the increased in deflection which include the possibility of inaccuracy of measurement tools used in 1997 and the occurrence of joint softening due to adhesive cracking or adhesive material degradation. Furthermore, based on on-site experience shared by structural engineers at Wagners Composite Fibre Technologies (WCFT), the difficulty in controlling the quality (adhered to manufacturer specifications) and allocation of curing period of adhesive bonds before pre-loading may compromise the joint strength. For these reasons, many engineering practitioners prefer to use mechanically fastened bolted joint for composite materials in civil applications.

2.3.3. Joint development of pultruded FRP hollow section

Pultruded GFRP hollow closed sections or tubular profiles that mimics thin-walled metallic sections have received growing interest from the engineering community due to better torsional rigidity, effective resistance of out-of-plane forces, high load transfer and improved strength and stiffness of the minor axis (Smith et al., 1998; DG9, 2004); therefore, are more preferable as girder elements compared to FRPs fabricated through moulding or filament winding. Despite these promising features, the

widespread acceptance of pultruded GFRP in the construction field is hampered by many challenges including inadequate connection system, which is a crucial element in determining their reliable performance and in providing satisfactory structural integrity.

Research focusing on jointing method of pultruded GFRP tubular members has recently expanded to include innovative concepts to fully utilise the composite material's attributes including better torsional rigidity, relatively high load transfer, and improved strength and stiffness of the minor axis (Smith et al., 1998; DG9, 2004). Early work on this matter, was carried out by Bank et al. (1994), whereby they had designed an improved wrapped angle connection for pultruded frame structures, while Singamsethi et al. (2005) had established monolithic cuff connections that can be easily attached to pultruded box members using epoxy adhesive to create a simple beam-cuff-column frame. Pfeil et al. (2009) had developed a new connection concept for dismountable bridge by adopting pre-stressing steel tendons inserted into tubular fibre section that could prevent tension forces during its service life. On the other hand, Bai and Yang (2013) had introduced a novel connector using pultruded glass FRP (GFRP) box profiles. By using simplified finite element modelling, the authors found that the configuration of space truss made up of pultruded GFRP can provide satisfactory structural stiffness at the structural level. Through-bolt connection is one of the alternatives when employing a hollow material type as a structural component, and with elements such as bolted sleeve and steel insert, mechanical improvements were observed by Luo et al. (2016b) and Mara et al. (2016) respectively. Further, for restricted accessibility for bolt tightening on tubular hollow shaped pultruded GFRP, Wu et al. (2015a) have successfully used a blind bolt as the connecting element as it only required one-sided access. Most recently, Zhang et al. (2018b) had presented an innovative bonded sleeve connector made from a steel tube that can be inserted at the vicinity of the joint area of hollow GFRP beam-column. Under static loading, this type of jointing method with sufficient bond length managed to achieve a ductile failure through yielding of the steel endplate. Further study on this bonded sleeve GFRP beam-column connection under cyclic loading has been carried out by Zhang et al. (2018a) whereby rotational stiffness, moment and rotation capacity, and local strain responses are investigated. The results obtained from both experimental and finite element analysis showed a successful development of bonded sleeve

connection by attaining an excellent ductility and energy dissipation capacity prior to the final connection failure.

2.3.4. Effect of bolt threads

The use of fully-threaded steel bolts (technically known as screws or all threaded rods) for connection cannot be eliminated in large construction where full FRP sections with thick walls are involved, as it speeds up the construction process while minimizing installation errors. Moreover, it can also reduce the number of different bolts on site, allowing better stock holding and improve construction efficiency. This material combination can be found in large scale constructions involving structural truss system such as industrial cooling towers, electric transmission towers and bridges. Studies on the effect of threaded bolts on the behaviour of bolted joints for pultruded FRP (Figure 2.8), however, are very limited and the design guidelines considering the use of threaded bolts in pultruded FRP construction is still not available. This issue has been identified by Mottram (2009) as one of the research gaps to be tackled in order for design rules to be improved and verified. In the ASCE pre-standard, (ASCE, 2010), it is recommended that, for bolted joint, smooth bolt shank must be in bearing into the FRP material.

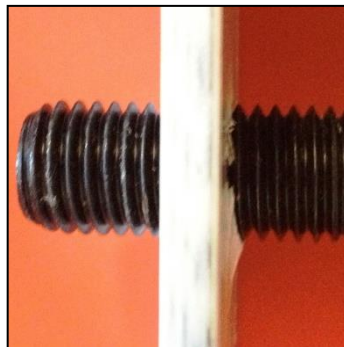


Figure 2.8. Bolt threads effect on composite laminate

For assembly purposes, the thread length should not exceed one third of plate thickness. Also, Matharu and Mottram (2012) mentioned that the presence of bolt thread in the contact zone of composite material is detrimental to the strength of connections in long term exposure, especially in an aggressive environment. Since the bolt threads may cause tearing through the pultruded layers creating narrow gaps between the bolts and the FRP, the connection system becomes more susceptible to

moisture entry. Application of threaded bolts in joining PFRP components to produce advanced composite structures are currently restricted in design and its performance in service is limited. Instead of looking to a new modern joining method, the latter case can be resolved through experimental investigations which results in adaptability and awareness of the issues among a wider group of practitioners.

2.4. FRP truss system

Trusses in engineering refer to structures assembled using two-force members that behave in unison when loaded. These members are generally arranged in repetitive triangle patterns and are assumed to carry only axial loads, either in tension or compression. This structural form is widely used in the 19th century commonly to stiffen structures such as roofs, bridges and transmission towers as it provides dimensional simplicity and low material-to-weight ratio (Zaharia and Dubina, 2006; Omar et al., 2008). Traditionally, steel, concrete and timbers were extensively used for the construction of trusses, but with the recent development in material technology of fibre reinforced polymer (FRP) composites, it is now possible to construct lightweight FRP trusses. Typically, they use much less material than solid web members and their framed nature allows pultruded material to be located where it has the greatest effect. It takes advantage of the unidirectional properties of fibre composites as truss members are subjected only to axial forces and effectively utilise its material strength (Hizam et al., 2012).

2.4.1. Truss systems and its joint concepts

One of the remarkable developments in the jointing system of FRP truss were produced by Goldsworthy and Hiel (1998) when they introduced the award-winning snap joint concept (Figure 2.9) for overhead transmission lines. While the joint design is quite simple, it is capable of distributing the stresses over a wide area and is successfully implemented in the construction of three Transmission Tower Structures near Los Angeles, USA. Since then, it has attracted the attention of other researchers to involve in the study and investigation on FRP truss system. Humphreys et al. (1999) introduced the Monocoque Fibre Composite (MFC) truss concept. In the development of MFC truss, they used the double skin concept whereby the fibre composite skins are separated by a core material. However, the MFC truss concept was not reliable in

lapping joints and improvement had been made by introducing the concept of strength and fill layers. Bradford et al. (2001) had contributed their masterpiece for emergency shelters and bridge decks by developing a modular composite truss panel concept. The modular panel was optimized by integrating the connection within the panel.

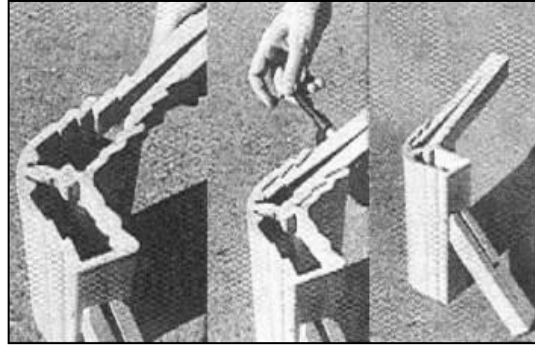


Figure 2.9. Snap joint concept by Goldsworthy & Hiel (1998)

Investigation on FRP truss continues when Keller et al. (2007a), carried out long term performance study of a two-span glass FRP truss bridge built in 1997 using five different pultruded GFRP profiles (angle profiles, square tubes, flat strips, U and I). The all-FRP composite Pontresina pedestrian bridge (Figure 2.10) where the main truss girders were connected by mechanically fastened and adhesive bonded had been tested under temperature -20°C to 25°C and structural safety. Similarly, its serviceability and durability were assessed after eight (8) years in service. In 2005, it was found that the bridge stiffness remains unchanged and the durability was mainly affected by inappropriate construction detailing. Further concern on feasibility of repairing fibre damages on FRP members was highlighted by the authors (Keller et al. , 2007a).



Figure 2.10. The all FRP composite Pontresina bridge (Keller et al. 2007)

Investigation of FRP truss in a military modular shelter system was carried out by Omar et al. (2007) at the University of Southern Queensland in Toowoomba. The deployable shelter concept required light-weight components to facilitate deployment and assembly without using heavy equipment. The main frames were constructed from modular fibre composite panels to fulfill the lightweight requirement and stressed in position by pre-stressing cables. The author had suggested that further research works should explore innovative joint systems due to the changing nature of the structure which affects its capacity and behaviour.

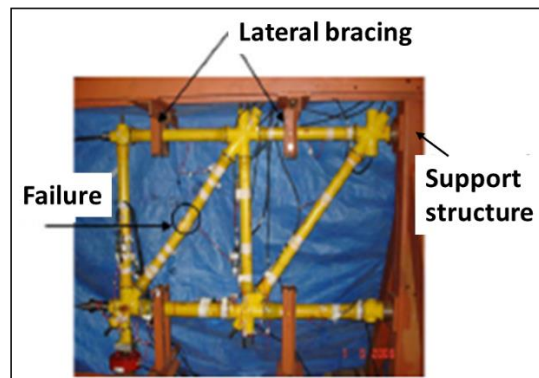


Figure 2.11. Cantilever trussed beam (Pfeil et al. , 2009)

Experimental tests on glass FRP (GFRP) truss modules for dismantlable bridge were investigated by Pfeil et al. (2009). The authors adopted a bearing connection instead of bolting or adhesive bonded. This concept required the pre-stressing steel tendons to be inserted into tubular fibre sections (Figure 2.11) to prevent tension forces during bridge service life. In order to achieve a higher failure load, the target of failure mechanism was designed to occur at the central region where fibers are continuous. Thus, the reinforcement using hand lay-up technique at tubular end section of the truss members had successfully increased 69% of compressive strength. The current study by Bai and Yang (2012) which involved forming all composite free-form space trusses using a novel connector constructed using pultruded GFRP profiles (Figure 2.12) shows a lot of potential. By using simplified finite element modeling, the authors found that the configuration of space truss made up of pultruded GFRP can provide satisfactory structural stiffness at the structural level.



Figure 2.12. Pultruded GFRP novel connector for space truss (Bai and Yang, 2013)

The abovementioned studies showed that fibre composites truss has a high potential to revolutionize the construction industry especially where the lightweight high-strength structures with high durability are needed. However, it was also evident that the structural integrity of FRP trusses largely depends on the joining system used to connect the individual components. Thus, a reliable joining system should be determined in order to advance the use of fibre composite trusses in practical applications.

2.4.2. Effects of eccentric loading

The use of pultruded FRP closed sections tends to limit its joint configuration and architectural design, as certain design may introduce the effects of eccentricity during load transfer between the members of the structure (Righman et al., 2004). During the construction phase, some changes in design may be necessary due to unforeseen issues or constructional imperfections. For example, the connection system may potentially develop accidental load eccentricity, reducing the continuity and global structural performance (Teixeira et al., 2014; dos Santos and Morais, 2015). In regards to the truss structure, this eccentric load may weaken the joint compressive resistance and affect the stability of the truss's compressed chord members (Zaharia and Dubina, 2006). This is not a problem when using thin-walled steel sections as the members can be aligned and connected on a single plane. Most recent research studies on FRP connections have been focussing on concentrically loaded connections (Zhang et al., 2018b; Satavissam et al., 2017; Feroldi and Russo, 2016; Mara et al., 2016).

Studies on eccentrically compressed pultruded GFRP tubular members are limited and as such, their structural behaviour is not fully understood. This has been

supported by the comprehensive review of Gand et al. (2013) which focussed on the developments of FRP closed sections, and the study of Mottram (2009) on the research gaps for connection design guidance, whereby the authors had outlined the behaviour of FRP tubular members under eccentric loading as one of the areas that need further research investigation. Nevertheless, a few published researches related to this topic were found to be on structural members with wide flange (WF) and I-section profiles. Structural members such as columns made up of pultruded GFRP were found to experience small unwarranted load eccentricity that restricts the establishment of universal design guidance (Lane and Mottram, 2002). Mottram et al. (2003) have attempted to address this problem on 'simple-braced' frames of pultruded WF cross-sections under the influence of combined compression and bending. The authors used conventional elastic theory to determine the major axis column behaviour under moment gradient. Another experimental study was conducted by Barbero and Turk (2000) on WF and I-sections of pultruded GFRP which were eccentrically loaded about the minor (weak) axis. It was reported that the main factors contributing to the beam-column failures were the eccentricity, the length of the tested members, and the specimen's geometrical and mechanical properties. A more recent study by Nunes et al. (2013) investigates the structural behaviour of pultruded GFRP columns subjected to small eccentric loading about the major axis, both experimentally and numerically. The authors found that even small eccentricities can have a significant impact on the behaviour of these columns. While initially, the axial stiffness of eccentrically loaded columns is comparable to that of concentrically loaded ones, the effects of bowing and second-order $P-\delta$ effect have expedited the deterioration of stiffness at higher loads. It was also highlighted that the eccentricity was responsible for up to 40% of linear reduction in the load carrying capacity of the columns. Focusing on the jointing area of a pultruded GFRP structure, for bolted connection design, the loading directions and fasteners must be arranged in a concentric manner (ASCE, 2010). However, as mentioned above, eccentricity may be developed during practice, and the discrete load paths employed by bolted connection to transfer forces and moments may also influence the behaviour of a pultruded structure. Thus, the studies of bolted connections with pultruded FRP sections under eccentric loading is of high importance in order to fully understand its effects on the overall performance of the structure during practical applications.

2.4.3. Behaviour under in-service elevated temperature

Inadequacy of information in joint design related to critical condition of service and its behaviour under variable environmental conditions partially contributes to the moderate coverage of its practice. Further research on the developed connections system is required especially in serviceability aspects in order to widen its applications. In many practical applications, the connection is exposed to different service environments including elevated temperature (Correia et al., 2015). For structural applications, all components and its connection must be able to withstand elevated temperatures while maintaining structural integrity. Owing to the different influences on the fibre and matrix, the failure mechanism seems to become non-linear and therefore rather complex. Due to the viscoelastic behaviour of polymer matrix in many composites, the physical properties of the composite can change drastically over relatively small changes in temperature. As the temperature increases, the matrix binding the fibres soften and eventually, the FRP composites may collapse as it further degrades when the glass transition temperature (T_g) is reached. This compromises the structural functionality of the material (Mouritz and Gibson, 2010).

Several studies have attempted to understand the effects of elevated temperature on the physical and mechanical properties of pultruded FRP. Structural performance of GFRP pultruded bolted connection had been tested under adverse environmental condition of ambient temperature, 60°C and 80°C. The specimens were also tested under moisture effect into two water immersion periods of 6.5 weeks and 13 weeks. It was concluded that, the period of immersion in water has caused lesser reduction in the load capacity of pultruded GFRP single bolt joints compared to temperature effect (Turvey and Wang, 2007). In addition, it was concluded by Manalo et al. (2017b) that the strength, stiffness and fibre/matrix interfacial bonding of the composite decreased with increased temperatures. The authors found that transversely cut glass FRP is affected more by the increase in temperature than the longitudinally cut specimens (along the direction of pultrusion). Similarly, Bai et al. (2008) observed that the elastic modulus of pultruded GFRP composites cut longitudinally is different from those cut transversely. Importantly, this type of composite suffers higher thermal degradation of shear and compressive strengths, as these properties are more influenced by the resin than the fibres, when compared to tensile strength (Correia et al., 2015). Therefore,

from these findings, it can be highlighted that the arrangement of the FRP components and the direction of loading are critical factors in thermal failure for pultruded FRP and this will contribute to the complexity of its joint performance at elevated temperatures. This was demonstrated by Turvey and Wang (2009) using Taguchi analysis of joint test data on pultruded FRP with a connection system of double-lap single-bolt tension joints. The study attempted to quantify the degrading effects of bolt/hole clearance, angle between the tension and pultrusion directions, elevated temperature and water immersion period on the failure loads of the joints and it was found that temperature was the most dominant factor. Further to this, it was observed that the effects of test temperature and joint geometry, in this case is the end distance to bolt hole diameter ratios (e/d_b), resulted in various failure modes (dominantly shear, tension, cleavage and bearing) depending on the combination of the two factors (Turvey and Sana, 2016).

2.5. Summary

As a structural material, pultruded GFRP has been widely accepted as alternatives to steel and timber, as advancements have been achieved through many research studies. This is contributed by its attractive characteristics that include ease of fabrication to meet specific structural performance, high axial resistance, high resistance to aggressive environment, relatively lightweight when compared to conventional materials, and quick installation time. However, the widespread acceptance of pultruded GFRP in the construction field is hampered by many challenges including inadequate connection system, which is a crucial element in determining their reliable performance and in providing satisfactory structural integrity. In analysis of joint behaviour for composite materials, it is essential to have a clear understanding of the load distribution paths that transmitted through various components of the joint due to the many possibilities of failure modes and the complexity of stress relieving mechanism. Thus, extensive research in understanding the behaviour of pultruded GFRP with different connection techniques have been carried out. The continuous interest from researchers shows the importance of joint as a vital component for transmitting loads in FRP structures and the importance of improving the gaps in this related area which lead a promising future of the material in civil industry. The selection of optimum connection parameters and materials are essential in order to

achieve the structural integrity and reliability in composite structures. Any joint in a composite structure, if not designed appropriately, may act as a damage initiation point and may lead to failure of the component at that location. Thus, some relevant issues focusing on pultruded FRP jointing elements were exposed during this review, and that will guide this research as follows:

1. Even though the numerous studies had covered the effect of geometric parameters, clamping pressure, and hole clearance requirement, but the effect of bolt thread and combination of latter factors are still unknown. Further investigation is needed in this area to scientifically evaluate the damage tolerance of GFRP profiles due the presence of bolt threads, and to determine clearly on how to account this type of joining system in connection design of composites.
2. In practice, changes in design may be necessary due to unforeseen issues or constructional imperfections which may result to applied accidental load eccentricity. However, joint behaviour on eccentrically loaded pultruded GFRP tubular members with bolted joints is not fully understood. This requires a detailed investigation and careful consideration in determining the overall structural performance and integrity of a pultruded GFRP truss structure.
3. Although inserts have been widely used in the aerospace industry, little result has been published for civil construction. Further tests that supplement crucial data on all thread through-bolt joint configuration should be conducted in order to assess the application of pultruded GFRP hollow profile, especially for truss structure. As of this writing, there is no scientific research on the mechanical insert filled the pultruded GFRP hollow profile and this is a key motivation in this study to explore this innovative joint system capable to improve load-bearing capacity and its mechanical behaviour and investigate its joint behaviour at a structural level (truss structure).
4. Owing to the different influences on the fibre and matrix, the mechanical properties of pultruded fibre reinforced polymer (FRP) and its joint performance are critically sensitive to elevated temperatures, causing the failure mechanism to become non-linear and therefore, rather complex. This limits its wide-spread application, especially in civil construction. Thus, further research on the developed connection systems for pultruded GFRP hollow

section under variable environmental conditions such as moisture, fatigue and elevated temperatures is critical in regards to serviceability aspects.

3. Study on the use of threaded bolt

3.1. Article I: Effect of bolt threads on the double lap joint strength of pultruded fibre reinforced polymer composite materials

A total of 150 double lap joint specimens were prepared and tested to evaluate the effects of threaded bolt and clamping pressure on the joint strength behaviour, failure mechanisms and joint efficiency of bolted joints in pultruded glass fibre reinforced polymer (GFRP). Double lap joints in both longitudinal and transverse (refer **Figure 3** of **Article I**) directions of the laminates and with different edge distance-to-bolt diameter (e/d_b) were prepared and tested in accordance with ASTM D5961 standards. The schematic diagram of the test set-up is shown in **Figure 5** of **Article I**. A summary of the experimental results for all tested specimens is presented in **Table 6** of **Article I**. The table lists the average maximum load, average displacement, and joint efficiency for all test parameters.

The experimental results showed that about 30%–40% reduction in joint strength was observed in the longitudinal direction due to the effects of laminate tearing by the bolt threads. Based on this result, a reduction factor of 0.6 is proposed for the preliminary design of pultruded FRP bolted connections using threaded bolts to account for the damaging effects of the threads. However, the introduction of lateral clamping pressure had lessened the effect of threads on the pultruded GFRP joints and increased the joint strength by 60% to 90%. The theoretical evaluation of the bolted joint strength used in **Article I** was based on existing design codes of ASCE pre-standard and Italian CNR and the computed results were compared to the experimental outputs as summarised in **Section 4**. More importantly, the outcomes of studies conducted in **Article I** provided an in-depth understanding of bolted GFRP joint behaviour with the presence of bolt threads. These findings are critical for the following studies whereby all-thread rods were used in through-bolt GFRP connection system, and the behaviour of this jointing system under elevated in-service temperature was evaluated in **Article II**. The published journal of **Article I** is included in **Appendix B.1**.

Effect of bolt threads on the double lap joint strength of pultruded fibre reinforced polymer composite materials

R.M. Hizam ¹, Allan C. Manalo ^{1*}, Warna Karunasena ¹ and Yu Bai ²

¹Centre of Future Materials, Faculty of Health, Engineering and Sciences, University Southern Queensland, QLD 4350, Australia.

²Department of Civil Engineering, Monash University, Clayton, VIC 3800, Australia.

*Corresponding Author:

manalo@usq.edu.au

Abstract

The ability to provide effective and adaptable joints for pultruded fibre reinforced polymer (PFRP) is crucial for its widespread application in civil infrastructure. This experimental based study on 150 double lap joints specimens investigated the effects of threaded bolt and clamping pressure on the joint strength behaviour, failure mechanisms and joint efficiency of bolted joints in PFRP. Double lap joints in both longitudinal and transverse directions of the laminates and with different edge distance-to-bolt diameter (e/d_b) were prepared and tested in accordance with ASTM D5961 standards. The joint strength in the longitudinal laminates with plain bolt increased for e/d_b ratio for up to 4 and with no appreciable strength gain after exceeding this ratio. On the other hand, about 30% - 40% reduction in joint strength was observed in the longitudinal direction due to the bolt thread tearing through the laminates. This leads to a recommendation of 0.6 reduction factor in preliminary design of PFRP bolted connections with bolt thread present. Meanwhile, only a marginal difference of 7% was observed in transverse direction. Furthermore, the introduction of lateral clamping pressure had increased the joint strength by 60%-90% and this has lessened the thread casualty effect on the pultruded composite joints.

Keywords: pultruded FRP; bolt threads; clamping; connection; joint; failure modes.

INTRODUCTION

The interest in using fibre reinforced polymer (FRP) composites in civil engineering and construction applications has increased significantly in recent years. This advanced material was initially introduced in structural applications as strengthening material for beams and columns of bridges and buildings (Bank et al., 1995; Bank, 2006; Hollaway, 2010). With advanced manufacturing process such as pultrusion, standard structural shapes for instance box section, I-beam, etc., which resemble closely that of structural steel sections, are now readily available for the construction industry. The attractive attributes such as high strength-to-weight ratios, high resistance to corrosive environment, and low life cycle cost have made FRP composites as material of choice in structures built in aggressive environment. In spite of these attractive features, the limitation in providing effective and reliable joining method has impeded the widespread use of pultruded FRP (PFRP) sections, especially in frame structures (Hizam et al., 2012; Mottram, 2009; Hai and Mutsuyoshi, 2012; Blaga et al., 2015; Russo, 2012).

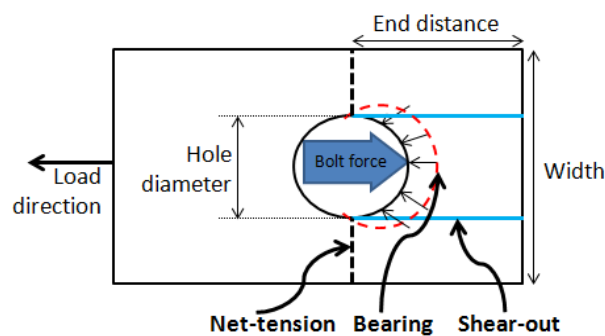


Figure 1. Type of failure modes in composite bolted joint

The ability to provide joint versatility for PFRP in civil structures industry is crucial for its application demands. Although there are many types of connection system available, the conventional steel bolt is mostly used to join the structural components

due to low cost, ease of assembly, ease of performing maintenance and inspection checks, and familiarity to the practitioners. Extensive research on bolted connections in FRP has been conducted by many researchers, focusing on the evaluation of joint performance as well as its failure modes and failure mechanism (SCI and BCSA, 2002; C.Cooper and G.J.Turvey, 1995; K.Hassan et al., 1996; Bank et al., 1994; Xiao and Ishikawa, 2005a; Khashaba et al., 2006; Keller et al., 2007a; Ascione et al., 2010; Bai and Yang, 2013; Lau et al., 2012; Luo et al., 2016b; Russo, 2016; Mottram and Turvey, 2003). This also has been well recognised in the recent design guidelines, i.e. ‘Pre-Standard for Load Resistance Factor Design (LRFD) of Pultruded FRP structures’ and ‘Guide for the Design and Construction of Structures made of FRP Pultruded Elements (CNR-DT 205/2007)’ wherein the detailed parameters and design requirements for joining composite materials are presented in Chapter 8 (ASCE, 2010) and Chapter 5 (CNR, 2008), respectively. As recommended by the both guidelines, fastening parameters such as joint geometry (width, spacing, end distance and bolt diameter), material thickness, clamping pressure, bolt hole tolerance, and loading conditions need to be carefully considered when designing FRP bolted connections. These parameters significantly influence the failure modes (Fig. 1) for instance bearing, shear-out, net tension and combinations of these which eventually dictate the strength of the joint connection. Meanwhile, recent review papers by Coelho and Mottram (2015) and Correia et al. (2015) provide a comprehensive list of published contributions covering bolted FRP joint behaviour and its mechanical response against various range of joint parameters and environment exposure conditions. Other than metallic fasteners, FRP fasteners (solid rod or bar) are adopted in rocks and soil engineering application as anchorage or strengthening strips (Terrasi et al., 2011). These FRP fasteners have the potential to be used in a variety of applications whereby its strength and stiffness properties are engineered according to different connection modes. It is ideal for applications that require fasteners to be non-corrosive, low in conductivity or no electromagnetic waves (Schmidt et al., 2012). FRP threaded rods are made by machining a thread on an FRP solid rod which can be used with metal hex nuts if the threads formed are a direct match and fit. Generally, however, the forming of thread has caused defects on the screw connections which resulted in a lower connection strength, about 20%-40% of the strength of the FRP solid bar itself (Min, 2008). Moreover, unlike steel fasteners, FRP threaded rods possess linear elasticity and

brittleness with anisotropic properties, making them ineffective as a joining component for advanced composites.

Currently, the use of fully-threaded steel bolts (technically known as screws or all threaded rods) for connection cannot be eliminated in large construction where full FRP sections with thick walls are involved, as it speeds up the construction process while minimizing installation errors. Moreover, it can also reduce the number of different bolts on site, allowing better stock holding and improve construction efficiency. This material combination can be found in large scale constructions involving structural truss system such as industrial cooling towers, electric transmission towers and bridges. The use of FRP composite materials for these structures are expected to show rapid growth in the near future (Plastics, 2002). It effectively exploits the FRP's high unidirectional strength as truss members are subjected only to axial forces. Studies on the effect of threaded bolts on the behaviour of bolted joints for PFRP, however, are very limited and the design guidelines considering the use of threaded bolts in PFRP construction is still not available. In the American pre-standard, ASCE (ASCE, 2010), it is recommended that, for bolted joint, smooth bolt shank must be in bearing into the FRP material. For assembly purposes, the thread length should not exceed one third of plate thickness. Matharu and Mottram (2012) also mentioned that the presence of bolt thread in the contact zone of composite material is detrimental to the strength of connections in long term exposure, especially in an aggressive environment. Since the bolt threads may cause tearing through the pultruded layers creating narrow gaps between the bolts and the FRP, the connection system becomes more susceptible to moisture entry.

Application of threaded bolts in joining PFRP components to produce advanced composite structures are currently restricted in design and its performance in service is limited. Instead of looking to a new modern joining method, the latter case can be resolved through experimental investigations which results in adaptability and awareness of the issues among a wider group of practitioners. It is the aim of this paper to provide a better level of understanding associated to the influence of bolt threads with the recognised joining parameters and to advice a factor that account the bolt threads effect in the preliminary FRP bolted design. This paper also reveals the joint

behaviour of bolt threads on FRP materials in microscopic scale to refine the understanding on the finding mode of failures and its mechanism.

This paper presents the results of an extensive experimental work, including the scanning electron microscope (SEM) imaging which investigates the effects of bolt threads on the joint strength and failure mechanisms of a double lap joint for composite laminates cut in the longitudinal and transverse directions of PFRP. Bolted FRP joints subjected to compression are less sensitive to joint geometry and are generally stronger than joints subjected to tensile forces (Mosallam, 2011). For this reason, FRP bolted connections in this paper were tested under axial force (tensile) to assess its strength and reliability. Assessment of bolt threads reduction factor in FRP bolted design, as well as the comparison of pultruded FRP joint strength and efficiency between plain bolts, threaded bolts, and clamped specimens were also presented.

EXPERIMENTAL PROGRAM

Pultruded FRP composites

The materials used in this study are 6.5 mm and 5 mm thick laminates, extracted from hollow glass PFRP composite sections, manufactured and supplied by Wagners Composite Fibre Technologies (WCFT). The coupon testing for both longitudinal and transverse directions have been carried out as recommended in Pre-Standard (LRFD) of pultruded FRP to assess its mechanical properties. The results are presented in Table 1. The conducted burn-out test at 600°C following ASTM D3171 (2011) (ASTMD3171, 2011) revealed that the stacking sequence of 6.5 mm and 5 mm thick PFRP specimens (Figure 2) are $[0^\circ/45^\circ/0^\circ/-45^\circ/\overline{0^\circ}]_s$. and $0^\circ/45^\circ/0^\circ/-45^\circ/0^\circ$, respectively. Additionally, there are thin protective veils present on the outermost surface of the PFRP. The fibre weight fractions were 61% and 65% for 6.5 mm and 5 mm thick pultruded samples, respectively.

Table 1. Mechanical properties of PFRP profiles

Properties ^a	6.5 mm plate	5 mm plate
Tensile Long ^b , Peak stress (MPa)	741.53 (44.91) ^d	686.43 (44.21)
Tensile Long, Elastic modulus (MPa)	42,983 (1257)	42,922 (2281)
Tensile Trans ^c , Peak stress (MPa)	66.41 (3.78)	46.84 (3.91)
Tensile Trans, Elastic modulus (MPa)	13,350 (2,131.06)	12,198 (1,110)
Compressive Long, Peak stress (MPa)	514.86 (15.27)	543.83 (43.95)
Compressive Trans, Peak stress (MPa)	161.66 (6.76)	147.70 (15.23)
In-plane shear Long, Peak stress (MPa)	113.60 (6.85)	88.95 (14.64)
In-plane shear Trans, Peak stress (MPa)	95.30 (4.72)	NA ^f
Pin-bearing (Plain), Peak stress (MPa)	291.44 (7.72)	260.12 (55.66)
Pin-bearing (Thread), Peak stress (MPa)	207.68 (11.08)	185 (7.21)
Fibre mass fraction, W_f	78.6%	81.4%
Fibre volume fraction, V_f	61%	65%
Density ^e (kg/m ³)	2030	

^aTesting were conducted based on relevant standards ^bLongitudinal ^cTransverse
^dStandard deviation ^eWCFT product specification ^fNot available

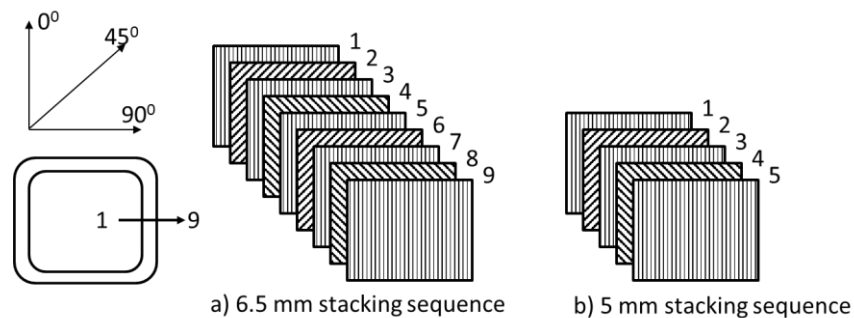


Figure 2. Stacking sequence of 6.5 mm and 5 mm PFRP specimens

High strength structural bolt

The bolts used in the double lap joint configuration are high strength structural bolts in accordance to Australian standards AS 1252:1996 (AS/NZS1252:1996, 1996a) and AS 1110-1995 (AS/NZS1110:1995, 1995). The Steel Construction Institute (2002) (SCI and BCSA, 2002) indicated that M20 x 60 mm long grade 8.8 all threaded bolts are used for 90% of the connections in a typical multi-storey steel frame. Thus, this type of bolt was used in this study. The M20 stainless steel (SS) 316 bolts were from commercially available sources and with properties presented in the next section. Table 2 shows the mechanical properties of class 8.8 SS bolts. The mechanical fasteners ultimate strength can be evaluated through simplification of internal forces redistribution based on designed experimental results. For this experimental program, the load transfer across the joint are classified as bearing type-bolts and pre-loaded friction-grip. Generally, in bolted connection, there are three ways the joint could break or fail which is by bolt failure, plate tearing (net-tension), and high extension of bolt hole or material tearing at the vicinity of the joint. Generally, the latter is more likely to occur when there is a difference in hardness between the materials. This phenomenon is widely observed when steel bolt is used to connect FRP materials, where the prominence failure modes of shear-out, bearing or cleavage are commonly identified. Based on the given bolt capacity and hardness differences, it is expected that the joint failure to occur on the jointed material instead of the connector.

Table 2. Bolt types and its mechanical properties (AS 1110-1995)

Item	Specification
Property class	8.8
Material type	Stainless steel S316
Diameter of bolt, D	20 mm (M20)
Nominal shank area	314 mm ²
Area of root of thread	225 mm ²
Minor diameter, Dc	19.67 mm
Pitch, P	2.50 mm
Minimum tensile strength	830 MPa

Item	Specification
Proof strength	600 MPa
Minimum yield strength	660 MPa
Minimum shear stress ^a	514.6 MPa
Min. breaking load in single shear (Shank)	163 kN
Min. breaking load in single shear (Thread)	117 kN
Minimum bolt tension ^b	145 kN

^aUltimate shear stress equals 62% of ultimate tensile strength

^bFull tightening

Specimen design and preparation

A total of 150 double lap, single bolt joint (DLSJ) specimens were produced from hollow pultruded glass FRP sections with different thicknesses, i.e. 6.5 mm and 5 mm. The tests were carried out in order to determine the influence of joint geometry, presence of bolt thread and the use of clamping pressure on the joint strength and efficiency. In this experiment, the joint was designed to promote bearing failure and this type of failure is preferable in composite joint due to its progressive nature and post-failure behaviour beyond its ultimate load (Ascione et al., 2010; B.Vangrimde and R.Boukhili, 2002; Xiao and Ishikawa, 2005a). In the calculation of the bearing resistance of pultruded FRP, the pin-bearing capacity on the composite laminates is an important design parameter. According to Matharu and Mottram (2012), the pin-bearing strength used in Equation (1) must be the ‘lowest’ characteristic strength which accounts for all detrimental effects,

$$R_{br} = t d_b F_{\theta}^{br} \quad (1)$$

Where t = thickness of FRP material (mm); d_b = nominal diameter of bolt (mm); F_{θ}^{br} = characteristic pin-bearing strength of FRP material, as stated in Table 1. The pin-bearing strength of the pultruded FRP used in this study was evaluated following the test procedure suggested by Keller et al. (2015). Their paper has addressed a few limitations with existing standards ASTM D953-02 (2010) (ASTMD953, 2010) and EN 13706-2:2002 (EN13706-2, 2002) and has called for an alternative test

arrangement. Thus, the pin-bearing test was executed adopting the set-up used by the Warwick University (2011) (Mottram and Zafari, 2011a) test setup, with a few adjustments on the bolt configuration and the test specimen's dimension. The test setup used steel bolts with a nominal diameter of 20 mm and a ratio of end distance to bolt diameter (e/d_b) up to 4. In this case, thread bolt was also included and its pin-bearing strength is presented in Table 3.

Table 3. Pin-bearing strength

Pin-bearing strength (MPa)				
Specimens	d_b/t ¹	Plain bolt, $F_{br,plain}$	Threaded bolt, $F_{br,thread}$	$\frac{F_{br,thread}}{F_{br,plain}}$ ³
6.5 mm	3.07	291.44 (7.72) ²	207.68 (11.08)	0.71
5 mm	4.00	260.12 (55.66)	185.00 (7.21)	0.71

¹bolt diameter to thickness ratio ²standard deviation

³thread to plain pin-bearing stress ratio

The results show that, the use of 20 mm diameter steel bolt with thread, has resulted in approximately 30% strength reduction compared to the bolt shank. The pin-bearing strength is also affected by about 11% reduction when the d_b/t increases from 3.07 to 4. It is comparable with the 15% reduction attained by Mottram and Zafari (2011a). These data are used in the theoretical analyses of the bearing failure load for FRP sections with double lap joints in Theoretical evaluation section. Table 4 shows the joint geometry of the specimens designed as per minimum geometric configurations as suggested by Bank (2006) (Bank, 2006). Due to material dimensional constraints of the used closed section (125 mm x 125 mm x 6.5 mm and 100 mm x 75 mm x 5 mm), the minimum plate width to bolt diameter ($w/d_b = 3$) ratio was chosen. The bolt hole was carefully drilled using diamond coated drill to ensure the accuracy of bolt holes and to avoid fibre damage as suggested by Persson et al. (1997).

Table 4. Geometric parameters for lap joint connections

Parameters	Bank (2006)	Test specimen geometry (longitudinal & transverse)	
		6.5mm	5mm
End Distance to bolt diameter, e/d_b	2	2.5, 3, 4,5	2.5, 3, 4,5
Plate width to bolt diameter, w/d_b	3	3	3
Bolt diameter to plate thickness, d_b/t_{pl}	0.5	3	4
Washer diameter to bolt diameter, d_w/d_b	2	2	2
Hole size clearance	1.6 mm ^a	0.50 – 0.55 mm	

^aMaximum clearance

Figure 3 shows the nominal dimensions of the tested pultruded FRP longitudinal and transverse specimens with an e/d_b of 2.5. The end distance, e , is varied as 50 mm, 60 mm, 80 mm and 100 mm in order to increase the ratio of e/d_b to 2.5, 3, 4, and 5, respectively.

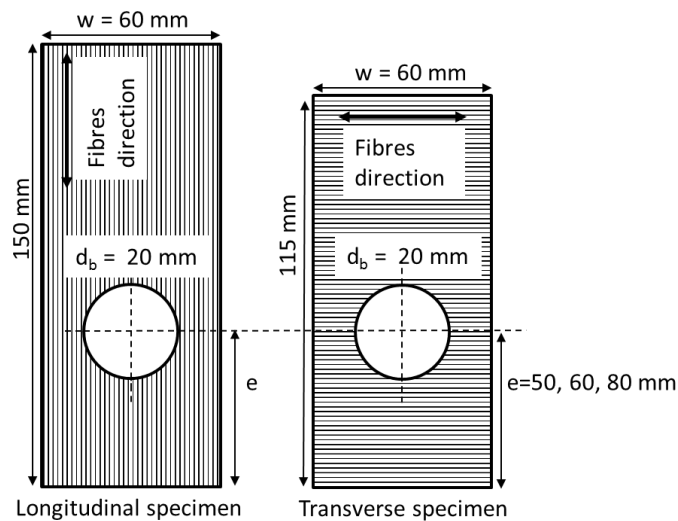


Figure 3. Nominal dimensions of $e/d_b = 2.5$ and $w/d_b = 3$

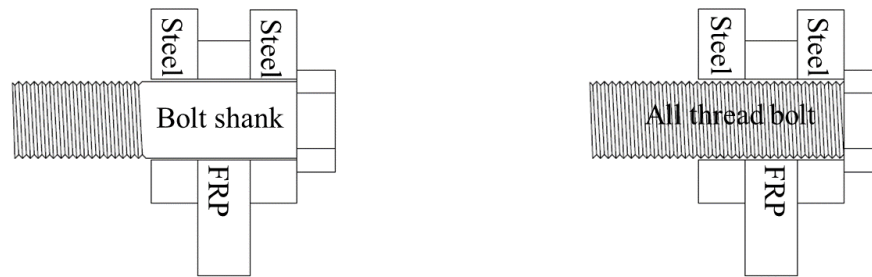
Table 5 outlines the experimental material groups, namely A and B which represent the 6.5 mm and 5 mm specimen thickness, respectively. The experimental program covers both longitudinal and transverse directions with different e/d_b ratios.

Table 5. Summary of pultruded FRP specimens

Specimen designation		e/d _b ratio	Direction	Bolt type	Clamp	No. of specimens
6.5 mm	5 mm					
A50LP	B50LP	2.5	Longitudinal	Plain	No	10
A60LP	B60LP	3	Longitudinal	Plain	No	10
A80LP	B80LP	4	Longitudinal	Plain	No	10
A100LP	B100LP	5	Longitudinal	Plain	No	10
A50LT	B50LT	2.5	Longitudinal	Thread	No	10
A60LT	B60LT	3	Longitudinal	Thread	No	10
A80LT	B80LT	4	Longitudinal	Thread	No	10
A50LPC	B50LPC	2.5	Longitudinal	Plain	Yes	10
A60LPC	B50LPC	3	Longitudinal	Plain	Yes	10
A80LPC	B50LPC	4	Longitudinal	Plain	Yes	10
A50LTC	B50LTC	2.5	Longitudinal	Thread	Yes	10
A60LTC	B60LTC	3	Longitudinal	Thread	Yes	10
A80LTC	B80LTC	4	Longitudinal	Thread	Yes	10
A50TP			Transverse	Plain	No	5
A50TT		2.5	Transverse	Thread	No	5
A50TPC			Transverse	Plain	Yes	5
A50TTC			Transverse	Thread	Yes	5

Based on other research works, pultruded base material requires high e/d_b ratio to achieve bearing failure mode due to high orthotropic nature. In some related literatures, it is recommended that the said ratio to be at least 4 and it was also mentioned that, when the e/d_b ratio is 5 or higher, no appreciable gain in the joint strength will be observed (Eurocomp, 1996; Matharu and Mottram, 2012). It is important to note that, these findings are dependent on the specific type of pultruded composite materials used by the researchers. Due to this reason, the current experimental work was designed to accommodate a certain range of e/d_b to observe its effect on the presence of threaded bolt and clamping pressure. Initially, the e/d_b ratio up to 5 was introduced for bolted joint using plain bolts for both A and B material groups. Based on the preliminary outcome, the applicable range of e/d_b was established for the remaining parameters.

Conversely, for specimens in transverse direction, only e/d_b ratio of 2.5 was considered due to the width limitation of the pultruded FRP section. Similarly, by providing grips on one end of the specimen has resulted in omission of more ratios of e/d_b for transverse specimens. The test specimens were divided into four main groups, namely plain pin (P), thread (T), plain pin with clamp (PC) and thread with clamp (TC).



a) Specimens with plain bolt

b) Specimens with threaded bolt

Figure 4. Illustrative diagrams of the steel bolt in contact with FRP laminate

Figure 4 shows the illustrative diagrams of plain bolt and threaded bolt when in contact with pultruded FRP laminate. The detailed description of the groups formed and numbers of specimens allocated for testing are presented in Table 5. For instance, A60LTC means that the specimen was prepared from the 6.5 mm thick laminates (Group A) in longitudinal direction (L) with 60 mm end distance (60) and connected using threaded bolt and was subjected to clamping pressure (TC).

Test configuration and instrumentation

Pultruded glass FRP specimens were tested to failure according to ASTM D5961 (2006) (ASTMD5961, 2006) to investigate the behaviour of bolted laminates in longitudinal and transverse directions. Figures 5 shows the schematic layout and photograph of double lap joint single-bolted pultruded FRP test specimens ready for testing.

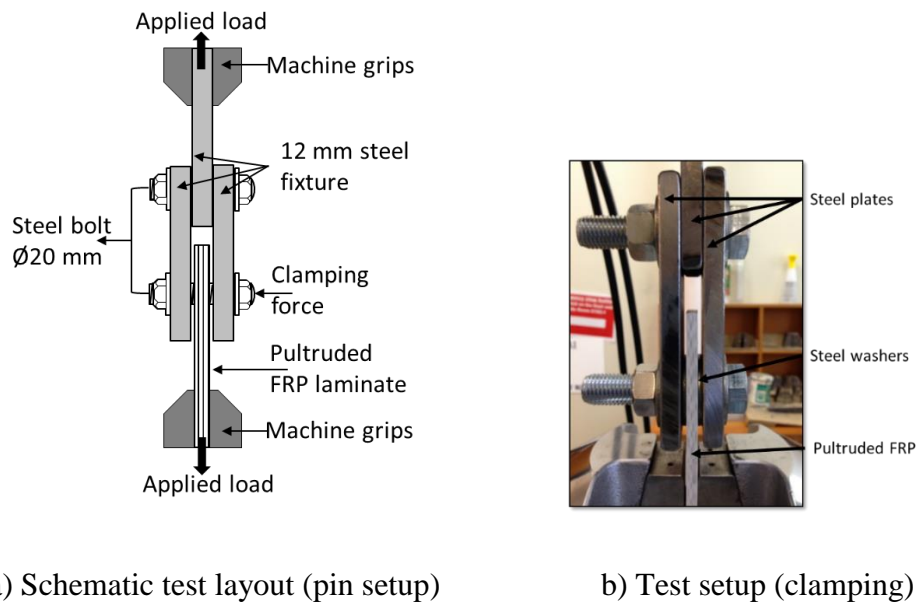


Figure 5. Double lap joint, single-bolted pultruded FRP test fixture

The pultruded FRP specimen was positioned between 12 mm machined steel plates and the other end was clamped by the hydraulic wedge with a grip pressure of approximately 8.5 MPa as per recommended by Guades (2013). Two types of stainless steel (SS) of 20 mm nominal bolt diameter or M20 were used, i.e. all threaded bolt and plain bolt shank with thread. Joints were tested in tension for two clamping conditions; the pin bearing condition (zero fastener torque) and the fully clamped condition. Figure 5a shows how the mechanical fastener was deployed in pin-bearing manner without any lateral restraint. However, loose SS nuts were placed for safety purposes. This DLSJ experimental test setup is similar to those reported by Hai and Mutsuyoshi (2012) and Turvey and Sana (2016). Figure 5b shows the joint configuration of test specimen with a recommended tightening torque of 25 Nm (Manalo and Mutsuyoshi, 2011). Steel washers with an outside diameter, d_w of 40 mm were inserted under the head bolt and at the gaps between the steel plates and laminates to ensure that the clamping pressure was uniformly applied. The bolted pultruded laminates and its steel fixtures were mounted at both ends in a 100 kN capacity servo-hydraulic 810 Material Test System (MTS) machine and were tested under tensile direction. The tests were conducted under the displacement control at a constant head-loading rate of 1.0 mm/min up to failure. The load and the system displacement were automatically measured and recorded for every 0.5s by the MTS Teststar IIs data logging. The failure

modes of each specimen were observed throughout the testing and a detailed assessment was carried out after the test.

RESULTS AND DISCUSSION

A summary of the experimental results for all tested specimens is presented in Table 6. The table lists the average maximum load, average displacement, and joint efficiency for all test parameters.

Table 6. Summary of results (Longitudinal and Transverse direction)

Specimens	Average Max. load (kN)	Standard deviation (kN)	Average Displacement (mm)	Standard deviation (mm)	Joint efficiency (%)	Mode of failure
A50LP	45.29	2.80	1.58	0.17	46.98	Shear-out
A60LP	47.25	3.64	1.92	0.42	49.01	Bearing
A80LP	52.37	1.64	1.58	0.02	54.32	Bearing
A100LP	51.97	2.69	1.97	0.21	53.91	Bearing
A50LT	30.17	2.82	2.04	0.17	31.29	Crushing
A60LT	30.66	2.38	2.06	0.12	31.81	Crushing
A80LT	29.54	1.85	1.96	0.10	31.64	Crushing
A50LPC	48.34	0.24	1.83	0.23	50.14	Shear-out
A60LPC	56.19	2.76	2.27	0.10	58.29	Shear-out
A80LPC	61.95	1.07	2.27	0.27	64.26	Shear-out
A50LTC	49.58	3.10	2.82	0.09	51.43	Shear-out
A60LTC	58.57	2.26	3.36	0.26	60.76	Shear-out
A80LTC	57.73	2.27	3.45	0.02	59.88	Shear-out
B50LP	25.65	2.61	1.15	0.18	37.36	Shear-out
B60LP	28.66	0.50	1.13	0.03	41.75	Bearing
B80LP	36.58	3.73	1.34	0.09	49.45	Bearing
B100LP	26.33	2.88	0.96	0.03	38.35	Bearing
B50LT	17.80	1.50	2.38	0.60	25.93	Crushing
B60LT	21.51	1.31	1.91	0.13	31.34	Crushing
B80LT	22.33	1.04	1.65	0.02	32.53	Crushing
B50LPC	29.31	1.49	1.36	0.05	42.70	Shear-out
B60LPC	39.88	1.78	1.71	0.20	58.11	Shear-out
B80LPC	47.47	2.87	1.94	0.18	69.16	Shear-out
B50LTC	28.30	2.28	2.24	0.18	41.22	Shear-out

Specimens	Average Max. load (kN)	Standard deviation (kN)	Average Displacement (mm)	Standard deviation (mm)	Joint efficiency (%)	Mode of failure
B60LTC	40.28	1.25	3.15	0.21	58.68	Shear-out
B80LTC	43.62	4.66	3.62	0.68	63.55	Shear-out
A50TP	12.98	2.23	0.92	0.12	50.11	Net-tension
A50TT	12.00	0.74	1.35	0.24	46.33	Net-tension
A50TPC	13.74	1.34	1.05	0.21	53.05	Net-tension
A50TTC	13.36	0.85	1.57	0.09	51.58	Net-tension

In this study, the ultimate failure load (Fig. 6) is defined as the maximum load just prior to unstable, nonlinear behaviour. In some cases, however, after the load undergoes reduction, it may start to increase again beyond the original failure load but at the expense of large displacement. From this data, it is apparent that the specimens with threaded bolt resulted in lower failure load compared to the specimens with plain bolt. An average of 30-40% strength reduction was obtained when compared with longitudinal plain specimens for both A and B groups. This level of strength reduction is comparable to the reduction in the pin-bearing characteristic of pultruded FRP using threaded bolt from that of plain bolt. Detailed examination of thread effect under scanning electron microscope (SEM) is presented in Influence of bolt threads section. The tests also revealed that the clamped specimens with threaded bolts attained 60%-90% higher joint strength than that of without the clamping pressure. Concisely, by providing a sufficient lateral restraint to the joint configuration, it has significantly improved the joint capacity of glass PFRP irrespective of bolting conditions (with or without threads).

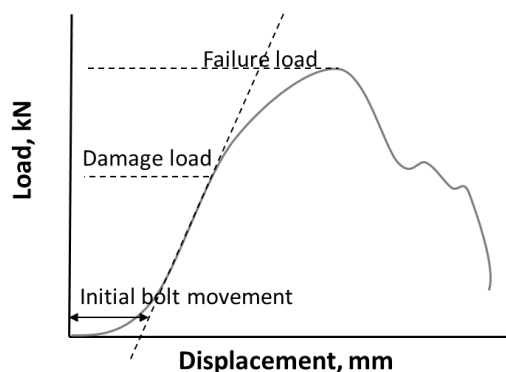


Figure 6. Typical load vs displacement of double lap single bolted FRP connection

Joint efficiency

Equation 2 is used to calculate the joint efficiency of a composite bolted joint which is based on net-strength. The joint efficiency, η , of the double lap joints, is defined as the ratio of the ultimate joint strength to the ultimate strength of the unjointed material. It also presents the design effectiveness of bolted joint compared to unjointed continuous member of the same size (Mosallam, 2011). S_j represents the ultimate joint strength (kN) of each parameter based on the experimental results. S_m is the ultimate load capacity of unnotched (unjointed) continuous member which can be determined by multiplying the pultruded FRP tensile strength with the affected sectional area. The affected section area is defined as the contact area between the bolt and pultruded FRP, whereby this area is likely to be the location where joint failure will occur.

$$\eta = \frac{S_j}{S_m} \quad (2)$$

In general, when comparing the results of the joint efficiency for the LP, LT, LPC and LTC groups, the LT group recorded the lowest joint efficiency. Groups LPC and LTC which obtained almost identical results for both A and B materials, recorded the highest joint efficiency, with more than half compared to unjointed members. In detail, B80LPC obtained the most joint efficiency at 69% when compared to unjointed 5 mm thickness specimen. It is worth to note that, specimens A80LPC, A60LTC, A80LTC and B80LTC achieved joint efficiency of at least 60%.

Failure mode

After the completion of each test, the specimens were disassembled from the test set-up to examine the damage on the FRP laminates. Table 6 presents the overall failure modes of each specimen. Figure 7 presents the common failure modes identified throughout the experimental programme which are shear-out, bearing, net-tension and local crushing. Shear out failure was visible for the specimens with $e/d_b = 2.5$, which can be found in specimens A50LP and B50LP as shown in Figure 7a). As the e/d_b increases, the failure mode changes from shear-out failure to bearing failure (Fig. 7b). Some of the previous studies reported that, the bearing failure of a single-bolt pultruded joint will likely occur for large widths and larger end distances (Vangrimde and Boukhili, 2003; Matharu and Mottram; Matharu and Mottram, 2012). A good

agreement was obtained with regard to the larger end distance condition, whereby, as the e/d_b increases, the mode of failure has changed from shear out to bearing failure. This can be seen clearly from the specimens at the e/d_b ratios of 3, 4, and 5. However, it is important to note that, if the pultruded FRP consists of highly orthotropic composite laminates, even at a very large end distance, the shear-out failure should be taken into consideration. Conversely, detailed observation has shown that the longitudinal specimen with threaded bolt were heavily crushed or broomed beneath the contact surface (Fig. 7e). Similar mode of failure was observed for all ALT and BLT specimens across the critical end distance range. This shows that, e/d_b ratio does not have any influence on the threaded specimen's failure mode.

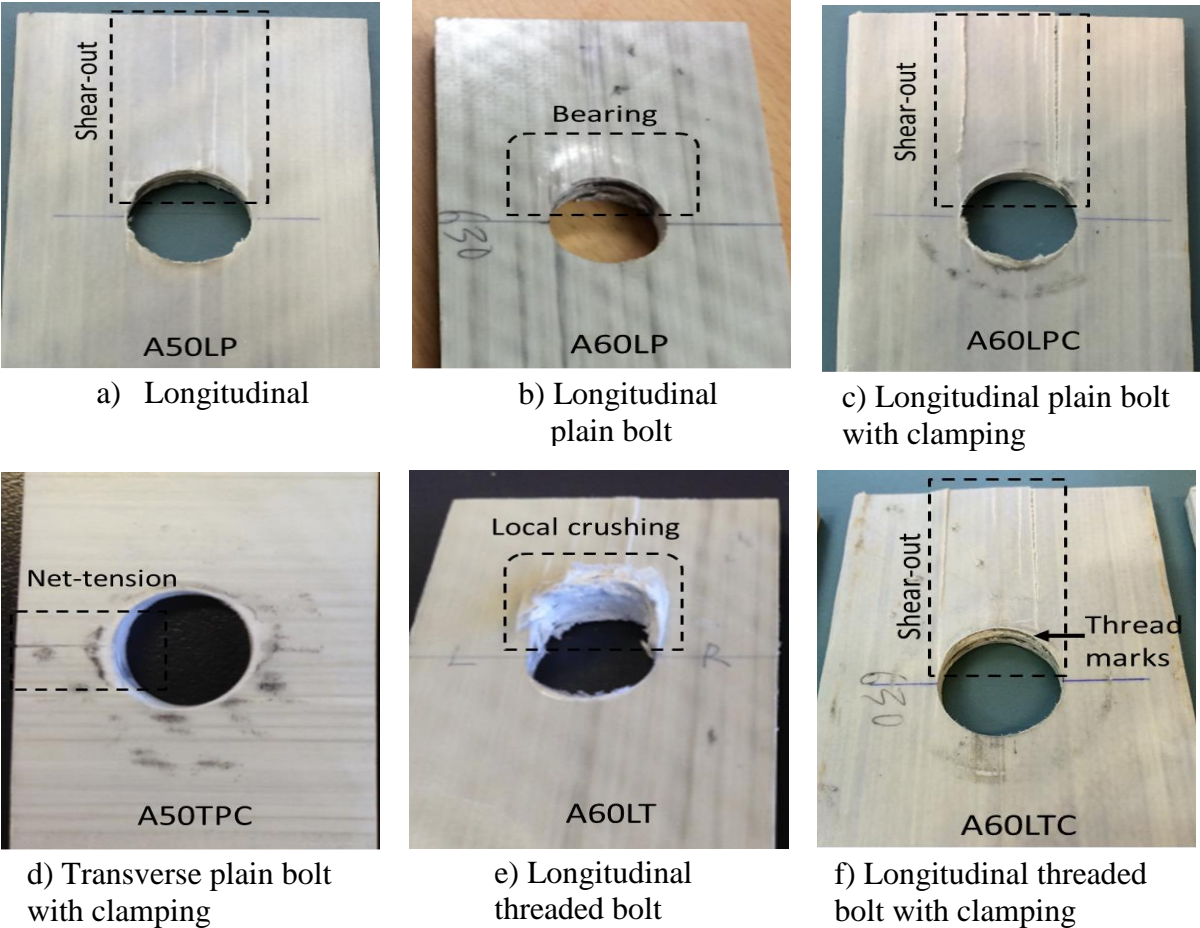


Figure 7. Common failure modes observed after the testing

Specimens with threads in the composite joints exhibited deterioration and delamination of both fibres and the resin matrix around the bolt hole, or what is known as the softened zone. This may have occurred due to the combined effect of the thread and the excessive compressive stress at the contact zone. When clamping pressure was

introduced to longitudinal plain and longitudinal thread specimens, the shear-out failure mode was examined (Fig. 7c and 7f). Similar failure mode was observed at different critical end distances. In different circumstances, all transverse specimens failed in net-tension mode (Fig. 7d). This was observed in specimen A50TP, A50TT, A50TPC and A50TTC. This indistinguishable mode of failure might have occurred predominantly due to very low ultimate tensile strength in transverse direction which caused the cracks to propagate perpendicular to the load direction.

Influence of laminate orientations

Figure 8 shows the comparison of experimental results between 6.5 mm longitudinal and transverse specimens with similar joint configurations. It is seen that the longitudinal specimens exhibit higher connection resistance than that of transverse specimens and similar findings were made by other researchers (Turvey, 1998a; Wang, 2002).

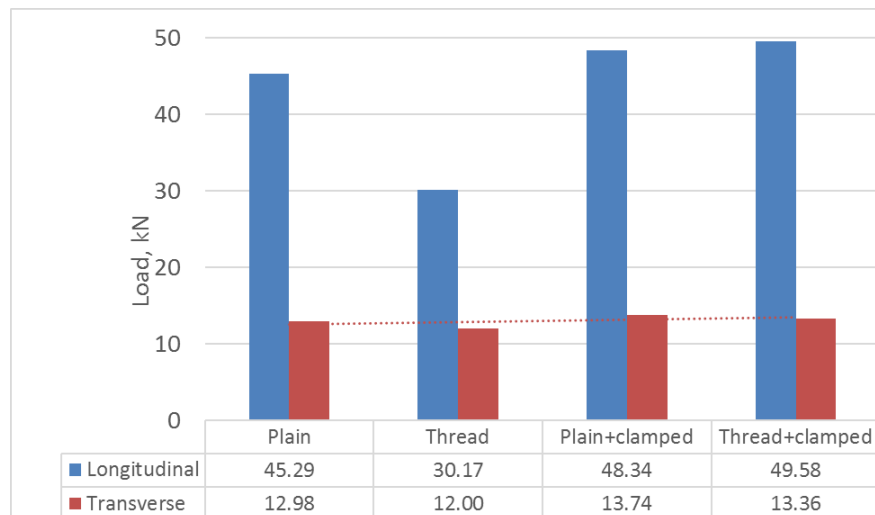


Figure 8. Comparison between longitudinal and transverse specimens for each parameter.

When fibre-to-load orientation changed from 0° to 90°, there was a massive reduction in joint resistance of about 70% for all parameters except for the joint tested with threaded bolt. On average, the threaded bolt specimens recorded about 60% lower joint capacity in the longitudinal direction than the one achieved by the transverse specimens. Significant differences of material strength between longitudinal and transverse direction of the specimens, as well as high stress concentration at the fibre-matrix interphases, especially at the hole edge region, may have contributed to the

substantial decrease of joint capacity. The joint strength of transverse specimens exhibited only marginal differences and bounded in the range of 12 kN to 14 kN, before rapidly declined as shown in Figure 9. The threaded bolt specimen, A50TT, experienced minor decrease in its joint capacity, by 7.5% of that of A50TP. On the contrary, with the tightening torque, the average maximum load of A50TPC was slightly increased by 5.9% of that of A50TP. Meanwhile, slight improvement of 11.3% is attained by A50TTC when compared with A50TT. Nearly constant results were obtained for clamped specimens A50TPC and A50TTC, with only a 0.3% difference between them.

Figure 9 shows that improvement of joint strength is gained with the introduction of clamping pressure but with the expense of higher joint displacement especially for specimen A50TTC. All transverse specimens prematurely failed by net-tension, meanwhile shear-out failure mode was largely observed in longitudinal specimens. The former may have occurred predominantly due to very low tensile strength in transverse direction and lower w/d_b ratio. This is expected as only the $\pm 45^\circ$ fibres are resisting the load. In term of w/d_b ratio, no adjustment can be made due to dimension limitation in preparing the transverse specimens from the structural shape.

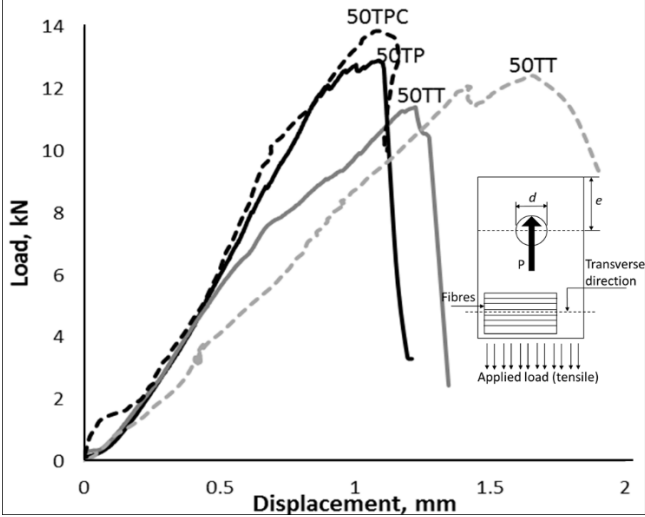


Figure 9. Load-displacement relationship of FRP bolted joints (transverse specimens)

Similar outcome is expected for 5 mm thickness specimen as it shows a comparable tensile strength in the transverse direction to the 6.5 mm thickness specimen. Thus, the

authors decided to discontinue any further testing on transverse direction and conclude the findings on threaded and clamping pressure effects.

Influence of e/d_b ratio on LP, LT, LPC and LTC

Figure 10a shows that the average maximum load attained by longitudinal specimens, LP in both group A and B increased with larger ratio of e/d_b up to 4. In group A, an increment of 4% and 14% was attained by specimen LP when the e/d_b ratio was increased from 2.5 to 3 and 4, respectively. For the same comparison, specimen BLP considerably increased its joint capacity by 12% and 43%, respectively. On the other hand, specimens A100LP and B100LP experienced a slight drop or can be considered as a constant joint strength when compared to A80LP and B80LP, respectively. A reduction of 0.8% and 28% were observed for both A100LP and B100LP, respectively. Hence, most likely the joint strength remained constant after e/d_b ratio exceeded 4. This is in agreement with some of the findings in the literatures (Eurocomp, 1996; Bank, 2006) that limits the e/d_b ratio in between 4 and 5 to characterise the bearing strength for a specific type of unidirectional pultruded composite. Similarly, for this specific pultruded FRP, when $e/d_b = 4$, the likely mode of failure is bearing and there is no appreciable gain in the joint strength after the ratio exceeded 4. Thus, $e/d_b = 5$ is intentionally excluded from further analysis in LT, LPC and LTC groups.

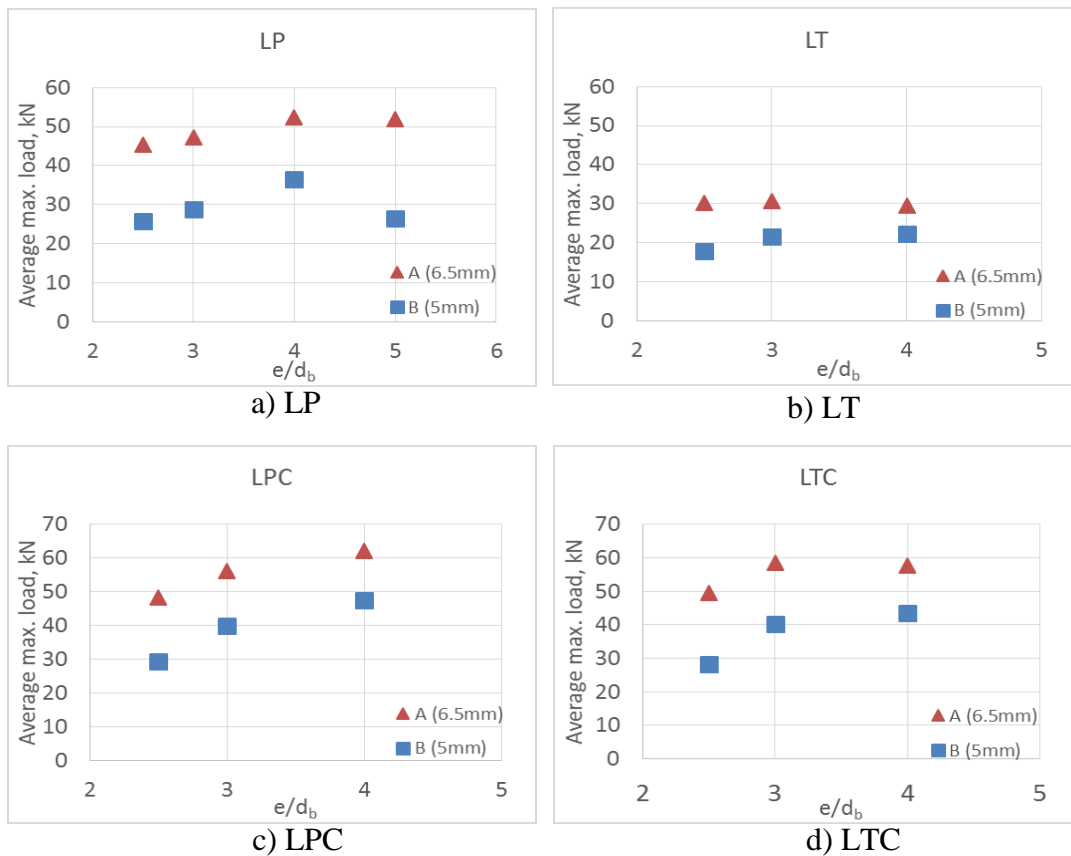


Figure 10. Comparison between group A (5 mm) and B (6.5 mm) for each parameter as e/d_b varies

As shown in Figure 10b, the joint capacity of specimens ALT and BLT with various end distances failed at average 30 kN and 20 kN, respectively. It may be observed that the e/d_b ratio has insignificant effect on the threaded joint, as the joint strength of LT group is virtually constant across the e/d_b range. Furthermore, the average maximum load attained by specimens ALPC, BLPC, ALTC and BLTC was increasing with increased e/d_b ratio. In this case, higher e/d_b ratio means that more continuous fibres are available at the end distance to provide better load carrying ability. Figure 10c shows that specimen B50LPC attained substantial improvements, almost 36% and 62% increment of joint strength when compared to specimens with $e/d_b = 3$ and 4, respectively. Meanwhile, A60LPC and A80LPC gained 16% and 28% increment of joint capacity. In Figure 10d, surprisingly, longitudinal clamping specimens with threaded bolt exhibited a promising improvement of joint capacity at higher critical end distance. However, it is important to note that, between e/d_b ratio of 3 and 4, marginal differences of joint capacity were found, whereby, only 8% increment of joint

capacity was gained by BLTC. Meanwhile, the joint capacity of ALPC remained constant.

Influence of laminate thickness

Figure 11 further demonstrates the comparison of different thickness for each parameter. It can be seen clearly that, the average maximum load of 6.5 mm thickness laminates (specimen A) was higher than 5 mm thickness laminates (specimen B) in all tested parameters. Specimen A, tested with plain bolt, exhibited an average difference of roughly 38% joint strength between e/d_b ratio of 2.5 and 4, when compared with specimen B. Meanwhile, when the joints tested with threaded bolt, thicker material provides more possibilities for bolt threads to entrench into pultruded layers. For M20 bolt with 2.5 mm pitch, it was observed that 2 and 3 threads cut through the 5 mm and 6.5 mm laminates, respectively as shown in Figure 11.

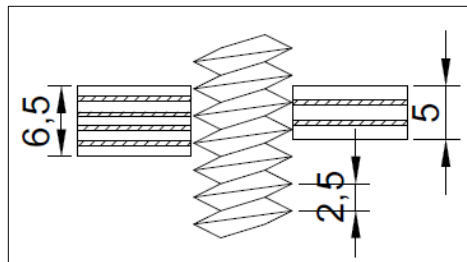


Figure 11. Bolt threads against different plate thicknesses

Despite having more threads in contact at vicinity of the joint, Figure 10b shows that the joint strength of specimen exhibited averagely 30% higher than that of specimen B. Eventually, by adding more laminas, which in turn increased the thickness of the laminate, the specimens are capable to accommodate further stresses and distribute them evenly. This outcome agrees with the research reported by Rosner and Rizkalla (1995), whereby, connection capacity increases linearly with the laminate thickness. This is consistent even with the presence of more threads at the joint contact area. Figure 10a and 10b present the comparison of joint capacity between LT and LP for both specimen group A and B, respectively. Since the presence of the threaded bolt seems to be irrelevant on the critical end distances, the 6.5 mm specimen experienced more damage due to higher strength reduction when compared to the specimen tested with plain bolt. Due to the threaded bolts, specimen ALP and specimen BLP experienced decrease in joint resistance at an average of 40% and 32%, respectively.

It may be seen that, the additional 1.5 mm thickness of the specimens, to some extent decreased the joint capacity by 8%.

Influence of bolt threads

Figure 12 presents the experimental data of 70 tested specimens in the form of comparison ratio of joint strength between the longitudinal bolt thread and longitudinal bolt plain specimens (LT/LP) across the e/d_b range of 2.5 to 4. The ratio explains the load-carrying capacity performance of different thickness of pultruded FRP bolted joint under undesirable 20 mm bolt thread effect. The higher ratio value interprets that the pultruded FRP bolted joint is less susceptible to the thread effect and vice versa. All the corresponding LT/LP ratio for specimen B were recorded higher than that of specimen A. At lower e/d_b , the corresponding LT/LP ratio is consistent at approximately 0.7. As e/d_b increases, the LT/LP for both specimens showed noticeable difference before declining at $e/d_b = 4$. Following this, the LT/LP ratio for specimen A is constricted at 0.6, which represents the lower bound of this overall observation. Therefore, it can be concluded that a ratio of 0.6 may serve as a reduction factor for FRP bolted connection design. This value is important in representing the effect of threads on bolts that causes an equivalent of 40% reduction in joint capacity of the FRP connection system.

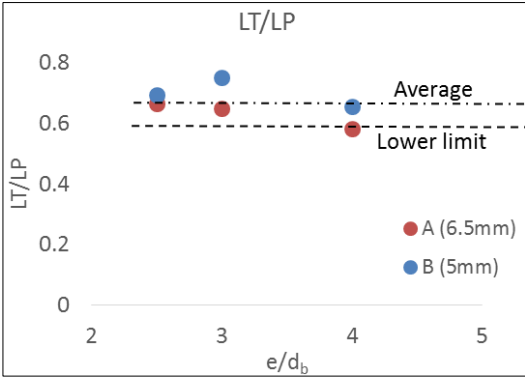


Figure 12. Corresponding LT / LP ratio.

The reduction in joint capacity as discussed above may be caused by the unevenness of contact surface between the thread and pultruded material (Ibrahim and Pettit, 2005). When the surfaces between the threaded bolt and pultruded material are subjected to a compressive load, it may initiate the separation of laminate layers due to thread embedment. Then, sufficient contact area was formed to continue to support

the load applied. However, this process may cause the thread to continuously damage the through-thickness of pultruded material and severely disrupt the stress dispersion between fibres. In addition, the thread cutting through the 45° angled fibre layers could critically damage the joint resistance more than that of unidirectional layers. On the other hand, Matharu and Mottram (2012) reported a reduction of 26% in joint strength when load is applied parallel to the pultrusion direction. It may be seen that, the key difference on the results reported is due to the pultruded stacking profile. The pultruded FRP used by Matharu and Mottram (2012) consists of unidirectional layers interspersed with a three layered (90°, ±45°) cross-stitched Continuous Fabric Mat (CFM) which improves transverse stiffness and could provide better resistance in dealing with threaded bolt. Images shown in Figure 13 were captured by scanning electron microscope (SEM) to observe the micro-failures of the contact surface area of softened zone, with and without the presence of the threaded bolt. In Figure 13a, it can be seen that, fibres were severely damaged and delaminated by the threads. A few void areas were observed which was caused by the threads indenting through the laminates. This could explain the failure development of softened zone at micro-level which resulted in a lower connection strength due to the presence of thread embedment. In comparison, Figure 13b indicates only the exposed fibres and eroded matrix after experiencing compressive stress from the bolt shank and no fibre damage is observed. Moreover, the presence of threads largely affects the hardness of contact surfaces which induced the deteriorating process on pultruded material.

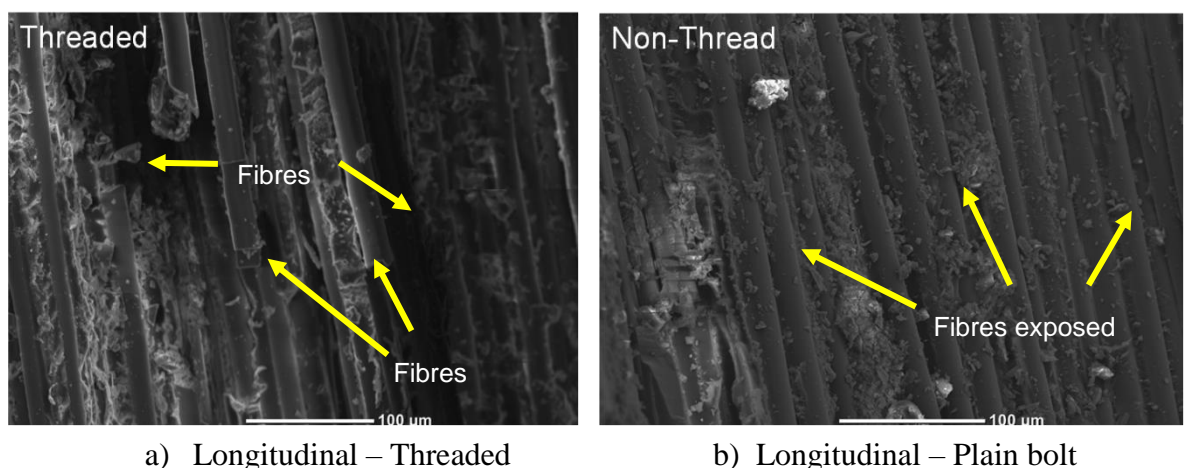


Figure 13. Failure modes observation of testing specimens using SEM.

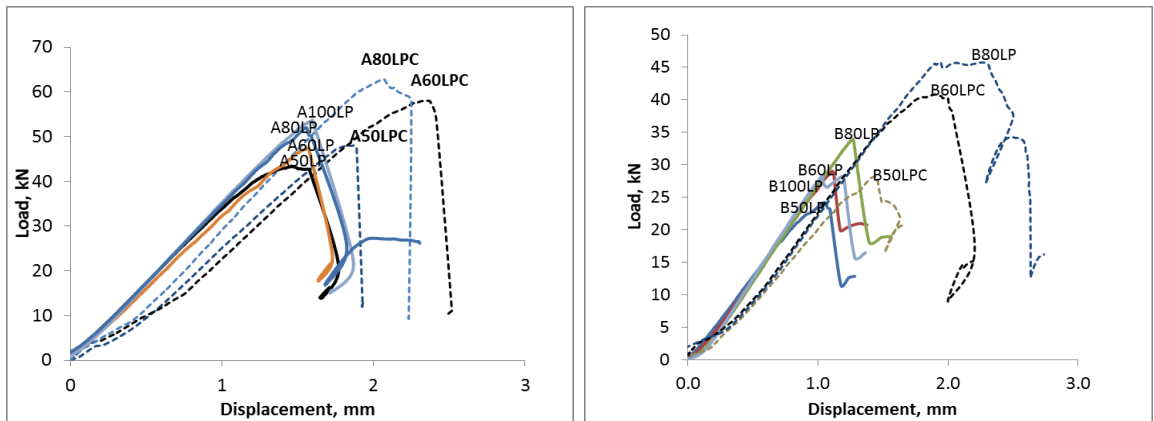
In the ASCE pre-standard (ASCE, 2010), it is noted that the bolt shank with thread should not exceed 1/3 of the thickness of pultruded plate to avoid undesirable thread effect. However, in some limitations, especially when using all threaded bolt, for this specific pultruded material under applied load in longitudinal direction, a reduction factor of 0.6 can be applied in preliminary joint design to anticipate the thread effect on the joint strength.

Influence of clamping pressure

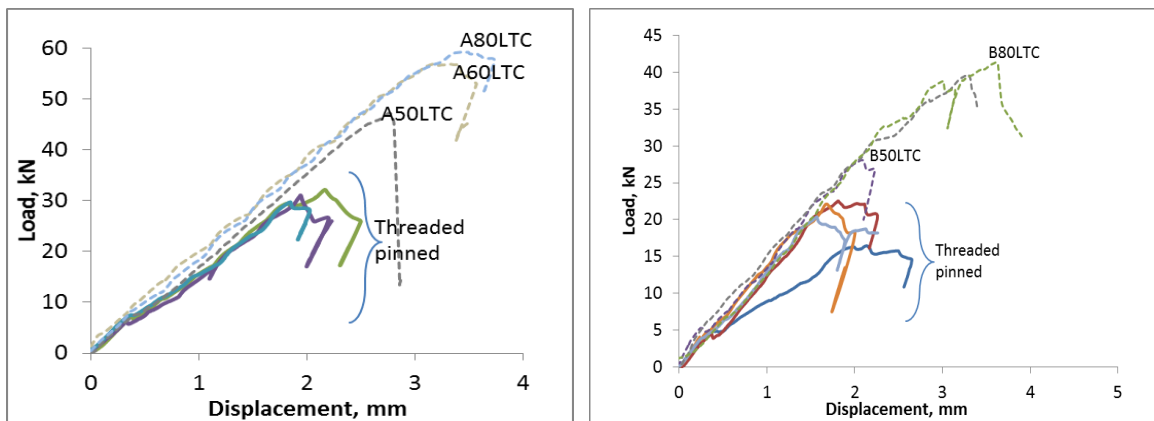
All connections with lateral restraints showed improvement of joint capacity and had altered the final failure mode to behave in a brittle manner. Based on Equation 3, the desirable axial bolt clamp force, F_p , can be estimated by dividing the applied clamping torque, T , with coefficient of friction, μ , and fastener bolt major diameter, d_b .

$$T = \mu d_b F_p \quad (3)$$

The clamping force of 8.3 kN was calculated using Equation 3 and it interacts well with the experimental results shown in Figure 14a.



a) Longitudinal plain pinned and plain clamped joint



b) Longitudinal threaded pinned and threaded clamped joint

Figure 14. Load-displacement relationship of FRP bolted joint (longitudinal specimens)

At the initial applied loading between 8 kN to 10 kN, LPCs attained less steeper slopes compared to that of LPs, and this could be due to the combined effects of pre-tensioned bolts reduction and initial slip load. At this point, the bolt may have settled on the material, together with the presence of static friction forces induced by clamping pressure. It was noticeable that, the joined laminates deform only elastically and no relative displacement between the laminates occurs. These local contacts between the fastener and pultruded material continue to induce large deformation and delamination failure near the contact edge of the hole. After reaching the peak load, sudden drop of applied load was observed as the pultruded laminates experienced final delamination failure in the direction parallel to the applied loading. Similar observation was made for LTC specimens (Figure 14b), whereby, the applied load is directly proportional to

the joint displacement until rapid failure occurred. Some identical nonlinearities or bumps across the slope were observed, which could indicate the development of threaded contact on the pultruded material. However, the 6.5 MPa clamping pressure produced by tightening torque (Figure 15) is important to retain the joint assembly. As the laminate is being pressed, this has suppressed the delamination defect progression. At the same time, it restrains the out-of-plane deformation and when the internal damage under the washer reached a critical state, a sudden incline in load response can be observed. For long-term service life issues relating to clamping pressure such as creep relaxation, a thread-locking sealant or locking nut could be used as an alternative to overcome possible nut loosening (ASCE, 2010).

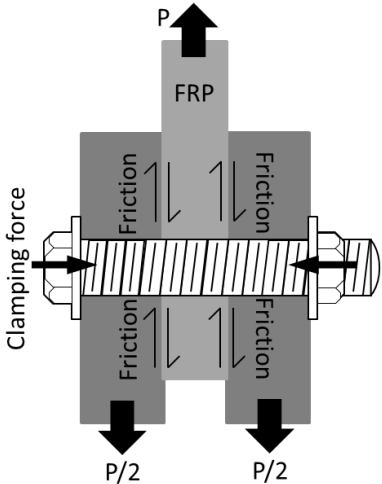


Figure 15. Clamping pressure and friction force distribution in double lap single bolted joint

Overall, the mechanically fastened joints in longitudinal specimens A and B that carry friction forces from the pre-tension of the bolt, attained almost 18% to 95% improvement in joint capacity. It eventually produced more than 50% of joint efficiency for all specimens with the addition of applied torque. When comparing LTC to LT as shown in Figure 16a, the joint capacity of both materials showed an increment almost directly proportional to e/d_b irrespective of threaded condition. At higher e/d_b , the LTC gained average 95% joint improvement to that of LT. The comparison between LTC and LPC in Figure 16b shows that, both parameters obtained comparable joint strength as e/d_b increases, with the average corresponding LTC/LPC ratio of 1.0. It seems that, with clamping force acting on the jointing material, it lessens the thread casualty effect on the pultruded composite joint. Thus, this 1.0 factor can be adopted

in the preliminary joint design whereby both threaded bolt and lateral restraint are featured in the FRP bolted connection.

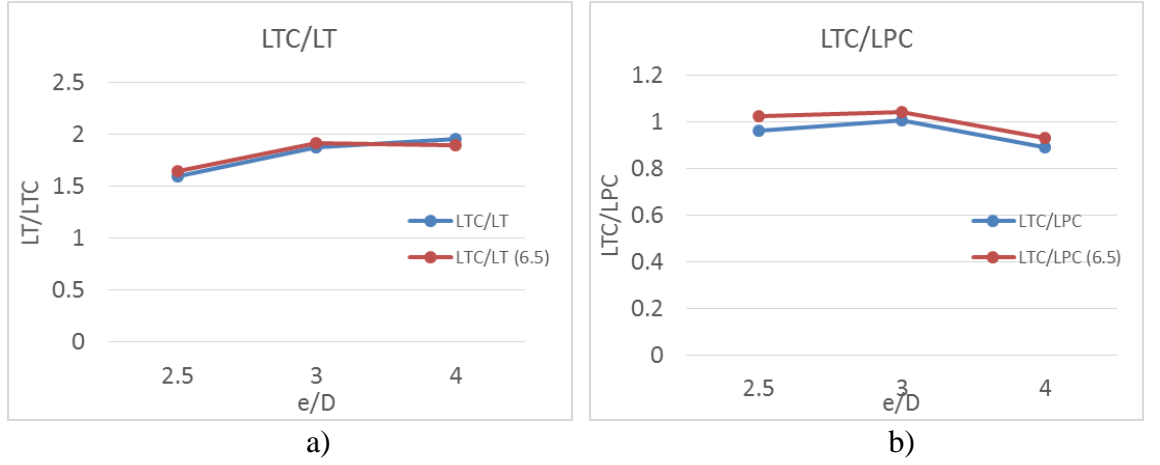


Figure 16. Comparison of LTC/LT and LTC/LPC as e/d_b varies

THEORETICAL EVALUATION OF BOLTED JOINT STRENGTH

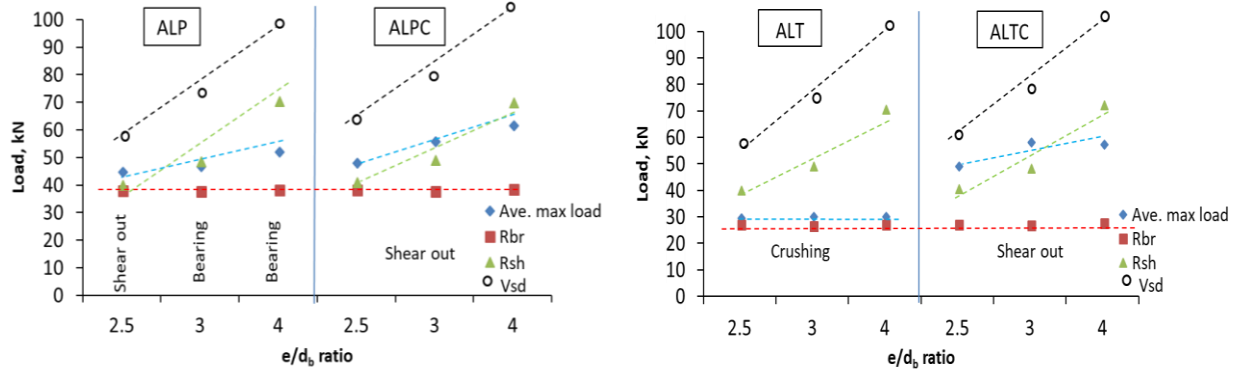
This section presents theoretical evaluation of the bolted joint strength and comparison with the experimental outcomes. This analytical approach focuses on both laminate orientations. For the longitudinal specimens, deliberate assessment especially at lower e/d_b ratio is required, where shear-out joint failure is frequently observed as a result of a bearing failure. Both longitudinal plain and longitudinal thread were analysed and its strength limit was validated based on the failure behaviour observed. Eq. 4 and Eq. 5 are evaluated to assess the bolted joint capacity under shear-out strength corresponding to the limit values suggested in the ASCE pre-standard (ASCE, 2010) and Italian CNR design guidelines (CNR, 2008).

$$R_{sh} = 1.4 \left(e_1 - \frac{d}{2} \right) t F_{sh} \quad (4)$$

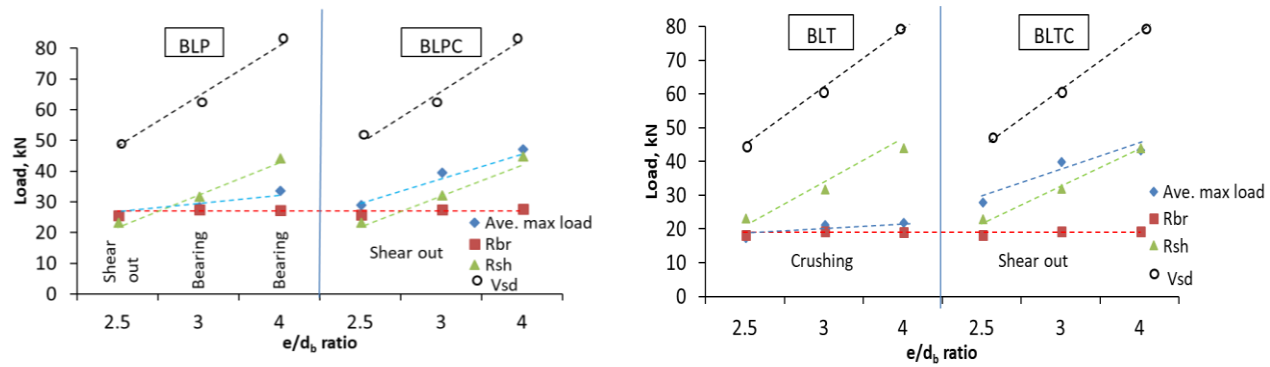
$$V_{sd} = F_{sh} (2e_1 - d) t \quad (5)$$

Where t = thickness of FRP material (mm); d = bolt hole diameter (mm); e_1 = end distance (mm); and F_{sh} = shear strength of FRP. This theoretical mechanics-based equation is a function of both joint geometry and composite material strength.

The load capacity due to pin-bearing strength, R_{br} , was calculated using Eq. 1 (similar equation also included in the Italian CNR design guidelines (CNR, 2008)). According to Matharu and Mottram (2012), the pin-bearing strength used must be the ‘lowest’ characteristic strength which accounts for all detrimental effects. Figure 17 shows the mode of failure between the theoretical evaluations and experimental results for the 6.5 mm and 5 mm thickness specimens as the e/d_b ratio increases. Overall, the comparisons are in agreement with the visual inspection findings reported in Table 6, except for the computed values from Eq. 5. This equation predicts a lesser conservative estimate of the shear-out strength limit compared to Eq. 4 which accommodates a reduction factor of 0.7. Apart from this, it is interesting to note that, with clamping pressure, it significantly alleviates the damage done by the threads by changing the mode of failure from local compression crushing to shear-out failure.



a) Failure modes for 6.5 mm specimens



b) Failure modes for 5 mm specimens

Figure 17. Failure modes comparison of longitudinal specimens using the theoretical approach

For transverse specimens, net-tension failure was observed to occur along the net section, predominantly due to very low tensile strength and unfavourable joint geometry such as low w/d_b ratios. When the strength properties of the material are exceeded, failure will occur initially at the stress concentration located at midpoint on the hole edge and will propagate towards the free edge along the net-section. The ultimate load for net-tension failure, P_u , can be obtained by the simple formulation as below:

$$P_u = F_T t (w - d) \quad (6)$$

Where F_T is the tensile strength in the transverse direction (MPa), t is the specimen thickness (mm), w is the plate width (mm) and d is the nominal bolt hole diameter (mm). Meanwhile, in Italian CNR design guidelines (CNR, 2008), the following

equation (Eq. 7) is used to assess the bolted joint capacity under net-tension failure, V_{sd} .

$$V_{sd} = \frac{1}{\gamma_{rd}} F_T (w - nd) t \quad (7)$$

This equation is almost similar to Eq. 6, with the inclusion of n , the number of holes and γ_{rd} , partial model coefficient, whereby for perforated section, it is assumed to be equal to 1.11. According to the ASCE pre-standard (ASCE, 2010), for single bolt connections, a correction factor must be used to calculate the stress concentration at the hole edge to allow for the various joint geometry. The nominal net tension strength, R_{nt} and, the stress concentration factor for a filled hole, K_{nt} shall be given by Equation (6):

$$R_{nt} = \frac{1}{K_{nt}} (w - nd) t F_T^t \quad (8)$$

$$K_{nt} = C_L \left(S_{pr} - 1.5 \frac{(S_{pr}-1)}{(S_{pr}+1)} \varphi \right) + 1 \quad (9)$$

$$\text{With } \varphi = 1.5 - 0.5 \frac{w}{e_1} \text{ for } \frac{e_1}{w} \leq 1, \quad \text{and} \quad \varphi = 1 \text{ for } \frac{e_1}{w} \geq 1$$

Where;

- t = minimum thickness of the connected component and/or member (mm)
- d = nominal hole diameter (mm)
- d_b = nominal bolt diameter (mm)
- n = number of bolts across the effective width (n = 1 a single bolt connection)
- w = plate width (mm)
- e₁ = plate end distance (mm)
- S_{pr} = w/d_b, and
- F_T^t = characteristic tensile strength in the transverse direction (MPa).

All Eq. 6, 7 and 8 are used when comparing with the experimental results of transverse specimens. Figure 18 shows that, overall, the experimental results exceeded both theoretical values except for specimen A50TT, which could be due to the presence of threaded bolt. It can be observed that, the calculated P_u and V_{sd} are in close proximity to the experimental data with an average difference of 3.8% and 3.9%, respectively.

On the other hand, with K_{nt} factor introduced in the net-tension formula (ASCE, 2010), the R_{nt} values obtained are about half the values from the experimental results and the calculated P_u and V_{sd} . The average calculated value of the stress concentration factor, K_{nt} is approximately 1.95. Based on theoretical values computed, the governing mode of failure is net-tension which agrees with the visual inspection of the transverse specimens after the testing.

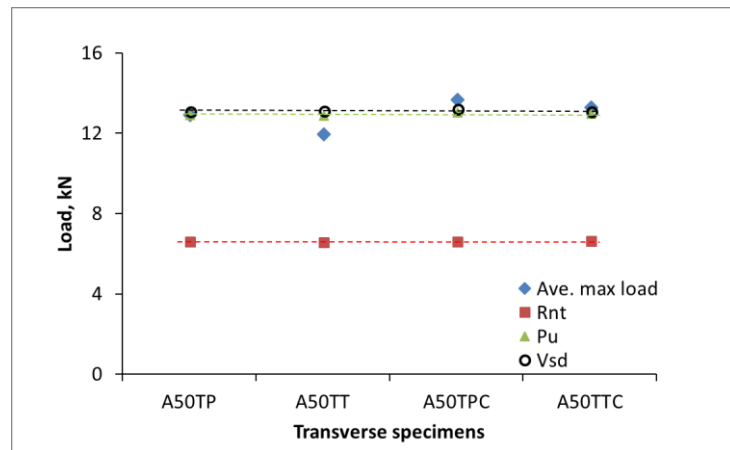


Figure 18. Net-tension failure mode comparison of transverse specimens using the theoretical approach.

CONCLUSION

An experimental investigation on the influence of M20 all threaded bolt and clamping pressure on double lap, single bolted joints of pultruded FRP materials prepared from 6.5 mm and 5 mm thick hollow section structural shapes has been described. All the 150 pultruded specimens with varied geometric ratio of e/d_b were loaded parallel to the direction of pultrusion axis and a tight fitting 20 mm diameter mechanical fastener was used. Based on the results, the following conclusions are made:

- 1) The joint strength in the longitudinal laminates with plain bolt increased for e/d_b ratio for up to 4. There is no appreciable gain in the joint strength after exceeding this ratio due to the failure mode changing from shear-out to bearing.
- 2) In contrast, as the e/d_b increases from 2.5 to 4, it has insignificant effect on the longitudinal laminate with threaded bolt and all the transverse bolted specimens as the joint strengths obtained are virtually constant.
- 3) In general, transverse bolted specimens exhibit much lower joint strength than that of longitudinal bolted specimens predominantly due to very low ultimate

tensile strength in transverse direction and unfavourable joint geometry of lower w/d_b ratio. These had influenced the cracks to propagate perpendicular to the load direction and failed in net-tension mode. Moreover, transverse bolted specimens with threaded bolt endured a significant drop in joint resistance of about 60% when compared to that of similar configuration in longitudinal direction.

- 4) The increase in laminate thickness from 5 mm to 6.5 mm increased the bolt strength by 38%. However, when dealing with threaded bolts, the thicker material provides more possibilities for bolt threads to entrench into the pultruded layers and consequently increased the damage impact on the joint capacity by 8%.
- 5) Based on the comparison ratio of joint strength between the longitudinal bolt thread and longitudinal bolt plain specimens (LT/LP), a reduction factor of 0.6 is proposed in preliminary FRP bolted connection design, where all threaded bolt is anticipated in pultruded joints. This value is important in representing the effect of threads on bolts that causes an equivalent of 40% reduction in joint capacity of the FRP connection system.
- 6) The combined effects of both the bolt threads and compressive stress at the contact zone in composite joints resulted in the deterioration and delamination of both fibres and the resin matrix. Under scanning electron microscope (SEM) observation, a few void areas were observed which was caused by the threads indenting through the laminates. This could explain the failure development of softened zone at micro-level which resulted in a lower connection strength due to the presence of thread embedment.
- 7) However, the bolted strength of pultruded composite joints with lateral restraint are less susceptible to thread effect. The damaged done by the threads had changed from vigorous fibre-matrix crushing to shear-out failure. Consequently, the lateral clamping pressure increases the strength of bolted joints for both threaded and unthreaded bolts in longitudinal specimens and exhibited more than 50% of joint efficiency when compared to unjointed specimens.
- 8) The derived mode of failures obtained from the theoretical assessment using the nominal strength approaches for both longitudinal and transverse

specimens, show very good agreement when compared to the experimental outcomes.

It is noted that the conclusions derived from this study are based on a specific type of pultruded composites and diameter of bolts considered. Further investigations on the thickness effects on threaded reduction factor, bolt diameters and its long-term outcome within an aggressive environment may be further explored.

ACKNOWLEDGEMENTS

The authors gratefully acknowledge Wagner Composite Fibre Technologies (WCFT) for the testing materials supplied. Special thanks to Mr. Mohan Trada for his kind support and technical expertise during the experimental work.

REFERENCES

- [1] L.C. Bank, J. Yin, M. Nadipelli, Local buckling of pultruded beams - nonlinearity, anisotropy and inhomogeneity, *Construction and Building Materials* 9(6) (1995) 325-331.
- [2] L.C. Bank, *Composites for Construction: Structural Design with FRP Materials*, John Wiley & Sons, Inc., New Jersey, 2006.
- [3] L.C. Hollaway, A review of the present and future utilisation of FRP composites in the civil infrastructure with reference to their important in-service properties, *Construction and Building Materials* 24(12) (2010) 2419-2445.
- [4] R.M. Hizam, A.C. Manalo, W. Karunasena, A review of FRP composite truss systems and its connections, in: C.S. Bijan Samali, Mario M. Attard (Ed.) 22nd Australasian Conference on the Mechanics of Structures and Materials, Taylor & Francis Ltd, Sydney, New South Wales, Australia, 2012.
- [5] J.T. Mottram, Design Guidance for Bolted Connections in Structures of Pultruded Shapes: Gaps in Knowledge, 17th International Conference on Composite Materials A1(6) (2009).
- [6] N.D. Hai, H. Mutsuyoshi, Structural behavior of double-lap joints of steel splice plates bolted/bonded to pultruded hybrid CFRP/GFRP laminates, *Construction and Building Materials* 30 (2012) 347-359.
- [7] L. Blaga, J.F. Dos Santos, R. Bancila, S.T. Amancio-Filho, Friction Riveting (FricRiveting) as a new joining technique in GFRP lightweight bridge construction, *Construction and Building Materials* 80 (2015) 167-179.
- [8] S. Russo, Experimental and finite element analysis of a very large pultruded FRP structure subjected to free vibration, *Composite Structures* 94 (2012) 1097-1105.
- [9] SCI, BCSA, *Joints in Steel Construction: Simple connections*, Steel Construction Institute/British Constructional Steelwork Association, 2002.
- [10] C.Cooper, G.J.Turvey, Effects of joint geometry and bolt torque on the structural performance of single bolt tension joints in pultruded GRP sheet material, *Composite Structures* 32 (1995) 217-226.

- [11] N. K.Hassan, M. A.Mohamedien, S. H.Rizkalla, Finite element analysis of bolted connections for PFRP composites, *Composites Part B: Engineering* 27B (1996) 339-349.
- [12] L.C. Bank, A.S. Mosallam, G.T. McCoy, Design and performance of connections for pultruded frame structures, *Journal of Reinforced Plastics and Composites* 13 (1994) 199-212.
- [13] Y. Xiao, T. Ishikawa, Bearing strength and failure behavior of bolted composite joints (part I: Experimental investigation), *Composites Science and Technology* 65(7-8) (2005) 1022-1031.
- [14] U.A. Khashaba, H.E.M. Sallam, A.E. Al-Shorbagy, M.A. Seif, Effect of washer size and tightening torque on the performance of bolted joints in composite structures, *Composite Structures* 73 (2006) 310-317.
- [15] T. Keller, Y. Bai, T. Vallée, Long-Term Performance of a Glass Fiber-Reinforced Polymer Truss Bridge, *Journal of Composites for Construction* 11(1) (2007).
- [16] F. Ascione, L. Feo, F. Maceri, On the pin-bearing failure load of GFRP bolted laminates: An experimental analysis on the influence of bolt diameter, *Composites Part B: Engineering* 41(6) (2010) 482-490.
- [17] Y. Bai, X. Yang, Novel joint for assembly of all-composite space truss structures: conceptual design and preliminary study, *Composites for Construction* 17(1) (2013) 130-8.
- [18] S.T.W. Lau, M.R. Said, M.Y. Yaakob, On the effect of geometrical designs and failure modes in composite axial crushing: A literature review, *Composite Structures* 94(3) (2012) 803-812.
- [19] F.J. Luo, X. Yang, Y. Bai, Member capacity of pultruded GFRP tubular profile with bolted sleeve joints for assembly of latticed structures, *Journal of Composites for Construction* 20 (2016) 1-12.
- [20] S. Russo, First investigation on mixed cracks and failure modes in multi-bolted FRP plates, *Composite Structures* 154 (2016) 17-30.
- [21] J.T. Mottram, G.J. Turvey, Physical test data for the appraisal of design procedures for bolted joints in pultruded FRP structural shapes and systems, *Progress in Structural Engineering and Materials* 5(4) (2003) 195-222.
- [22] ASCE, Pre-Standard for Load and Resistance Factor Design (LFRD) of Pultruded Fibre Reinforced Polymer (FRP) Structures, 2010.
- [23] CNR, Guide for the Design and Construction of Structures made of FRP Pultruded Elements, National Research Council of Italy, Rome, 2008.
- [24] A.M.G. Coelho, J.T. Mottram, A review of the behaviour and analysis of bolted connections and joints in pultruded fibre reinforced polymers, *Materials & Design* 74 (2015) 86-107.
- [25] J.R. Correia, Y. Bai, T. Keller, A review of the fire behaviour of pultruded GFRP structural profiles for civil engineering applications, *Composite Structures* 127 (2015) 267-287.
- [26] G.P. Terrasi, C. Affolter, M. Barbezat, Numerical Optimization of a Compact and Reusable Pretensioning Anchorage System for CFRP Tendons, *Journal of Composites for Construction* 15(2) (2011) 126.
- [27] J.W. Schmidt, A. Bennitz, B. Täljsten, P. Goltermann, H. Pedersen, Mechanical anchorage of FRP tendons – A literature review, *Construction and Building Materials* 32 (2012) 110-121.
- [28] W. Min, The finite element value simulation of composite bolt threaded nut contact and experimental study, School of Material Science and Engineering, Taiyuan University of Science and Technology, China, 2008.

- [29] R. Plastics, Pultrusion industry grows steadily in US, *Reinforced Plastics* (2002).
- [30] N.S. Matharu, J.T. Mottram, Laterally unrestrained bolt bearing strength: Plain pin and threaded values, 6th International Conference on FRP Composites in Civil Engineering, Rome, Italy, 2012.
- [31] A.S. Mosallam, *Design Guide for FRP Composite Connections*, American Society of Civil Engineers (ASCE)2011.
- [32] ASTM D3171, *Standard Test Methods for Constituent Content of Composite Materials*, American Society for Testing and Materials (ASTM) Standard, 2011.
- [33] WCFT, *Wagners Composite Fibre Technologies: Product Guide*, Wagners CFT Manufacturing Pty Ltd, Toowoomba, Australia, 2016.
- [34] AS/NZS1252:1996, *High-strength steel bolts with associated nuts and washers for structural engineering*, Standards Australia and Standards New Zealand, Australia and New Zealand, 1996.
- [35] AS/NZS1110:1995, *ISO metric precision hexagon bolts and screws.*, Standards Australia and Standards New Zealand., Australia and New Zealand, 1995.
- [36] B.Vangrimde, R.Boukhili, Analysis of the bearing response test for polymer matrix composite laminates bearing stiffness measurement and simulation, *Composite Structures* 56 (2002) 359-374.
- [37] T. Keller, N. Theodorou, A. Vassilopoulos, J. de Castro, Effect of Natural Weathering on Durability of Pultruded Glass Fiber–Reinforced Bridge and Building Structures, *Journal of Composites for Construction* 20(1) (2015) 04015025.
- [38] ASTM D953, *Standard Test Method for Bearing Strength of Plastics*, American Society for Testing and Materials (ASTM) Standard, 2010.
- [39] EN13706-2, *Reinforced plastics composites. Specifications for pultruded profiles. Method of test and general requirements.*, British Standards Institution., 2002.
- [40] J.T. Mottram, B. Zafari, Pin-bearing strengths for bolted connection in FRP structures, *Structures and Buildings* (2011).
- [41] E. Persson, I. Eriksson, L. Zackrisson, Effects of hole machining defects on strength & fatigue life of composite, *Composites Part A: Applied Science and Manufacturing* 28A (1997) 141-151.
- [42] Eurocomp, *Structural Design of Polymer Composites*, E & FN Spon, London, 1996.
- [43] ASTM D5961, *Standard Test Method for Bearing Response of Polymer Matrix Composite Laminates*, American Society for Testing and Materials (ASTM) Standard, 2006.
- [44] E.J. Guades, *Behaviour of Glass FRP Composite Tubes Under Repeated Impact for Piling Application*, Centre of Excellence in Engineered Fibre Composites, University of Southern Queensland, Queensland, Australia, 2013.
- [45] G.J. Turvey, A. Sana, Pultruded GFRP double-lap single-bolt tension joints – Temperature effects on mean and characteristic failure stresses and knock-down factors, *Composite Structures* 153 (2016) 624-631.
- [46] A.C. Manalo, H. Mutsuyoshi, Behavior of fiber-reinforced composite beams with mechanical joints., *Journal of composite materials* (0 (0)) (2011) 1-14.
- [47] B. Vangrimde, R. Boukhili, Descriptive relationships between bearing response and macroscopic damage in GRP bolted joints, *Composites Part B: Engineering* 34(7) (2003) 593-605.
- [48] N.S. Matharu, J.T. Mottram, Laterally unrestrained bolt bearing strength: Plain pin and threaded values, 1-8.

- [49] G.J. Turvey, Single-bolt tension joint tests on pultruded GRP plate: effects of the orientation of the tension direction relative to pultrusion direction, *Composite Structures* 42(4) (1998) 341-351.
- [50] Y. Wang, Bearing behaviour of joints in pultruded composites, *Journal of Composite Materials* 36(18) (2002) 2199-2216.
- [51] C.N. Rosner, S.H. Rizkalla, Bolted connections for fiber-reinforced composite structural members: analytical model and design recommendations, *Journal of Materials in Civil Engineering* 7(4) (1995) 232-238.
- [52] R.A. Ibrahim, C.L. Pettit, Uncertainties and dynamic problems of bolted joints and other fasteners, *Journal of Sound and Vibration* 279(3-5) (2005) 857-936.

4. Study on the use of mechanical inserts

4.1. Article II: Joint strength of single-bolted pultruded GFRP SHS sections with mechanical inserts under elevated temperatures

The key findings of **Article I** had provided a better understanding associated to the influence of threaded bolt with other joining parameters to anticipate its behaviour in pultruded GFRP hollow sections and to further explore against environmental durability. This paper addressed the **second objective** of this study by critically evaluating the joint performance of bolted connection pultruded GFRP using all-thread bolt under in-service elevated temperatures ranging between room temperature to 80°C. Additionally, the influence of employing inserts to the connection system was also assessed throughout the study. The filled-type connection element was installed within the hollow sections of the pultruded FRP joint configuration in two ways; tight-fit attachment without adhesive and bonded attachment using epoxy adhesive. The experimental set-up is shown in **Figure 5** of **Article II**. The experimental results showed that, under room temperature, the introduction of mechanical inserts through tight-fitting and through adhesion improved the joint load-carrying capacity by approximately 24% and 113%, respectively. Deterioration in joint strength and joint stiffness were observed for all specimens, regardless of joint configuration, when exposed to elevated temperatures. However, the use of mechanical inserts in bolted connections of pultruded GFRP hollow sections had improved the load-carrying capacity of the specimens and demonstrated adequate joint performance during serviceability. The proposed joint strength prediction equation, which incorporates the strength reduction factors and modification factors based on the different joint configurations involving mechanical insert was evaluated and compared with the experimental results. In addition, the threaded pin-bearing strength of pultruded GFRP determined in **Article I** is applied in **Equation 5** of **Article II** to incorporate the effects of threads in the joint strength evaluation. Further investigation on this type of joint configuration under different loading conditions was conducted and the results are presented, analysed, and discussed in **Article III**.

Joint strength of single-bolted pultruded GFRP square hollow sections with mechanical inserts under elevated temperatures

R.M. Hizam ¹, Allan C. Manalo ², Warna Karunasena ³ and Yu Bai ⁴

ABSTRACT

The sensitivity of the joint performance of pultruded fibre reinforced polymer (FRP) to elevated temperature has been known to limit the widespread application of FRP in civil construction. This paper addresses the study of the effect of elevated temperature and mechanical inserts on the joint strength and failure mechanism of square hollow section (SHS) of pultruded glass FRP. Three pultruded FRP bolted joint configurations were implemented, namely joint without mechanical insert (N), joint with mechanical insert with tight-fit attachment (I) and joint with mechanical insert bonded with epoxy adhesive (G). A total of sixty (60) square pultruded GFRPs with a single all threaded bolt connection was tested up to failure at room temperature, 40°C, 60°C, and 80°C. Specimen G exhibited the highest joint strength, with twice more than that of specimen N across the temperature range. Shear-out failure has been observed on specimens N and I at higher temperature mainly due to the deterioration of the interfacial bond between the fibres and its matrix. The strength reduction factor, k and modification factor, m which incorporates the increasing temperatures and the designed joint configurations showed excellent agreement when compared to the experimental results.

KEYWORDS

Pultrusion, FRP, Insert, Temperature, Failure modes, Bolted, Box section, Connection.

¹PhD Candidate, Centre of Future Materials, Faculty of Health, Engineering and Sciences, University Southern Queensland, QLD 4350, Australia.

E-mail: mohammadhizamshah.rusmi@usq.edu.au

²Associate Professor, Centre of Future Materials, Faculty of Health, Engineering and Sciences, University Southern Queensland, QLD 4350, Australia.

E-mail: allan.manalo@usq.edu.au

³Professor, Centre of Future Materials, Faculty of Health, Engineering and Sciences, University Southern Queensland, QLD 4350, Australia.

E-mail: karu.karunasena@usq.edu.au

⁴Senior Lecturer, Department of Civil Engineering, Monash University, Clayton, VIC 3800, Australia.

E-mail: yu.bai@monash.edu.au

INTRODUCTION

Pultruded fibre reinforced polymer (FRP) composites has been the subject of several research studies and its breakthrough came in the early 1990's (Turvey and Wang, 2007; Hollaway, 2010). It has gained wide recognition from design engineers for a number of factors including its ability to tailor its structural performance, high axial resistance and its high resistance to aggressive environment. It is also significantly lightweight when compared to conventional materials and promotes quick installation time. Presently, pultrusion is the more preferred method compared to other methods in manufacturing FRP cross sections similar to steel profiles, for instance square and rectangular hollow sections, angle, standard I-beam and channel (Qureshi and Mottram, 2015). Meanwhile, glass fibre is one of the most common fibres used in the construction industry as it is relatively economical compared to other fibres such as carbon, aramid, and basalt (Manalo et al., 2017a). Despite its successful applications in several infrastructure projects, there are still a considerable resistance in the widespread use of pultruded FRP in civil engineering and construction.

Generally, the mechanical properties of pultruded FRP are more sensitive to temperature compared to steel and the sensitivity of the properties is further complicated by the lack of understanding on its joint performance. Many earlier

studies on connection of pultruded components were done based on the concepts widely used in steel industry (Bank, 2006; Mottram, 2009; Mosallam, 2011) and the three common techniques used are bolted joint, adhesively bonded and a combination of both (Hizam et al., 2012). Other ways to connect components in steel construction such as single-plate or welded connection are not yet practical for pultruded FRP sections. Some innovative concepts for connecting pultruded members have been developed to fully benefit the improved strength and stiffness provided by the closed section in pultruded composite structures. Early work on this matter, was carried out by Bank et al. (1994), whereby they had designed an improved wrapped angle connection for pultruded frame structures, while Singamsethi et al. (2005) had established monolithic cuff connections that can be easily attached to pultruded box members using epoxy adhesive to create a simple beam-cuff-column frame. Pfeil et al. (2009) had developed a new connection concept for dismountable bridge by adopting pre-stressing steel tendons inserted into tubular fibre section that could prevent tension forces during its service life. On the other hand, Bai and Yang (2013) had introduced a novel connector using pultruded glass FRP (GFRP) box profiles. By using simplified finite element modelling, the authors found that the configuration of space truss made up of pultruded GFRP can provide satisfactory structural stiffness at the structural level. Through-bolt connection is one of the alternatives when employing a hollow material type as a structural component, and with elements such as bolted sleeve and steel insert, mechanical improvements were observed by Luo et al. (2016b) and Mara et al. (2016) respectively. Most recently, Zhang et al. (2018b) had presented an innovative bonded sleeve connector made from a steel tube that can be inserted at the vicinity of the joint area of hollow GFRP beam-column. Under static loading, this type of jointing method with sufficient bond length managed to achieve a ductile failure through yielding of the steel endplate. Further study on this bonded sleeve GFRP beam-column connection under cyclic loading has been carried out by Zhang et al. (2018a) whereby rotational stiffness, moment and rotation capacity, and local strain responses are investigated. The results obtained from both experimental and finite element analysis showed a successful development of bonded sleeve connection by attaining an excellent ductility and energy dissipation capacity prior to the final connection failure.

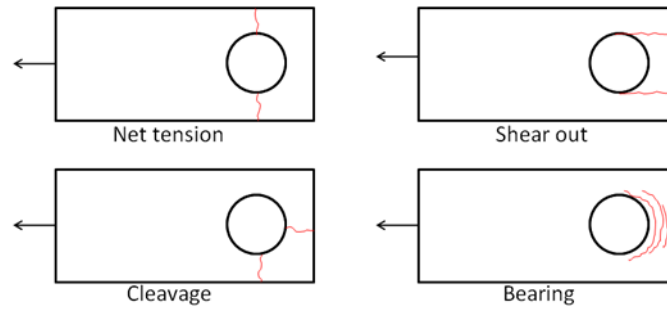


Fig. 1. Failure modes in FRP connection

Based on the extensive studies focusing on FRP bolted lap joints (S.Ramakrishna et al., 1995; Ibrahim and Pettit, 2005; Xiao and Ishikawa, 2005a; Lau et al., 2012) four (4) common mode of failures have been identified which are bearing, shear-out, cleavage, and net-tension (Fig. 1). Combination of these failure modes are also possible to occur. Unlike steel connections, fastening parameters such as geometry (width, spacing, end distance, etc), joint type, plate thickness, clamping force, hole tolerance and loading condition are among the important parameters to be considered when designing FRP bolted connection (Eurocomp, 1996; CNR, 2008; ASCE, 2010). Besides bolted connection, adhesive bonded shows promising potential as a connector for pultruded FRP. It can transmit forces and moments continuously between FRP structures and avoid fibres breakage and stress concentrated due to presence of bolt holes (Zhang and Keller, 2008; Keller and Vallée, 2005). Alternatively, a combination of both bolting and adhesive bonding is capable to provide excellent connection performance as reported by (Manalo and Mutsuyoshi, 2011).

Inadequacy of information in joint design related to critical condition of service and its behaviour under variable environmental conditions partially contributes to the moderate coverage of its practice. Further research on the developed connections system is required especially in serviceability aspects in order to widen its applications. In many practical applications, the connection behaviour under service environments such as moisture, fatigue, and elevated temperatures is of great concern (Correia et al., 2015). One example is that the pultruded materials deployed as structural components and its connection must be able to withstand elevated temperatures while maintaining structural integrity. Owing to the different influences on the fibre and matrix, the failure mechanism seems to become non-linear and therefore rather complex. Due to the viscoelastic behaviour of polymer matrix in many composites, the physical

properties of the composite can change drastically over relatively small changes in temperature (Fig. 2). As the temperature increases, the matrix binding the fibres soften and eventually, the FRP composites may collapse as it further degrades when the glass transition temperature (T_g) is reached. This compromises the structural functionality of the material (Mouritz and Gibson, 2010)

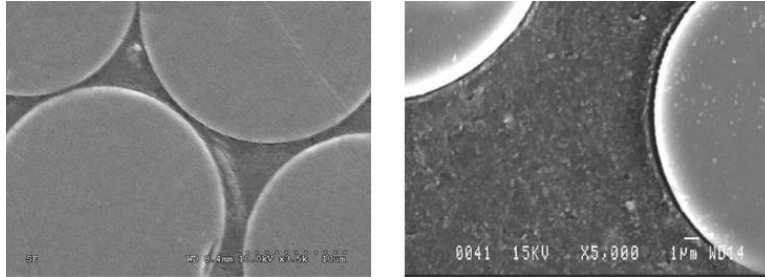


Fig. 2. Fibre/matrix interface for glass FRP bar aged in air at 80 °C for 2 hours (Mathieu et al. 2010)

Several studies have attempted to understand the effects of elevated temperature on the physical and mechanical properties of pultruded FRP. It was concluded by Manalo et al. (2017b) that the strength, stiffness and fibre/matrix interfacial bonding of the composite decreased with increased temperatures. The authors found that transversely cut glass FRP is affected more by the increase in temperature than the longitudinally cut specimens (along the direction of pultrusion). Similarly, Bai et al. (2008) observed that the elastic modulus of pultruded GFRP composites cut longitudinally is different from those cut transversely. Importantly, this type of composite suffers higher thermal degradation of shear and compressive strengths, as these properties are more influenced by the resin than the fibres, when compared to tensile strength (Correia et al., 2015). Therefore, from these findings, it can be highlighted that the arrangement of the FRP components and the direction of loading are critical factors in thermal failure for pultruded FRP and this will contribute to the complexity of its joint performance at elevated temperatures. This was demonstrated by Turvey and Wang (2009) using Taguchi analysis of joint test data on pultruded FRP with a connection system of double-lap single-bolt tension joints. The study attempted to quantify the degrading effects of bolt/hole clearance, angle between the tension and pultrusion directions, elevated temperature and water immersion period on the failure loads of the joints and it was found that temperature was the most dominant factor. Further to

this, it was observed that the effects of test temperature and joint geometry, in this case is the end distance to bolt hole diameter ratios (e/d_b), resulted in various failure modes (dominantly shear, tension, cleavage and bearing) depending on the combination of the two factors (Turvey and Sana, 2016).

In this study, all-thread single-bolted connection is employed in square hollow section (SHS) pultruded GFRP and the specimens were tested under tensile loading at elevated in-service temperatures. The use of threaded steel bolts for connection cannot be eliminated in heavy construction for instance industrial cooling towers and bridges, as it speeds up the construction process while minimising installation errors. However, application of threaded bolt in joining pultruded composites are restricted in design and based on the previous work by the authors, a reduction factor that account the bolt threads effect should be introduced in the preliminary FRP bolted design (Hizam et al., 2018). Tensile test was conducted to evaluate the joint performance of this specimens as this condition is deemed more critical. Under compression forces, the FRP joints are less sensitive to the joint geometries and can generally sustain higher loading than when subjected to tensile forces (Mosallam, 2011). The selection of hollow profile structures is a better option for pultruded GFRP as it can provide better torsional rigidity, relatively capable to transfer high load and improve its weak axis strength and stiffness (Smith et al., 1998; DG9, 2004). Aiming to take advantage of those properties especially high axial resistance, this joint configuration of pultruded tubular section can be adopted as truss components (such as bottom and top chord members) in all-composite bridge systems. Despite their advantageous characteristics, the joint performance associated with pultruded hollow section was poor in term of localised load application (McCormick, 1999) and will be further analysed in this paper.

This shows advancement in knowledge on effective connection method is a critical issue here (Pfeil et al., 2009; Ibrahim and Pettit, 2005) especially under elevated temperatures. Additionally, to deal with those deficiencies in hollow joint, mechanical inserts are proposed at the vicinity of the joint area. This introduction of filled-type connection element is anticipated to further improve the compressive strength at the bearing connection. Thus, this paper focuses mainly on the effect of mechanical insert

on the joint strength of through-bolt SHS pultruded GFRP under elevated temperatures and its failure behaviours are thoroughly investigated.

EXPERIMENTAL PROGRAM

Material Properties

Table 1 presents the mechanical properties determined through GFRP coupon specimens from 125 mm x 125 mm x 6.5 mm pultruded square hollow sections (SHS). These pultruded GFRP tubular profiles were supplied and manufactured by Wagner's Composite Fibre Technologies (WCFT) in Toowoomba, Australia. In the pultrusion process, multi-directional of glass fibres are pulled through a bath of vinyl ester resin, then through a heated die that provides the shape of the SHS cross-section to the final product. This WCFT composite material consists of high volume, symmetrical layers of fibres, in long continuous uni-direction (0°), contributing to the material's high tensile strength and elastic modulus. Meanwhile, the reinforcement from continuous stitch fabrics ($\pm 45^\circ$) has improved its transverse strength. From the burn-out test following ASTM D3171 (ASTMD3171, 2011), the amount of fibres in this composite material is 78% by weight.

Table 1. Mechanical properties of 125 mm x 125 mm x 6.5 mm

Properties	6.5 mm plate	Test method
Tensile Long ^a , Peak stress (MPa)	741.53 (44.91) ^c	
Tensile Long, Elastic modulus (MPa)	42,983 (1257)	ASTM D638
Tensile Trans ^b , Peak stress (MPa)	66.41 (3.78)	
Tensile Trans, Elastic modulus (MPa)	13,350 (2,131.06)	
Compressive Long, Peak stress (MPa)	514.86 (15.27)	ASTM D695
Compressive Trans, Peak stress (MPa)	161.66 (6.76)	
In-plane shear Long, Peak stress (MPa)	113.60 (6.85)	ASTM D5379
In-plane shear Trans, Peak stress (MPa)	95.30 (4.72)	
Pin-bearing (Plain), Peak stress (MPa)	291.44 (7.72)	ASTM D953
Pin-bearing (Thread), Peak stress (MPa)	207.68 (11.08)	
Glass transition temperature (T _g) ^d	115.61°C	ASTM E1356

^aLongitudinal ^bTransverse ^cStandard deviation ^dManalo et al. 2017

Mechanical Insert

An insert is part of a detachable fixation device, which enables the connection between other structural parts. The mechanical connection is achieved through the hollow part of the insert, which in most cases is threaded but can also be an unthreaded clearance hole for a through-the-thickness type insert (ECSS, 2011). The load transfer is achieved via the contribution of various structural elements. Although inserts have been widely used in the aerospace industry, little result has been published for civil construction (Humphreys, 2003). The mechanical insert (Fig. 3) or so-called anti-crush insert are available with bolt hole diameters of 14, 18, 22 and 26 mm. Since it is difficult to position the insert exactly at the point at which it is needed for connection purposes, a margin of 2 mm of hole diameter is required for any misalignment.

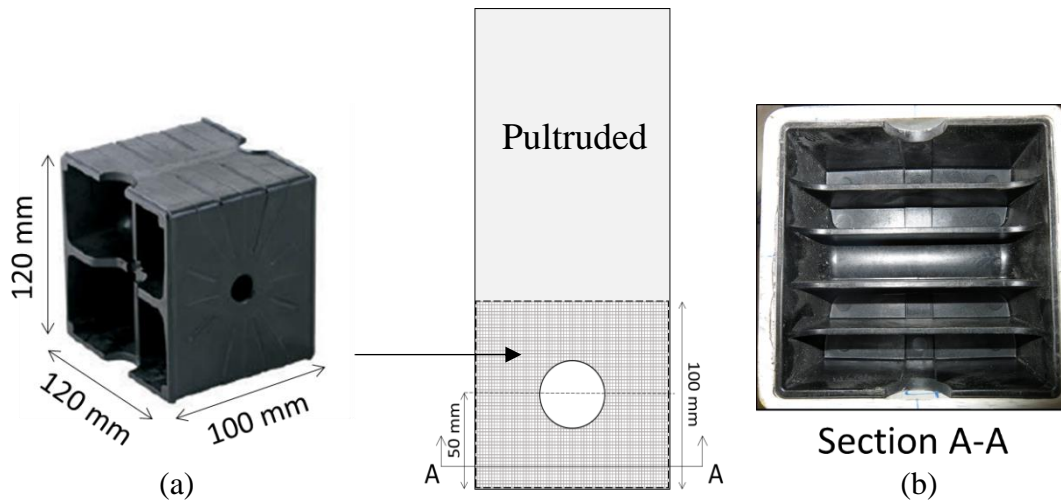


Fig. 3. (a) Anti-crush insert (WCFT 2016) (b) Insert filled pultruded GFRP

For this reason, mechanical insert of 22 mm hole diameter is used for 20 mm bolt diameter. The mechanical insert is made from moulded thermoplastic alloy (TPA) filled with approximately 49.35% of short glass fibres, determined in accordance with the ISO 1172 (ISO1172, 1996). Following the ASTM E1356 (ASTME1356-08, 2014), the glass transition temperature, T_g was determined by differential scanning calorimetry (DSC) using the TA instrument model Q100C. Small samples were precisely cut from the moulded WCFT insert to fittingly well in a small DSC aluminium pan. The analysis took scans from room temperature up to 250°C by having a heating rate of 10°C/ min. Based on the results computed by TA Universal Analysis software, the average T_g for the mechanical insert was obtained at value of 99.35°C.

Adhesive material (Epoxy adhesive)

The epoxy adhesive namely Techniglu-HP R26 supplied by ATL Composites Pty. Ltd. is used to provide a connection between the mechanical insert and the surrounding pultruded GFRP walls. The adhesive is primarily important to ensure a proper shear load transfer from the insert to the surrounding pultruded GFRP walls in order to gain maximum strength. Table 2 presents the related mechanical properties of adhesive used in this study. Following the ASTM E1356 (ASTME1356-08, 2014) with similar testing parameters used for insert, the average T_g of the epoxy adhesive using DSC analysis was determined as 99.17°C.

Table 2. WCFT adhesive properties (WCFT 2016)

Properties	Value	Test method
Tensile strength (f_t)	34.1 MPa	ISO 527-2
Tensile modulus (E_t)	2409 MPa	ISO 527-2
Lap shear strength (f_v)	11.9 MPa	ASTM D3163
Heat deflection temperature (HDT)	85°C	ISO 75-1

Notes:

1. The values in the table are based on a cure schedule of 24 hrs at ambient and 8 hrs at 80 °C.
2. The values in the table are the design values to be used in normal ambient conditions. It does not include adjustment factors to account for temperature, humidity and chemical environments.

All-thread bolt

The stainless steel (SS) bolts used for pultruded GFRP box section is a high strength all-thread structural bolts in accordance to Australian standard AS 1252:1996 (AS/NZS1252:1996, 1996b) and AS 1110:1995 (AS/NZS1110:1995, 1995). The Steel Construction Institute (SCI and BCSCA, 2002) indicated that M20 x 60 mm long grade 8.8 all-threaded bolts are used for 90% of the connections in a typical multi-storey steel frame. For practical use, this specific type and diameter of bolt was used in this study. By standardising the size and the grade of all-thread bolts, it will lead into simple connection fabrications which eventually reduce the workmanship costs. Table 3 shows the properties of the bolt strength property class 8.8.

Table 3. Bolt types and its mechanical properties

Items	Specification
Property class:	8.8
Material type:	Stainless steel S316
Diameter of bolt, D:	20 mm (M20)
Nominal shank area:	314 mm ²
Area of root of thread:	225 mm ²
Minor diameter, D _c :	19.67 mm
Pitch, P mm:	2.50 mm
Minimum tensile strength:	830 MPa

Items	Specification
Proof strength:	600 MPa
Minimum yield strength:	660 MPa
Minimum shear stress ^a :	514.6 MPa
Min. breaking load in single shear (Shank):	163 kN
Min. breaking load in single shear (Thread):	117 kN
Minimum bolt tension ^b :	145 kN

^aUltimate shear stress equals 62% of ultimate tensile strength ^bFull tightening

Specimen preparation

A total of sixty (60) SHS pultruded GFRP profile with nominal dimension of 125 mm x 125 mm x 6.5 mm, 345 mm length were prepared with approximately 20 mm nominal bolt hole diameter at the end of face 2 and face 4 (refer Fig. 4). These holes were drilled using diamond coated drilled to ensure the accuracy of bolt holes and to avoid fibre damage (Persson et al., 1997). Table 4 presents the geometric parameters for lap joint bolted connection which were selected as per recommendations by Bank (2006).

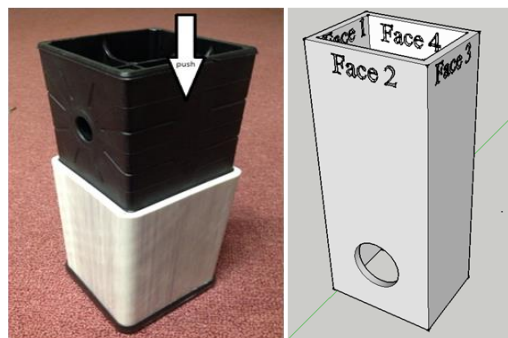


Fig. 4. Pultruded glass FRP with mechanical insert and bolt holes location

Table 4. Recommended geometric parameters for lap joint connections

Parameters	Bank, 2006	Test specimen geometry
End Distance to bolt diameter, e/d_b	2	2.5
Plate width to bolt diameter, w/d_b	3	5.5
Bolt diameter to plate thickness, d_b/t_{pl}	0.5	3
Washer diameter to bolt diameter, d_w/d_b	2	2
Hole size clearance (mm) ^a	1.6 mm	0.5-0.55 mm

^aMaximum clearance

The test specimens were designed to fail by bearing failure in the pultruded base material in the longitudinal direction. Bearing failure is preferable in this preliminary test due to its progressive nature and it can sustain post-failure loads beyond the ultimate load (Xiao and Ishikawa, 2005b). For the mechanical fastener part, M20 stainless steel (SS) 316 through bolts (all threaded) with 215 mm length was deployed in pin-bearing manner (no lateral restrained). However, SS nuts were placed at the both ends of the through bolt for safety purposes.

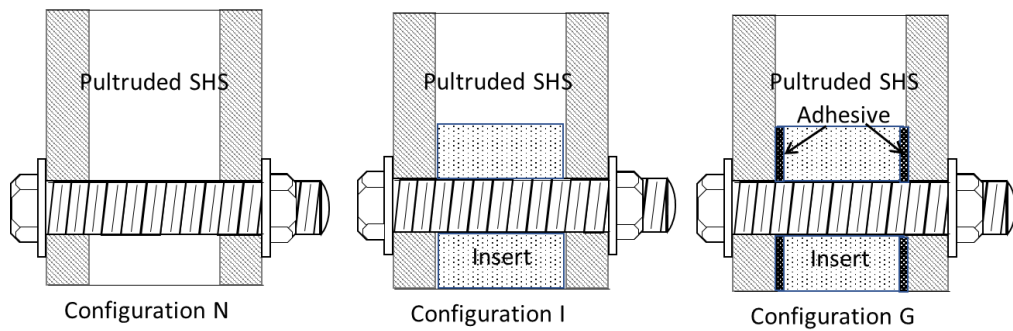


Fig. 5. Illustration of the single-bolted joint configurations (cross-section view)

In this test, twenty (20) square pultruded GFRP were allocated for each experimental model as illustrated in Figure 5, namely pultruded GFRP with no insert (N), pultruded GFRP with tight-fit insert (I) and pultruded GFRP with adhesively bonded insert (G). Figure 4 illustrates how the mechanical insert was placed inside the SHS pultruded in the vicinity of the bolt-holes. The installation was done in industry using special equipment which is capable in pushing the insert inside the square pultruded GFRP

member to produce a tight-fit attachment. Meanwhile, for specimen G, epoxy adhesive was injected to fill the spaces in between the insert and SHS pultruded GFRP thin-walled. When evaluating the durability of FRP, many researchers (Bakis et al., 1998; Mathieu et al., 2010; Garrido et al., 2015) have used a wide range of temperatures to understand how the material reacts in certain exposure conditions. Turvey and Sana (2016) had selected the temperature range for their experimental work based on the recommendation from *EXTREN fibreglass design manual* which stated that the pultruded GFRP working temperature should not be above 65°C. However, the Queensland’s Department of Transport and Main Roads (TMR, 2014) has specified that the maximum allowable temperature for a bridge construction and other related structures in outdoor environment shall be 68°C. Based on this, the testing temperatures for this research work were set at room temperature (23°C), 40°C, 60°C and 80°C and are presented by the notations RT, 40, 60, and 80, respectively. The first three temperatures were selected below the recommended maximum temperature by TMR (2014) to simulate varying summer conditions. Testing at 80°C is conducted to observe any substantial decrease in joint failure loads and its failure mode behaviour when the materials are exposed above the recommended temperature of 68°C. Table 5 summarised the specimen groups and number of specimens allocated for testing. For example, the specimen G-40 is a square pultruded GFRP section with adhesively bonded insert and tested at 40°C.

Table 5. Summary of SHS pultruded GFRP specimens

Group of specimens	Joint configuration	Test temperatures (°C)	No. of specimens
N	Single threaded bolt	RT (23)	5
		40	5
		60	5
		80	5
I	Single threaded bolt and tight-fit insert	RT (23)	5
		40	5
		60	5
		80	5
G	Single threaded bolt and adhesively bonded insert	RT (23)	5
		40	5
		60	5
		80	5

Note: RT = room temperature or ambient temperature.

Experimental setup and instrumentation

The specimens were tested up to failure under axial (tensile) loading using a 220 kN capacity testing machine. The experimental setup is shown in Figure 6 (a). The specimen was mounted at both ends using special fabricated test fixtures and threaded bolts (Fig. 6 (b)). Two approximately 20 mm hole diameters were drilled in line at the upper part of the specimens and both joint vicinities were filled with the inserts.

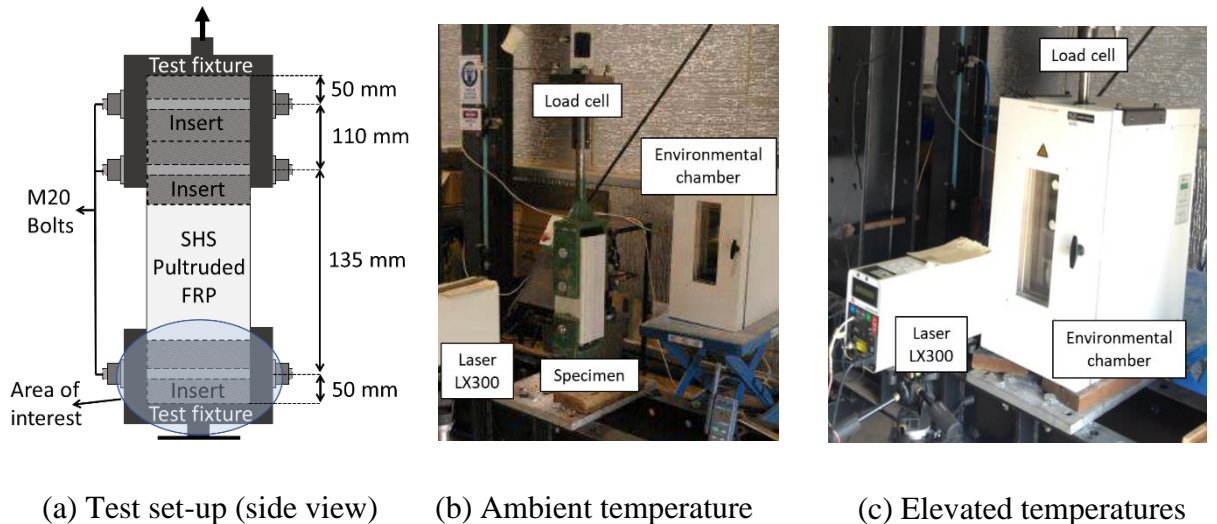


Fig. 6. Pultruded GFRP bolted joint test set-up

It was designed to provide stronger fixed connection to ensure the failures are shifted to occur only at the lower end of the fixture. The upper end test fixture was anchored to the load cell of the testing machine to measure the applied load while the bottom was tightly secured to resist any movement. A calibrated contactless MTS LX300 laser extensometer was used to measure the hole elongation. The LX measures the joint's displacement (hole elongation) by detecting the reflective tape markings positioned under the head bolt (with a 30 mm gauge length). For the elevated temperature testing (Fig. 6 (c)), the specimens were conditioned for 30 mins in Instron 3119-408 environmental chamber in order to achieve the required test temperature prior applying the tensile loading. Data logger (System 5000) was used to record the load applied. The failure modes of each specimen were observed during the loading and after the test had been completed.

RESULTS AND DISCUSSION

Table 6 shows a summary of the experimental results of SHS pultruded GFRP with different joint configurations consisting of mechanical insert under elevated temperature. The results are presented in term of the average maximum load and its corresponding hole elongation.

Table 6. Summary of experimental results

Specimen	Ave. max. load (kN)	Std* (kN)	Ave. elongation (mm)	Std (mm)	Ave. bearing Stress (MPa)	Std (MPa)	Ave. joint stiffness (kN/mm)	Std (kN/mm)
N-RT	56.47	1.86	6.30	0.51	215.56	6.72	8.84	0.76
N-40	45.09	8.77	6.68	0.77	175.22	33.59	6.76	1.19
N-60	42.56	3.39	6.84	0.45	165.46	13.24	6.25	0.76
N-80	38.86	0.55	6.73	0.75	151.14	2.21	5.83	0.69
I-RT	70.11	6.00	4.63	0.94	272.61	23.44	15.47	2.34
I-40	62.80	0.24	5.07	0.49	244.29	13.87	12.48	1.33
I-60	62.24	0.24	6.25	0.92	242.12	7.06	10.16	1.62
I-80	54.20	0.19	5.77	0.61	191.41	38.92	9.49	1.35
G-RT	108.52	8.31	2.84	0.28	421.12	31.31	37.23	3.65
G-40	105.23	0.40	3.81	0.97	404.73	38.77	28.79	6.02
G-60	91.96	0.36	4.38	0.39	357.69	21.42	21.15	2.58
G-80	82.88	0.32	5.03	1.27	321.93	21.17	17.15	3.44

Note: Std = Standard deviation; Ave = average; max = maximum.

The average bearing stress is calculated by dividing the average maximum load to the mean cross-sectional area. Whereas, the average joint stiffness is calculated by dividing the average maximum load to the mean hole elongation of the five nominally identical joints.

At room temperature, the lowest average load of 56.47 kN was attained by the control specimen N-RT, with an average elongation of 6.30 mm. Other experimental models,

specimen I and G, produced higher connection strength of 70.11 kN and 108.52 kN, respectively. Table 6 shows that, the average elongation of the test joints at room temperature are consistently lower than those of the joints tested at higher temperatures. Additionally, it shows that specimens I-RT and G-RT obtained lesser elongation at the bolt hole when compared to specimen N-RT, with 4.63 mm and 2.84 mm, respectively. It can be noted that, specimen G exhibited higher average maximum joint load across the temperature range when compared to specimen N and I while, specimen I constantly ranked in between specimen N and G. As the temperature increases, it appears that the average maximum loads and bearing stresses decreases. Specimen I recorded the highest joint strength improvement of 46% relative to N at 60°C. Meanwhile, specimen G exhibited the highest joint strength improvement relative to N at 40°C by 133%. At the highest test temperature of 80°C, all specimen N, I and G experienced their lowest joint capacity of 38.8 kN, 54.2 kN, and 82.8 kN, respectively. It should be noted that, marginal declined of average maximum load between 40°C and 60°C was observed throughout all specimen models. Overall, the bolted joint strength showed fair improvement of joint capacity with the presence of insert in the interior of SHS. Further development of joint resistance can be observed evidently with the addition of epoxy adhesive around the mechanical insert.

Whereas, to assess the joint performance of each configuration at room temperature, the joint efficiency (defined as the ratio of ultimate joint strength to ultimate strength of unjointed pultruded material) was determined. This evaluation represents the design effectiveness of each bolted joint configuration with reference to the performance of the same pultruded section without connections. Therefore, it was calculated that specimens N and I showed 31% and 37% efficiency, respectively, whereas specimen G showed 60% efficiency when compared to corresponding sections without connection. Due to the effect of bolt thread, similar joint efficiency for specimen N was obtained in a previous study by the authors (Hizam et al., 2018). Meanwhile, the higher joint efficiency attained by specimen G was expected due to the presence of the adhesively bonded insert in the vicinity of the jointing area. Nonetheless, the pultruded GFRP box section single-bolt connection is vulnerable to a decrease in strength and stiffness as temperature increases. From the authors' previous findings on the degradation of flexural strength of similar pultruded FRP material under elevated temperatures (Manalo et al., 2017b), it is expected that the loss in mechanical

properties of the material will adversely impact the joint efficiency of its connection system. Hence, the effect of elevated temperature, effect of mechanical insert with and without adhesives and its failure mechanism are discussed in detail in the following sections.

Load vs Hole elongation response

The deformation behaviours of specimens N and I at room temperature (Fig. 7 (a)) show that, at the early stage of load application, the curves increased linearly, followed by various degrees of knees up to the peaks. Post-peaks show that the specimens continued to sustain load but suffer large deformation until failure. A similar curve pattern was observed in Figure 7 (b), (c) and (d), however at elevated temperature, the behaviour of the tested specimens gradually changed. Generally, the curves for each specimen exhibited lower stiffness at the linear phase, then continued with extended non-linear responses over elongation before attaining lower peak loads.

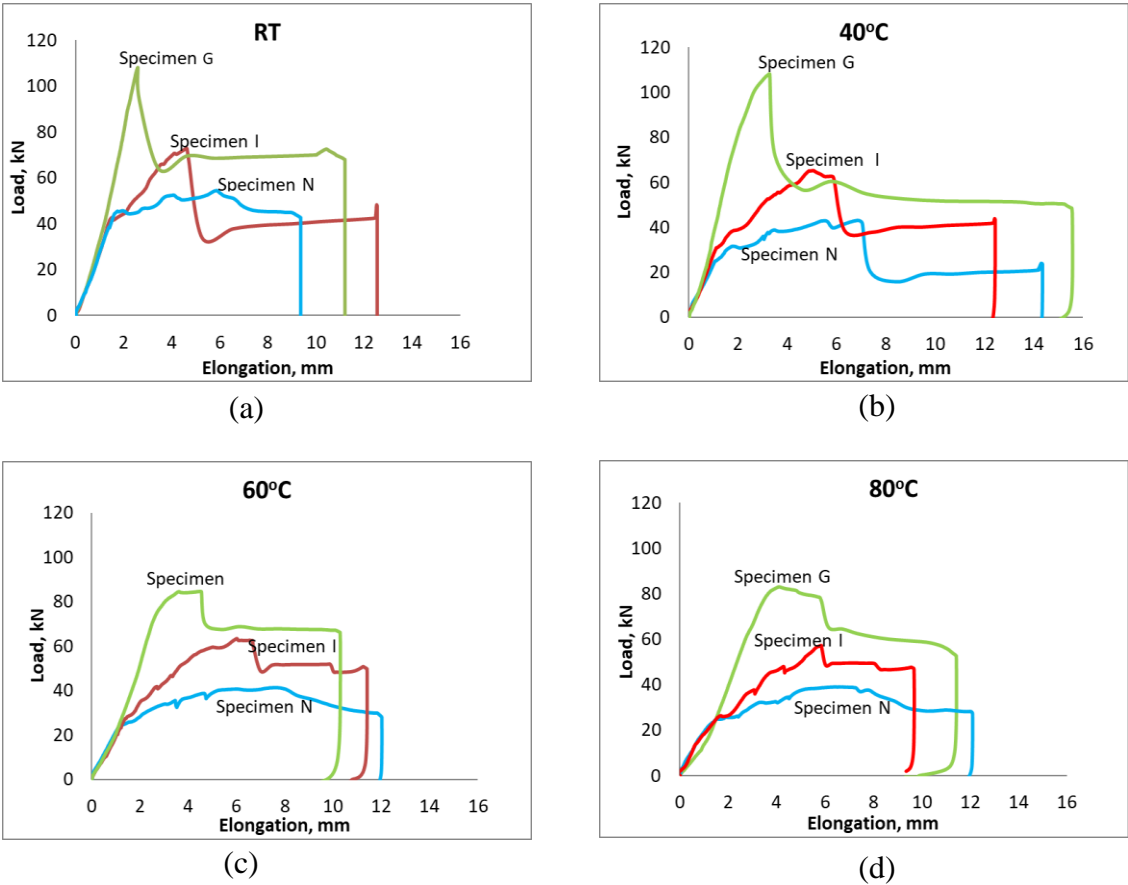


Fig. 7. Load vs hole elongation across temperature range

Interestingly, specimens N and I had similar initial points of non-linear segment where the slope of the graph, which represents the joint stiffness, starts to degrade. These points are approximately 44 kN, 29 kN, 25 kN, 18 kN at RT, 40°C, 60°C, and 80°C, respectively. This may indicate that, when subjected to compressive load, some initial internal damage had occurred at the contact zone between the bolt and pultruded thin-walled. The thread embedment may initiate the separation of laminate layers which causes ply delamination. After this point, the behaviour between these specimens were easily distinguishable, mainly due to the presence of mechanical insert which provides additional resistance against the threaded bolt and delaying the damaging process. Meanwhile, in reference to Figure 7 (a) and (b), specimen G showed almost linear behaviour without any apparent non-linearity, until final failure. This extended linear behaviour can be explained by the contribution of adhesives surrounding the insert, that has efficiently transferred the load and provided a steady resistance against slipping. This also represents the joint stiffness of the undamaged pultruded GFRP and mechanical insert, owing to the elastic behaviour of the adhesive. Subsequently, a significant descending response in sudden and brittle manner can be observed which followed by various degrees of non-linearity as the configuration breaks.

As the temperature rose to 60°C and 80°C, higher non-linearity was observed for all specimens as shown in Figure 7 (c) and (d). This could be attributed to the vinyl ester matrix softening which may exacerbate the initiation and propagation of ply delamination (Manalo et al., 2017b). Generally, even though slope reduction (consisting of several knees) was observed especially at the middle segment of specimens N and I curves, these specimens are still capable to carry the increased loading but with higher deformation until failure. After failure, specimen N showed gradual reduction in joint resistance and exhibited its ability to sustain post-failure load. As for specimen I, a sharper drop in joint resistance was observed which may be triggered by a different mode of failure and due to the sudden slip of the mechanical insert. In contrast, specimen G experienced some ductility (adhesive softening) at the peak of both graphs in Figure 7 (c) and (d) before sharply losing its load-sustaining ability which was mainly caused by the broken mechanical insert. From these observations, it can be seen that the installation of the mechanical inserts, with and without adhesive, has caused reasonable improvement in joint carrying capacity at an average of 113% and 37%, respectively, across the entire range of testing

temperatures. Additionally, the non-linearity observed from the load-elongation graphs can be associated with the stiffness reduction of the specimens during the testing at all temperature conditions as shown in Figure 8.

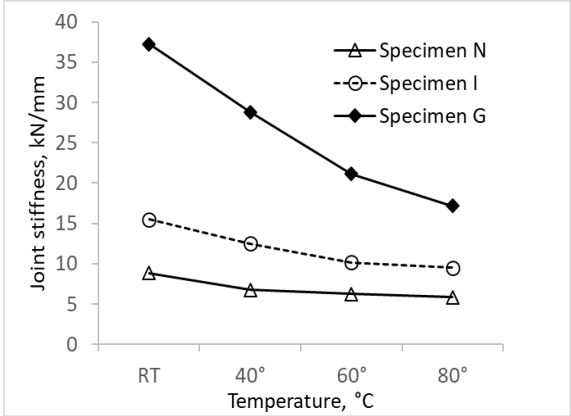


Fig. 8. Joint stiffness as function of elevated temperature

The joint stiffness for specimen N-RT dropped significantly with an approximately of 24%, 29% and 34% when compared to N-40, N-60, and N-80, respectively. However, there was less pronounced reduction of joint stiffness observed at the temperature regions of 40°C to 60°C (7%) and 60°C to 80°C (8%). Similar stiffness response (at constant rate) can be observed for specimen I between 60°C and 80°C. This indicates that the stiffness of these specimens is more influenced by the properties of the fibres, hence composite materials composed of glass fibres, like pultruded GFRP tend to be stable in large temperature range. On the other hand, the strength of the specimens is predominantly influenced by their fibre-matrix interface as its condition severely affects the joint strength at higher temperatures as discussed earlier. On average, the improvement of joint stiffness throughout the temperature range is about 68% for specimen I compared to specimen N. Overall, specimen G possesses higher joint stiffness capacity across the temperature range when compared to specimens N and I, approximately at an average of 72% and 53%, respectively. This may have been achieved due to the presence of epoxy adhesive in specimen G that promotes better composite action by allowing the effective use of mechanical insert. In addition, high volume of glass fibres composed in both mechanical insert and pultruded GFRP had contributed in improved joint stiffness. As temperature rose, the joint stiffness of specimen G declined in a linear pattern. This phenomenon may have occurred because

of the gradual softening of the adhesive, progressively weakening the contact interface between the pultruded GFRP and the mechanical insert.

Effect of level of temperature on joint capacity and bearing stress

Figure 9 compares the reduction in bolted joint capacity (in percentage) of pultruded GFRP box section at the various testing temperatures. The measured losses (%) of joint resistance relative to room temperature was found to increase at higher temperatures which directly indicate the degree of deterioration experienced by the tested specimens.

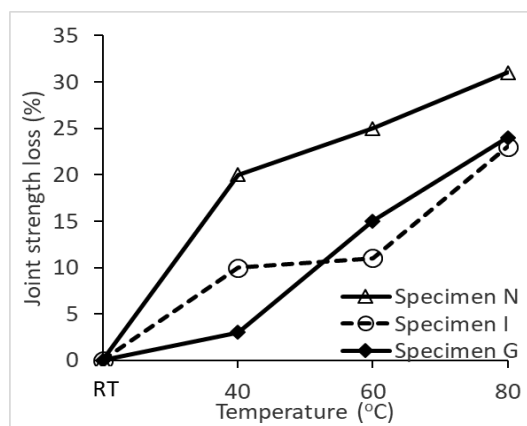


Fig. 9. Joint strength loss (%) at elevated temperature relative to RT

As expected, specimen N endured the most significant reduction of joint load-carrying capability when exposed to elevated temperatures compared to specimens I and G. Specimen N's joint strength tends to decline steadily, causing significant losses of 20%, 25% and 31% when exposed at 40°C, 60°C and 80°C, respectively. A similar trend of strength degradation at a constant gradient was observed by Manalo et al. (2017b) for the same pultruded GFRP section tested under typical three-point static bending test at seven different temperatures. It can be explained that the decrease in joint strength at higher temperatures is mainly due to the softening of the resin matrix which deteriorates the effectiveness of stress transfer between the glass fibres (Manalo et al., 2017b; Turvey and Sana, 2016; Mathieu et al., 2010). As aforementioned, at higher temperatures, the adhesion between the glass fibre and vinyl ester matrix may have been de-bonded as this was also observed by Mathieu et al. (2010) and Azwa and Yousif (2017) under scanning electron microscopy (SEM) of several polymeric composite materials. When the pultruded GFRP was exposed to 80°C approaching its

T_g value (115°C), resin matrix softened further resulted in matrix compression cracking (Ireman et al., 2000) and fibre buckling at bolt-hole contact interface.

The joint strength of specimen I and G were also negatively affected as the temperature rose but they exhibited lesser reduction compared to that of specimen N. When the temperature increased from RT to 40°C, the loss in joint load capacity was calculated to be approximately 10% and 3% for specimens I and G, respectively. From here, it can be seen that specimen G underwent marginal decline in joint strength due to the combined response achieved from mechanical insert and bonded adhesive. This assembly critically provides a significant in-plane resistance at the joint contact zone which are exposed to both compression stress and temperature effects. When the temperature increased up to 60°C, notably, specimen I exhibited only marginal additional joint loss of 0.9% before undergoing steeper linear degradation at 80°C. Insignificant joint strength loss observed between 40°C and 60°C (temperatures relatively far below T_g) may demonstrate constant thermal expansion coefficient of the pultruded GFRP and mechanical insert within this temperature range. Closer to T_g , the thermal expansion coefficient of these materials will rapidly increase (Mathieu et al., 2010). Therefore, with constant expansion, the configuration of the pultruded GFRP filled mechanical insert can be maintained through-out the loading up to failure. At higher temperature close to T_g , both composite resin materials gradually demonstrated higher viscoelastic behaviour leading to declination of material density. Together with the effect of softened resin matrix, it weakened the contact region of pultruded-insert and made the mechanical insert susceptible to slippage. This had lessened the impact of mechanical insert and lower the overall joint capacity.

Specimen G, in contrast, tends to exhibit a linear joint strength loss at elevated temperatures in a similar mode to that of specimen N as shown in Figure 9. With the application of epoxy adhesive, it has effectively promoted the composite action by strongly binding the mechanical insert and pultruded GFRP together, resulting in very minimal loss of joint capacity (about 3%) at 40°C. However, at higher temperatures of 60°C and 80°C, specimen G experienced considerable decline in joint carrying capacity by 15% and 24%, respectively. This indicates that the epoxy resin may begin to be negatively affected by the heat, subsequently weaken the pultruded-insert interface region. This is supported by Turi (1997) observation, whereby certain

properties of resin start to decline at a temperature as low as 50°C. Hence, the load transfer through this region was reduced, impairing the composite action. In addition, both the pultruded GFRP and mechanical insert had also undergone depreciation of stress distribution between fibres due to resin matrix softening, causing the overall system to lose its load-sustaining ability.

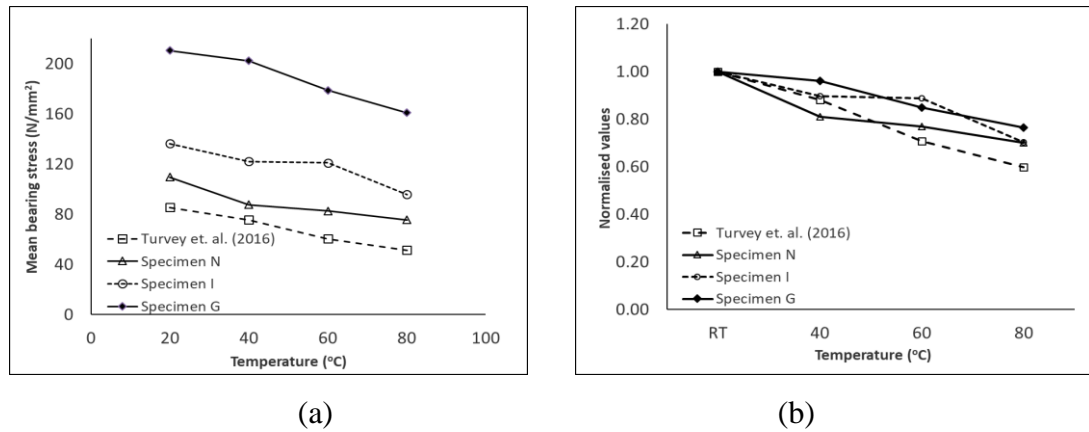


Fig. 10. Mean bearing stress (a) and normalised values (b) in relation to elevated temperatures

Figure 10 (a) presents the mean bearing stress in relation to elevated temperatures. A series of descending linear lines were recorded for all the tested specimens, including the test results obtained by Turvey and Sana (2016). The data from Turvey and Sana (2016) were comparable as the material used in the study was pultruded GFRP with an average thickness of 6.4 mm. Furthermore, both experimental programs comprised similar joint configurations (single-bolt under tensile loading), matched e/d_b ratio of 2.5, and identical tested temperature range. Despite all similarities, the cross-sectional shape of the material used in this paper is SHS pultruded, while Turvey and Sana (2016) used plate pultruded material. Additionally, there are different values in tensile properties where, 299.2 MPa and 741.5 MPa were documented for *EXTREN*[®] 500 series and WCFT composite, respectively. This was attributed to the difference in the type and configuration of the fibres within the composite materials, as well as the fibre-resin interphase properties. Due to this, it was observed that specimen N is capable of recording a higher mean bearing stress than that of the results obtained by Turvey and Sana (2016) as shown in Figure 10 (a). Nonetheless, the joint bearing stress of specimen N responded in a similar way to that of Turvey and Sana's specimen, where it progressively deteriorated at a comparable rate in relation to elevated temperatures.

As the bearing contact area are subjected to compression, it critically relies upon the polymer resin ability to efficiently transfer the stresses between fibres. However, this might not have worked adequately due to the softening of polymer resin structure at higher temperature, and this directly decreased the joint resistance. Figure 10 (b) plots the joint bearing stress of the tested specimens as a function of temperature normalised to that measured at RT. It was apparent from Figure 10 (b) that the normalised values obtained by Turvey and Sana (2016) declined in a linear manner at constant gradient across the temperature range. However, specimen N recorded the lowest value at 40°C which might be due to the presence of threaded bolt, before declining at a lower gradient (between 60°C and 80°C) when compared to that of Turvey and Sana’s specimen. The lesser joint degradation endured by specimen N was contributed by the high volume of longitudinally oriented fibres which crosslinked the softened resin matrix, providing resistance to the applied load (Manalo et al., 2016).

Effect of test temperature on mechanical insert (with and without adhesive)

Figure 11 suggests that with the mechanical insert featured in specimens I and G, the joint strength obtained is much higher than that of specimen N. The difference in connection strength achieved by specimen I compared to specimen N is 24%, 39%, 46%, and 39% higher at RT, 40°C, 60°C, and 80°C, respectively. For specimen G, it enables efficient load transfer between the components which had considerably enhanced the joint strength up to 50% across the test temperature. Further, specimen G exhibited more than doubled the joint capacity that of specimen N across the increased temperature range.

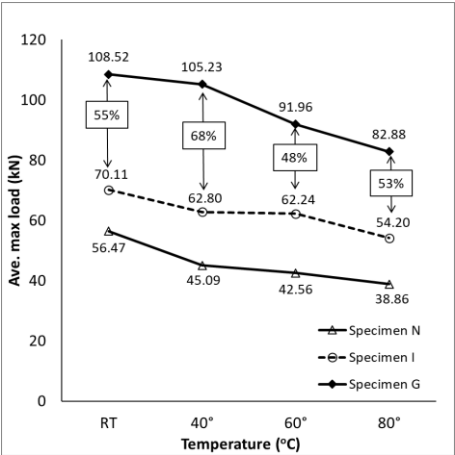


Fig. 11. Average maximum joint load at test temperatures

The presence of insert has increased the contact area at the vicinity of the joint and alleviates the threaded effect on the thin-walls. For this reason, it could improve the joint resistance and stabilises the all threaded bolt and pultruded thin walls against buckling. Having said that, at much higher load, it was observed that, in specimen I, the undamaged insert was slipping from its original position which allowed the bolt to gradually shear the pultruded thin walls. Subsequently, the injected epoxy adhesive had enhanced the bond between the insert and the pultruded thin walls. From close visual inspection, the bonded assembly managed to stop the slipping of the insert which had occurred at lower load in specimen I that led to premature failure. Critically, the bonded assembly had improved its stress distribution and fully utilised the mechanical insert load-carrying capability especially at the contact zone. In that case, it indicates that the combination of insert and adhesive can sustain higher connection shear resistance and had proven to strengthen the bolted connection area in SHS pultruded GFRP material.

Effect of test temperature on failure modes

After completion of the mechanical testings, the specimens were disassembled from the test set-up and further investigations on failure behaviour were carried out once the specimens had cooled down.

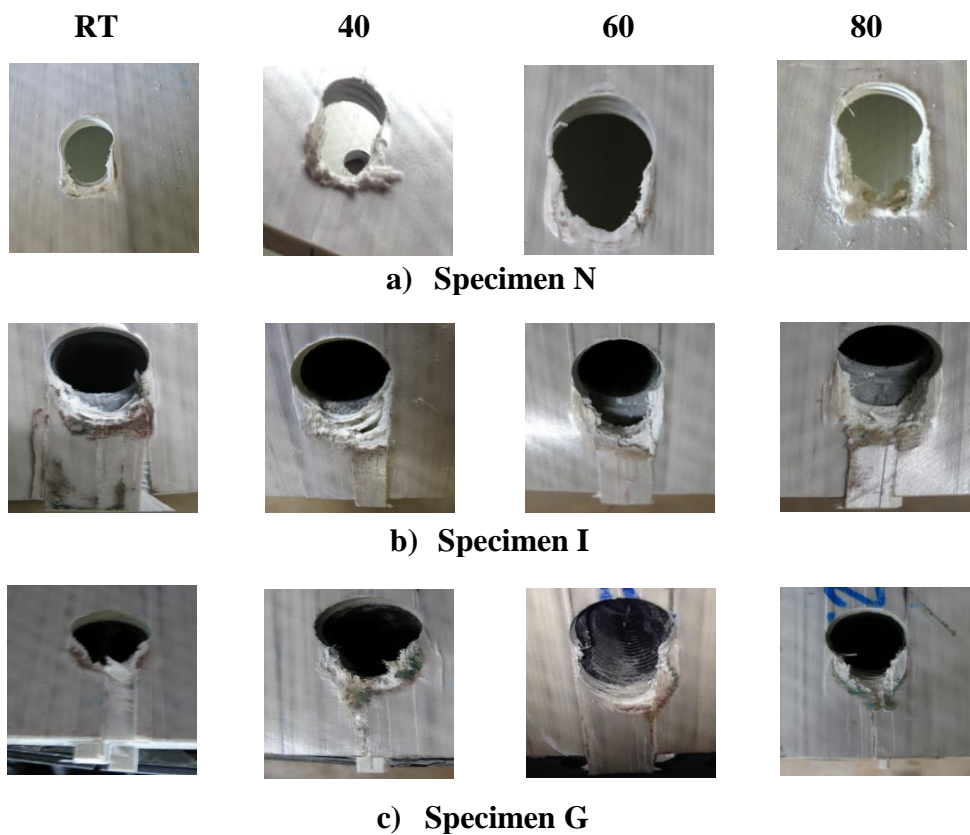


Fig. 12. Failure modes of specimens N, I and G

The final failure modes were identified and the photographs of specimens N, I and G are presented in Figure 11. Most of the specimens showed identical failure modes at both sides of the thin walls where the holes of the mechanically fastened joints were located. However, there were specimens that showed variation in failure modes which may occur due the sensitivity of load distribution in regards to geometric imperfections (eg. bolt-hole clearance). Thus, repeatability is vital in this testing program in order to better assess the differences of the results obtained.

For specimen N-RT, a combination of local crushing and bearing failure modes can be observed directly beneath the bolt/hole contact surface as shown in Figure 12 (a). With an e/d_b ratio of 2.5 and a high w/d_b ratio of 5.5, bearing failure was achieved as the specimen is able to sustain post-failure loads and this can be seen from the load-elongation graph in Figure 7. This also agrees well with observations from other experimental works done by Cooper and Turvey (1995), Vangrimde and Boukhili (2003), Matharu and Mottram (2012) and Luo et al. (2016b). As the temperature

increases, the polymer resin at the thin walls had softened and this consequently allowed the bolt thread to easily entrench into the material. Figure 12 (a) shows that at higher temperatures, the bolt thread had gradually damaged the pultruded composite material in a crushing manner. Meanwhile, Turvey and Sana (2016) discovered that, at e/d_b ratio of 2 and 2.5, the pultruded GFRP experienced shear failure mode when tested at 20°C and 40°C temperature. The difference of observed failure mode was influenced by the use of plain bolt instead of all-threaded bolt as a connector. Furthermore, lower selection of w/d_b ratio of 4.0 (less than 5) tends to promote shear-out failure. For specimens I and G, some indication of bearing damage was observed for the entire temperature range. The pultruded FRP laminates together with the mechanical inserts, bear the load from the advancing bolt and experienced some compressive damages with less local crushing before failing abruptly. Subsequently, the final failure mode was a shear-out whereby the delamination of outer plies can be observed clearly at the end distance. The presence of mechanical insert had provided extra resistance against the threaded bolt and alleviated the stress concentrations in the region of the bolt holes. These improvements had resulted in a higher joint load-carrying capacity and delayed the occurrence of final fracture.

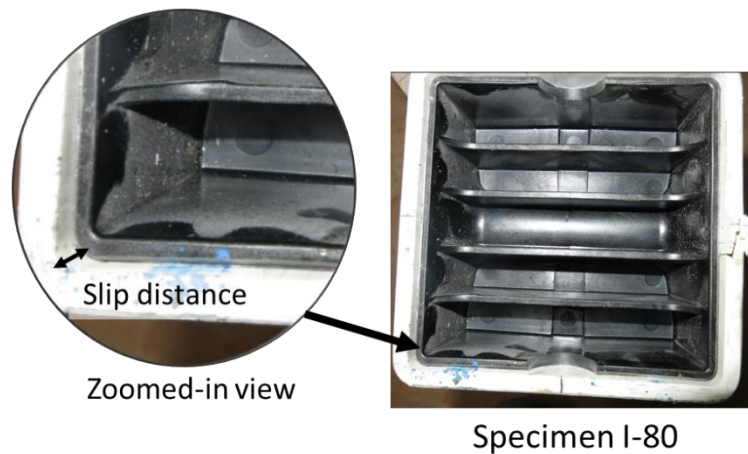


Fig. 12. Slipped insert of specimen I at 80°C

With a tight-fit attachment of mechanical insert in specimen I, it was observed that the mechanical insert was displaced from its original position and no external damage on the insert was noticeable as shown in Figure 13. From Figure 12 (b) and 13, when subjected to thermal loading, the mechanical insert may easily displace further from its initial position. When both the pultruded GFRP and mechanical insert are exposed

to higher temperature conditions, the materials become less dense with smoother surfaces due to the softening of resin matrix. As a result, the surface friction or contact force at the insert-pultruded interface may have been disrupted, leading to increased chance of slippage and poor load distribution, therefore causing the mechanical insert to be ineffective on the joint performance.

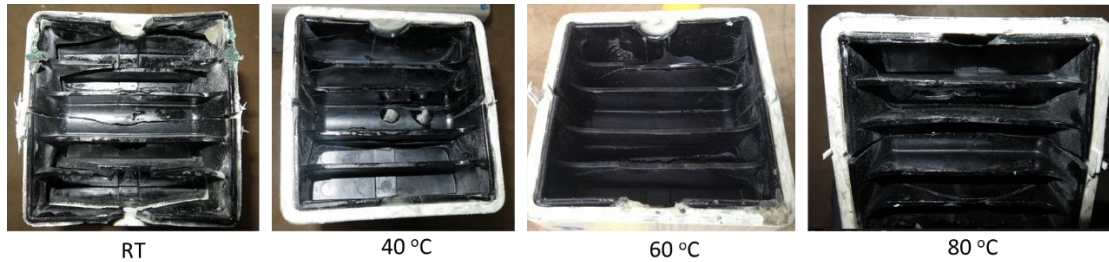


Fig. 13. Broken insert of specimen G

With epoxy adhesive injected in between the pultruded material and mechanical insert, specimen G failed in a catastrophic manner whereby sudden loss in joint resistance became apparent. After reaching the peak loads, the specimen failed, accompanied with a bursting sound at all temperature conditions indicating that the insert has broken as shown in Figure 13. Close visual inspection at the locations of failure in Figure 12 (c) demonstrates that, initial bearing was observed along the orientation of fibre direction preceding final failure in the shear-out mode. At higher temperatures, the interfacial bond between glass fibres and the surrounding polymer resin may have weakened, making the pultruded material more susceptible to ply delamination and promoting shear-out failure. The same mechanism may also affect the mechanical insert, whereby load transfer were ineffective as the interphase between the short fibres and the surrounding adhesive degrades, cumulatively compromised the joint's overall load-carrying capability. Notably, no visible premature slipping of the insert was observed. The loading was continuously applied and this caused further displacement of the cracked mechanical insert to the bottom end of the SHS pultruded profile.

THEORETICAL ASSESSMENT

A theoretical approach was used to analyse the strength limits of specimen N and I based on the failure behaviour observed at room temperature. Equation 1 and Equation 2 (ASCE 2010) were used to assess the bolted joint capacity under bearing strength R_{br} and shear-out strength, R_{sh}

$$R_{br} = t d F_{\theta}^{br} \quad (1)$$

$$R_{sh} = 1.4 \left(e_1 - \frac{d_n}{2} \right) t F_{sh} \quad (2)$$

where t = thickness of FRP material (mm); d = nominal diameter of bolt (mm); d_n = bolt hole diameter (mm); e_1 = end distance (mm); F_{θ}^{br} = characteristic pin-bearing strength of FRP material and F_{sh} = shear strength of FRP.

For F_{θ}^{br} , the threaded pin-bearing strength of FRP is employed as stated earlier in Table 1 is employed in order to take account the influence of bolt threads against pultruded laminates. The computed theoretical joint bearing strength of 54.34 kN is comparable to the average maximum load of specimen N tested at RT and it shows that the selected F_{θ}^{br} (threaded) value adequately represented the condition around the bolted hole. In fact, the observed mode of failure was found to be in good agreement with Eq (1). On the other hand, the computed theoretical shear-out strength based on Eq. (2) was about 79 kN, slightly higher when compared to the experimental result attained in specimen I at RT. Even though the experimental result is a little bit lower (13%), the observed failure had already shown the clearly defined shear-out plane along the principal material direction. Additionally, using a linear regression analyses, the strength reduction factor (SRF), k is presented which is defined as the ratio of the average maximum joint capacity achieved at elevated temperatures to the strength at RT. The analysis is conducted for specimens N and G, disregarding specimen I as the slippage causes higher unpredictability and affects the actual reduction in strength. Meanwhile, Table 7 presents the modification factor, m , which have been determined by quantitative relation between the experimental mean joint failure across the specimen groups and the mean joint failure at RT. The distributions of obtained results show that the joint capacity of specimens I and G are averagely increased by 40% and 100%, respectively when compared to specimen N. These percentages are reasonably

closed with the calculated improvement of 37% and 113% discussed in Load vs Hole elongation section earlier.

Table 7. Modification factor, *m* values

<i>m</i> values	Description
1.00	Pultruded GFRP bolted joint without any filled / mechanical insert.
1.40	Pultruded GFRP bolted joint with mechanical insert without adhesive.
2.00	Pultruded GFRP bolted joint with mechanical insert and adhesive.

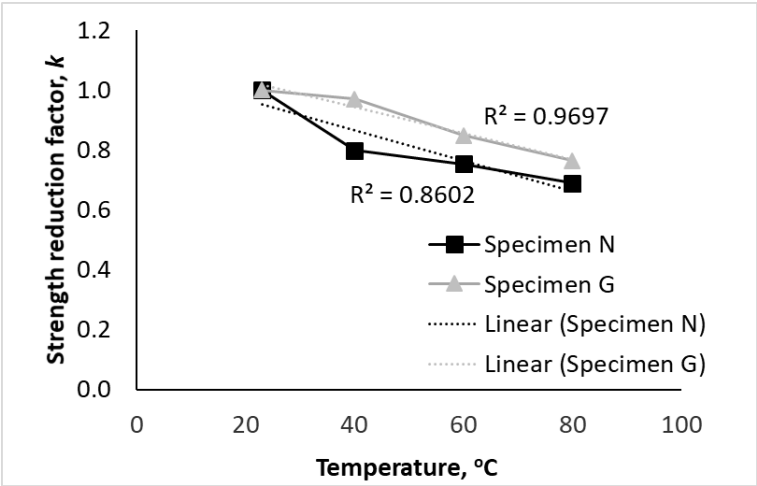


Fig. 14. Strength reduction factor at different temperatures

From Figure 14, the results indicate that the best responses for both specimens N and G can be determined by a linear regression analyses with an R-squared value of 0.86 and 0.97, respectively. The corresponding equations are as follows:

Specimen N:

$$k = 1.067 - 0.0051T \quad \text{when } RT \leq T \leq 80^{\circ}C \quad (3)$$

Specimen G:

$$k = 1.117 - 0.0044T \quad \text{when } RT \leq T \leq 80^{\circ}C \quad (4)$$

Based on these observations, k factor is averagely improved by about 12% by introducing the adhesively bonded mechanical insert at the hollow joint of pultruded GFRP. Effect of joint configurations such as all threaded bolt and the bonded insert under elevated temperatures were taken into account when introducing the SRF interaction. It can be seen that all joint configurations demonstrated some development of bearing damage in the bolt-hole region prior to their respective final failure modes. During the load transfer from the all-threaded bolt to the pultruded laminates, the predominant damage state was mainly governed through compressive damage. This had been supported by the introduction of mechanical insert that may provide improved stress redistribution at the edge of the bolt bores and delayed the propagation of internal damage. Therefore, the bearing equation with a combination of the derived factors was used to predict the joint load-carrying capacity of specimen N and G. Several assumptions were made when predicting the maximum loads using the following equation (Eq. 5), for instance, clamping force was neglected, and the elevated temperatures in the all threaded bolt does not influence the overall joint strength (Luo et al., 2016a; Wu et al., 2015a). A following joint bearing strength equation incorporates the strength reduction and modification factor is proposed to predict the ultimate joint capacity of pultruded GFRP hollow section under elevated temperatures.

$$P_o = k.m.(2 t d F_{\theta}^{br})$$

or

$$P_o = k.m.R_{br} \quad (5)$$

It should be noted that, the derived k and m presented earlier are for these particular pultruded composite materials using the designed joint configurations under the designed elevated temperatures ($RT \leq T \leq 80^{\circ}C$). In Eq. (5), P_o is the predicted ultimate bolted joint capacity of SHS pultruded GFRP, R_{br} is the bearing capacity of SHS pultruded GFRP bolted joint as mentioned in Eq. (1) and m is the modification factor for the different joint configurations stated in Table 7. For SHS profile, there are two thin walls area affected by the bolt, thus Eq. (5) should be multiplied by 2 and F_{θ}^{br} is chosen to accommodate the threaded pin-bearing effect. Further, Eq (5). is multiplied by the strength reduction factor, k and modification factor, m to incorporate

the pultruded GFRP mechanical properties account for temperature effect and the different joint assembly, respectively.

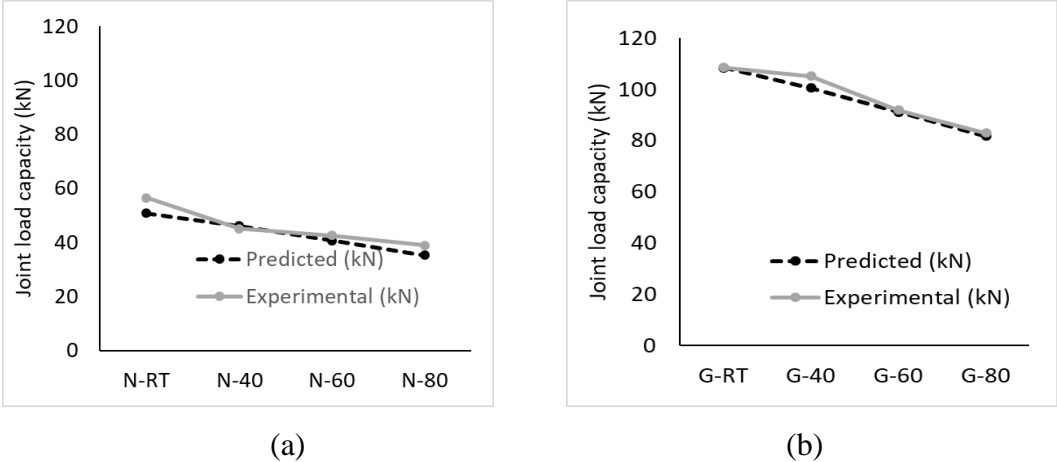


Fig. 15. Comparison of joint load carrying capacity at elevated temperatures

Figure 15 shows the comparison of the predicted formulation with the experimental results. As can be seen, the graphs plot an array of straight lines of negative slope which means that the degradation of joint capacity is linearly proportional to the increased temperature. Most of the data computed using Eq. (5) are predicted reasonably well and are plotted slightly below the experimental results. This shows that the proposed Eq. (5) satisfies the lower bound values that are suitable for a preliminary joint design exposed to these related temperatures. Also, the ratio of joint strength from the predicted equation to the experimental results for all specimens showed excellent agreement whereby most of the ratios are approaching 1.0.

CONCLUSIONS

This study was conducted to investigate the effect of elevated temperature on the joint strength of mechanical insert with and without adhesive used in the single-bolt joint of square pultruded GFRP tubular profile. A total of sixty (60) SHS pultruded GFRPs were tested under tensile loading, and its joint performance and failure mechanism were assessed. Based on the experimental results, the following conclusions can be drawn:

1. The introduction of mechanical insert with tight-fit arrangement at the jointing region can enhance the joint capacity up to 24% at room temperature when compared with the specimen without the mechanical insert. Further

improvement of 39% and 46% was gained at 40°C and 60°C, respectively, before it slightly reduced at 80°C.

2. At similar temperature exposure, the full composite action achieved in specimen G exhibited the highest joint strength, with an average of about 113% compared to that of specimen N. Critically, the mechanical insert with bonded assembly had improved its stress distribution and fully utilised the insert in sustaining higher load-carrying capability.
3. At elevated temperature between 40°C to 80°C, a marginal reduction of joint stiffness, approximately 1% and 3%, were observed for both specimens N and I, respectively. This indicates that the joint stiffness is contributed by the fibre properties of the composite as materials composed of glass fibres such as pultruded GFRP and the mechanical insert tend to be stable in large temperature range and results a relatively less stiffness loss.
4. Standard pultruded GFRP single-bolt joint endured the most significant reduction of joint load-carrying capability when exposed to elevated temperatures compared to specimens with mechanical inserts, with or without epoxy adhesive. The former joint strength tends to decline steadily, causing significant losses of 20%, 25% and 31% when tested at 40°C, 60°C and 80°C, respectively.
5. Pultruded GFRP supported with mechanical insert exhibited only marginal additional joint loss of 0.9% from 40°C to 60°C, possibly due to constant thermal expansion coefficient of the pultruded GFRP and mechanical insert between this temperature range which is well below T_g .
6. Pultruded GFRP with the bonded mechanical insert, in contrast, encountered a linear joint strength loss at elevated temperatures. With an inclusion of epoxy adhesive, it effectively promoted the composite action between the pultruded GFRP and the mechanical insert and endured lesser decline in joint capacity by 3%, 15% and 24% at 40°C, 60°C, and 80°C, respectively.
7. At higher temperature, localised crushing mode of failure was observed for the standard square pultruded GFRP due to the combined effect of threaded bolt and elevated temperatures. The softening of resin matrix caused higher deterioration rate especially at the contact point between the threaded bolt and pultruded material.

8. On the other hand, shear-out failure was observed on the test specimens with the mechanical insert, with and without the adhesive bond at the jointing area. At higher temperatures, the interfacial bond between fibres and the polymer resin may deteriorate, making the pultruded material more susceptible to ply delamination and promoting brittle shear-out failure.
9. The proposed joint strength prediction equation, which incorporates the strength reduction and modification factors based on different joint configurations involving mechanical insert, calculated reasonable outcomes against experimental failure load. In addition, the ratio of joint strength from the proposed equation to the experimental results for all specimens showed excellent agreement whereby most of the ratios are close to 1.
10. The use of mechanical inserts to strengthen bolted connections in SHS of pultruded GFRP shows promising future. Further research on this type of configuration in terms of its serviceability aspects will build confidence among practitioners and widen its industrial applications.

It is noted that the reduction factor, k and modification factor, m , derived from this study are based on a specific type of pultruded composites and mechanical insert considered under this particular range of elevated temperatures. Further investigations on the different dimensions of SHS pultruded GFRP material and its joint geometries can be explored in order to extend the understanding of established factors.

ACKNOWLEDGMENTS

The first author gratefully acknowledges the Australian Commonwealth Government for the contribution through Research Training Program (RTP) scheme. The authors also gratefully acknowledge Wagner Composite Fibre Technologies (WCFT) for the testing materials and experimental data supplied. Special thanks to Dr. Mario Springolo and Mr. Wayne Crowell for their kind support and guidance during the experimental work.

REFERENCES

AS/NZS1110:1995 (1995). " ISO metric precision hexagon bolts and screws.", Standards Australia and Standards New Zealand., Australia and New Zealand.

- AS/NZS1252:1996 (1996). "High-strength steel bolts with associated nuts and washers for structural engineering. Australia and New Zealand." Standards Australia and Standards New Zealand.
- ASCE (2010). "Pre-Standard for Load and Resistance Factor Design (LFRD) of Pultruded Fibre Reinforced Polymer (FRP) Structures."
- ASTMD3171 (2011). "Standard Test Methods for Constituent Content of Composite Materials." American Society for Testing and Materials (ASTM) Standard.
- ASTME1356-08 (2014). "Standard Test Method for Assignment of the Glass Transition Temperatures by Differential Scanning Calorimetry." American Society for Testing and Materials (ASTM) Standard, United States.
- Azwa, Z. N., and Yousif, B. F. (2017). "Physical and mechanical properties of bamboo fibre / polyester composites subjected to moisture and hygrothermal conditions." *Journal of Materials: Design and applications*, 0(0), 1-15.
- Bai, Y., Post, N. L., Lesko, J. J., and Keller, T. (2008). "Experimental investigations on temperature-dependent thermo-physical and mechanical properties of pultruded GFRP composites." *Thermochimica Acta*, 469(1-2), 28-35.
- Bai, Y., and Yang, X. (2013). "Novel joint for assembly of all-composite space truss structures: conceptual design and preliminary study." *Composites for Construction*, 17(1), 130-138.
- Bakis, C. E., Preimanis, A. I., Gremel, D., and Nanni, A. "Effect of resin material on bond and tensile properties of unconditioned and conditioned FRP reinforcement roads." *Proc., The 1st International Conference on Durability of FRP Composites for Construction (CDCC98)*, CDCC, 525-533.
- Bank, L. C. (2006). *Composites for Construction: Structural Design with FRP Materials*, John Wiley & Sons, Inc., New Jersey.
- Bank, L. C., Mosallam, A. S., and McCoy, G. T. (1994). "Design and performance of connections for pultruded frame structures." *Journal of Reinforced Plastics and Composites*, 13, 199-212.
- CNR (2008). "Guide for the Design and Construction of Structures made of FRP Pultruded Elements." National Research Council of Italy, Rome.
- Cooper, C., and Turvey, G. J. (1995). "Effects of joint geometry and bolt torque on the structural performance of single bolt tension joints in pultruded GRP sheet material." *Composite Structures*, 32, 217-226.
- Correia, J. R., Bai, Y., and Keller, T. (2015). "A review of the fire behaviour of pultruded GFRP structural profiles for civil engineering applications." *Composite Structures*, 127, 267-287.
- DG9 (2004). "Design guide 9: For Structural Hollow Section Column Connections." The International Committee for Research and Technical Support for Hollow Section Structures (CIDECT), Germany.
- ECSS (2011). "Insert design handbook." European Cooperation for Space Standardization, Noordwijk, The Netherlands.
- Eurocomp (1996). *Structural Design of Polymer Composites*, E & FN Spon, London.
- Garrido, M., Correia, J. R., and Keller, T. (2015). "Effects of elevated temperature on the shear response of PET and PUR foams used in composite sandwich panels." *Construction and Building Materials*, 76, 150-157.
- Hizam, R. M., Manalo, A. C., and Karunasena, W. (2012). "A review of FRP composite truss systems and its connections." *22nd Australasian Conference on the Mechanics of Structures and Materials*, C. S. Bijan Samali, Mario M. Attard, ed., Taylor & Francis Ltd, Sydney, New South Wales, Australia.

- Hollaway, L. C. (2010). "A review of the present and future utilisation of FRP composites in the civil infrastructure with reference to their important in-service properties." *Construction and Building Materials*, 24(12), 2419-2445.
- Humphreys, M. F. (2003). "Development and structural investigation of monocoque fibre composite trusses." Queensland University of Technology.
- Ibrahim, R. A., and Pettit, C. L. (2005). "Uncertainties and dynamic problems of bolted joints and other fasteners." *Journal of Sound and Vibration*, 279(3-5), 857-936.
- Ireman, T., Ranvik, T., and Eriksson, I. (2000). "On damage development in mechanically fastened composite laminates." *Composite Structures*, 49, 151-171.
- ISO1172 (1996). "Textile-glass-reinforced plastics, prepegs, moulding compounds and laminates: Determination of the textile-glass and mineral-filler content- Calcination methods." International Organization for Standardization (ISO).
- Keller, T., and Vallée, T. (2005). "Adhesively bonded lap joints from pultruded GFRP profiles. Part I: stress-strain analysis and failure modes." *Composites Part B: Engineering*, 36(4), 331-340.
- Lau, S. T. W., Said, M. R., and Yaakob, M. Y. (2012). "On the effect of geometrical designs and failure modes in composite axial crushing: A literature review." *Composite Structures*, 94(3), 803-812.
- Luo, F. J., Bai, Y., Yang, X., and Lu, Y. (2016). "Bolted sleeve joints for connecting pultruded FRP tubular components." *Composites for Construction*, 20(1), 04015024.
- Luo, F. J., Yang, X., and Bai, Y. (2016). "Member capacity of pultruded GFRP tubular profile with bolted sleeve joints for assembly of latticed structures." *Journal of Composites for Construction*, 20, 1-12.
- Manalo, A., Aravinthan, T., Fam, A., and Benmokrane, B. (2017). "State-of-the-Art Review on FRP Sandwich Systems for Lightweight Civil Infrastructure." *Journal of Composites for Construction*, 21(1).
- Manalo, A., Maranan, G., Sharma, S., Karunasena, W., and Bai, Y. (2017). "Temperature-sensitive mechanical properties of GFRP composites in longitudinal and transverse directions: A comparative study." *Composite Structures*, 173, 255-267.
- Manalo, A., Surendar, S., Van Erp, G., and Benmokrane, B. (2016). "Flexural behavior of an FRP sandwich system with glass-fiber skins and a phenolic core at elevated in-service temperature." *Composite Structures*, 152, 96-105.
- Manalo, A. C., and Mutsuyoshi, H. (2011). "Behavior of fiber-reinforced composite beams with mechanical joints." *Journal of composite materials*(0 (0)), 1-14.
- Mara, V., Haghani, R., and Al-Emrani, M. (2016). "Improving the performance of bolted joints in composite structures using metal inserts." *Journal of composite materials*, 50(21), 3001-3018.
- Matharu, N. S., and Mottram, J. T. (2012). "Laterally unrestrained bolt bearing strength: Plain pin and threaded values." *6th International Conference on FRP Composites in Civil Engineering*Rome, Italy.
- Mathieu, R., Peng, W., Patrice, C., and Brahim, B. (2010). "Temperature as an Accelerating Factor for Long-Term Durability Testing of FRPs: Should There Be Any Limitations?" *Journal of Composites for Construction*, 14(4), 361-367.
- McCormick, L. (1999). "The Static Load Response of Fibre Composite Trusses." Undergraduate Thesis, University of Southern Queensland, Toowoomba, Australia.

- Mosallam, A. S. (2011). *Design Guide for FRP Composite Connections*, American Society of Civil Engineers (ASCE).
- Mottram, J. T. (2009). "Design Guidance for Bolted Connections in Structures of Pultruded Shapes: Gaps in Knowledge." *17th International Conference on Composite Materials*, A1(6).
- Mouritz, A. P., and Gibson, A. G. (2010). *Fire properties of polymer composite material*, Springer, Netherlands.
- Persson, E., Eriksson, I., and Zackrisson, L. (1997). "Effects of hole machining defects on strength & fatigue life of composite." *Composites Part A: Applied Science and Manufacturing*, 28A, 141-151.
- Pfeil, M. S., Teixeira, A. M. A. J., and Battista, R. C. (2009). "Experimental tests on GFRP truss modules for dismountable bridges." *Composite Structures*, 89(1), 70-76.
- Qureshi, J., and Mottram, J. T. (2015). "Moment-rotation response of nominally pinned beam-to-column joints for frames of pultruded fibre reinforced polymer." *Construction and Building Materials*, 77, 396-403.
- S.Ramakrishna, H.Hamada, and M.Nishiwaki (1995). "Bolted joints of pultruded sandwich composite laminates." *Composite Structures*, 32, 227-235.
- Singamsethi, S. K., LaFave, J. M., and Hjelmstad, K. D. (2005). "Fabrication and Testing of Cuff Connection for GFRP Box Sections." *Journal of Composites for Construction*, 9(6), 536-544.
- Smith, S. J., Parsons, I. D., and Hjelmstad, K. D. (1998). "An experimental study of the behaviour of connection for pultruded GFRP- I beams and rectangular tubes." *Composites Structures* (42), 281 - 290.
- TMR (2014). "Design criteria for bridges and other structures." Q. T. a. M. R. (TMR), ed. Queensland, Australia.
- Turi, E. A. (1997). "Thermal characterization of polymer materials." *Academic*, 2.
- Turvey, G. J., and Sana, A. (2016). "Pultruded GFRP double-lap single-bolt tension joints – Temperature effects on mean and characteristic failure stresses and knock-down factors." *Composite Structures*, 153, 624-631.
- Turvey, G. J., and Wang, P. (2007). "Failure of pultruded GRP single-bolt tension joints under hot–wet conditions." *Composite Structures*, 77(4), 514-520.
- Turvey, G. J., and Wang, P. "Failure of pultruded GFRP bolted joints: a Taguchi analysis." *Proc., Engineering and Computational Mechanics*, Institution of Civil Engineers (ICE), 155-166.
- Vangrimde, B., and Boukhili, R. (2003). "Descriptive relationships between bearing response and macroscopic damage in GRP bolted joints." *Composites Part B: Engineering*, 34(7), 593-605.
- Wu, C., Bai, Y., and Toby Mottram, J. (2015). "Effect of Elevated Temperatures on the Mechanical Performance of Pultruded FRP Joints with a Single Ordinary or Blind Bolt." *Journal of Composites for Construction*, 20(2), 04015045.
- Xiao, Y., and Ishikawa, T. (2005). "Bearing strength and failure behavior of bolted composite joints (part I: Experimental investigation)." *Composites Science and Technology*, 65(7-8), 1022-1031.
- Xiao, Y., and Ishikawa, T. (2005). "Bearing strength and failure behavior of bolted composite joints (part II: modeling and simulation)." *Composites Science and Technology*, 65(7-8), 1032-1043.
- Zhang, Y., and Keller, T. (2008). "Progressive failure process of adhesively bonded joints composed of pultruded GFRP." *Composites Science and Technology*, 68(2), 461-470.

- Zhang, Z., Bai, Y., He, X., Jin, L., and Zhu, L. (2018). "Cyclic performance of bonded sleeve beam-column connections for FRP tubular sections." *Composites Part B: Engineering*.
- Zhang, Z., Bai, Y., and Xiao, X. (2018). "Bonded sleeve connections for joining tubular glass fiber reinforced polymer beams and columns: an experimental and numerical study." *Composites for Construction*.

5. Study on the effect of eccentric loading

5.1. Article III: Behaviour of through-bolt connection for pultruded GFRP T-joint

The outcomes of **Article II** had suggested the effectiveness of through-bolt with mechanical insert connection system in pultruded GFRP hollow sections under adverse temperatures. Further investigation due to possible construction errors such as eccentric loading is important for its practical use. As part of the study's **third objective**, the effects of eccentric loading on the joint resistance of pultruded GFRP hollow sections and the subsequent failure mechanism was investigated in **Article III**. The pultruded GFRP materials were assembled using all-threaded through-bolt connection system to form T-joints, representing structural components found in bridge trusses. Additionally, the influence of employing mechanical inserts at the connection system on the eccentric loading was examined. The configurations of the T-joints included both single and double bottom chords, with the former imbalanced configuration intended to impart load eccentricity as shown in **Figures 4 and 5** of **Article III**. The results indicated that the single bottom chord T-joint, with and without mechanical insert, achieved 41% and 61% lower joint strength, respectively, when compared to their double bottom chord counterparts. This reduction in joint strength was contributed by the additional stresses developed due to eccentricity which was evident from the observed mode of failure as highlighted in **Failure mode** section of **Article III**. Meanwhile, all T-joints with mechanical inserts exhibited higher joint load-carrying capacity than the insert-less joints, implying that the inserts promoted better bending resistance as illustrated in **Figure 10** of **Article III**. The theoretical evaluation in **Theoretical assessment** section, considering the combined effects of axial compression and bending stress, was incorporated with modification factors derived in **Article II**. The outcomes of this paper demonstrated that the through-bolt connection with bonded mechanical insert is an effective alternative joint system for pultruded GFRP hollow sections. This connection system was employed at a structural level, specifically on one-meter span pultruded truss structures were conducted and the results are presented, analysed and discussed in **Article IV**.

Behaviour of through-bolt connection for pultruded GFRP T-joint under eccentric loading

R.M. Hizam ¹, Allan C. Manalo ^{1*}, Warna Karunasena ¹ and Yu Bai ²

¹Centre of Future Materials, Faculty of Health, Engineering and Sciences, University Southern Queensland, QLD 4350, Australia.

²Department of Civil Engineering, Monash University, Clayton, VIC 3800, Australia.

*Corresponding Author:

manalo@usq.edu.au

ABSTRACT

This paper investigates the effect of eccentric loading on the bolted joint resistance and failure mechanism of pultruded glass fibre reinforced polymer (GFRP) T-joint between the chord and vertical members. The rectangular hollow sections (RHS) of 100 mm x 75 mm x 5 mm were assembled as a T-joint using all-threaded steel bolts that represents structural components in a bridge truss. The configurations of the T-joints included both single and double bottom chords, with the former imbalanced configuration intended to impart load eccentricity, which can be found in composite truss bridges. Both configurations were further subjected to the effect of mechanical inserts as a filled-type connection element in the vicinity of bolted joints. The experimental results showed that, due to the developed eccentricity, the vertical component of pultruded GFRP thin wall had suffered from local compression which induced web buckling coupled with apparent plies delamination. In addition, the single bottom chord T-joint with and without mechanical insert, achieved 41% and 61% lower joint strength, respectively, when compared to their double bottom chord counterparts. Meanwhile, the T-joints with the mechanical inserts exhibited higher joint load-carrying capacity than the insert-less joint due to the insert promoting better bending resistance whereby no evidence of web buckling was visible. Furthermore, the theoretical equations of combined axial compression and bending stress with

modification factors to consider the influence of mechanical insert predicted the resistance of GFRP T-joints reliably.

Keywords: Bolted Joint, Connection, Eccentricity, Pultruded FRP, T-Joint

INTRODUCTION

The applications of fibre reinforced polymer (FRP) composites in civil engineering have increased significantly in the last 20 years, both in infrastructures and building construction (Satavisam et al., 2017; Manalo et al., 2016; Keller et al., 2015; Correia et al., 2015). In particular, glass fibre reinforced polymer (GFRP) composites are preferred over carbon, aramid, and basalt due to its lower cost (Uddin and Abro, 2008; Manalo et al., 2017a). GFRP cross sections which resemble thin-walled metallic sections, such as square and rectangular hollow sections, angle, standard I-beam and channel are also now manufactured efficiently through pultrusion (Keller, 2001; Bai and Yang, 2013). The pultrusion manufacturing process allows bulk production at low operating costs, high fibre-to-matrix ratio, reproducibility of product, and dimensional tolerances (Manalo et al., 2017a). As a structural material, pultruded GFRP has been widely accepted as alternatives to steel and timber, as advancements have been achieved through many research studies (Turvey and Wang, 2007; Hollaway, 2010). This is contributed by its attractive characteristics that include ease of fabrication to meet specific structural performance, high axial resistance, high resistance to aggressive environment, relatively lightweight when compared to conventional materials, and quick installation time (Omar et al., 2008). Despite these promising features, the widespread acceptance of pultruded GFRP in the construction field is hampered by many challenges including inadequate connection system, which is a crucial element in determining their reliable performance and in providing satisfactory structural integrity.

Early works conducted on investigating suitable connection methods for pultruded components were based around steel bolted joints due to its low cost, ease of installation and removal, and design familiarity (Turvey, 2000; Bank, 2006; Mottram, 2009; Mosallam, 2011). Compared to steel fasteners, FRP fasteners (solid rod or bar) as an alternative, provide excellent mechanical performance such as higher resistance against corrosion, lightweight and lower heat conductivity (Schmidt et al., 2012).

However, they are not widely used due to its anisotropic properties that exhibit severe concerns in regards to joint ductility (Min, 2008; Gand et al., 2013). While other methods, such as single-plate or welded connection are still impractical for pultruded FRP sections, some essential fastening parameters that need to be considered when designing FRP bolted connections includes geometry (width, spacings, end distance, etc.), joint type, plate thickness, clamping force, hole tolerance and loading conditions (CNR, 2008; ASCE, 2010; Coelho and Mottram, 2015).

Research focusing on jointing method of pultruded GFRP tubular members has recently expanded to include innovative concepts to fully utilise the composite material's attributes including better torsional rigidity, relatively high load transfer, and improved strength and stiffness of the minor axis (Smith et al., 1998; DG9, 2004). Early efforts by Bank et al. (1994) had seen the improvement in the design of wrapped angle connection for pultruded frame structures. Monolithic cuff connections that are adhesively bonded to pultruded box members were introduced by Singamsethi et al. (2005) to create a simple beam-cuff-column frame. Similarly, this type of connection was also used in truss structure assembly of FRP tubular sections (Luo et al., 2016a). Another concept was introduced by Bai and Yang (2013) involving a novel connector using pultruded glass FRP box profiles which the authors claim provided satisfactory structural stiffness as analysed by simplified finite element modelling. This study was further expanded to assess the concept used in a large-scale space frame and its performance under fatigue (Yang et al., 2016; Yang et al., 2015). Another alternatives explored is using through-bolts to connect the pultruded GFRP tubular members. Luo et al. (2016b) and Hizam et al. (2013) have investigated the influence of bolted sleeve and mechanical insert, respectively, on through-bolt joint design, whereby significant improvements in term of joint resistance were observed. Further, for restricted accessibility for bolt tightening on tubular hollow shaped pultruded GFRP, Wu et al. (2015a) have successfully used a blind bolt as the connecting element as it only required one-sided access.

Bridge construction is one of the civil engineering applications where FRP tubular members are used as as main structural components, for instance, truss girders and decks. Generally, to provide better lateral stability and sufficient bending stiffness of the overall structural system, each side of the bridge decks is supported by pairs of

truss girders (Teixeira et al., 2014). However, the use of FRP closed sections tends to limit its joint configuration and architectural design, as certain design may introduce the effects of eccentricity during load transfer between the members of the structure (Righman et al., 2004). During the construction phase, some changes in design may be necessary due to unforeseen issues or constructional imperfections. For example, the connection system may potentially develop accidental load eccentricity, reducing the continuity and global structural performance (Teixeira et al., 2014; dos Santos and Morais, 2015). In regards to the truss structure, this eccentric load may weaken the joint compressive resistance and affect the stability of the truss's compressed chord members (Zaharia and Dubina, 2006). This is not a problem when using thin-walled steel sections as the members can be aligned and connected on a single plane. Most recent research studies on FRP connections have been focussing on concentrically loaded connections (Zhang et al., 2018b; Satavisam et al., 2017; Feroldi and Russo, 2016; Mara et al., 2016).

Studies on eccentrically compressed pultruded GFRP tubular members are limited and as such, their structural behaviour is not fully understood. This has been supported by the comprehensive review of Gand et al. (2013) which focussed on the developments of FRP closed sections, and the study of Mottram (2009) on the research gaps for connection design guidance, whereby the authors had outlined the behaviour of FRP tubular members under eccentric loading as one of the areas that need further research investigation. Nevertheless, a few published researches related to this topic were found to be on structural members with wide flange (WF) and I-section profiles. Structural members such as columns made up of pultruded GFRP were found to experience small unwarranted load eccentricity that restricts the establishment of universal design guidance (Lane and Mottram, 2002). Mottram et al. (2003) have attempted to address this problem on 'simple-braced' frames of pultruded WF cross-sections under the influence of combined compression and bending. The authors used conventional elastic theory to determine the major axis column behaviour under moment gradient. Another experimental study was conducted by Barbero and Turk (2000) on WF and I-sections of pultruded GFRP which were eccentrically loaded about the minor (weak) axis. It was reported that the main factors contributing to the beam-column failures were the eccentricity, the length of the tested members, and the specimen's geometrical and mechanical properties. A more recent study by Nunes et al. (2013) investigates the

structural behaviour of pultruded GFRP columns subjected to small eccentric loading about the major axis, both experimentally and numerically. The authors found that even small eccentricities can have a significant impact on the behaviour of these columns. While initially, the axial stiffness of eccentrically loaded columns is comparable to that of concentrically loaded ones, the effects of bowing and second-order $P-\delta$ effect have expedited the deterioration of stiffness at higher loads. It was also highlighted that the eccentricity was responsible for up to 40% of linear reduction in the load carrying capacity of the columns. Focusing on the jointing area of a pultruded GFRP structure, for bolted connection design, the loading directions and fasteners must be arranged in a concentric manner (ASCE, 2010). However, as mentioned above, eccentricity may be developed during practice, and the discrete load paths employed by bolted connection to transfer forces and moments may also influence the behaviour of a pultruded structure. Thus, the studies of bolted connections with pultruded FRP sections under eccentric loading is of high importance in order to fully understand its effects on the overall performance of the structure during practical applications. The selection of T-joint configurations in this study represents truss structural components whereby the behaviour of a centre member loaded along the parallel-to-fibre-direction and the supported side members loaded along the perpendicular-to-fibre direction are examined.

In this research paper, the behaviour of a pultruded GFRP bolted T-joint with a single bottom chord under eccentric loading is investigated. A comparison is made against another configuration that utilises double bottom chords which represents a more concentrically loaded joint. A through-bolt connection is employed in rectangular hollow section (RHS) pultruded GFRP. The paper also evaluates the effect of the mechanical insert on the joint strength of these configurations. The pultruded GFRP T-joint specimens are tested under tensile loading, and the failure behaviours are thoroughly investigated.

EXPERIMENTAL WORK

In the following sections, the material properties, jointing assembly, and experimental setup are described in detail.

Materials

The main structural components used in this study are made from rectangular pultruded GFRP tubular sections with a dimension of 100 mm x 75 mm x 5 mm. These rectangular hollow sections (RHS) were supplied by Wagners Composite Fibre Technologies (WCFT) in Toowoomba, Australia and were manufactured through pultrusion process using catalysed vinyl ester resin and E-glass fibre reinforcement. From the burn-out test conducted as per ASTM D3171 (2011), it was revealed that the pultruded GFRP laminates have a stacking sequence (Fig. 1) in the form of $[0/\pm 45/\bar{0}]_s$ with a high volume of fibre weight fraction of approximately 81%. Table 1 presents the mechanical properties determined through GFRP coupon specimens from 100 mm x 75 mm x 5 mm pultruded RHS.

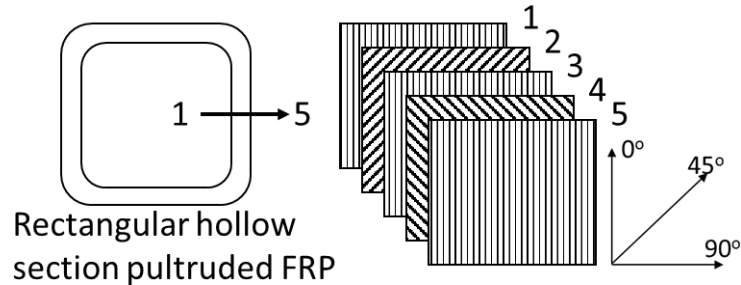


Figure 1: Pultruded GFRP stacking sequence.

Table 1. Mechanical properties of 100 mm x 75 mm x 5 mm RHS

Properties	5 mm plate	Test methods
Tensile Long ^a , Peak stress (MPa)	686.43 (44.21) ^c	
Tensile Long, Elastic modulus (MPa)	42,922 (2281)	ASTMD638 (2010)
Tensile Trans ^b , Peak stress (MPa)	46.84 (3.91)	
Tensile Trans, Elastic modulus (MPa)	12,198 (1,110)	
Compressive Long, Peak stress (MPa)	543.83 (43.95)	ASTMD695 (2010)
Compressive Trans, Peak stress (MPa)	147.70 (15.23)	
In-plane shear Long, Peak stress (MPa)	88.95 (14.64)	ASTMD5379 (2005)
Pin-bearing (Plain), Peak stress (MPa)	260.12 (55.66)	ASTMD953 (2010)
Pin-bearing (Thread), Peak stress (MPa)	185 (7.21)	
Fibre mass fraction, W_f	81.4%	ASTMD3171 (2011)
Fibre volume fraction, V_f	65%	
Density ^d (kg/m ³)	2030	

^aLongitudinal ^bTransverse

^cStandard deviation ^dWCFT product specification

Test specimens and jointing assembly details

In the experimental works, pultruded GFRP tubular profiles with a nominal dimension of 100 mm x 75 mm x 5 mm (Fig. 2) were used to form twelve (12) T-joint components. The total lengths of the vertical and bottom chord components were 500 mm and 650 mm, respectively. The bolt holes with approximately 22 mm nominal diameter were drilled on both sides of the thin-walled tubular pultruded GFRP. The vertical components have bolt holes at either end to fix onto both the testing equipment and bottom chord profiles. For bottom chord components, the bolt holes were drilled at the midspan of the chords. All these holes were carefully drilled using a diamond coated drill bit to control the diameter accuracy of the bolt hole and to minimise fibre damage as suggested by Persson et al. (1997).



Figure 2: Vertical components of pultruded GFRP T-joint.

The mechanical fasteners used were all-thread stainless steel (SS) 316 of 20 mm nominal diameter (M20) together with SS washers and nuts. This high strength all-thread bolts of property class 8.8 have the minimum tensile strength and shear strength of 830 MPa and 514.6 MPa, respectively. Table 2 presents the essential properties of the all-thread bolt in accordance with AS/NZS1252.1 (2016) and AS/NZS4291.2 (2016).

Table 2. Bolt types and its mechanical properties

Items	Specification
Property class:	8.8 (M20)
Minor diameter, Dc:	19.67 mm
Area of root of thread:	225 mm ²
Pitch, P mm:	2.50 mm
Minimum tensile strength:	830 MPa
Proof strength:	600 MPa
Minimum yield strength:	660 MPa
Minimum shear stress ^a :	514.6 MPa
Min. breaking load in single shear (Thread):	117 kN
Minimum bolt tension ^b :	145 kN

^aUltimate shear stress equals 62% of ultimate tensile strength ^bFull tightening

Tightening torque of 25 N.m as suggested by Manalo and Mutsuyoshi (2011) was applied to provide considerably lateral restraint as it can increase the joint strength and affect the displacement characteristic of the joint (Cooper and Turvey, 1995). Further,

to study the effect of the mechanical inserts on the T-joints, the WCFT mechanical inserts (Fig. 3) of 22 mm hole diameter were installed at the vicinity of the pultruded GFRP T-joint, filling its tubular interior. The inserts are made of thermoplastic alloy (TPA) composed of 49.35% short E-glass fibres, determined in accordance with ISO 1172 (ISO1172, 1996). The mechanical insert installation was done by WCFT using a special equipment, whereby the insert was pushed inside the RHS pultruded GFRP member, creating a tight-fit attachment. Next, the adhesive epoxy was injected and forced to fill the tight space between the insert and RHS walls. The insert performance was improved by providing stronger adhesion and leads to the increased of joint capacity of the pultruded GFRP.



Figure 3. WCFT’s mechanical bolt insert

In this study, four (4) experimental models were prepared and labelled as 1B-N, 2B-N, 1B-Ins, and 2B-Ins. The terms ‘1B’ and ‘2B’ stand for single bottom chord and double bottom chords, respectively, while terms ‘N’ and ‘Ins’ represent the T-joint without mechanical inserts and the T-joint with mechanical inserts, respectively. Table 3 provides a summary description of each experimental model. The pultruded GFRP T-joint with one bottom chord configuration was assembled to provide eccentricity during loading, whereas the pultruded GFRP T-joint with two bottom chords is often preferred for FRP bridge construction due to its balanced configuration (Keller et al., 2007a).

Table 3. Summary of RHS pultruded GFRP specimens.

Specimens	Description	No. of test
1B-N	T-joint with one bottom chord	3
1B-ins	T-joint with one bottom chord; with insert	3
2B-N	T-joint with two bottom chords	3
2B-ins	T-joint with two bottom chords; with insert	3

Figure 4 details out the front view and side view of pultruded GFRP T-joint components used in this experiment. It represents the 1B and 2B specimens where no inserts are installed at jointing area of the vertical and chord components. Figure 5, meanwhile, shows the detail locations of installed mechanical inserts in 1B-Ins and 2B-Ins. Both Figures 4 and 5 show the mechanical inserts were also installed at the other end of the vertical component. This provides a strengthening mechanism at the jointing area between the specimens and the testing equipment to ensure the failure will occur at the T-joints. In Figure 4, the joint geometry of e/d_b (end distance to bolt diameter) and w/d_b (plate width to bolt diameter) of the perpendicular elements of the T-joints are 2.5 and 3.5, respectively. These can be expressed as $e = 2.5d$ and $w = 3.5d$ which have met the minimum requirements as outlined (Table 4) in the Pre-Standard for Load and Resistance Factor Design (LFRD) (ASCE, 2010).

Table 4: Minimum requirements for bolted connection geometries.

Notation	Definition	Minimum required spacing (or distance in terms of bolt diameters)
$e_{1,min}^{[a]}$	End distance	Tension load
	Single row of bolts	$4d^{[a]}$
	Two or three bolt rows	$2d$
	End distance	Compression load
$e_{2,min}$	All connections	$2d$
	Edge distance / width	$1.5d$

Source: *Pre-Standard for Load and Resistance Factor Design (LFRD) of Pultruded FRP Structures*

Notes:

[a] d is the nominal diameter of bolt

[b] Minimum $e_{1,min}$ may be reduced to $2d$ when the connected member has a perpendicular element attached to the end that the connection force is acting towards.

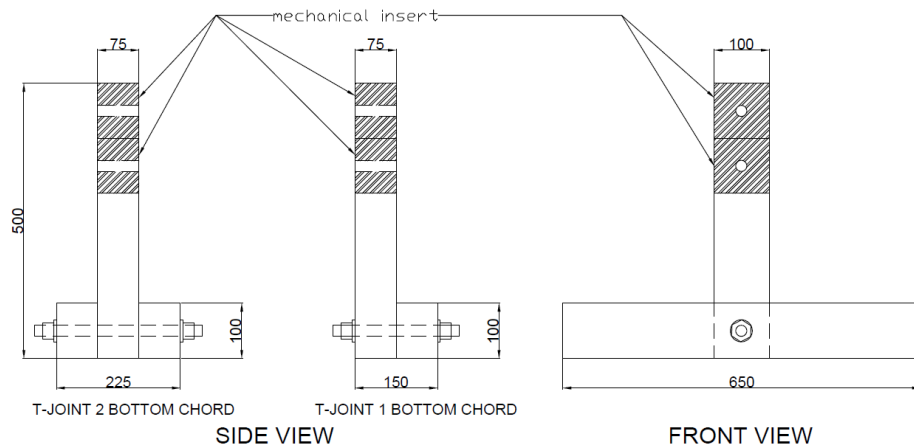


Figure 4. Pultruded GFRP T-joint bolted configurations (dimensional unit in mm)

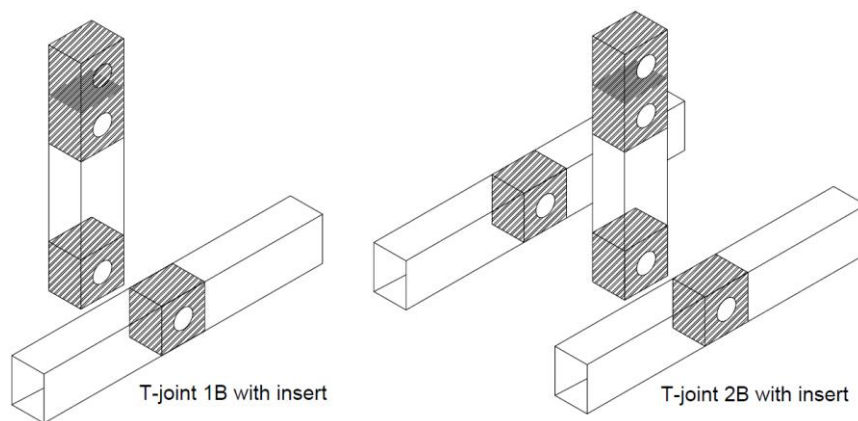


Figure 5. Pultruded GFRP T-joint with the mechanical inserts configuration

Test set-up and instrumentation

All pultruded GFRP bolted T-joint specimens were tested up to failure under axial (tensile) loading at P11 Structural Laboratory at the University of Southern Queensland (USQ). The testing program was conducted using a loading machine (Transducer Techniques, model SWO-50K) with a load capacity of 222 kN. A steel test fixture was specially designed and fabricated to mount the top end of the perpendicular members of the T-joint specimens to the loading machine. Prior to this, the top end of these members were drilled with two 22 mm diameter bolt holes and were fixed with inserts in order to produce stronger connection at the fitting point between the specimens and the loading machine. This will reduce the influence from

equipment errors on the failures that may occur at the joints of the specimens. Meanwhile, a machine test frame comprised of steel girders was used to restrain the specimen's bottom chords from moving upwards while tensile loading was applied. The detailed experimental setup is shown in Figure 6. Data logger (system 5000) was used to record the load applied and displacement. A draw-wire (string pot) displacement transducer with a sensitivity of 64.50 mV/V/inch was used to measure the overall displacement of the pultruded GFRP T-joint fixtures. Calibrations of those instrumentations were performed prior to the commencement of the testing program. The failure modes of each specimen were observed during loading and after the test had been completed.

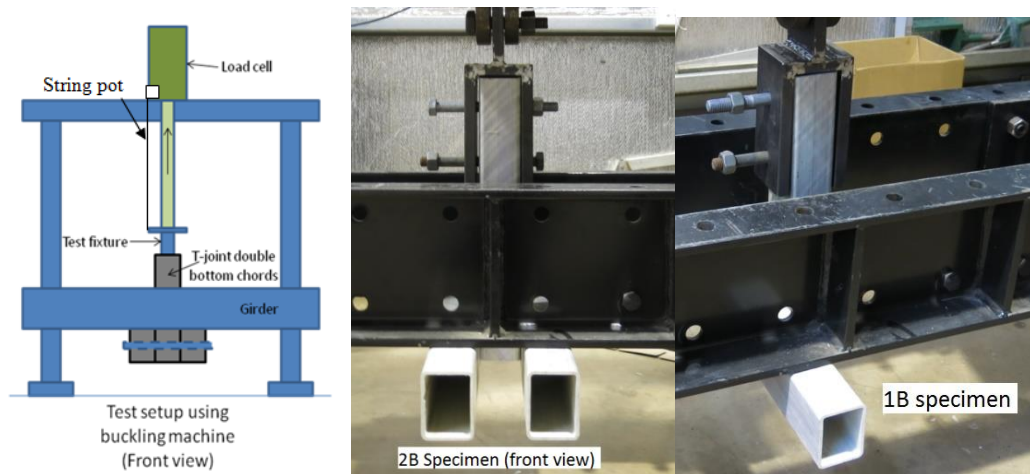


Figure 6: Pultruded GFRP T-joint experimental setup

TEST RESULTS AND DISCUSSION

Load-displacement

Table 5 presents a summary of the experimental results of rectangular pultruded GFRP T-joints under tensile loading with different bolted joint configurations. The results are presented in terms of average maximum joint load, average fixture displacement and initial fixture stiffness. The maximum load or peak load here is defined as the failure load due to significant damage observed when the curve reached this point. At the initial stage of loadings (from 0.8- 2.0 kN), bolt movement occurred due to the gaps present within the fixture components and this was recorded by the machine. As the

loading increases, the gaps were closed, and the load-displacement slopes appeared to be practically linear. Thus, the displacement data were presented with an offset of early displacement clearance. The initial fixture stiffness is determined from the gradient of the initial linear region of the curves, prior to the point where a noticeable decline in the curve slope is observed. This is known as the damage point.

Table 5: Summary of the experimental results

Specimens	Average max. load (kN)	Average fixture displacement (mm)	Average initial fixture stiffness (kN/mm)
1B-N	14.45 (1.41)	17.38 (1.50)	1.29 (0.18)
1B-Ins	46.43 (3.20)	26.50 (4.26)	2.26 (0.20)
2B-N	37.24 (1.76)	13.03 (0.94)	3.44 (0.79)
2B-Ins	78.23 (8.24)	20.44 (4.81)	4.45 (0.76)

Note: The numbers inside () are the standard deviations.

As shown in Table 5, specimen 1B-N obtained the lowest average joint capacity of 14.45 kN with an average displacement of 17.38 mm. This is followed by specimens 2B-N and 1B-Ins with 37.24 kN and 46.43 kN, respectively. Meanwhile, specimen 2B-Ins exhibited the highest average joint resistance load of 78.23 kN at an average displacement of 20.44 mm. It can be seen that the specimens with the mechanical inserts yielded higher load-carrying capacity irrespective of the bottom chord configurations. Figure 7 presents the typical load-displacement curves of one representative from each of the tested pultruded GFRP T-joint configurations. Specimens 1B-N and 2B-N experienced almost similar behaviour where initially, they show linear elastic characteristics up until the peak. After reaching the peak, the load-carrying capacity of 1B-N and 2B-N dropped gradually, followed by a progressively noticeable non-linear region until the end of load application. These descending non-linear lines present the continuous damage occurring at both the tubular members and joining region. Meanwhile, specimens 1B-Ins and 2B-Ins exhibited almost identical curve behaviour, with 2B-Ins showing steeper gradient which ended at a much higher peak. Both curves are initially characterised by a linear elastic region up until the peak load. It should be noted that 1B-Ins exhibited a damage load of approximately 33 kN which may be contributed by the fibre cracking at the vicinity of the joint due to the

unbalanced configuration. At the peak region, several knees response were observed before a sudden drop in the joint capacity, showing a brittle like mode of failure. The sharp loss of this joint capacity is caused by the sudden breakage of the mechanical insert, coupled with the crushing of fibre and resin matrix.

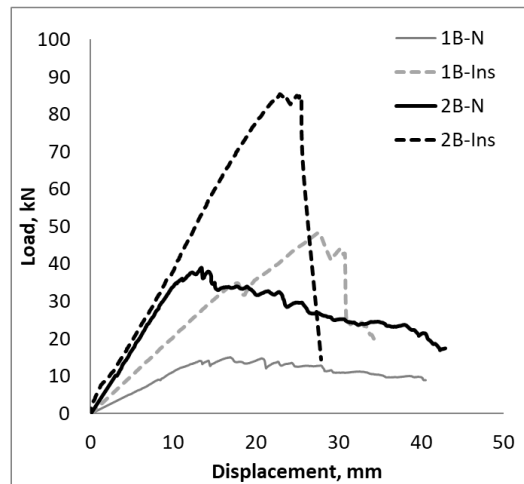


Figure 7. Average load-displacement curves of tested T-joints in all joint configurations.

As expected, with double bottom chord members, 2B-N and 2B-Ins showed higher joint strength of the pultruded GFRP T-joints by 158% and 68%, respectively when compared to that of 1B-N and 1B-Ins, respectively. On the other hand, with the mechanical insert fitted at 1B-Ins and 2B-Ins, it has improved the joint strength of the pultruded GFRP T-joint by 221% and 110%, respectively, when compared to that of 1B-N and 2B-N, respectively. Surprisingly, one bottom chord T-joint with mechanical insert surpassed the joint resistance of 2B-N by 25% but at the expense of higher displacement, which was about twice that of 2B-N. Clearly, by having both balanced T-joint configuration and insert reinforcement at the jointing area, it has positively influenced the structure's ability to resist the applied loading and significantly improved its overall load-carrying capacity.

Initial stiffness

Figure 8 shows the relationship of load-carrying capacity and stiffness of all tested pultruded GFRP T-joints. It also presents the comparison of joint load-carrying capacity between theoretical and experimental results for all specimens, which will be

discussed later in Theoretical assessment section. The stiffness presented was measured from the initial linear elastic slope of the load-displacement curves shown in Figure 7. As can be seen, with the presence of mechanical insert or double bottom chord members, or the combination of both, the pultruded GFRP T-joints exhibit reasonable improvement on its stiffness compared to that of 1B-N. This improvement of fixture stiffness of 75%, 167%, 245% was achieved by 1B-Ins, 2B-N, and 2B-Ins, respectively.

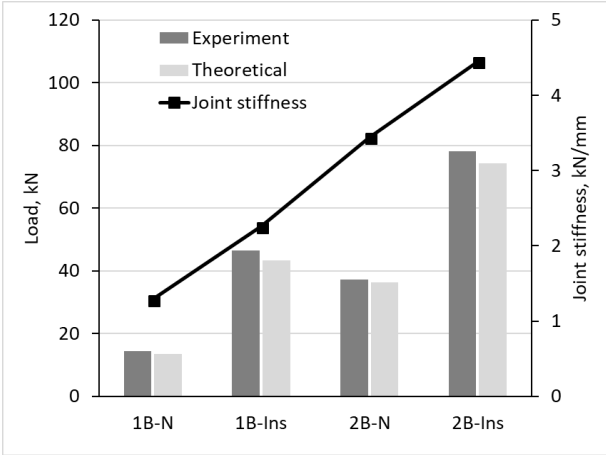


Figure 8. Comparison between load-carrying capacity (experiment and theoretical) and stiffness for each parameter.

With an imbalanced T-joint configuration, the introduction of mechanical insert has significantly lessened the effect of load eccentricity and the corresponding bending moment. This may be due to the full composite action achieved between the bonded insert and the pultruded GFRP which enabled the exploitation of its high glass fibre volume and contributed to the improved overall joint stiffness. Besides, with mechanical insert, better resistance was provided to the T-joint connection against bolt bearing and also prevented the web/flange buckling phenomenon induced by bending moment. It was apparent that 1B-Ins recorded higher maximum joint load of about 25% than that of 2B-N. However, the latter managed to promote higher stiffness of about 52% than that of the former, which suggests that the double bottom chord configuration responded better to the deformation of the overall structural assembly in response to the applied loading. In addition, under balanced loading (negligible joint

eccentricity), the unidirectional fibre properties composed in the pultruded GFRP were effectively utilised, therefore, this predominantly influenced the structural stiffness performance.

Failure mode

Figure 9 presents the typical mode of failure of the tested pultruded GFRP T-joint configurations subjected to tensile loading. The behaviour represents the post-failure condition whereby the applied load was maintained for an approximately 1 minute after reaching its maximum capacity. Once the tensile testing is completed, the pultruded GFRP T-joint components were disassembled to carefully examine the damages experienced by the pultruded GFRP members and the connection assembly (fastener and insert). Based on the overall observation, the primary failure of all tested specimens occurred at the vertical (centre) member and its joint, while the bottom chord or side member(s) only endured initial splitting or minor delamination of the surface plies near the hole region as shown in Fig. 9 a). In addition, all the bottom chord members of 1B-Ins, 2B-N and 2B-Ins were in excellent condition, and no damage was observed. The following discussion will focus more on the vertical members and its joint where the principal failure had been detected.

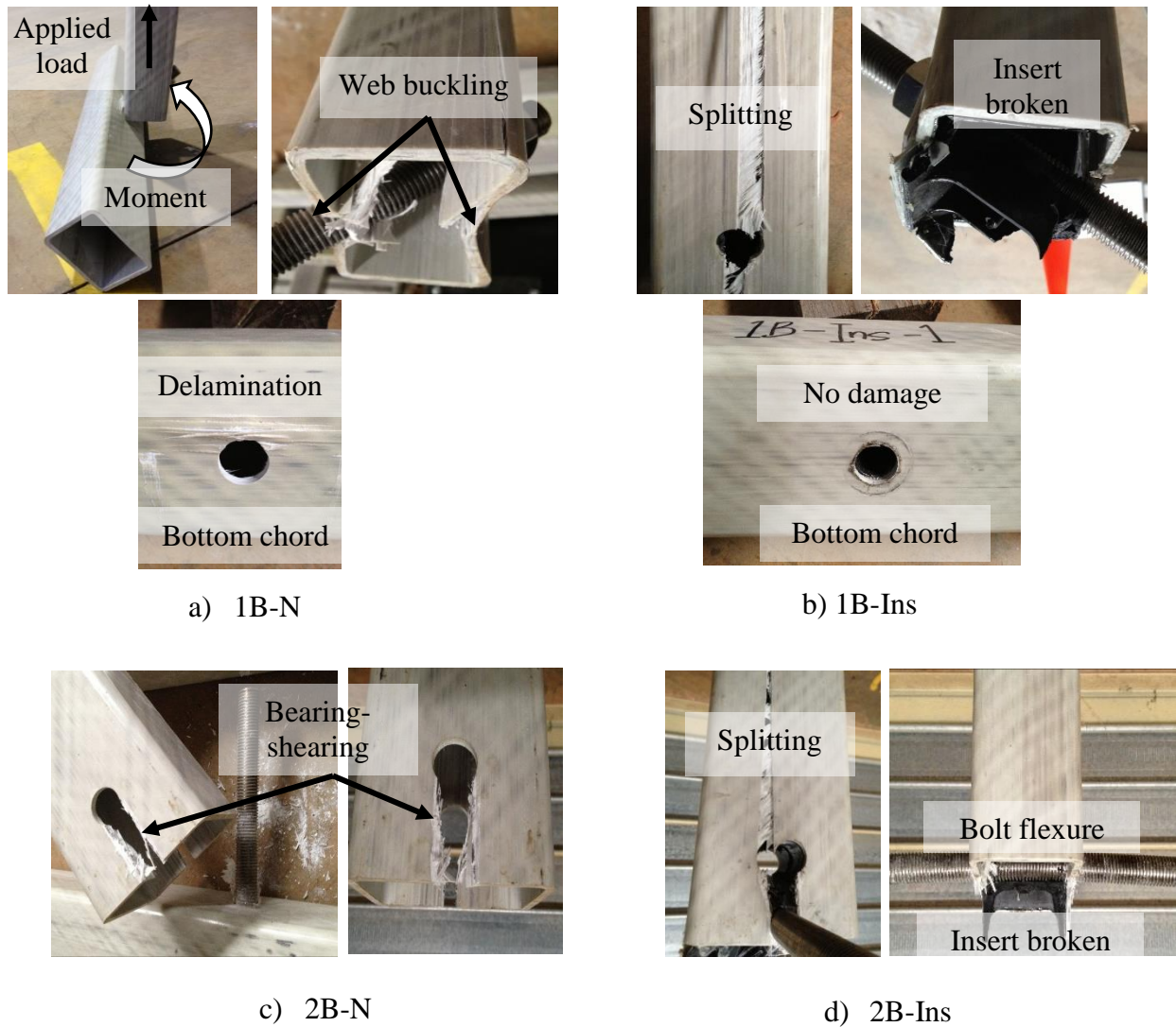


Figure 9. Typical failure modes achieved by the different pultruded GFRP T-joint configurations

Figures 9 a) and b) show the failure modes of pultruded GFRP T-joints under intended eccentricity. It is evidence that both pultruded thin-walled specimens, 1B-N and 1B-Ins suffered from local compression directly located at bolt hole region (at nut and washer side) which resulted from the moment-rotation of the bolt (approximately 40 degrees). However, a distinguishable difference of the final outcome was observed between the specimens, with and without mechanical insert at the joint area. The 1B-N vertical member exhibited apparent web buckling (causing the thin-walled to bend inwards) coupled with plies delamination which resulted from the steel nut and washer plate punching into the web. Another reason that induced the web to buckle instead of crushing failure is due to high slenderness ratio (web height divided by web thickness)

between 12.3 to 19.5 value based on the experimental findings by Wu and Bai (2014). Whereas, the failure on the other side of the thin wall was governed by bolt bearing-shearing failure along the shear planes. It was observed that the threaded bolt had vigorously crushed the fibre-matrix of the web.

Specimen 1B-Ins, on the contrary, promotes a better bending resistance whereby no evidence of web buckling was visible. This resistance to bending is influenced by the presence of mechanical insert that increased the structural member's area moment of inertia. At loadings higher than the capacity of 1B-N, it was noted that several loud cracks were audible at 45 kN followed by a sudden drop of load-carrying capacity. Due to the eccentric loading, the bolt was subjected to rotation which created uneven loading distribution along the bolt. This has developed a high concentrated compressive force locally around the bolt-end at A-B region (Fig. 10 b)), initiating fracture on the insert which occurred at approximately 33 kN as can be seen in Figure 7. Subsequently, the crack propagates along the insert-bolt hole line (A to C) until complete failure (Fig. 10 b). This reaction of the broken insert has developed an internal expansion force which simultaneously promotes sudden splitting transversely to the direction of the connection force. Also, the split propagation was quite prominent due to the material's low tensile strength in the transverse direction.

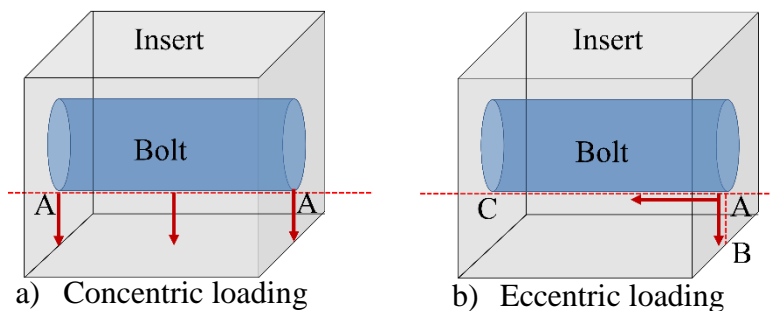


Figure 10. Failure mechanism of mechanical inserts under different loading conditions.

As for the balanced pultruded GFRP T-joint configuration of 2B-N and 2B-Ins, both sides of the pultruded GFRP thin walls endured identical deteriorations at the contact surface around the mechanical steel fastener. There was no visible damage induced by

bolt rotation and web buckling at its thin walls. 2B-N exhibited a more pseudo-ductile failure as reflected in their load-displacement curve (Fig. 7) with a progressive damage growth owing to the lateral restraint of the connection (Park, 2001). This helps delay the occurrence of ply delamination and fibre rupture. As the loading increases, the threaded bolt progressively damages the joint end distance and the final outcome of crushed fibres and matrix can be seen in Figure 9 c).

Specimen 2B-Ins, in contrast, experienced brittle compression directly below the contact point between the fastener and the pultruded GFRP elements. This is followed by a snapping sound which indicates the breakage of the mechanical insert (Fig. 9 d)). Due to the balanced configuration, the evenly distributed force has caused the bolt to compress and fracture the insert at the area along the insert-bolt hole region (line A-A) as shown in Figure 10 (a), before splitting the bottom part of the insert in half. Once the insert is fractured, stress transfer between the fasteners is no longer effective, and this is exhibited by a sharp drop in joint resistance of the specimens. It was also found that the threaded bolt endured minor bolt flexure which was evident from the difficulty faced while dismantling the T-joint components. This circumstance will be further assessed in the Theoretical assessment section of this paper. In addition, 2B-Ins exhibited almost similar response to that of 1B-Ins after reaching maximum load, whereby an internal failure of the mechanical insert had induced a high transverse expansion. This caused the pultruded GFRP laminate to crack, originating from the bolt hole boundary and then split towards the midspan in the transverse direction.

Effect of eccentric loading

Under pure axial tensile load, the testing specimens with double bottom chord configuration developed compressive stresses at the edge of the bolt holes which was evenly distributed across the rectangular hollow pultruded GFRP sections. However, with only one bottom chord, a couple moment was introduced which has to be resisted by the specimens, especially at the connection area. It should be noted that, with increasing eccentricity, higher magnitude of bending moment need to be resisted by the pultruded GFRP sections (Hadi, 2007; Dubina, 2008; Nunes et al., 2013) which will negatively impact their joint resistance against the axial loading. Without any mechanical inserts, the presence of eccentricity at the connection has decreased the overall joint resistance due to the localised bending moment acting on the joint, as well

as the loads that it is experiencing (such as bearing and shearing). Also, due to low compressive and shear strength in the transverse direction, the bending effect was exacerbated which caused the webs at the connection to be susceptible to the buckling action as discussed in failure mode section. Figure 11 shows the joint load carrying capacity under different loading conditions and joint configurations. Regardless of its bottom chord configuration, the pultruded GFRP T-joints with the mechanical inserts exhibited higher joint load-carrying capacity as much as 221% and 110% when compared to that of 1B-N and 2B-N, respectively.

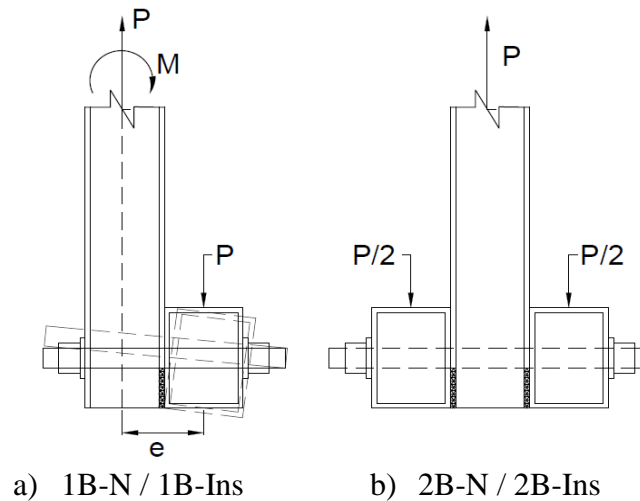


Figure 11. Loading distributions and affected joints area.

As can be seen for the 1B specimens, the mechanical insert had strengthened the pultruded GFRP hollow section against the developed bending moment resulted from eccentric loading. Several factors may have contributed to the improved performance of this connection. Firstly, the mechanical insert was installed at the weakest point of specimen 1B-Ins, which is at its connection region. This allows the forces, including the additional stresses developed due to eccentricity, to be transferred from the tubular side plates and the fastener to the mechanical insert, which is a stiffer and stronger structural element compared to the tubular thin-wall (Smith et al., 1998). Secondly, it increases the second area moment of inertia of the pultruded GFRP cross-section that is perpendicular to the axis of intended bending. With these considerable improvements, the pultruded GFRP section can further resist against web buckling and

web-flange junction fracture that may be resulted from the bending moment. As a result, the webs on the thin-walled pultruded GFRP remained intact and the section is stabilised against out of plane buckling up until failure, whereby the insert is finally crushed. Generally, embedding between the threaded fastener and fibrous materials (FRP or wood) would exhibit an initial non-linear load-displacement curve, and the materials are subjected to noticeable surface damages at the vicinity of the bolt holes (Hizam et al., 2018; dos Santos and Morais, 2015; Matharu and Mottram, 2012). However, based on the results obtained, the specimens with mechanical insert did not suffer from those shortcomings as discussed in Load-displacement and Initial stiffness sections. Interestingly, the mechanical insert may improve the joint bearing resistance against the embedment effect of the threaded bolt, as well as evenly distribute the stress around the hole edge.

THEORETICAL ASSESSMENT AND COMPARISON WITH EXPERIMENTAL RESULTS

Based on the allowable capacities of all-thread bolt stated in Table 2, the bolts were sufficiently reliable to retain the connection assembly and to transmit the loads between the connected members without undergoing any breakage, particularly fracture in shear. Failure mode section provides further evidence that no bolt fracture was observed, and all the threaded bolts were still in good condition. However, it was found that the bolt connecting 2B-Ins pultruded GFRP components was slightly bended which may be caused by the combination of tension and shear load acting along the 225 mm length of the bolt. Hence, in this specific case, flexural beam equation (Eq. 1) was used to predict the flexural strength of the threaded bolt. Based on the 2B-Ins joint configuration, the resulting stress was determined under the loads in four-point bending setup as follows:

$$\sigma_{b,f} = \frac{P_o(L-L_i)}{\pi.R^3} \quad (1)$$

where $\sigma_{b,f}$ = flexural strength of all-thread bolt (MPa); L = length of the bolt between its supports (mm); L_i = span between two loadings (mm); R = radius of all-thread bolt (mm); and P_o = 2B-Ins ultimate joint capacity (N).

Since there is no flexural strength data available from Table 2, due to material homogeneity, it is assumed that the bolt flexural strength will be similar to the bolt tensile strength. From Figure 4, the supports span (L) and loading span (L_i) was approximately determined as 150 mm and 75 mm, respectively. It was concluded that the calculated flexural strength of 977 MPa using Eq. 1 was 18% higher than that of the maximum tensile strength. This may have caused the all-thread bolt to endure permanent bending which agrees with the close visual findings at the connection region of 2B-Ins. Meanwhile, the bearing strength, R_{br} of specimen 2B-N was assessed based on the equation (Eq. 2) in the pre-standard for load & resistance factor design (LRFD) of pultruded FRP structures (ASCE 2011). The test specimen joint geometries were designed to fail by bearing failure with a larger w/d_b ratio of 5 and an e/d_b ratio of 2.5 (Ascione et al., 2010; Xiao and Ishikawa, 2005a; Cooper and Turvey, 1995). In addition, with the lateral clamping pressure applied to the bolted joint, it is expected that the specimens have higher joint bearing strength (Park, 2001) and improved capability to sustain post-failure loads.

$$R_{br} = t \cdot d \cdot F_{\theta}^{br} \quad (2)$$

$$P_o = 2 \cdot m \cdot R_{br} \quad (3)$$

where t = thickness of FRP material (mm); d = nominal diameter of bolt (mm); m = modification factor; F_{θ}^{br} = characteristic pin-bearing strength of FRP material (MPa) and R_{br} = joint bearing capacity (kN) and P_o = ultimate joint capacity (kN).

Table 6: Modification factor due to the presence of mechanical insert

m values	Joint configurations of pultruded GFRP tubular section
1.00	Single-bolted joint
1.40	Single-bolted joint with mechanical insert
2.00	Single-bolted joint with bonded mechanical insert

In calculating the joint bearing capacity, R_{br} , the characteristic of the threaded pin-bearing strength was applied as stated in Table 1. The measured F_{θ}^{br} threaded value (185 MPa) gives a close representation of the joint configuration setup, as it accounts

for the threaded effect on thin-walled pultruded GFRP. Next, Eq. (3) is employed to predict the joint load-carrying capacity of both 2B-N and 2B-Ins by multiplying the determined joint bearing capacity, R_{br} by 2 (two thin walls area affected by the bolt) as shown in Figure 11 (b) and its corresponding modification factor, m , as shown in Table 5. These m factors were computed by the authors from the quantitative relationship of the experimental results of sixty (60) single-bolted square section of pultruded GFRP profiles under different single-bolted joint configurations (Table 6).

The distributions of obtained results showed that the joint capacity of single-bolted joint with mechanical insert and with bonded mechanical insert were averagely increased by 40% and 100%, respectively, when compared to single-bolted joint without mechanical insert. Hence, for 2B-N and 2B-Ins, the m factors of 1 and 2, respectively, were used in Eq. (3).

$$\sigma_m = \frac{P_o}{m.A} + \frac{M.y}{I} \quad (4)$$

$$P_o = \frac{m.\sigma_m.A.I}{I+(m.e.y.A)} \quad (5)$$

where σ_m = maximum compressive stress of FRP material (MPa); A = cross-sectional area (mm^2); m = modification factor; I = area moment of inertia (mm^4); y = largest distance from the neutral axis (mm); M = couple moment (Nmm); e = eccentricity (mm); and P_o = ultimate joint capacity (N).

For 1B-N and 1B-Ins, a different theoretical approach is used due to the presence of couple moment generated by two parallel, but in opposite directions, axial forces that did not share a line of action as shown in Fig. 11 (a). In other words, couple moment is the product of two forces identical in magnitude (P) with a perpendicular distance between their lines of action (e is about 75 mm). In this assessment, Eq. (5) is applied to predict the joint load-carrying capacity of specimen 1B-N and 1B-Ins. This equation was formulated considering the combined axial and bending stress of Eq. (4), and by re-arranging the unknown P_o on one side of the equation. As observed in this study, the failure behaviour was governed by the compressive failure under the contact area between the bolt and the thin-walled pultruded GFRP. Thus, for the allowable stress, σ_m , the pin-bearing strength of pultruded GFRP is used in this evaluation. Another

important parameter in understanding the material resistance to bending is the area moment of inertia. It is also known as second moment of area which can be defined as a geometrical property of an area that is perpendicular to the axis of that intended bending. Specimens 1B-N and 1B-Ins have different values of second moment of area as a function of their shapes, whereby the latter contained a mechanical insert at the vicinity of its joint area. It should be noted that several assumptions were made while conducting this assessment, for instance, the test configuration is subjected to pure moment, the affected cross-section is a homogeneous material, and specimens remain on the same plane during bending.

Figure 8 presents the comparison of joint load-carrying capacity between theoretical and experimental results for all specimens. It can be seen that all the theoretical predictions based on Eq. (3) and Eq. (5) are slightly lower than the experimental data. The percentage differences between the theoretical and experimental values of 1B-N, 1B-Ins, 2B-N, and 2B-Ins are 6.78%, 6.63%, 2.28% and 4.96%, respectively. These marginal differences show that the conventional theoretical prediction equations incorporated with a modification factor are in good agreement with the experimental results. In fact, these equations have carefully included the effects of threaded bolt, mechanical insert and bending moment acting on the joint. Therefore, these predicted equations can be used as a preliminary calculation tool when evaluating the joint load-carrying capacity of pultruded GFRP tubular profiles under concentric or eccentric loading. However, it is important to note that the modification factors, m , are for these particular pultruded GFRP adopting its unique mechanical insert in single-bolted joint configurations.

CONCLUSION

This study investigated the effect of eccentric loading on the joint strength of rectangular pultruded GFRP tubular profile with different joint configurations. A total of twelve (12) pultruded GFRP T-joint components had been assembled using a through-threaded bolt, with or without the mechanical inserts installed at the vicinity of the joint areas. The specimens were tested under tensile loading and its joint performance, failure mechanism and theoretical predictions were evaluated. Based on the results of this study, the following conclusions have been drawn:

- The eccentric loading created by the single bottom chord in pultruded GFRP T-joint specimens had a negative impact on the joint resistance. The joint resistance of T-joint with one chord was only a third that of T-joint with double chords as a result of a couple moment developed from the eccentric loading. Due to the moment-rotation of the bolt, the vertical pultruded GFRP thin wall suffered from local compression directly located at the bolt hole region (at nut and washer side) and caused web buckling (bend inwards) coupled with apparent plies delamination. On the opposite of thin walls, the failure was governed by fibre and matrix crushing, occurring along the shear-out planes on the hole boundary.
- Pultruded GFRP T-joint with double bottom chords with or without mechanical inserts, exhibited reasonable improvement on stiffness compared to that of insert-less single bottom chord specimen, achieving improved fixture stiffness of 245%, 167%, respectively. This showed that the double bottom chord configuration responds better to the deformation of the overall structural assembly and effectively utilised the unidirectional fibre properties of the pultruded GFRP. Both specimens endured identical deteriorations at the contact surface around the mechanical fasteners and had no visible damage induced by bolt rotation and web buckling at the vicinity of the joint and the pultruded GFRP thin walls. Insert-less double bottom chord specimen exhibited a more pseudo-ductile failure with progressive damage owing to the lateral restraint of its connection, resulting in delayed ply delamination and fibre rupture. Meanwhile, with the presence of inserts, this configuration suffers brittle compression directly below the contact point between the fastener and the pultruded GFRP elements.
- The presence of mechanical inserts in both single and double bottom chords of the T-joints had improved the joint strength by 221% and 110%, respectively, when compared to their insert-less counterparts. This allows the forces, including the additional stresses developed due to eccentricity, to be transferred from the tubular side plates and the fastener to the mechanical insert. The insert that was installed within the hollow section of the pultruded GFRP has increased the area moment of inertia property of the configuration, and this contributed to the improvement in bending resistance. No evidence of flexural

deformation or web buckling was visible at its thin walls. The specimen exhibited brittle-failure behaviour at higher load, which failed due to the breaking of the insert.

- The theoretical equations considering the combined axial compression and bending stress and incorporating modification factors to consider the influence of mechanical insert on the predicted joint resistance of the specimens had shown good agreement with the experimental results. The difference between the theoretical and experimental joint strength is at a maximum 6.78% indicating that these equations can be used as a preliminary calculation tool when evaluating the joint load-carrying capacity of pultruded GFRP tubular profile under concentric or eccentric loading.

ACKNOWLEDGEMENTS

The first author gratefully acknowledges the Australian Commonwealth Government for the contribution through Research Training Program (RTP) scheme. The authors also gratefully acknowledge Wagner Composite Fibre Technologies (WCFT) for the testing materials supplied. Special thanks to Mr Wayne Crowell for his kind support and guidance during the experimental work.

REFERENCES

- [1] Satavisam S, Feng P, Bai Y, Caprani C. Composite actions within steel-FRP composite beam systems with novel blind bolt shear connections. *engineering Structures*. 2017;138:63-73.
- [2] Manalo A, Surendar S, Van Erp G, Benmokrane B. Flexural behavior of an FRP sandwich system with glass-fiber skins and a phenolic core at elevated in-service temperature. *Composite Structures*. 2016;152:96-105.
- [3] Keller T, Theodorou N, Vassilopoulos A, de Castro J. Effect of Natural Weathering on Durability of Pultruded Glass Fiber-Reinforced Bridge and Building Structures. *Journal of Composites for Construction*. 2015;20:04015025.
- [4] Correia JR, Bai Y, Keller T. A review of the fire behaviour of pultruded GFRP structural profiles for civil engineering applications. *Composite Structures*. 2015;127:267-87.
- [5] Uddin N, Abro AM. Design and manufacturing of low cost thermoplastic composite bridge superstructures. *engineering Structures*. 2008;30.
- [6] Manalo A, Aravinthan T, Fam A, Benmokrane B. State-of-the-Art Review on FRP Sandwich Systems for Lightweight Civil Infrastructure. *Journal of Composites for Construction*. 2017;21.
- [7] Keller T. Recent all-composite and hybrid fibre-reinforced polymer bridges and buildings. *Progress in Structural Engineering and Materials*. 2001;3:132-40.

- [8] Bai Y, Yang X. Novel joint for assembly of all-composite space truss structures: conceptual design and preliminary study. *Composites for Construction*. 2013;17:130-8.
- [9] Turvey GJ, Wang P. Failure of pultruded GRP single-bolt tension joints under hot-wet conditions. *Composite Structures*. 2007;77:514-20.
- [10] Hollaway LC. A review of the present and future utilisation of FRP composites in the civil infrastructure with reference to their important in-service properties. *Construction and Building Materials*. 2010;24:2419-45.
- [11] Omar T, Erp GV, Aravinthan T, Heldt T. Truss fibre deployable shelter. Australia: University of Southern Queensland, 2008.
- [12] Turvey GJ. Bolted connections in PFRP structures. *Progress in Structural Engineering and Materials*. 2000;2:146-56.
- [13] Bank LC. *Composites for Construction: Structural Design with FRP Materials*. New Jersey: John Wiley & Sons, Inc., 2006.
- [14] Mottram JT. Design Guidance for Bolted Connections in Structures of Pultruded Shapes: Gaps in Knowledge. 17th International Conference on Composite Materials. 2009;A1.
- [15] Mosallam AS. *Design Guide for FRP Composite Connections: American Society of Civil Engineers (ASCE)*, 2011.
- [16] Schmidt JW, Bennitz A, Täljsten B, Goltermann P, Pedersen H. Mechanical anchorage of FRP tendons – A literature review. *Construction and Building Materials*. 2012;32:110-21.
- [17] Min W. The finite element value simulation of composite bolt threaded nut contact and experimental study. China: Taiyuan University of Science and Technology, 2008.
- [18] Gand AK, Chan T-M, Mottram JT. Civil and structural engineering applications, recent trends, research and developments on pultruded fibre reinforced polymer closed sections: a review. *Frontiers of Structural and Civil Engineering*. 2013;7:227-44.
- [19] CNR. *Guide for the Design and Construction of Structures made of FRP Pultruded Elements*. Rome: National Research Council of Italy; 2008.
- [20] ASCE. *Pre-Standard for Load and Resistance Factor Design (LFRD) of Pultruded Fibre Reinforced Polymer (FRP) Structures*. 2010.
- [21] Coelho AMG, Mottram JT. A review of the behaviour and analysis of bolted connections and joints in pultruded fibre reinforced polymers. *Materials & Design*. 2015;74:86-107.
- [22] Smith SJ, Parsons ID, Hjelmstad KD. An experimental study of the behaviour of connection for pultruded GFRP- I beams and rectangular tubes. *Composites Structures*. 1998:281 - 90.
- [23] DG9. *Design guide 9: For Structural Hollow Section Column Connections*. Germany: The International Committee for Research and Technical Support for Hollow Section Structures (CIDECT); 2004.
- [24] Bank LC, Mosallam AS, McCoy GT. Design and performance of connections for pultruded frame structures. *Journal of Reinforced Plastics and Composites*. 1994;13:199-212.
- [25] Singamsethi SK, LaFave JM, Hjelmstad KD. Fabrication and Testing of Cuff Connection for GFRP Box Sections. *Journal of Composites for Construction*. 2005;9:536-44.
- [26] Luo FJ, Bai Y, Yang X, Lu Y. Bolted sleeve joints for connecting pultruded FRP tubular components. *Composites for Construction*. 2016;20:04015024.

- [27] Yang X, Bai Y, Luo FJ, Zhao XL, Ding F. Dynamic and fatigue performances of a large-scale space frame assembled using pultruded GFRP composites. *Composite Structures*. 2016;138:227-36.
- [28] Yang X, Bai Y, Ding F. Structural performance of a large-scale space frame assembled using pultruded GFRP composites. *Composite Structures*. 2015;133:986-96.
- [29] Luo FJ, Yang X, Bai Y. Member capacity of pultruded GFRP tubular profile with bolted sleeve joints for assembly of latticed structures. *Journal of Composites for Construction*. 2016;20:1-12.
- [30] Hizam RM, Karunasena W, Manalo AC. Effect of mechanical insert on the behaviour of pultruded reinforced polymer (FRP) bolted joint. *Fourth Asia-Pacific Conference on FRP in Structures (APFIS)*. Melbourne, Australia: International Institute for FRP in Construction (IIFC); 2013.
- [31] Wu C, Bai Y, Toby Mottram J. Effect of Elevated Temperatures on the Mechanical Performance of Pultruded FRP Joints with a Single Ordinary or Blind Bolt. *Journal of Composites for Construction*. 2015;20:04015045.
- [32] Teixeira AMAJ, Pfeil MS, Battista RC. Structural evaluation of a GFRP truss girder for deployable bridge. *Composites Structures*. 2014;110:29-38.
- [33] Righman J, Barth K, Davalos J. Development of an Efficient Connector System for Fiber Reinforced Polymer Bridge Decks to Steel Girders. *Journal of Composites for Construction*. 2004;8:279-88.
- [34] dos Santos CL, Morais JLL. Mechanical behaviour of wood T-joints. Experimental and numerical investigation. *Frattura ed Integrita Strutturale*. 2015;31:23-37.
- [35] Zaharia R, Dubina D. Stiffness of joints in bolted connected cold-formed steel trusses. *Constructional Steel Research*. 2006;62:240-9.
- [36] Zhang Z, Bai Y, Xiao X. Bonded sleeve connections for joining tubular glass fiber reinforced polymer beams and columns: an experimental and numerical study. *Composites for Construction*. 2018.
- [37] Feroldi F, Russo S. Structural Behavior of All-FRP Beam-Column Plate-Bolted Joints. *Journal of Composites for Construction*. 2016;20:04016004.
- [38] Mara V, Haghani R, Al-Emrani M. Improving the performance of bolted joints in composite structures using metal inserts. *Journal of composite materials*. 2016;50:3001-18.
- [39] Lane A, Mottram JT. The influence of modal coupling upon the buckling of concentrically pultruded fibre-reinforced plastic columns. *Proc Inst of Mechanical Engineers Part L: Journal of Materials - Design and Applications*. 2002;216:133-44.
- [40] Mottram JT, Brown ND, Anderson D. Buckling characteristics of pultruded glass fibre reinforced plastic columns under moment gradient. *Thin-Walled Structures*. 2003;41:619-38.
- [41] Barbero EJ, Turk M. Experimental investigation of beam-column behavior of pultruded structural shapes. *Reinforced Plastics and Composites*. 2000;19:249-65.
- [42] Nunes F, Correia M, Correia JR, Silvestre N, Moreira A. Experimental and numerical study on the structural behavior of eccentrically loaded GFRP columns. *Thin-Walled Structures*. 2013;72:175-87.
- [43] ASTM D3171. Standard Test Methods for Constituent Content of Composite Materials. American Society for Testing and Materials (ASTM) Standard; 2011.
- [44] ASTM D638. Standard test method for tensile properties of plastics. American Society for Testing and Materials (ASTM) Standard; 2010.

- [45] ASTM D695. Standard test method for compressive properties of rigid plastics. American Society for Testing and Materials (ASTM) Standard; 2010.
- [46] ASTM D5379. Standard test method for shear properties of composite materials by the V-notched beam method. American Society for Testing and Materials (ASTM) Standard; 2005.
- [47] ASTM D953. Standard Test Method for Bearing Strength of Plastics. American Society for Testing and Materials (ASTM) Standard; 2010.
- [48] Persson E, Eriksson I, Zackrisson L. Effects of hole machining defects on strength & fatigue life of composite. *Composites Part A: Applied Science and Manufacturing*. 1997;28A:141-51.
- [49] AS/NZS 1252.1. High-strength steel fastener assemblies for structural engineering - Bolts, nuts and washers: Part 1 - Technical requirements. Australian/New Zealand Standard; 2016.
- [50] AS/NZS 4291.2. Mechanical properties of fasteners made of carbon steel and alloy steel - Nuts with specified property classes - Coarse thread and fine pitch thread. Australian/New Zealand standard; 2016.
- [51] Manalo AC, Mutsuyoshi H. Behavior of fiber-reinforced composite beams with mechanical joints. *Journal of composite materials*. 2011;1-14.
- [52] Cooper C, Turvey GJ. Effects of joint geometry and bolt torque on the structural performance of single bolt tension joints in pultruded GRP sheet material. *Composite Structures*. 1995;32:217-26.
- [53] ISO 1172. Textile-glass-reinforced plastics, prepegs, moulding compounds and laminates: Determination of the textile-glass and mineral-filler content- Calcination methods. International Organization for Standardization (ISO); 1996.
- [54] Keller T, Bai Y, Vallée T. Long-Term Performance of a Glass Fiber-Reinforced Polymer Truss Bridge. *Journal of Composites for Construction*. 2007;11.
- [55] Wu C, Bai Y. Web crippling behaviour of pultruded glass fibre reinforced polymer sections. *Composite Structures*. 2014;108:789-800.
- [56] Park HJ. Effects of stacking sequence and clamping force on the bearing strengths of mechanically fastened joints in composite laminates. *Composite Structures*. 2001;53:213-21.
- [57] Hadi MNS. The behaviour of FRP wrapped HSC columns under different eccentric loads. *Composite Structures*. 2007;78:560-6.
- [58] Dubina D. Structural analysis and design assisted by testing of cold-formed steel structures. *Thin-Walled Structures*. 2008;46:741-64.
- [59] Hizam RM, Manalo AC, Karunasena W, Bai Y. Effect of bolt threads on the double lap joint strength of pultruded fibre reinforced polymer composite materials. *Construction and Building Materials (Accepted)*. 2018.
- [60] Matharu NS, Mottram JT. Laterally unrestrained bolt bearing strength: Plain pin and threaded values. 6th International Conference on FRP Composites in Civil Engineering. Rome, Italy 2012.
- [61] Ascione F, Feo L, Maceri F. On the pin-bearing failure load of GFRP bolted laminates: An experimental analysis on the influence of bolt diameter. *Composites Part B: Engineering*. 2010;41:482-90.
- [62] Xiao Y, Ishikawa T. Bearing strength and failure behavior of bolted composite joints (part I: Experimental investigation). *Composites Science and Technology*. 2005;65:1022-31.

6. Study on pultruded GFRP truss connection system

6.1. Article IV: Behaviour of pultruded GFRP truss system connected using through-bolt with mechanical insert

The results of **Article III** showed that the mechanical inserts had prevented bolt flexure and contributed to the improvement in bending resistance when subjected to a couple moment developed due to eccentricity. Also, the double-chord pultruded T-joint with bonded mechanical insert exhibited the highest joint strength and fixture stiffness compared to other configurations and therefore, it will be further investigated on its suitability in a truss structure. The structural and joint behaviour of double-chorded pultruded GFRP trusses connected using all-thread through-bolts with bonded mechanical inserts was evaluated and presented in **Article IV** which addressed the **fourth objective** of the study. Assembled trusses consisting of pultruded GFRP rectangular hollow section members, with adhesively bonded mechanical inserts installed within the hollow area of the joints were loaded under two different load conditions as shown in **Figure 4**. The trusses were tested under 4-point bending (Load Case 1) and 3-point bending (Load Case 2). From this experimental program, the load-vertical deflection behaviour of the truss, internal forces distribution in the members and joint behaviour were investigated and analysed. Based on the experimental results, the pultruded GFRP truss under Load Case 1 was capable of resisting the maximum load capacity of the testing equipment at 450 kN with the lowest factor of safety of 1.10 was attained by the external diagonal members. Meanwhile, the truss under Load Case 2 failed at 160 kN with the continuous top chords ruptured in flexural bending manner as shown in **Figure 7** of **Article IV**. The joints of the trusses were inspected upon unloading and it was concluded that the truss structures tested under both load cases did not suffer any major failure. The theoretical evaluation using both Strand7 modelling and strength limit equations proposed by ASCE pre-standard presented in **Theoretical assessment** section showed a good agreement with the experimental results. The theoretical evaluation incorporated the pin-bearing strength for bolt thread effects obtained from **Article I** and the modification factor of 2 for bonded mechanical

insert effects obtained from **Article II**. The factors have proven consistent in providing comparable values to the experimental outcomes. This experimental program, focussing on the interaction of pultruded GFRP connection system at a structural level, had addressed the main objective of this study and showed that the structural joint of pultruded GFRP hollow sections using a through-bolt connection with bonded mechanical insert is a promising connection system for GFRP in civil engineering applications

Behaviour of pultruded GFRP truss system connected using through-bolt with mechanical insert

R.M. Hizam ¹, Allan C. Manalo ^{1*}, Warna Karunasena ¹

¹Centre of Future Materials, Faculty of Health, Engineering and Sciences,
University Southern Queensland, QLD 4350, Australia.

*Corresponding Author:

Allan.manalo@usq.edu.au

Abstract

This paper presents the experimental and analytical studies of double-chord composite truss system connected using stainless steel through-bolts with mechanical inserts. The composite trusses were assembled using rectangular hollow sections of pultruded glass fibre reinforced polymer (GFRP) where adhesively bonded mechanical inserts were introduced at the vicinity of the joining areas. The trusses were tested under 4-point bending (Load Case 1) and 3-point bending (Load Case 2). From this experimental program, the load-vertical deflection behaviour of the truss, internal forces distribution in the members and joint behaviour were investigated. The pultruded GFRP truss under Load Case 1 was capable of resisting the maximum load capacity of the testing equipment at 450 kN with the lowest factor of safety of 1.10 was attained by the external diagonal members. High axial compression forces experienced by the external diagonal members has exceeded the American pre-standard theoretical joint bearing capacity by 2%, and this was reflected by the minor bearing damage observed on the joints of these members. Meanwhile, the truss under Load Case 2 failed at 160 kN with the continuous top chords ruptured in flexural bending manner. The satisfactory comparisons between the Strand 7 truss model and experimental results demonstrated the validity of the adopted simplified numerical model. Additionally, the theoretical strength limits of pultruded GFRP truss members in tension, compression and flexure according to American pre-standard are in close agreement with the experimental results.

KEYWORDS

Pultruded FRP, Truss, Tubular section, Hollow section, Bolted connection, Joint insert.

INTRODUCTION

Trusses in engineering refer to structures assembled using two-force members that behave in unison when loaded. These members are generally arranged in repetitive triangle patterns and are assumed to carry only axial loads, either in tension or compression. This structural form is widely used in the 19th century commonly to stiffen structures such as roofs, bridges and transmission towers as it provides dimensional simplicity and low material-to-weight ratio (Zaharia and Dubina, 2006; Omar et al., 2008). Traditionally, steel, concrete and timbers were extensively used for the construction of trusses, but with the recent development in material technology of fibre reinforced polymer (FRP) composites, it is now possible to construct lightweight FRP trusses. In particular, glass fibre reinforced polymer (GFRP) composites are preferred over carbon, aramid, and basalt due to its lower cost (Uddin and Abro, 2008; Manalo et al., 2017a). Other attractive properties of FRP include high strength-to-weight ratio, quick installation time, low maintenance requirements, superior corrosion resistance and electromagnetic neutrality (Gand et al., 2013; Coelho and Mottram, 2015). Pultrusion is a continuous manufacturing process that involves the pulling of multi-directional fibres through a bath of resin and heated die, producing constant cross-sections for instance, square and rectangular hollow sections, angles, standard I-beams, and channels (Carlone et al., 2006). This gives the GFRP material excellent unidirectional properties, compatible to transfer the axial loads in a truss system effectively. The high axial strength also contributes to low material usage in the truss production, offsetting the high material cost of FRPs compared to steel or timber (Plastics, 2002). Pultruded GFRP hollow closed sections or tubular profiles that mimics thin-walled metallic sections have received growing interest from the engineering community due to better torsional rigidity, effective resistance of out-of-plane forces, high load transfer and improved strength and stiffness of the minor axis (Smith et al., 1998; DG9, 2004); therefore, are more preferable as girder elements compared to FRPs fabricated through moulding or filament winding.

However, despite these advantageous characteristics, there seems to be some reluctance in the widespread use of pultruded GFRP among civil engineering practitioners due to several drawbacks. One of the significant issues is pertaining to the inadequacy or unpredictability of the connection system of structures made from pultruded GFRP members (Mottram, 2009; Mosallam, 2011; Turvey, 2000). The connection system or joints in trusses are assumed to be frictionless hinges or pins to allow slight rotations of members, creating a stable shape or configuration. Thus, it is a critical area to be considered in determining the overall structural performance and integrity of a truss system. Generally, there are three common techniques used to connect FRP structural members, i.e. bolted joint, adhesively bonded and a combination of both (Hizam et al., 2012). Early works conducted on investigating suitable connection methods for pultruded components were based around bolted joints due to its low cost, ease of installation and removal, and design familiarity (Turvey, 2000; Bank, 2006; Mottram, 2009; Mosallam, 2011). Also, Zhou and Keller (2006) have stressed that the holes for bolting should be drilled using diamond tipped bits to minimise the breaking of glass fibres and to avoid local stress concentration at the bolt-hole region. A combination of both bolting and adhesive bonding is seen to be a more reliable method, incorporating strengths from both connecting elements thus providing excellent joint performance as reported by Manalo and Mutsuyoshi (2011). The mechanical properties of pultruded GFRPs are more sensitive to the change in different load conditions as compared to steel especially on its joint bearing capacity, due to its multi-layered orthotropic behaviour (Pfeil et al., 2009; Vangrimde and Boukhili, 2003; Pisano and Fuschi, 2011). As in the case of pultruded GFRP structural frame applications, bolted joint designs based on steel practice may not be applicable due to lack of optimisation concerning its joint strength and stiffness.

The design and construction of FRP trusses will be influenced by the types and cross sections of the FRP materials used, as well as the truss configuration required. Therefore, the jointing techniques employed must be adapted to meet the construction demands. Thus, it is essential to investigate the system behaviour of FRP trusses and its connections to produce a safe and economical design. Presently, extensive research in understanding the behaviour of pultruded GFRP with different connection techniques such as mechanical fasteners and adhesively bonded at components (coupons) level have been carried out (Lau et al., 2012; Coelho and Mottram, 2015;

Boyd et al., 2004; Hashim and Nisar, 2013; de Castro and Keller, 2008; Lee et al., 2015). However, the authors have found only a handful of literature focussing on the interaction of pultruded GFRP connection system at a structural level. It was concluded from the review paper that further research work needs to be carried out to explore innovative joint systems of truss structures to improve load-bearing capacity and mechanical behaviour (Hizam et al., 2012). Previously, for FRP truss system, several jointing concepts were examined which include the award-winning snap joint for overhead transmission tower produced by Goldsworthy and Hiel (1998), and the introduction of Monocoque Fibre Composite (MFC) concept by Humphreys et al. (1999). Other studies on jointing concepts of trusses also included modular composite truss panel concept with integrated connection system by Bradford (2004) and the mechanically fastened and adhesive bonded all-FRP composite Pontresina pedestrian bridge by Keller et al. (2007a). The research area also expands to newer FRP truss applications that take advantage of the light-weight components, for instance, deployable military modular shelters (Omar et al., 2007), truss modules for dismountable bridges (Pfeil et al., 2009) and truss girders for deployable bridge (Teixeira et al., 2014). More recent studies in regards to pultruded GFRP tubular section connection are the investigation of conceptual novel connector for large-space frame (Bai and Yang, 2013; Yang et al., 2015) and the assessment of bolted sleeve joints for assembly of latticed structures (Luo et al., 2016a; Luo et al., 2016b). Further, for limited accessibility for bolt tightening on tubular hollow shapes pultruded GFRP, Wu et al. (2015a) and Satavisam et al. (2017) have successfully used the blind bolt as the connecting element as it only required one-sided access.

In this current study, a bolted connection system using through-bolt or all-thread rod is adopted for truss structures consisting of pultruded GFRP hollow section members. In large-scale constructions of structural truss system such as cooling towers, transmission towers and bridges, the use of all-thread bolt for connection is important to speed up the construction progress and improve construction efficiency. Apart from that, it can reduce the number of different bolt sizes on site which results in better stock holding and minimising installation errors. The use of mechanical insert and lateral restraint were also introduced as additional jointing elements, which were developed to support and alleviate the presence of threads that could mainly affect the bolted joint performance (Hizam et al., 2013; Hizam et al., 2018). It also increases joint stiffness

by filling in the gaps of the tubular sections. The mechanical connection is achieved through the hollow part of the insert, which in most cases is threaded but can also be an unthreaded clearance hole for a through-the-thickness type insert (ECSS, 2011). Although inserts have been widely used in the aerospace industry, little result has been published for civil construction (Humphreys, 2003). As per previous studies conducted by the authors, it was found that an insert-less connection system for the same pultruded GFRP member yields 20% lower joint strength compared to samples with mechanical inserts. By applying epoxy adhesive between the inserts and the pultruded GFRP inner walls, a further 55% increment in joint strength was achieved as the bonding prevented slippage of the inserts during loading, resulting in effective shear load transfer from the insert to the surrounding pultruded GFRP walls. Based on these previous findings, the current study incorporated both the mechanical insert and the adhesive resin in the connection system of the truss, as well as stainless steel through-bolts as mechanical fasteners.

In this paper, 1 m span composite trusses were constructed by assembling pultruded FRP hollow sections into a double chord configuration using stainless steel bolted joints. Adhesive bonded mechanical inserts were installed at the vicinity of the bolted areas, within the inner walls of the hollow sections. Two load cases were applied at the top chords of the trusses and the overall system behaviour (vertical displacement and axial forces), as well as the local behaviour of its connections, were investigated using experimental and theoretical approaches. The results are presented and discussed in order to analyse the effectiveness of the proposed connection system on the double-chorded pultruded GFRP truss structure.

EXPERIMENTAL PROGRAM

Truss configuration

As for the configuration, a double chord truss system was used in this study due to the constraint in joint design provided by the pultruded GFRP hollow sections. This type of configuration has previously been used for steel and concrete trusses. Early finite element study on planar tabular steel trusses consisting of rectangular hollow sections showed that double chord trusses outperform their single chord counterparts unless stiffening plates were utilised to provide comparable end moments of members (Mirza

et al., 1982; Shehata et al., 1987). Additionally, for the same RHS material, Korol (1986) concluded that double-chord arrangement for both K and T-joints have higher joint strength and stiffness than the single-chord arrangement. The spacing apart of the double chords also provides lateral stability, reducing the need for bracing. The current authors also observed this improvement in joint performance of double-chord configuration on a preliminary study performed on T-joints of pultruded GFRP rectangular hollow sections. It was found that the joint resistance of T-joint with one chord was only a third that of T-joint with double chords as a result of a couple moment developed from the eccentric loading. With the insert incorporated into the double chord T-joint, the joint stiffness is 245% higher than the single chord insert-less joint. Therefore, this current study intends to expand these findings on individual double chord T-joints to an overall structural performance of a truss system.

Materials properties

The main experimental program carried out in this study involves load compression testing of an FRP truss system. The material used for all truss members is pultruded GFRP rectangular hollow sections with a dimension of 100 mm x 75 mm x 5 mm. It has a density of 2030 kg/m³ and a gross section area of 1580 mm². These structural components were supplied by Wagners Composite Fibre Technologies (WCFT) in Toowoomba, Australia and were manufactured through pultrusion process. Pultrusion, performed in WCFT's factory, involves the pulling of multi-directional E-glass fibres through a bath of vinyl ester resin and heated die, giving a constant final shape. Coupon specimens were extracted from this GFRP material and tests were conducted to determine its mechanical properties as presented in Table 1. According to ASTM 3171 (ASTMD3171, 2011), a burn-out test revealed the fibre weight fraction and fibre volume fraction of the GFRP material to be 81.5% and 65%, respectively, as well as its stacking sequence of [0°/+45°/0°/-45°/0°] as shown in Figure 1. The higher contents of continuous unidirectional fibres (0°) contributes to the high tensile strength and elastic modulus of this GFRP material.

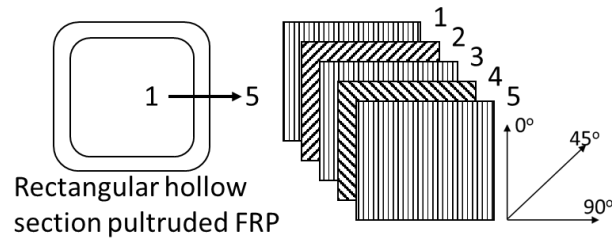


Figure 1. Pultruded GFRP stacking sequence

Table 1. Mechanical properties of 100 mm X 75 mm X 5 mm.

Properties	Notation	5 mm plate	Test method
Tensile Long ^a , Peak stress (MPa)	f_{Lt}	686.43 (44.21) ^c	
Tensile Long, Elastic modulus (GPa)	E_{Lt}	42.92 (2.28)	ASTM D638 (ASTMD638, 2010)
Poisson's Ratio Long	ν_L	0.30 (0.02)	
Tensile Trans ^b , Peak stress (MPa)	f_{Tt}	46.84 (3.91)	
Tensile Trans, Elastic modulus (GPa)	E_{Tt}	12.19 (1.11)	
Poisson's Ratio Trans	ν_T	0.15 (0.07)	
Compressive Long, Peak stress (MPa)	f_{Lc}	543.83 (43.95)	ASTM D695
Compressive Long, Elastic modulus (GPa)	E_{Lc}	39.59 (1.71)	(ASTMD695, 2010)
Compressive Trans, Peak stress (MPa)	f_{Tc}	147.70 (15.23)	
Compressive Trans, Elastic modulus (GPa)	E_{Tc}	14.76 (1.55)	
In-plane shear, Peak stress (MPa)	f_{Lv}	88.95 (14.64)	ASTM D5379 (ASTMD5379, 2005)
In-plane shear, Elastic modulus (GPa)	G_L	5.42 (0.23)	
Pin-bearing (Plain), Peak stress (MPa)	$f_{br,plain}$	260	ASTM D953 (ASTMD953, 2010)
Pin-bearing (Thread), Peak stress (MPa)	$f_{br,thread}$	185	

^aLongitudinal ^bTransverse ^cStandard deviation

Connection components

The GFRP members were connected through a jointing system that consists of through-bolts and adhesive bonded mechanical inserts which were installed in the vicinity of every joint in the truss structure. These mechanical inserts are expected to provide improved joint strength, and consequently, the overall performance of the GFRP truss system. The main connection components are the 20 mm diameter all-thread bolt which are made of stainless steel (SS). These are high strength all-thread structural bolts suitable for pultruded GFRP box section as in accordance to Australian

standard AS 1252:1996 (AS/NZS1252:1996, 1996b) and AS 1110:1995 (AS/NZS1110:1995, 1995). Furthermore, these bolts meet the requirement of a minimum yield strength of 372 MPa (54 ksi) to give an adequate margin of safety against slippage of the connected parts when sufficiently tightened as stated in Guide to Design Criteria for Bolted and Riveted Joints (AISC, 2001). Table 2 shows the bolt strength properties for Class 8.8.

Table 2. Bolt types and its mechanical properties.

Items	Specification
Property class:	8.8 (M20)
Minor diameter, D _c :	19.67 mm
Area of root of thread:	225 mm ²
Pitch, P:	2.50 mm
Minimum tensile strength:	830 MPa
Proof strength:	600 MPa
Minimum yield strength:	660 MPa
Minimum shear stress ^a :	514.6 MPa
Min. breaking load in single shear (Thread):	117 kN
Minimum bolt tension ^b :	145 kN

^aUltimate shear stress equals 62% of ultimate tensile strength ^bFull tightening

Mechanical inserts with 22 mm bolt holes, also known as anti-crush inserts, were installed at the bolted areas in the hollow sections of the GFRP to provide further joint strengthening. These inserts as shown in Figure 2 were moulded in WCFT’s factory from thermoplastic alloy (TPA) filled with approximately 49.35% of short glass fibres, determined in accordance with ISO 1172 (ISO1172, 1996).



Figure 2. WCFT’s mechanical bolt insert

An adhesive resin is applied at the insert-GFRP interface to provide bonding for higher joint stability and effective load transfer between the mechanical inserts and the inner-walls of the GFRP members. The adhesive resin used is an epoxy-based called Techniglu-HP R26 supplied by ATL Composites Pty. Ltd. Table 3 presents the related mechanical properties of the adhesive used in this study.

Table 3. Properties of Techniglu-HP R26 (WCFT, 2016).

Properties	Value	Test method
Tensile strength	34.1 MPa	ISO 527-2 (ISO527-2, 1996)
Tensile modulus	2409 MPa	ISO 527-2 (ISO527-2, 1996)
Lap shear strength	11.9 MPa	ASTM D3163 (ASTMD3163-01, 2014)
Heat deflection temperature	85°C	ISO 75-1 (ISO75-1, 2004)

Notes:

3. The values in the table are based on a cure schedule of 24 hrs at ambient and 8 hrs at 80°C.
4. The values in the table are the design values to be used in normal ambient conditions. It does not include adjustment factors to account for temperature, humidity and chemical environments

Structural assembly

For the assembly of the truss, the pultruded GFRP rectangular hollow sections of 100 mm x 75 x 5 mm were used as truss members and connected using through-bolts with bonded mechanical inserts in a configuration as shown in Figure 3a. A symmetrical double chorded truss configuration was used to provide balance load transfer and eliminate eccentricity effects (Ragheb, 2010). The hollow sections used as continuous chords and diagonal members provide better stability and buckling resistance, especially in the vertical plane of the truss (Smith et al., 1998; Wu et al., 2015b). However, by using hollow sections for double chorded truss, the through-bolt adopted may be subjected to high bolt flexure, affecting the bearing stress across the thickness of the joint component (ASCE, 2010). To alleviate this issue, the use of the mechanical inserts at the vicinity of the connection area is expected to support the bolts from flexural failure. To build the truss structure, the pultruded GFRP were cut into two members with lengths of 765 mm for the top chords and two members with lengths of 1130 mm for the bottom chords. The length of the middle vertical member was 600

mm while the length of all diagonal members was 625 mm. Ten bolt holes with a diameter of 22 mm were drilled in each side of the pultruded FRP hollow sections at the location shown in Figure 3b, with a 50 mm distance from hole centres to the edge of the pultruded RHS profile. The detailed joint geometry of e/d_b (end distance to bolt diameter) and w/d_b (plate width to bolt diameter) adopted at pultruded truss members are 2.5 and 3.5, respectively. These can be expressed as $e = 2.5d$ and $w = 3.5d$ which have met the minimum requirements as outlined (Table 4) in the ASCE Pre-Standard for Load and Resistance Factor Design (LRFD) (ASCE, 2010).

Table 4: Minimum requirements for bolted connection geometries.

Notation	Definition	Minimum required spacing (or distance in terms of bolt diameters)
$e_{1,min}^{[b]}$	End distance	Tension load
	Single row of bolts	$4d^{[a]}$
	Two or three bolt rows	$2d$
	End distance	Compression load
	All connections	$2d$
$e_{2,min}$	Edge distance / width	$1.5d$

Source: *Pre-Standard for Load and Resistance Factor Design (LRFD) of Pultruded FRP Structures*

Notes:

[a] d is the nominal diameter of bolt

[b] Minimum $e_{1,min}$ may be reduced to $2d$ when the connected member has a perpendicular element attached to the end that the connection force is acting towards.

The truss members were assembled using M20 stainless steel all-thread bolts with a length of 275 mm, which is sufficiently long to pass through the thickness of the double chords as well as the diagonal/vertical members. It is important to control the bolt placement when assembling the pultruded GFRP truss structures to lessen poor redistribution of stresses due to lack of fit (Feroldi and Russo, 2016). Thus, a tightening torque of 25 N.m as suggested by Manalo and Mutsuyoshi (2011) was applied to

provide considerably lateral restraint as it can increase the joint strength and affect the displacement characteristic of the joint (Cooper and Turvey, 1995). Also, this lateral clamping pressure can provide compressive resistance between the double chord members and minimise bolt slippage. Finally, two (2) pultruded GFRP truss structures were assembled to be tested with different load cases.

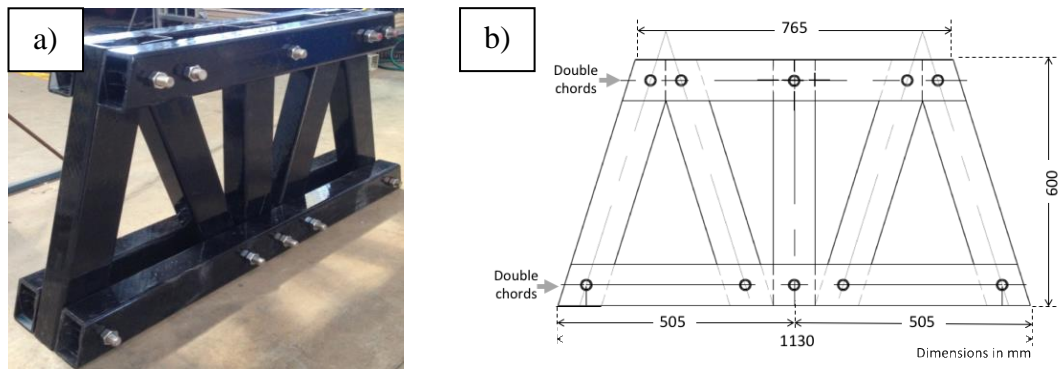


Figure 3. Double chord pultruded GFRP truss

Experimental setup

The composite truss system was simply supported and tested at different load conditions as shown in Figure 4. For Load Case 1 (LC1), the pultruded FRP composite truss was tested in uniaxial compressive loading under 4-point bending configuration as presented in Figure 4a. The load cell of 450 kN capacity was applied manually using a hydraulic jack and transmitted evenly by a load distribution frame at the left and right joints of the top chords (Joints B and F). For Load Case 2 (LC2), using the same test setup (refer Figure 4b), only one continuous point load was applied at the centre of the top chords (Joint A) until complete failure was achieved. A 10 mm rubber pad was placed under the point load to better distribute the load to the joint and to avoid direct contact between load cell and the pultruded material which could be damaging.

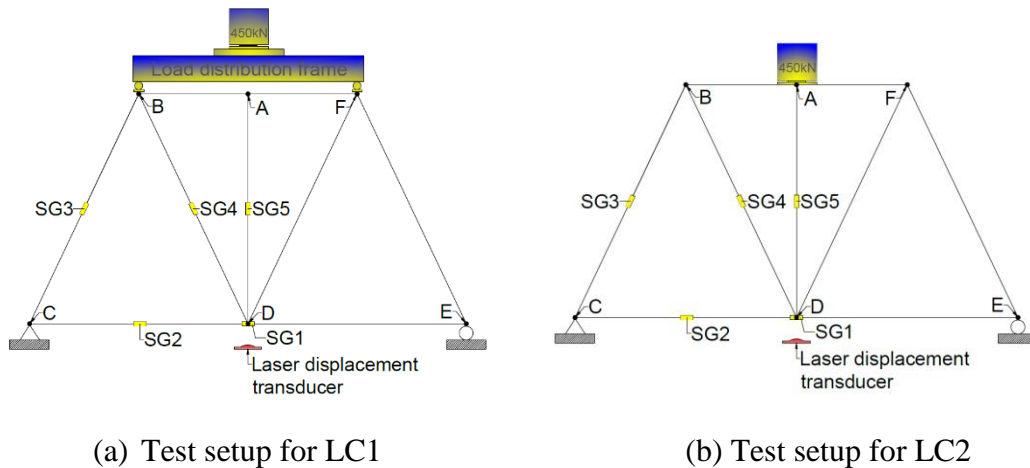


Figure 4. Experimental setup and instrumentation of pultruded GFRP truss

In both load cases, a laser displacement transducer was placed at the centre of the bottom chords and vertical displacements of the trusses were recorded during loading. To measure the strains of the FRP members throughout the test of LC1, five (5) strain gauges (SG) were fixed onto the members as shown in Figure 4b. It should be noted that only members connected between nodes A-B-C-D were evaluated in this study. As the truss is symmetrical, the same results were expected for members in between nodes A-F-E-D. After the tests were completed, the pultruded FRP trusses were disassembled to carefully observe any physical damages at jointing areas, including the all-thread bolts, adhesive resins and mechanical inserts.

RESULTS AND DISCUSSION

Load-deflection behaviour

The applied load and the vertical deflection measured (positive downwards) at the mid-span of the trusses were recorded throughout the loading process. Figures 5a and 5b exhibit the deflection behaviour under LC1 and LC2, respectively, presenting the full deflection data recorded by the laser displacement transducer, the deflection data with an offset of early displacement clearance and the theoretical displacement obtained from Strand7 finite element software. The latter will be discussed further in Through-bolt connection with mechanical insert section. Under LC1, the structural pultruded GFRP truss members remained physically undamaged as the maximum capacity of the equipment of 450 kN is reached, although a decline in stiffness was apparent prior to this. This indicates that the adopted through-bolt connections with mechanical insert

are capable to sustain higher joint load-carrying capacity and adequately transmitted the internal forces to other members by providing a uniform stress distribution along the length of the members. As shown in Figures 5a and 5b, four apparent stages could be identified based on the slope transition of the curve. These stages demonstrate the common behaviour of bolted joints of structures subjected to compression loading (AISC, 2001).

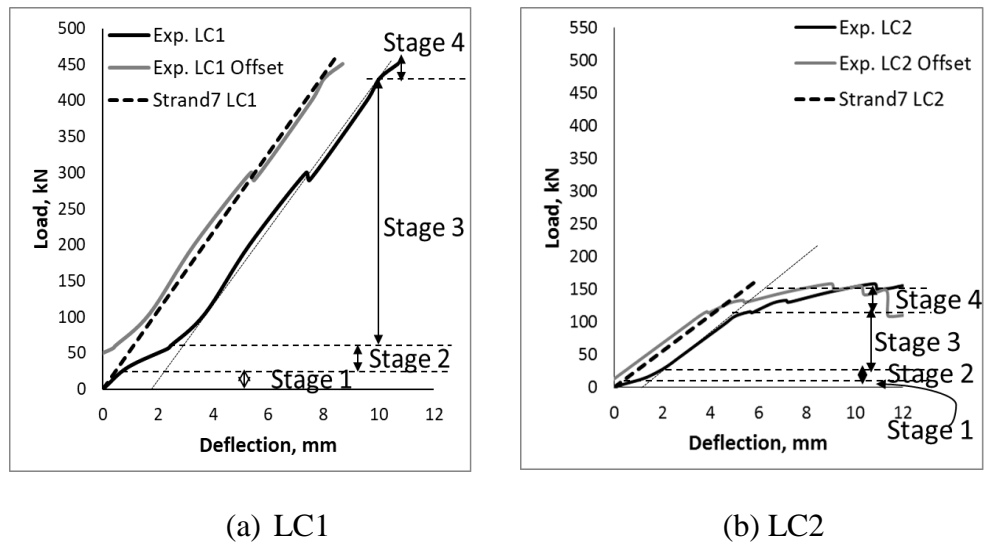


Figure 5. Load-vertical deflection (experimental and theoretical) at mid-span of the truss

Stage 1: shows a linear response to the lower loadings as the residual clamping force of the connectors were slowly overcome, however, slip of bolts were prevented due to static friction. *Stage 2:* The load has now exceeded the frictional resistance causing bolts to slip into bearing. Two factors influence this bolt slip; clearance slip and deformation slip. Clearance slip refers to the maximum clearance between the bolts and the bolt holes. As the bolt diameter is 20 mm, while the holes drilled on the GFRP members and mechanical inserts were 22 mm, it is expected that the maximum clearance of 2 mm would contribute to this slip with the assumption that the bolt shank is not centrally located within the holes of the connecting members. Additionally, slip deformation may also occur which is contributed by the distortion of bolts and members during that initial loading. A study performed by Ungkurapinan (2000) on individual joints showed that as the numbers of bolts per joint increased, the load required to enter stage 2 would also be higher. The author reported for a single joint with four bolts, the joint will fully slip at 46.95 kN and ideally remain constant for a

maximum slippage of 2.21 mm. For this current study, as there are multiple joints involved, for LC1, a higher load of approximately 65 kN was required to cause full slippage of 2.2 mm but is more progressive in nature due to overlapping effects between stages. Meanwhile, under LC2, the different distribution of the load directly affects lesser joints; thus, it can be seen that a lower load of approximately 30 kN is needed to cause a slippage of 1.8 mm. Moreover, for both cases, joints at the top chords where the loads were applied are expected to settle first as they endured higher stresses.

Stage 3: Under LC1, the external loads applied to joints B and F that connect the diagonal members provided a more favourable distribution of internal forces within the members. Due to that, higher stress will be endured by the diagonal members, especially the external components with end support restrains, while adequately transmitting the forces to the chord members. In this case, the satisfactory performance of the composite joints is crucial to transfer the stress effectively. This can be achieved by the presence of mechanical inserts that provide steady resistance against bolt shearing which delayed the damaging process. With adhesives surrounding the insert, it has enabled positive composite action with the pultruded GFRP members, efficiently exploiting the high glass fibre volume property and resulted in improved overall structural stiffness. This has been supported by the authors' observation in regards to the influence of bonded mechanical insert installed in single-bolted pultruded GFRP hollow sections. It was concluded that specimens assembled with bonded mechanical inserts showed improved joint-carrying capacity by 113% compared to that of similar specimens without inserts. This behaviour reflected on the curve response in Stage 3 that rises linearly as the fasteners and members deform elastically implicating the stiffness property of the truss system as shown in Figure 5a. This fixture or structural stiffness is determined from the slope of the linear region before the point where a noticeable decline in the curve slope is observed. Further for LC1, as the load reached approximately 300 kN, minor cracking sounds from the tested specimen were audible and the curve responded with a slight slope reduction. The sound may be caused by the de-bonding process between the mechanical inserts and pultruded members as inspected post-loading. This will be discussed in more detail in Failure mode section. Following this, it was suspected that the mechanical inserts have started to slip from its original position after the adhesive resin becomes ineffective, and local deformation have occurred at the bolt-pultruded GFRP member contact region while continuing to

provide resistance against bearing. Under LC2, a concentrated load applied at the centre of the top chords of the truss structure has placed joint A under higher stress and this primarily affected the overall load distribution paths. Subsequently, more insight into the failure behaviour of the truss system can be gained which was not achieved under LC1. Under moderate loading between 20 kN to 100 kN, similar behaviour was observed as per LC1 whereby the deflection and section forces are directly proportional to the load applied and this implies that the material is deformed without any increase in stress. However, at higher loads, the linear graph started to deviate which can be an indication of internal material damage. This behaviour could be associated to the response of the top chords (BAF) that were loaded along the perpendicular-to-fibre direction which has a significantly lower modulus of elasticity (E_{Tf}) compared to the E_{Lf} value in the longitudinal direction.

Stage 4: For LC1, the pultruded GFRP truss structure demonstrated a gradual decline in stiffness but is still capable of resisting the increased loading until the maximum capacity of the testing machine (around 450 kN) was reached, and with a final vertical displacement of approximately 10.5 mm. However, yielding of the members and/or the joint components were observed and if the load is further increased to higher than 450 kN, member fracture or shearing of fasteners will be expected. Meanwhile, for LC2, stage 4 is reached just prior to the point circled in Figure 5b, after which noticeable change in stiffness was observed through several knees response with lowered gradient. At this point, it was assumed that the failure load of approximately 118 kN had been reached with a vertical displacement of 4 mm, potentially due to the crushing of fibres and cracking of resin matrix on the web surface plies under the point load. At around 130 kN to 160 kN, compressive failure may have progressively occurred in the outermost part of the tubular cross-section, and beyond this point, the load-carrying capacity dropped gradually until the end of the load application. This descending non-linear curve presents the structural failure resulted from the continuous internal damage occurring at the mid-span of the double top chords and joint A region. It is essential to prolong the loading time after the maximum load is reached to understand the response of the through-bolt and bonded mechanical insert connection system in this truss structure. As can be seen in Figure 5b, the system has shown some ductility although with the expense of higher displacement. This is a critical requirement for serviceability limit states of FRP material when designing for

civil infrastructure (Manalo et al., 2017a) and therefore, in this case, the ductile behaviour at failure of the whole truss system is preferable (Keller and de Castro, 2005; Bai and Zhang, 2012).

Internal members' forces

Table 5 presents the axial member forces at the maximum load of LC1 and LC2, obtained from the strain measurements summarised in Figure 4a and 4b. The data was obtained from single element strain gauges attached at mid-span (SG1) and quarter-length (SG2) of the bottom chord member, and mid-length of external diagonal (SG3), internal diagonal (SG4) and vertical (SG5) members. The estimated member's capacity in tension and compression were computed using detailed equations as presented in Member resistance in tension and compression sections, respectively. Based on this experimental studies, the corresponding factor of safety (FoS) was determined as a ratio between the ultimate capacity of member strength and the measured internal force experienced by the truss member. Commonly, many structural design codes (ASCE, 2010; DG9, 2004; CNR, 2008; Clarke, 1996) specify FoS ranging from about 1.6 to 3.0 (or larger) for structural members and connections and it was assumed that the member will fail when the FoS is less than 1. As can be seen for both load cases, the internal forces of the bottom chord members were in tension while the internal forces of the vertical and external diagonal members were under compression.

Table 5. Internal member's forces at maximum load under LC1 and LC2

Data	Load Case 1 – 450 kN					Load Case 2 (LC2) – 160 kN				
	SG1	SG2	SG3	SG4	SG5	SG1	SG2	SG3	SG4	SG5
Exp. ³ (kN)	77.18	35.46	170.98	37.70	18.54	29.65	14.83	60.30	3.39	54.44
Strand7 (kN)	75.16	37.58	198.81	39.83	22.31	30.21	15.11	63.17	4.87	54.85
Type of forces	T ¹	T	C ²	C	C	T	T	C	T	C
FoS ⁴	3.65	7.95	1.10	4.97	10.11	9.50	19.00	3.11	83.13	3.44

Note: ¹Tension ²Compression ³Experimental ⁴Factor of Safety

For LC1, the maximum internal tension force of 77.18 kN was recorded at the mid-span of the bottom chord, while the maximum internal compression force was measured at 170.98 kN for the external diagonal members. Under this load condition, the load is directly distributed to members BC and FE and with the presence of support restraint at their ends, they were able to sustain greater internal forces compared to other members. However, to transfer loads to other structural members, joints B, C, E and F endured very high stresses as indicated by SG3 and often lead to the initiation of joint failure. Detailed discussion on the observed joint damage is presented in the next section. Based on the evaluated FoS, all the structural members were capable of carrying the load safely for LC1, with the lowest FoS of 1.10 was attained by the external diagonal member. This ratio is slightly higher than 1 which indicates that the affected member is nominally safe but has minimal margin for errors, such that may be caused by variability in loads. Any additional loadings acting on the structure will possibly cause the external diagonal members and their joints to fail in compression (rupture) and bearing, respectively. SG2 and SG4, in contrast, showed smaller internal forces through-out the loading process. At the unloaded joint A, where three (3) members are connected, with two of them being a continuous chord (BA and AF), the vertical member AD is theoretically a zero force member. However, SG5 which was placed on member AD recorded some internal forces, notably much less compared to the other members. This, in reality, indicates that member AD may be subjected to some forces from the loads and also provide stability by preventing buckling of the structures if variations are introduced in the external loading configuration, for instance under LC2.

For LC2, the maximum axial tension force of 30.21 kN was measured at the bottom chord member. On the other hand, higher axial compression forces (almost twice of the axial tension) of 60.30 kN and 54.44 kN were recorded for the external diagonal member and the vertical member, respectively. In this case, joint A was crucial in transmitting the direct compression load to member AD before equally distributing it through members AB and AF to the external diagonal members with the end supports. The load paths taken aim to avoid overload of structural elements, therefore, prolonging structural safety and robustness. Table 5 shows that the lower FoS of 3.44 and 3.11 were determined at the vertical and external diagonal members, respectively. These members did not experience any buckling and had met the required slenderness

ratio of < 300 as per ASCE pre-standard (ASCE, 2010). However, the horizontal continuous top chords failed in bending at mid-span as a result of significant bending stress acting on the sections. It was found that pultruded GFRP are prone to compression (buckling) failure due to the relatively low shear stiffness that composites generally exhibit (Mottram, 1992; Davalos and Qiao, 1997). Also, due to the tubular geometry of the pultruded GFRP that is characterised by its slender proportions (Ascione et al., 2013), the effect of buckling (rather than just strength limitations) may also be considered. For safety factor estimation, the ultimate strength of the members in tension and compression is not directly comparable in regards to flexural strength (buckling load) of the material since it could fail in a different number of modes. Thus, this case is further analysed in Member resistance in flexural section in evaluating member BF resistance against buckling failure.

Failure mode

After the unloading of the pultruded GFRP truss structure subjected to LC1, the truss components were disassembled to closely examine for any physical damage on the pultruded GFRP members and the connection assembly. It was found that the bolts at joints B and F connecting the external diagonal members (located at the top chords) were difficult to dislodge from the holes due to some embedment observed on the GFRP material by the bolt threads as shown in Figure 6b. It is worth noting that there was no lateral instability issue observed on the pultruded truss structure for both load cases. At maximum load of 450 kN, overall, the truss members were in excellent condition whereby no cracks or damages were observed along the length of the members. The connector elements (bolts and mechanical inserts) were in good condition as there were no cracks on the mechanical inserts, nor there was any bolts flexure observed.

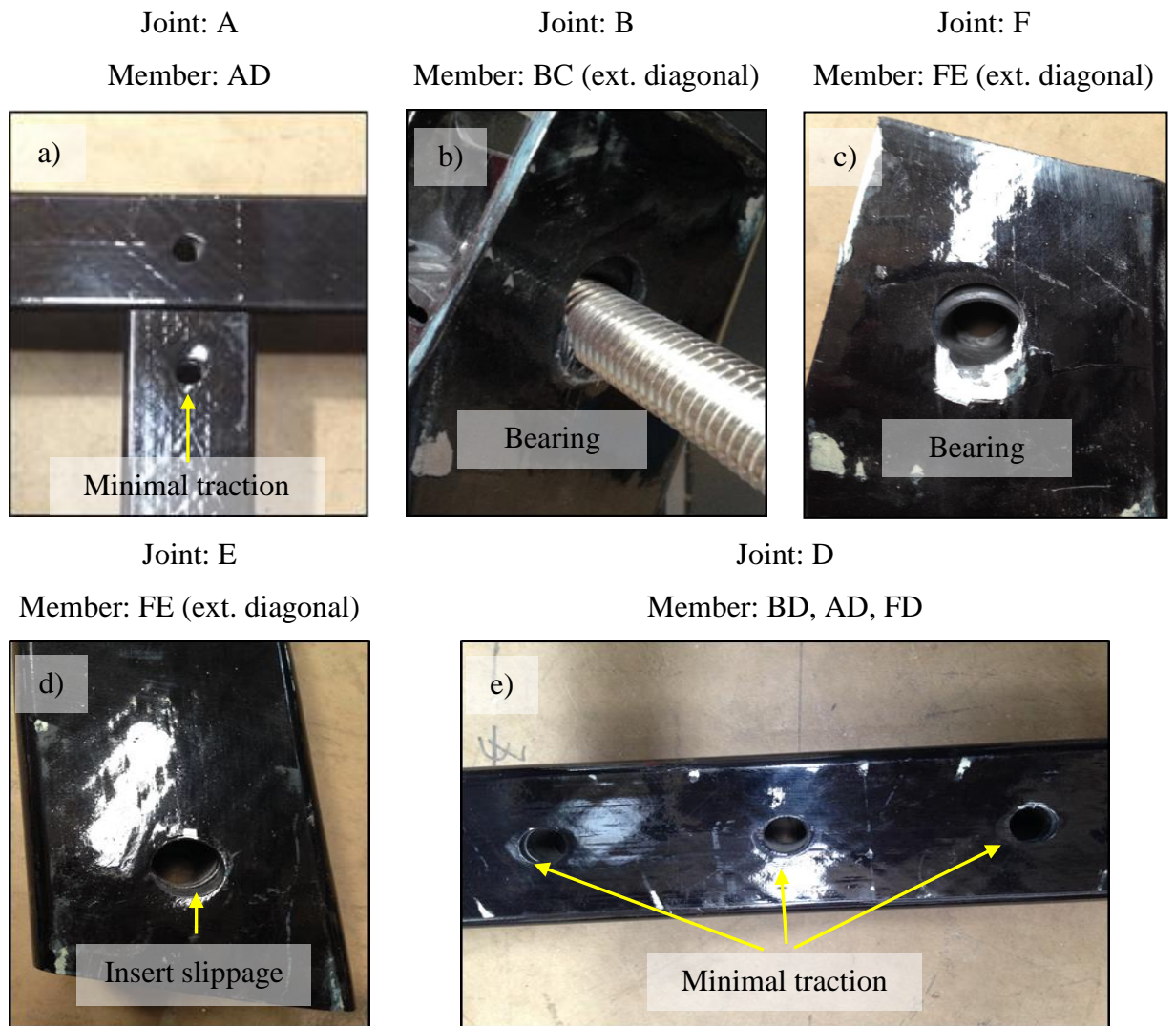


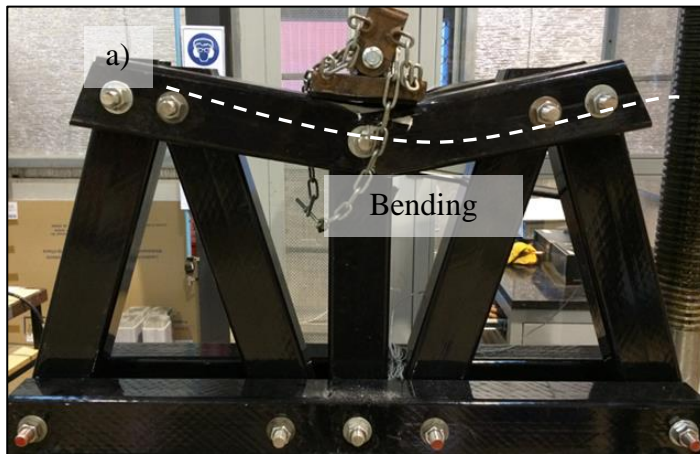
Figure 6. Common damage modes observed on the joints post-loading of LC1

Figure 6 presents the common damages observed at the jointing area of the truss after loading under LC1. Generally, most of the joints experienced minor indentation directly beneath the bolt-hole contact surface of the FRP members due to bolt traction/bearing as highlighted in Figures 6a and 6e. This indicates that the adopted joining method has provided adequate reinforcement on the connection area, preventing any premature failure and losses in load-carrying capacity. However, there were two (2) joints as shown in Figures 6b and 6c that exhibited obvious local delamination of fibres and resin matrix around the bolt-hole interface. Both joints B and F suffered initial signs of shearing through the combined action of high compressive stress at the contact zone and the thread embedment effect, creating a bearing area around the damaged hole. The location of this bearing area correlates well

with the direction of the resultant connection force, which acts towards the restrained edges as shown in Figure 9. Under this condition, additional resistance is provided against shear out and cleavage modes of failure. This was where the truss members BC and FE bear the highest compressive stresses under LC1. In addition, the mechanical inserts at these joints were displaced from their original position due to bolt movement. Similar condition was observed at the other ends of these members, at joint E (refer Fig. 6d)) and joint C, whereby slippage of mechanical inserts with minimal bearing effect were also noted. This may indicate that bearing damage is starting to develop at other joints especially at the bottom chord members which may be caused by the higher vertical deflection occurring mid-span of member CE.

Overall truss structure

Affected member: BF (Top chord)



Joint A (close-up)

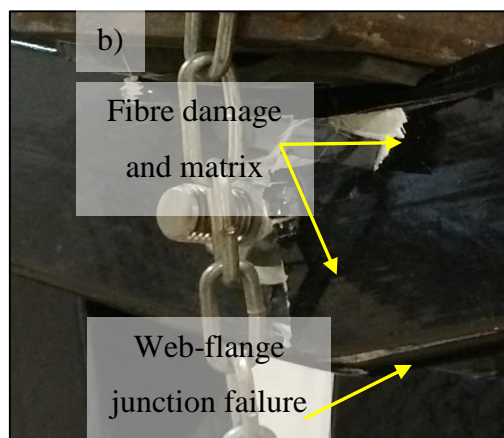


Figure 7: Principal mode of failure in LC2

Figure 7 presents the mode of failure of the tested pultruded GFRP truss under LC2. It demonstrates the post-failure condition of the truss as the compressive load was continuously applied until no apparent increase in the loading resistance was observed. At maximum load (160 kN), the principal failure was observed at the top double chords where both parallel pultruded GFRP members failed identically under flexural bending (refer Fig. 7a)) at mid-span, causing total failure of the truss structure. By closely inspecting the cross-section of these failed members, it was found that the top edges of the web of the rectangular hollow sections suffered significant local compression damages through delamination and cracking, which progressed to the bottom edges (web-flange junction failure) as highlighted in Figure 7b. Some fibres splitting and matrix cracking of the surface plies (developed perpendicular to the longitudinal axis) were observed near the hole region of joint A, indicating the effect of buckling and resulting in losses in mechanical properties and joint load-carrying capacity. Similar observations were reported by Muttashar et al. (2017), Bai et al. (2013) and Turvey and Zhang (2006). In addition, the presence of mechanical inserts, especially at joint A, contributed to the structure's ability to sustain much higher moment and had prevented local buckling of the flange wall due to in-plane compression which hollow sections generally exhibit. Furthermore, the load distribution path in this case is similar to a simply supported slender beam subjected to central loading. This principle can be used as a theoretical validation of the damaged pultruded member subjected to bending which is discussed in Member resistance in flexural section.

Through-bolt connection with mechanical insert

Figure 8 shows the detailed cross-section of the through-bolt connection with mechanical insert employed in the pultruded GFRP truss structures, with the diagonal member subjected to axial tension force. As discussed in the previous sections, both truss structures tested under LC1 and LC2 did not suffer any major failure at their connection areas which is considered to be one of the important outcomes of this experimental work.

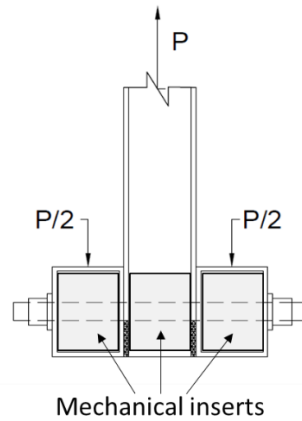


Figure 8. Double-chorded truss cross section and its through-bolt connection with mechanical insert

Only minimal damage in bearing was observed as consequences of high compressive stresses developed around the contact point between the bolt and the thin-walled pultruded GFRP members. For LC2, this was found mainly on the diagonal members that endured highest axial compression force acting along the axis of the components as observed in the previous section. It is important to ensure that the principal failure mode is not caused by the collapse of the connection system as it is highly responsible for the overall stiffness of the structure as well as the structural performance in regards to its serviceability limit states. Nevertheless, these joints failed in a more preferable manner which was through bearing failure due to its progressive nature and the ability to sustain post-failure loads beyond the ultimate load (Xiao and Ishikawa, 2005b). On the other hand, all the joint areas of the GFRP members that is perpendicular to the direction of the connection force were in satisfactory condition due to the restrained edge distance provided by the box section geometry as shown in Figure 9. This has provided additional connection resistance against shear out and cleavage mode of failure according to the ASCE pre-standard LRFD (ASCE, 2010). Under this condition, the shear-out strength and cleavage strength were not critical in the bolted connection design.

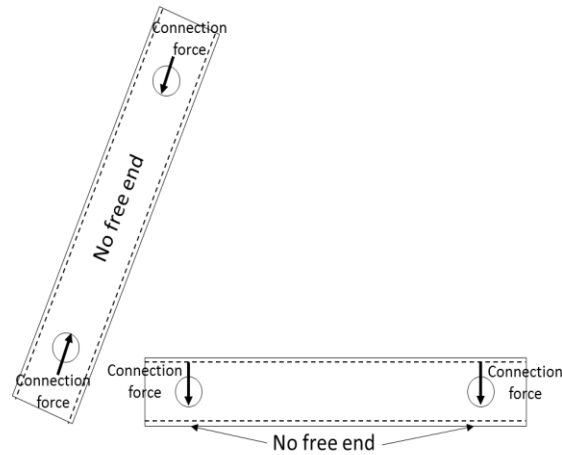


Figure 9. Restrained edges perpendicular to connection forces of the diagonal and horizontal members

The introduction of mechanical insert has improved the stress distribution of the connection system by providing better load paths from the bolt to the edge of the bolt holes, and it has significantly reduced the embedding effect between the threaded fasteners and fibrous materials. Without the inserts occupying the void spaces of the RHS joints, the through-bolt is susceptible to bolt flexure, causing poor bearing distribution across the thickness of the contact zone. This effect of non-uniform bearing pressure due to bolt shank flexure has been alleviated with the presence of the mechanical inserts. Otherwise, a reduction factor of 0.5 has to be applied to the pin-bearing strength in order to consider the effect of this non-uniform bearing pressure. Prior to this study, the authors have done extensive experimental works at component (coupon) levels pertaining to the effect of all-thread bolt (Hizam et al., 2018), mechanical insert (Hizam et al., 2013), and joint eccentricity on the strength of bolted connection of pultruded GFRP. The joint stiffness and modification factors are some of the key findings of the studies and were analysed by the authors based on the quantitative relationship of the experimental results of sixty (60) single-bolted hollow section of pultruded GFRP profiles under different joint configurations.

Table 6. Joint stiffness and modification factor due to the presence of mechanical insert

Description	Joint stiffness (kN/mm)	Modification factor, m
Pultruded GFRP bolted joint without any filled / mechanical insert.	8.84	1.0
Pultruded GFRP bolted joint with mechanical insert without adhesive.	15.47	1.4
Pultruded GFRP bolted joint with mechanical insert and adhesive.	37.23	2.0

The information in Table 6 can be adopted when evaluating or designing this specific through-bolted connection with mechanical insert (bearing-type connection) for pultruded GFRP members. Therefore, for this truss system which employs the same connection system, the joint stiffness and m value will be incorporated for the joint analysis. As per the ASCE pre-standard LRFD (ASCE, 2010), Equation 1 was used to evaluate the bearing strength, R_{br} at joints C and D where the external diagonal members experienced highest axial compression force under LC1. Overall, the pultruded GFRP truss joint geometries were designed to fail by bearing mode of failure with a large w/d_b ratio of 5 and an e/d_b ratio of 2.5 (Ascione et al., 2010; Xiao and Ishikawa, 2005a; Cooper and Turvey, 1995). In addition, with the lateral clamping pressure applied to the bolted joints, it is expected that the specimens have higher joint bearing strength (Park, 2001) and improved capability to sustain post-failure loads

$$R_{br} = t \cdot d \cdot F_{\theta}^{br} \quad (1)$$

$$P_o = 2 \cdot m \cdot R_{br} \quad (2)$$

where t = thickness of FRP material (mm); d = nominal diameter of bolt (mm); m = modification factor; F_{θ}^{br} = characteristic pin-bearing strength of FRP material (MPa) and R_{br} = joint bearing capacity (kN) and P_o = ultimate joint capacity (kN).

The mean value of the pin-bearing strength in Table 1 was used for F_{θ}^{br} and modification factor, $m = 2$, is applied to take into account the effect of bonded mechanical insert. This is important to portray a close representation of the joint configuration setup when defining the joint load-carrying capacity in Equation 2. The determined R_{br} is multiplied by 2 with respect to two (2) thin walls affected by the bolt as shown in Figure 8. Then, the P_o was assessed at the members that experienced the highest internal forces. The computed P_o capacity of joints B and C were compared to the measured axial compression force sustained by the external diagonal members under LC1. The joints are subjected to a slightly higher stress about 2% than their allowable capacity, and this is visually evident by the presence of minor bearing damage observed in Failure mode section.

THEORETICAL EVALUATION AND COMPARISON WITH EXPERIMENTAL RESULTS

Evaluation of the member forces and deflection using Strand7

Figure 10 shows a two-dimensional numerical model constructed to simulate the behaviour of the pultruded GFRP truss structure using Strand 7 finite element analysis software (Strand7, 2015). The rectangular hollow sections of the truss members were represented by a beam element with six degrees of freedom (DoF) at each node, capable to carry axial force, torque, shear forces and bending moments in its principal planes.

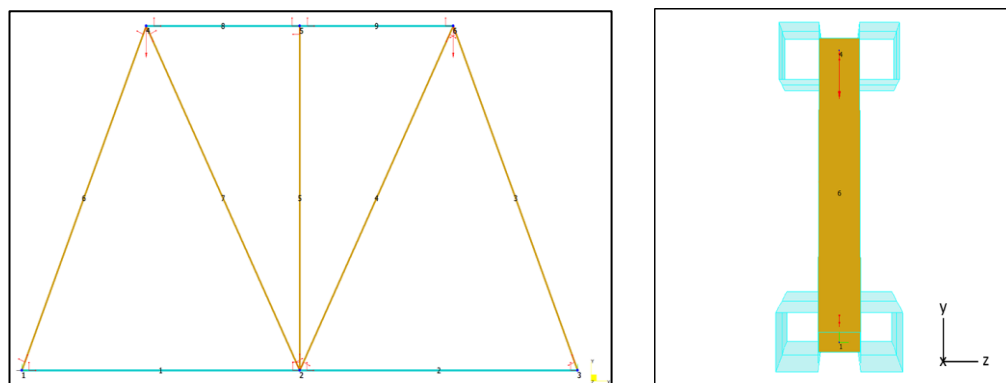


Figure 10. Numerical model of simply supported pultruded truss structure

This element is also best suited for the continuous pultruded GFRP members used for the upper and bottom chords which were modelled with double parallel member configuration as shown in Figure 11c. Meanwhile, Figure 11b represents the vertical and diagonal members of the truss structure. For this particular model, the translation end release or connection rigidity of the beam needs to incorporate the influence of bonded mechanical insert at the nodes. Figure 11a shows the three components in the beam's principal axis system and the beam may be fixed, released or partially released in certain directions based on the design of the connection system. For a pinned connection in the specified direction, full release can be assigned to the model. Meanwhile, partial release can be applied for additional springs of the specified stiffness connected between the end of the beam and the node. Commonly, in modelling a slotted bolted joint, the beam is restrained in translation 1 (lateral) and translation 2 (vertical) by bolt tension and bolt shear, respectively. However, in order to include the mechanical insert, both translation 2 (vertical) and 3 (axial) were changed to partially resist translational sliding by including the required joint stiffness, while translation 1 remained fixed. This approach simplifies the modelling of the connection resistance that was promoted by the presence of bonded mechanical insert and successfully demonstrates its effects on the beam nodes in vertical and axial directions. The joint stiffness of 74.46 kN/mm (refer Table 5) was multiplied by 2 to define the influence of mechanical inserts in the double top and bottom chord configurations. Finally, the numerical model based on LC1 and LC2 were analysed under linear elastic approach and the truss behaviour in terms of its overall vertical deflection and member axial forces were acquired.

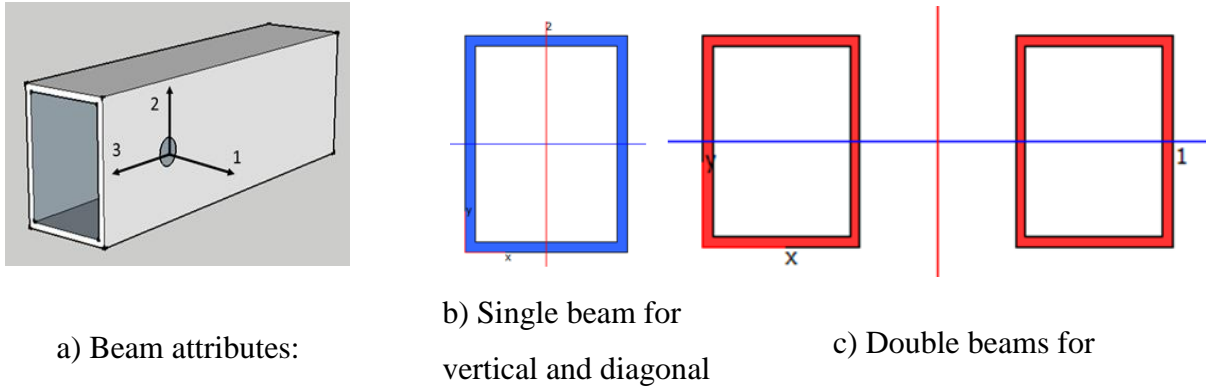


Figure 11. Beam attributes and geometry properties used for the truss assembly in Strand 7

Figure 5 shows the vertical displacement measured at mid-span of the truss with increasing load, comparing both the experimental and the theoretical Strand 7 models. It can be seen for both cases (LC1 and LC2), the structural stiffness of the numerical models was almost identical when compared to the experimental results. However, slight difference in response of the structural deflection was observed. This was attributed to the effect of bolt slippage as discussed earlier which was not considered in the numerical model. Table 5 compares the absolute values of axial forces obtained experimentally (from strain data) and theoretically (from Strand 7) at the maximum applied load of LC1 and LC2. Overall, the theoretical results produced higher axial stresses compared to the experimental data, but the correlation between the two approaches were satisfactory, with the largest discrepancy of 17% and 30% obtained for LC1 SG5 and LC2 SG4, respectively. It will be challenging to get closer outcomes due to the complexity of modelling the semi-rigid connections mechanisms and providing precise geometrical property (such as second moment of area, stacking sequence) of pultruded GFRP members and mechanical inserts. However, based on the comparable data obtained from the vertical displacement and member axial forces, the adopted simplified numerical method is sufficient to validate the behaviour of the double chord pultruded GFRP truss with bolted connection and mechanical insert.

In the following sub-sections, truss members subjected to highest stresses in tension, compression and flexure based on the strain data are evaluated against the strength limit states according to ASCE pre-standard LRFD (ASCE, 2010). For comparison purposes, the mean strength values listed in Table 1 were used for the corresponding characteristic values required in the following equations. In addition, the time effect factor, $\lambda = 0.4$ was used in all design assessments to signify the external load as the design load acting on the truss structure during its entire service life, equal to or exceeding 50 years.

Member resistance in tension

Equation 3 was used to assess the pultruded GFRP structural shape under tension loads acting parallelly along a member's longitudinal axis, incorporating adjustment in terms of time factor and resistance factor. Equation 4 was used to produce a limit state which equals the lowest nominal axial strength, P_n that is associated with the truss member susceptible to tensile rupture in its gross cross-sectional area.

$$P_u \leq \lambda \phi P_n \quad (3)$$

$$P_n = F_n A_g \quad (4)$$

where P_u = required axial tensile strength due to factored loads (N); P_n = nominal axial tensile strength (N); F_n = Nominal tensile strength from the characteristic value of coupon tests (MPa); A_g = gross cross-sectional area (mm); λ = time effect factor and ϕ = resistance factor

In this case, longitudinal tensile strength, f_{Lt} , was substituted for F_n and ϕ is taken as 0.65 for the failure of a material section under tension rupture. The computed theoretical axial tensile strength of 281 kN is about 264% higher when compared to the highest tensile stress value of 77.18 kN experienced by the bottom chord members under LC1. Also, it yields the factor of safety of 3.65.

Member resistance in compression

Equation 5 is used to assess the pultruded GFRP material strength under axial compression force, applied through the centroidal axis of the member. In calculating the nominal axial compression, P_n , the factored critical stress ($\phi_c F_{cr}$) shall be determined according to the pultruded GFRP rectangular tube sections defined by Equations 7 and 8.

$$P_u \leq \lambda \phi_c P_n \leq 0.7 \lambda F_L^c A_g \quad (5)$$

$$\phi_c P_n = \phi_c F_{cr} A_g \quad (6)$$

where P_u = required compression strength due to factored loads (N); P_n = nominal axial compression strength (N); F_L^c = minimum longitudinal compression material strength (MPa); A_g = gross cross-sectional area (mm); λ = time effect factor and ϕ_c = resistance factor for failure of a section under compression of the material; and $\phi_c F_{cr}$ = Factored critical stress

$$F_{cr} = \frac{\pi^2 E_L}{\left(\frac{KL_e}{r}\right)^2} \text{ and } \phi_c = 0.7 \quad (7)$$

$$F_{crw} = \frac{\left(\frac{\pi^2}{6}\right) \left[\sqrt{E_{L,w} E_{T,w} + \nu_{LT} E_{T,w} + 2G_{LT}} \right]}{\beta_w^2} \text{ and } \phi_c = 0.8 \quad (8)$$

where E_L = minimum longitudinal compression elastic modulus (MPa); $E_{L,w}$ = Characteristic value of the longitudinal compression modulus of the element under consideration (MPa); $E_{T,w}$ = characteristic value of the transverse compression modulus of the element under consideration (MPa); ν_{LT} = poisson's ratio associated with transverse deformation when compression is applied in the longitudinal direction; G_{LT} = characteristic value of the transverse compression; r = radius of gyration; L_e = effective length (distance between truss nodes); β_w = maximum width-to-thickness ratio, whichever is larger; and $K = 1$ for the member effective length factor.

In this case, E_{Lc} , E_{Lt} , and G_L listed in Table 1 were substituted for $E_{L,w}$, $E_{T,w}$, G_{LT} , respectively. Meanwhile, r , L_e and β_w was measured at 36.8 mm, 520 mm and 20, respectively. Another important parameter to check is the compression member effective slenderness ratio, $\frac{KL_e}{r}$. The calculated slenderness ratio of the member under compression is equal to 200 which meets the requirement of ASCE, whereby the ratio shall not exceed 300. The determined $\phi_c F_{cr}$ shall be taken as the lower values of $\phi_c F_{cr}$ (Equation 5) and $\phi_c F_{crw}$ (Equation 6). The minimum value was obtained by $\phi_c F_{crw} = 118.58$ MPa and was used as the factored critical stress in Equation 6. The computed theoretical axial compression strength based on Equation 5 was about 187 kN, and it was slightly higher by 10% when compared to the ultimate axial compression force experienced at the external diagonal members under LC1. This agrees well with the observation made in Failure mode section, where the pultruded GFRP member was still in good condition and no rupture in compression was observed.

Member resistance in flexural

This theoretical assessment focused on the truss structure under LC2, whereby member BF (representing the double top chords of the truss) is subjected to bending about the

plane of the neutral axis. In Failure mode section, the flexure member BF failed due to rupture of the material in compression at the location of the point load, as well as in tension at the lower end of the member's web. In this case, no observation of local buckling and lateral-torsional buckling at the flange or web was found. Thus, the following theoretical equations was carried out based on the governed mode of failure.

$$M_u \leq \lambda \phi M_n \quad (9)$$

$$M_n = \frac{F_L I}{y} \quad (10)$$

where M_u = required flexural strength (N.mm); M_n = nominal flexural strength (N.mm); F_L = characteristic longitudinal strength (in tension or compression) of the member (MPa); I = moment of inertia of the member about the axis of bending (mm^4); λ = time effect factor and ϕ = resistance factor for failure due to rupture of the material in tension or compression shall be taken as 0.65; and y = distance from the neutral axis to the extreme fibre of the member (mm)

Equation 10 was considered to determine the factored nominal flexural strength of members, ϕM_n which was subjected to material rupture. The equation has been simplified as the difference in elastic moduli of the pultruded GFRP longitudinal flanges and webs are within 15%. The mean value of longitudinal compressive strength, f_{Lc} and tensile strength, f_{Lt} was substituted for F_L , and the distance of y is 50 mm, measured from the neutral axis of the pultruded GFRP member to its farthest fibre. Moreover, the moment of inertia should be calculated to include the mechanical insert installed in the hollow area of member BF as it can influence the material resistance against bending. The computed allowable flexural strength, M_u , in consideration of both longitudinal compression and tension zones were 15,050 kNmm and 19,013 kNmm, respectively. These values were then compared to the experimental moment of force that is normally used in slender beams. It is the product of the magnitude of the external force multiplied with the distance between the force and the point of interest. The calculated bending moment attained was 52% and 21% higher than that of required flexural strength, M_u (Equation 9) in longitudinal compression and tension, respectively. This theoretical check reflects and validates the outcome of the

test under LC2 whereby the experimental values exceeded the member's allowable capacities, therefore resulted in failure of the truss structure.

CONCLUSION

The current paper presented the experimental results and theoretical analyse of pultruded GFRP truss system connected using through-bolted connection with mechanical insert. The trusses were tested under two different loading configurations to examine the mid-span deflection of the truss structure, internal forces of pultruded members and joint load-carrying capacity. A truss model using Strand7 and theoretical evaluation according to ASCE pre-standard were used to predict and evaluate the behaviour of the tested truss system. Based on the results, the following conclusions can be drawn:

- Under Load Case 1, the structural pultruded GFRP truss members remained physically undamaged as the maximum capacity of the equipment of 450 kN is reached, although a decline in stiffness was apparent prior to this. The maximum internal tension force of 77.18 kN was recorded at the mid-span of the bottom chord, while the maximum internal compression force was measured at 170.98 kN for the external diagonal members. Based on the evaluated factor of safety, all the structural members are capable of carrying the load safely, with the lowest factor of safety of 1.10 was attained by the external diagonal members.
- This also indicates that the adopted through-bolt with mechanical insert connection system are capable of sustaining higher joint load-carrying capacity and adequately transmitted the internal forces to other members by providing a uniform stress distribution along the length of the members. This was reflected on the load-deflection curve (Stage 3), which increased linearly as the fasteners and members deformed elastically implicating the stiffness property of the truss system. In terms of the mode of failure, most of the joints experienced minimal indentation directly beneath the bolt-hole contact surface of the FRP members due to bolt traction/bearing. However, joints B and F suffered initial signs of shearing through the combined action of high compressive stress at the contact zone and the thread embedment effect, creating a bearing area around the damaged hole.

- Under Load Case 2, the top chords members and joint A have been placed under greater stress and this largely affected the overall load distribution paths. The maximum axial tension force of 30.21 kN was measured at the bottom chord member, while, higher axial compression forces of 60.30 kN and 54.44 kN were recorded for the external diagonal member and the vertical member, respectively. Based on the load-deflection curve, at around 130 kN to 160 kN, compressive failure may have progressively occurred in the outermost part of the tubular cross-section, and beyond this point, the load-carrying capacity dropped gradually until the end of the load application. Under prolong loading time, the system has shown some ductility although with the expense of higher displacement. In this case, the ductile behaviour at failure of the whole truss system is preferable.
- At maximum load of 160 kN, the horizontal continuous top chords failed in bending at mid-span as a result of significant bending stress acting on the sections. It was found that pultruded GFRP hollow sections are prone to compression (buckling) failure due to the relatively low shear stiffness that composites generally exhibit. By closely inspecting the cross-section of these failed members, it was found that the top edges of the web of the rectangular hollow sections suffered significant local compression damages through delamination and cracking, which later progressed to the bottom edges (web-flange junction failure).
- High axial compression forces experienced by the external diagonal members of LC1 had exceeded the ASCE pre-standard theoretical joint bearing capacity by 2%, and this was reflected by the minor bearing damage observed on the joints of these members. The assessment included the modification factor, $m = 2$, to take into account the effect of bonded mechanical insert. This is important to portray a close representation of the joint configuration setup when defining the joint load-carrying capacity
- The favourable comparison between the Strand 7 truss model and experimental results obtained in terms of vertical deflections and axial member forces demonstrate the validity of the adopted simplified numerical model. This can be achieved by presenting the truss members as a beam element and modified

the beam translation end release (connection rigidity) to incorporate the influence of bonded mechanical insert at the nodes.

- The theoretical strength limits of pultruded GFRP truss members in tension, compression and flexural according to ASCE pre-standard are in close agreement with the experimental results.

ACKNOWLEDGEMENTS

The first author gratefully acknowledges the Australian Commonwealth Government for the contribution through Research Training Program (RTP) scheme. The authors also gratefully acknowledge Wagner Composite Fibre Technologies (WCFT) for providing all the pultruded GFRP tubes in the experimental programme. Special thanks to Mr. Wayne Crowell for kind support and guidance during the experimental work.

REFERENCES

- [1] Zaharia R, Dubina D. Stiffness of joints in bolted connected cold-formed steel trusses. *Constructional Steel Research*. 2006;62:240-9.
- [2] Omar T, Erp GV, Aravinthan T, Heldt T. Truss fibre deployable shelter. Australia: University of Southern Queensland, 2008.
- [3] Uddin N, Abro AM. Design and manufacturing of low cost thermoplastic composite bridge superstructures. *engineering Structures*. 2008;30.
- [4] Manalo A, Aravinthan T, Fam A, Benmokrane B. State-of-the-Art Review on FRP Sandwich Systems for Lightweight Civil Infrastructure. *Journal of Composites for Construction*. 2017;21.
- [5] Gand AK, Chan T-M, Mottram JT. Civil and structural engineering applications, recent trends, research and developments on pultruded fibre reinforced polymer closed sections: a review. *Frontiers of Structural and Civil Engineering*. 2013;7:227-44.
- [6] Coelho AMG, Mottram JT. A review of the behaviour and analysis of bolted connections and joints in pultruded fibre reinforced polymers. *Materials & Design*. 2015;74:86-107.
- [7] Carlone P, Palazzo GS, Pasquino R. Pultrusion manufacturing process development by computational modelling and methods. *Mathematical and Computer Modelling*. 2006;44:701-9.
- [8] Plastics R. Pultrusion industry grows steadily in US. *Reinforced Plastics*. 2002.
- [9] Smith SJ, Parsons ID, Hjelmstad KD. An experimental study of the behaviour of connection for pultruded GFRP- I beams and rectangular tubes. *Composites Structures*. 1998:281 - 90.
- [10] DG9. Design guide 9: For Structural Hollow Section Column Connections. Germany: The International Committee for Research and Technical Support for Hollow Section Structures (CIDECT); 2004.

- [11] Mottram JT. Design Guidance for Bolted Connections in Structures of Pultruded Shapes: Gaps in Knowledge. 17th International Conference on Composite Materials. 2009;A1.
- [12] Mosallam AS. Design Guide for FRP Composite Connections: American Society of Civil Engineers (ASCE), 2011.
- [13] Turvey GJ. Bolted connections in PFRP structures. *Progress in Structural Engineering and Materials*. 2000;2:146-56.
- [14] Hizam RM, Manalo AC, Karunasena W. A review of FRP composite truss systems and its connections. In: Bijan Samali CS, Mario M. Attard, editor. 22nd Australasian Conference on the Mechanics of Structures and Materials. Sydney, New South Wales, Australia: Taylor & Francis Ltd; 2012.
- [15] Bank LC. *Composites for Construction: Structural Design with FRP Materials*. New Jersey: John Wiley & Sons, Inc., 2006.
- [16] Zhou A, Keller T. Joining techniques for fiber reinforced polymer composite bridge deck systems. *Composites Structures*. 2006;69:336-45.
- [17] Manalo AC, Mutsuyoshi H. Behavior of fiber-reinforced composite beams with mechanical joints. *Journal of composite materials*. 2011:1-14.
- [18] Pfeil MS, Teixeira AMAJ, Battista RC. Experimental tests on GFRP truss modules for dismountable bridges. *Composite Structures*. 2009;89:70-6.
- [19] Vangrimde B, Boukhili R. Descriptive relationships between bearing response and macroscopic damage in GRP bolted joints. *Composites Part B: Engineering*. 2003;34:593-605.
- [20] Pisano A, Fuschi P. Mechanically fastened joints in composite laminates: Evaluation of load bearing capacity. *Composites Part B: Engineering*. 2011;42:949-61.
- [21] Lau STW, Said MR, Yaakob MY. On the effect of geometrical designs and failure modes in composite axial crushing: A literature review. *Composite Structures*. 2012;94:803-12.
- [22] Boyd SW, Winkle IE, Day AH. Bonded butt joints in pultruded GRP panels—an experimental study. *International Journal of Adhesion and Adhesives*. 2004;24:263-75.
- [23] Hashim SA, Nisar JA. An investigation into failure and behaviour of GFRP pultrusion joints. *International Journal of Adhesion and Adhesives*. 2013;40:80-8.
- [24] de Castro J, Keller T. Ductile double-lap joints from brittle GFRP laminates and ductile adhesives, Part I: Experimental investigation. *Composites Part B: Engineering*. 2008;39:271-81.
- [25] Lee Y-G, Choi E, Yoon S-J. Effect of geometric parameters on the mechanical behavior of PFRP single bolted connection. *Composites Part B: Engineering*. 2015;75:1-10.
- [26] Goldsworthy WB, Hiel C. *Composite structures*. *SAMPE Journal*. 1998;34:24-30.
- [27] Humphreys MF, Erp GV, Tranberg CH. The structural behavior of monocoque FRP truss joints. *Advanced Composite Letters*. 1999;8:173-80.
- [28] Bradford NM. *Design optimization of FRP composite panel building system: Emergency shelter applications*: University of South Florida, 2004.
- [29] Keller T, Bai Y, Vallée T. Long-Term Performance of a Glass Fiber-Reinforced Polymer Truss Bridge. *Journal of Composites for Construction*. 2007;11.
- [30] Omar T, Van Erp G, Aravinthan T, Key PW. Innovative all composite multi pultrusion truss system for stressed-arch deployable shelters. *Sixth Alexandria International Conference on Structural and Geotechnical Engineering*. 2007.

- [31] Teixeira AMAJ, Pfeil MS, Battista RC. Structural evaluation of a GFRP truss girder for deployable bridge. *Composites Structures*. 2014;110:29-38.
- [32] Bai Y, Yang X. Novel joint for assembly of all-composite space truss structures: conceptual design and preliminary study. *Composites for Construction*. 2013;17:130-8.
- [33] Yang X, Bai Y, Ding F. Structural performance of a large-scale space frame assembled using pultruded GFRP composites. *Composite Structures*. 2015;133:986-96.
- [34] Luo FJ, Bai Y, Yang X, Lu Y. Bolted sleeve joints for connecting pultruded FRP tubular components. *Composites for Construction*. 2016;20:04015024.
- [35] Luo FJ, Yang X, Bai Y. Member capacity of pultruded GFRP tubular profile with bolted sleeve joints for assembly of latticed structures. *Journal of Composites for Construction*. 2016;20:1-12.
- [36] Wu C, Bai Y, Toby Mottram J. Effect of Elevated Temperatures on the Mechanical Performance of Pultruded FRP Joints with a Single Ordinary or Blind Bolt. *Journal of Composites for Construction*. 2015;20:04015045.
- [37] Satavisam S, Feng P, Bai Y, Caprani C. Composite actions within steel-FRP composite beam systems with novel blind bolt shear connections. *engineering Structures*. 2017;138:63-73.
- [38] Hizam RM, Karunasena W, Manalo AC. Effect of mechanical insert on the behaviour of pultruded reinforced polymer (FRP) bolted joint. Fourth Asia-Pacific Conference on FRP in Structures (APFIS). Melbourne, Australia: International Institute for FRP in Construction (IIFC); 2013.
- [39] Hizam RM, Manalo AC, Karunasena W, Bai Y. Effect of bolt threads on the double lap joint strength of pultruded fibre reinforced polymer composite materials. *Construction and Building Materials*. 2018;181:185-98.
- [40] ECSS. Insert design handbook. Noordwijk, The Netherlands: European Cooperation for Space Standardization; 2011.
- [41] Humphreys MF. Development and structural investigation of monocoque fibre composite trusses: Queensland University of Technology, 2003.
- [42] Mirza FA, Shehata AA, Korol RM. Modelling of double chord rectangular hollow section T-joints by finite element method. *Computers & Structures*. 1982;15:123-9.
- [43] Shehata AA, Korol R, Mirza FA. Joint flexibility effects on rectangular hollow section vierendeel trusses. *Mechanics of Structures and Machines*. 1987;15:89-107.
- [44] Korol R. Double Chords as an Alternative in Tubular Trusses. *Journal of Structural Engineering*. 1986;112:2665-78.
- [45] ASTM D3171. Standard Test Methods for Constituent Content of Composite Materials. American Society for Testing and Materials (ASTM) Standard; 2011.
- [46] ASTM D638. Standard test method for tensile properties of plastics. American Society for Testing and Materials (ASTM) Standard; 2010.
- [47] ASTM D695. Standard test method for compressive properties of rigid plastics. American Society for Testing and Materials (ASTM) Standard; 2010.
- [48] ASTM D5379. Standard test method for shear properties of composite materials by the V-notched beam method. American Society for Testing and Materials (ASTM) Standard; 2005.
- [49] ASTM D953. Standard Test Method for Bearing Strength of Plastics. American Society for Testing and Materials (ASTM) Standard; 2010.
- [50] AS/NZS 1252:1996. High-strength steel bolts with associated nuts and washers for structural engineering. Australia and New Zealand. Standards Australia and Standards New Zealand.; 1996.

- [51] AS/NZS1110:1995. ISO metric precision hexagon bolts and screws. Australia and New Zealand: Standards Australia and Standards New Zealand.; 1995.
- [52] AISC. Guide to Design Criteria for Bolted and Riveted Joints. Second Edition. Chicago, USA: American Institute of Steel Construction (AISC); 2001.
- [53] ISO1172. Textile-glass-reinforced plastics, prepegs, moulding compounds and laminates: Determination of the textile-glass and mineral-filler content- Calcination methods. International Organization for Standardization (ISO); 1996.
- [54] WCFT. Wagners Composite Fibre Technologies: Product Guide. Toowoomba, Australia: Wagners CFT Manufacturing Pty Ltd; 2016.
- [55] ISO527-2. Plastics: Determination of tensile properties. International Organization for Standardization (ISO); 1996.
- [56] ASTM D3163-01. Standard Test Method for Determining Strength of Adhesively Bonded Rigid Plastic Lap-Shear Joints in Shear by Tension Loading. American Society for Testing and Materials (ASTM) Standard; 2014.
- [57] ISO75-1. Plastics - Determination of temperature of deflection under load International Organization for Standardization (ISO); 2004.
- [58] Ragheb WF. Local buckling analysis of pultruded FRP structural shapes subjected to eccentric compression. *Thin-Walled Structures*. 2010;48:709-17.
- [59] Wu C, Bai Y, Zhao XL. Improved bearing capacities of pultruded glass fibre reinforced polymer square hollow sections strengthened by thin-walled steel or CFRP. *Thin-Walled Structures*. 2015;89:67-75.
- [60] ASCE. Pre-Standard for Load and Resistance Factor Design (LFRD) of Pultruded Fibre Reinforced Polymer (FRP) Structures. 2010.
- [61] Feroldi F, Russo S. Structural Behavior of All-FRP Beam-Column Plate-Bolted Joints. *Journal of Composites for Construction*. 2016;20:04016004.
- [62] Cooper C, Turvey GJ. Effects of joint geometry and bolt torque on the structural performance of single bolt tension joints in pultruded GRP sheet material. *Composite Structures*. 1995;32:217-26.
- [63] Ungkurapinan N. A study of joint slip in galvanised bolted angle connections. Canada: University of Manitoba, 2000.
- [64] Keller T, de Castro J. System ductility and redundancy of FRP beam structures with ductile adhesive joints. *Composites Part B: Engineering*. 2005;36:586-96.
- [65] Bai Y, Zhang C. Capacity of nonlinear large deformation for trusses assembled by brittle FRP composites. *Composite Structures*. 2012;94:3347-53.
- [66] CNR. Guide for the Design and Construction of Structures made of FRP Pultruded Elements. Rome: National Research Council of Italy; 2008.
- [67] Clarke JL. Structural design of polymer composites: EUROCOMP design code and handbook. London: E & FN Spon, 1996.
- [68] Mottram J. Lateral-torsional buckling of a pultruded I-beam. *Composites*. 1992;23:81-92.
- [69] Davalos JF, Qiao P. Analytical and experimental study of lateral and distortional buckling of FRP wide-flange beams. *Journal of Composites for Construction*. 1997;1:150-9.
- [70] Ascione L, Berardi VP, Giordano A, Spadea S. Buckling failure modes of FRP thin-walled beams. *Composites Part B: Engineering*. 2013;47:357-64.
- [71] Muttashar M, Manalo A, Karunasena W, Lokuge W. Flexural behaviour of multi-celled GFRP composite beams with concrete infill: Experiment and theoretical analysis. *Composite Structures*. 2017;159:21-33.
- [72] Bai Y, Keller T, Wu C. Pre-buckling and post-buckling failure at web-flange junction of pultruded GFRP beams. *Materials and structures*. 2013;46:1143-54.

- [73] Turvey GJ, Zhang Y. Shear failure strength of web-flange junctions in pultruded GRP WF profiles. *Construction and Building Materials*. 2006;20:81-9.
- [74] Xiao Y, Ishikawa T. Bearing strength and failure behavior of bolted composite joints (part II: modeling and simulation). *Composites Science and Technology*. 2005;65:1032-43.
- [75] Ascione F, Feo L, Maceri F. On the pin-bearing failure load of GFRP bolted laminates: An experimental analysis on the influence of bolt diameter. *Composites Part B: Engineering*. 2010;41:482-90.
- [76] Xiao Y, Ishikawa T. Bearing strength and failure behavior of bolted composite joints (part I: Experimental investigation). *Composites Science and Technology*. 2005;65:1022-31.
- [77] Park HJ. Effects of stacking sequence and clamping force on the bearing strengths of mechanically fastened joints in composite laminates. *Composite Structures*. 2001;53:213-21.
- [78] Strand7. Strand7 Release 2.4.6. Sydney, Australia 2015.

7.0 CONCLUSION

Pultruded glass fibre reinforced polymer (GFRP) composites have now been widely accepted as alternative structural materials to steel and timber. This is contributed by its numerous advantageous characteristics including high axial resistance, high resistance to aggressive environment, lightweight, and ease of fabrication and installation time. However, the integrity and reliability of joining systems in assembling structures made from pultruded GFRP profiles is crucial for its widespread acceptance in civil infrastructure. While a number of research works have been carried out in understanding the behaviour of pultruded GFRP with different connection techniques at a coupon level, only a few have investigated at a systems and structural level. This study experimentally and analytically evaluated the structural behaviour of pultruded GFRP trusses which were constructed by assembling pultruded GFRP hollow sections connected together using through-bolt with mechanical inserts. The systems behaviour of this truss connection was conducted in four phases:

1. Determination of the influence of bolt threads on the joint geometric parameters and clamping pressure using double lap single bolt joint (DLSJ) configuration and tested in accordance with ASTM D5961.
2. Investigation of the influence of mechanical inserts with and without adhesive in through-bolt connection of pultruded GFRP hollow sections under in-service elevated temperatures.
3. Examination of the influence of eccentric loading on the behaviour of through-bolt connection of pultruded GFRP T-joint using single bottom chords.
4. Assessment of the structural and joint performance of pultruded GFRP trusses connected using through-bolt with mechanical insert connection system under different load cases.

7.1. Effect of bolt threads in GFRP bolted connection

The effect of bolt threads on the joint behaviour of GFRP laminates were thoroughly investigated under different parameters including end distance-to-bolt diameter (e/d_b), laminate thickness, clamping pressure and laminate orientations (longitudinal

and transverse). Comparative evaluation on the joint strength behaviour, joint efficiency and mode of failure for GFRP laminates using plain was also conducted. Based on the test results, the following conclusions were derived:

- Both plain and threaded bolts were found to affect the joint strength of the pultruded GFRP laminates. Using plain bolts, the joint strength increased up to e/d_b of 4, with higher ratio showing no appreciable gain as the failure mode changes from shear-out to bearing. On the other hand, the joint strength was similar for threaded bolts for the e/d_b ratios considered as the failure was governed by the deterioration and delamination of both fibres and the resin matrix around the bolt hole.
- The transverse bolted specimens exhibited much lower joint strength than that of longitudinal bolted specimens predominantly due to very low ultimate tensile strength in transverse direction and unfavourable joint geometry. This effect was more pronounced with threaded bolts as a 60% drop in joint strength was observed when compared to that of similar configuration in longitudinal direction.
- The increase in laminate thickness from 5 mm to 6.5 mm achieved 38% higher bolt strength using plain bolts. However, the damaging effects of thread entrenchment using threaded bolts reduced the joint capacity by 8%.
- At microscopic level, threads indentations on the laminates were apparent through appearance of voids on the scanning electron micrographs which may explain the failure development of softened zone resulting in a lower connection strength. A reduction factor of 0.6 is therefore proposed in preliminary pultruded GFRP bolted connection design to consider the effects of bolt threads on the joint capacity.
- With the introduction of lateral clamping pressure, the damage done by the bolt threads were less profound, changing from fibre-matrix crushing to shear-out failure. Consequently, the lateral clamping pressure increases the joint strength for both threaded and unthreaded bolts in longitudinal specimens.
- An in-depth understanding of the effects of bolt threads, in combination with other fastening parameters, on the joint strength of pultruded GFRP had been achieved. These key findings were important to provide support in designing through-bolt connection system for pultruded GFRP hollow sections.

7.2. Behaviour of through-bolt with mechanical insert

The use of mechanical insert as a filled-type connection element in pultruded GFRP hollow sections had been studied by preparing and testing sixty (60) square pultruded GFRPs with a single all-threaded bolt connection, with and without mechanical inserts. The test was implemented at room temperature, 40°C, 60°C, and 80°C to investigate the effect of in-service elevated temperature of the joint performance. Additionally, a comparison and evaluation of different bolted joint configurations of pultruded GFRP hollow sections, i.e. joint without mechanical insert, joint with tight-fit mechanical insert and joint with mechanical insert bonded using epoxy adhesive was conducted. The main findings of this study are as follows:

- The introduction of mechanical inserts in the hollow GFRP bolted joints resulted in 24% increase in joint strength at room temperature, but by providing adhesion between the insert and the inner wall of the GFRP, the increment is 113% compared to that of the insert-less specimen. This was achieved through effective composite action between the pultruded GFRP and the mechanical insert, therefore, improving the stress distribution and fully utilising the insert in sustaining higher load-carrying capability.
- Under elevated temperatures, ranging from 40°C to 80°C, insert-less specimens endured highest reduction in joint strength, declining steadily with 20%, 25% and 31% loss when tested at 40°C, 60°C and 80°C, respectively. As the temperature increases, the bolt thread had gradually damaged the softened pultruded composite material in a local crushing manner.
- Under similar exposure, with bonded mechanical inserts, these figures are much lesser, i.e. 3%, 15% and 24% at 40°C, 60°C, and 80°C, respectively, indicating the effectiveness of the inserts in improving the joint strength. Interestingly, with inserts tight-fit attachment, marginal additional joint loss of 0.9% from 40°C to 60°C was observed, possibly due to constant thermal expansion of the pultruded GFRP and mechanical insert, as this temperature range is still well below T_g . Also, the final mode of failure of shear-out had occurred for the entire temperature range which can be observed clearly at its end distance.
- In terms of joint stiffness, negligible reduction was recorded for specimen without mechanical insert and specimen with mechanical insert tight-fit attachment, as

stiffness is contributed by the fibre properties of the pultruded GFRP and the mechanical insert which is stable in this temperature range.

- The joint stiffness of specimen with bonded mechanical insert declined in a linear pattern across the temperature range and overall, possess higher stiffness capacity compared to other specimens. This may have been achieved due to the composite action produced by the epoxy adhesive that the mechanical insert able to play its role effectively. High volume of glass fibres composed in both mechanical insert and pultruded GFRP had improved the joint stiffness, however, the linear decline at high temperatures may be attributed to epoxy adhesive softening effect at pultruded-insert interface.
- Strength reduction factor (k) and modification factors (m) based on different joint configurations involving mechanical insert were proposed to accurately predict the joint strength of pultruded GFRP hollow sections. The joint strength from the proposed equation showed excellent agreement to the experimental results.
- This promising connection system, consisting of through-bolt with bonded mechanical insert, had been assessed on its joint capacity at elevated temperatures. Further work on this connection system under different loading condition, such as eccentricity that may arise due to possible construction errors, is crucial to give more understanding on its joint performance and its interaction with the connected pultruded GFRP members.

7.3. Behaviour of GFRP T-joint under eccentric loading

A total of twelve (12) pultruded GFRP T-joint components had been assembled to investigate the behaviour of through-bolt connection with mechanical insert under eccentric loading. The configurations of the T-joints included both single and double bottom chords, with the former imbalanced configuration intended to impart load eccentricity. The single and double bottom chord T-joints were compared to similar specimens without mechanical inserts. Based on the experimental and analytical results, the following conclusions can be drawn:

- The eccentric loading on the T-joint of the pultruded GFRP severely impacted its joint resistance, achieving only a third of the resistance of the T-joint under

concentric loading. This was due to the couple moment, specifically the moment-rotation of the bolt, developed from the eccentricity.

- Under eccentric loading, the vertical pultruded GFRP thin wall suffered from local compression directly located at the bolt hole region (at nut and washer side) and caused web buckling coupled with apparent plies delamination due to the moment rotation of the bolt. On the opposite of thin walls, the failure was governed by fibre and matrix crushing, occurring along the shear-out planes on the hole boundary.
- The presence of mechanical inserts in both eccentrically and concentrically loaded T-joints improved the joint strengths by 221% and 110%, respectively, when compared to their insert-less counterparts. This allowed the forces, including the additional stresses developed due to eccentricity, to be transferred from the tubular side plates and the fastener to the mechanical insert. The insert that was installed within the hollow section of the pultruded GFRP has increased the area moment of inertia of the configuration, and this contributed to the improvement in bending resistance.
- The theoretical equations considering the combined axial compression and bending stress and incorporating modification factors to consider the influence of mechanical insert on the predicted joint resistance of the specimens had shown good agreement with the experimental results. The proposed modification factor, $m=2$, sufficiently represented the effect of the mechanical inserts on the theoretical joint strength of the pultruded GFRP, yielding comparable values to the experimental outcomes.
- This study has provided the ability for practitioners to predict the joint capacity of these T-joint configurations and understand the governed failure modes under eccentricity. These findings were applied on a full-scale truss structure and the structural and joint behaviours were further investigated to expand the data for civil applications.

7.4. Structural and joint behaviour of GFRP truss

The structural and joints performance of pultruded GFRP trusses which were constructed by assembling pultruded GFRP hollow sections into a double-chord truss

configuration using through-bolt with insert connection system were investigated under 4-point bending (Load Case 1) and 3-point bending (Load Case 2). From the results of this experimental program, the following conclusions are drawn:

- The pultruded GFRP truss under Load Case 1 was capable of resisting the maximum load capacity of the testing equipment at 450 kN with the lowest factor of safety of 1.10 was attained by the external diagonal members. High axial compression forces experienced by the external diagonal members has exceeded the American pre-standard theoretical joint bearing capacity by 2%, and this was reflected by the minor bearing damage observed on the joints of these members.
- In terms of the mode of failure, most of the joints experienced minimal indentation directly beneath the bolt-hole contact surface of the GFRP members due to bolt traction/bearing which indicates that the connection system is capable of sustaining higher joint strength capacity and adequately transmitted the internal forces to other members by providing a uniform stress distribution along the length of the members.
- The composite truss under Load Case 2 failed at 160 kN with the continuous top chords ruptured in flexural bending manner. The top edges of the web of the rectangular hollow sections suffered significant local compression damages through delamination and cracking, which later progressed to the bottom edges (web-flange junction failure). Under prolong loading time, however, the system has shown some ductility which is a preferred failure behaviour for a composite truss system.
- The theoretical strength limits of the pultruded GFRP truss members in tension, compression and flexural, as well as the joint strength were calculated using design equations prescribed by ASCE pre-standard and the results are in close agreement with the experimental values.
- Strand 7 truss model predicted accurately the vertical deflections and axial member forces of the composite truss system with bolted joints. This was achieved by presenting the truss members as a beam element and modified the beam translation end release (connection rigidity) to incorporate the influence of bonded mechanical insert at the nodes.
- The bolt thread pin-bearing strength and the modification factor of 2 for bonded mechanical insert effects were incorporated in both the theoretical and modelling

approaches to portray a close representation of the joint configuration setup when defining the joint load-carrying capacity. The factors have proven consistent in providing comparable values to the experimental outcomes.

7.5. Contributions of the study

The results obtained from this study showed that the structural joint of pultruded GFRP hollow sections using a through-bolt connection with bonded mechanical insert is an appropriate connection system in civil engineering applications. The significance of the outcomes from this research are as follows:

1. The results of this study provided a detailed understanding on the mechanism of damage initiation and propagation at the joint component of pultruded GFRP truss structure. Determination of failure modes and strength of pultruded GFRP truss structure under a different type of loadings will help to close gaps in designing efficient jointing methods.
2. The outcome of this study enhanced the understanding of bolting joint technology pertaining to the effect of bolt threads and the introduction of mechanical insert at the vicinity of jointing area. This will address the research gaps highlighted and contribute to improving the existing design codes for bolted connections of pultruded FRP.
3. The findings from the eccentricity study on T-joint component truss structures are useful for the practitioners to assess the joint load-carrying capacity and its behaviour. Even though in bolted connection design, the loading directions and fasteners should be arranged in a concentric manner, eccentricity may be unavoidable due to practical limitations in fabrication or erection. This will potentially increase the adaptability of bolted pultruded GFRP configuration under certain conditions.
4. The vital information gained from the tubular pultruded FRP bolted joint under elevated temperature is essential to evaluate the extent of deterioration of joint capacity in actual environmental conditions. In turn, it will develop a better understanding of pultruded GFRP bolted joint used under the hostile environment.

5. The evaluation of the large-scale pultruded GFRP truss structure provided useful and important data on the joint strength behaviour and its interactions with truss members, which mainly controls the overall structural integrity and capacity. This will promote the expansion of pultruded GFRP of hollow section for truss structure using through-bolt with mechanical inserts.

7.6. Areas for further study

The study of all-thread through-bolt connection with bonded mechanical insert for pultruded GFRP hollow sections is at an early stage and requires further experimental and analytical studies to expand its versatility in civil construction applications. Based on the findings of this study, the following recommendations for future investigations are drawn:

1. Further experimental works on bolted joint of pultruded GFRP hollow section incorporating the effects of other parameters, such as various bolt thread pitches, joint angles and multi-bolted connection with two or more rows of bolts, with and without the presence of mechanical inserts should be evaluated to be able to calibrate the previous proposed prediction equation. Also, effect of fatigue loadings and creeping behavior of FRP should be investigated in order to have a detailed understanding on how the loads are resisted, transferred, and distributed to each component and to design them safely and economically.
2. Long term performance of through-bolt connection with mechanical insert exposed under natural weathering is deemed necessary to evaluate structural performance and its joint durability which is governed by serviceability requirements in building and infrastructure applications. Besides, environmental ageing investigation associated to hot-wet conditions can be used to simulate common outdoor environments.
3. The investigation of this proposed pultruded GFRP tubular joint connection should be extended to the evaluation of the structural joints in framed structures, for instance beam-to-column joints, which exhibit a nonlinear

behaviour due to the moments and forces transferred and the interaction of other elements such as bolt contact and joint slip.

4. In addition, it is necessary to construct precise finite element (FE) modelling of through-bolt connection with bonded mechanical insert to capture the materials nonlinearities, damage initiation, and bolt interactions such as compressive interface stresses and possibility of slip. This comprehensive coverage using an advanced FE technique should be developed to generate parametric studies that will contribute to establishment of reliable design guidelines.

8. References

- AISC. (2001) Guide to Design Criteria for Bolted and Riveted Joints. *Second Edition*. Chicago, USA: American Institute of Steel Construction (AISC).
- AS/NZS1110:1995. (1995) ISO metric precision hexagon bolts and screws. Australia and New Zealand: Standards Australia and Standards New Zealand.
- AS/NZS1252.1. (2016) High-strength steel fastener assemblies for structural engineering - Bolts, nuts and washers: Part 1 - Technical requirements. Australian/New Zealand Standard.
- AS/NZS1252:1996. (1996a) High-strength steel bolts with associated nuts and washers for structural engineering. Australia and New Zealand: Standards Australia and Standards New Zealand.
- AS/NZS1252:1996. (1996b) High-strength steel bolts with associated nuts and washers for structural engineering. Australia and New Zealand. Standards Australia and Standards New Zealand.
- AS/NZS4291.2. (2016) Mechanical properties of fasteners made of carbon steel and alloy steel - Nuts with specified property classes - Coarse thread and fine pitch thread. Australian/New Zealand standard.
- ASCE. (2010) Pre-Standard for Load and Resistance Factor Design (LFRD) of Pultruded Fibre Reinforced Polymer (FRP) Structures.
- Ascione F. (2010) A preliminary numerical and experimental investigation on the shear stress distribution on multi-row bolted FRP joints. *Mechanics Research Communications* 37: 164-168.
- Ascione F, Feo L and Maceri F. (2010) On the pin-bearing failure load of GFRP bolted laminates: An experimental analysis on the influence of bolt diameter. *Composites Part B: Engineering* 41: 482-490.
- Ascione L, Berardi VP, Giordano A, et al. (2013) Buckling failure modes of FRP thin-walled beams. *Composites Part B: Engineering* 47: 357-364.
- Ascione L, Caron J-F, Godonou P, et al. (2016) *Prospect for new guidance in the design of FRP: Support to the implementation, harmonization and further development of the Eurocodes*: Publications Office of the European Union.
- ASTMD638. (2010) Standard test method for tensile properties of plastics. American Society for Testing and Materials (ASTM) Standard.
- ASTMD695. (2010) Standard test method for compressive properties of rigid plastics. American Society for Testing and Materials (ASTM) Standard.
- ASTMD953. (2010) Standard Test Method for Bearing Strength of Plastics. American Society for Testing and Materials (ASTM) Standard.
- ASTMD3163-01. (2014) Standard Test Method for Determining Strength of Adhesively Bonded Rigid Plastic Lap-Shear Joints in Shear by Tension Loading. American Society for Testing and Materials (ASTM) Standard.
- ASTMD3171. (2011) Standard Test Methods for Constituent Content of Composite Materials. American Society for Testing and Materials (ASTM) Standard.
- ASTMD5379. (2005) Standard test method for shear properties of composite materials by the V-notched beam method. American Society for Testing and Materials (ASTM) Standard.

- ASTMD5961. (2006) Standard Test Method for Bearing Response of Polymer Matrix Composite Laminates. American Society for Testing and Materials (ASTM) Standard.
- ASTME1356-08. (2014) Standard Test Method for Assignment of the Glass Transition Temperatures by Differential Scanning Calorimetry. United States: American Society for Testing and Materials (ASTM) Standard.
- Azwa ZN and Yousif BF. (2017) Physical and mechanical properties of bamboo fibre / polyester composites subjected to moisture and hygrothermal conditions. *Journal of Materials: Design and applications* 0: 1-15.
- B. Vangrimde and R. Boukhili. (2002) Analysis of the bearing response test for polymer matrix composite laminates bearing stiffness measurement and simulation. *Composite Structures* 56: 359-374.
- Bai Y, Keller T and Wu C. (2013) Pre-buckling and post-buckling failure at web-flange junction of pultruded GFRP beams. *Materials and structures* 46: 1143-1154.
- Bai Y, Post NL, Lesko JJ, et al. (2008) Experimental investigations on temperature-dependent thermo-physical and mechanical properties of pultruded GFRP composites. *Thermochimica Acta* 469: 28-35.
- Bai Y and Yang X. (2012) A Novel Joint for Assembly of All-Composite Space Truss Structures: Conceptual Design and Preliminary Study. *Journal of Composites for Construction*: 120807053619007.
- Bai Y and Yang X. (2013) Novel joint for assembly of all-composite space truss structures: conceptual design and preliminary study. *Composites for Construction* 17: 130-138.
- Bai Y and Zhang C. (2012) Capacity of nonlinear large deformation for trusses assembled by brittle FRP composites. *Composite Structures* 94: 3347-3353.
- Bakis CE, Freimanis AI, Gremel D, et al. (1998) Effect of resin material on bond and tensile properties of unconditioned and conditioned FRP reinforcement rods. In: Benmokrane B and Rahman H (eds) *The 1st International Conference on Durability of FRP Composites for Construction (CDCC98)*. Sherbrooke: CDCC, 525-533.
- Bank LC. (2006) *Composites for Construction: Structural Design with FRP Materials*, New Jersey: John Wiley & Sons, Inc.
- Bank LC. (2013) Progressive Failure and Ductility of FRP Composites for Construction: Review. *Composites for Construction* 17: 406-419.
- Bank LC, Gentry TR, Nuss KH, et al. (2000) Construction of a Pultruded Composite Structure: Case Study. *Journal of Composites for Construction* 4: 112-119.
- Bank LC, Mosallam AS and McCoy GT. (1994) Design and performance of connections for pultruded frame structures. *Journal of Reinforced Plastics and Composites* 13: 199-212.
- Bank LC, Yin J and Nadipelli M. (1995) Local buckling of pultruded beams - nonlinearity, anisotropy and inhomogeneity. *Construction and Building Materials* 9: 325-331.
- Barbero EJ and Turk M. (2000) Experimental investigation of beam-column behavior of pultruded structural shapes. *Reinforced Plastics and Composites* 19: 249-265.
- Berg CA, McGarry FJ and Elliot SY. (1973) Composite Material: Testing and Design (3rd conference). ASTM Special Technical Publication.

- Biscaia HC and Chastre C. (2018) Theoretical analysis of fracture in double overlap bonded joints with FRP composites and thin steel plates. *Engineering Fracture Mechanics* 190: 435-460.
- Blaga L, Dos Santos JF, Bancila R, et al. (2015) Friction Riveting (FricRiveting) as a new joining technique in GFRP lightweight bridge construction. *Construction and Building Materials* 80: 167-179.
- Bourban PE, Bogli A, Bonjour F, et al. (1998) Integrated processing of thermoplastic composites. *Composites Science and Technology* 58: 633-637.
- Boyd SW, Winkle IE and Day AH. (2004) Bonded butt joints in pultruded GRP panels—an experimental study. *International Journal of Adhesion and Adhesives* 24: 263-275.
- Bradford NM. (2004) Design optimization of FRP composite panel building system: Emergency shelter applications. *Department of Civil and Environmental Engineering*. University of South Florida.
- C.Cooper and G.J.Turvey. (1995) Effects of joint geometry and bolt torque on the structural performance of single bolt tension joints in pultruded GRP sheet material. *Composite Structures* 32: 217-226.
- Carlone P, Palazzo GS and Pasquino R. (2006) Pultrusion manufacturing process development by computational modelling and methods. *Mathematical and Computer Modelling* 44: 701-709.
- Chen Y and Wang C. (2015) Web crippling behavior of pultruded GFRP rectangular hollow sections. *Composite Part B* 77: 112-121.
- Clarke JL. (1996) *Structural design of polymer composites: EUROCOMP design code and handbook*, London: E & FN Spon.
- CNR. (2008) Guide for the Design and Construction of Structures made of FRP Pultruded Elements. Rome: National Research Council of Italy.
- Coelho AMG and Mottram JT. (2015) A review of the behaviour and analysis of bolted connections and joints in pultruded fibre reinforced polymers. *Materials & Design* 74: 86-107.
- Cooper C and Turvey GJ. (1995) Effects of joint geometry and bolt torque on the structural performance of single bolt tension joints in pultruded GRP sheet material. *Composite Structures* 32: 217-226.
- Correia JR, Bai Y and Keller T. (2015) A review of the fire behaviour of pultruded GFRP structural profiles for civil engineering applications. *Composite Structures* 127: 267-287.
- Davalos JF and Qiao P. (1997) Analytical and experimental study of lateral and distortional buckling of FRP wide-flange beams. *Journal of Composites for Construction* 1: 150-159.
- Davalos JF, Salim HA, Qiao P, et al. (1996) Analysis and design of pultruded FRP shapes under bending. *Composite Part B: Engineering* 27B: 295-305.
- de Castro J and Keller T. (2008) Ductile double-lap joints from brittle GFRP laminates and ductile adhesives, Part I: Experimental investigation. *Composites Part B: Engineering* 39: 271-281.
- DG9. (2004) Design guide 9: For Structural Hollow Section Column Connections. Germany: The International Committee for Research and Technical Support for Hollow Section Structures (CIDECT).
- dos Santos CL and Morais JLL. (2015) Mechanical behaviour of wood T-joints. Experimental and numerical investigation. *Frattura ed Integrita Strutturale* 31: 23-37.

- Dubina D. (2008) Structural analysis and design assisted by testing of cold-formed steel structures. *Thin-Walled Structures* 46: 741-764.
- ECSS. (2011) Insert design handbook. Noordwijk, The Netherlands: European Cooperation for Space Standardization.
- Einde LVD, Zhao L and Seible F. (2003) Use of FRP composites in civil structural applications. *Construction and Building Materials* 17: 389-403.
- EN13706-2. (2002) Reinforced plastics composites. Specifications for pultruded profiles. Method of test and general requirements.: British Standards Institution.
- Eurocomp. (1996) *Structural Design of Polymer Composites*, London: E & FN Spon.
- Feng P, Wang J, Tian Y, et al. (2016) Mechanical Behavior and Design of FRP Structural Members at High and Low Service Temperatures. *Journal of Composites for Construction* 20: 04016021.
- Feroldi F and Russo S. (2016) Structural Behavior of All-FRP Beam-Column Plate-Bolted Joints. *Journal of Composites for Construction* 20: 04016004.
- Foster DC, Richards D and Bogner BR. (2004) Design and Installation of Fiber-Reinforced Polymer Composite Bridge. *Journal of Composites for Construction* 4: 33-37.
- Gand AK, Chan T-M and Mottram JT. (2013) Civil and structural engineering applications, recent trends, research and developments on pultruded fibre reinforced polymer closed sections: a review. *Frontiers of Structural and Civil Engineering* 7: 227-244.
- Garrido M, Correia JR and Keller T. (2015) Effects of elevated temperature on the shear response of PET and PUR foams used in composite sandwich panels. *Construction and Building Materials* 76: 150-157.
- Goldsworthy WB and Hiel C. (1998) Composite structures. *SAMPE Journal* 34: 24-30.
- Guades EJ. (2013) Behaviour of Glass FRP Composite Tubes Under Repeated Impact for Piling Application. *Centre of Excellence in Engineered Fibre Composites*. Queensland, Australia: University of Southern Queensland.
- Hadi MNS. (2007) The behaviour of FRP wrapped HSC columns under different eccentric loads. *Composite Structures* 78: 560-566.
- Hai ND and Mutsuyoshi H. (2012) Structural behavior of double-lap joints of steel splice plates bolted/bonded to pultruded hybrid CFRP/GFRP laminates. *Construction and Building Materials* 30: 347-359.
- Hashim SA. (2009) Strength of resin-coated-adhesive-bonded double lap-shear pultrusion joints at ambient temperature. *International Journal of Adhesion and Adhesives* 29: 294-301.
- Hashim SA and Nisar JA. (2013) An investigation into failure and behaviour of GFRP pultrusion joints. *International Journal of Adhesion and Adhesives* 40: 80-88.
- Heshmati M, Haghani R and Al-Emrani M. (2017) Durability of bonded FRP-to-steel joints: Effects of moisture, de-icing salt solution, temperature and FRP type. *Composites Part B: Engineering* 119: 153-167.
- Hizam RM, Karunasena W and Manalo AC. (2013) Effect of mechanical insert on the behaviour of pultruded reinforced polymer (FRP) bolted joint. *Fourth Asia-Pacific Conference on FRP in Structures (APFIS)*. Melbourne, Australia: International Institute for FRP in Construction (IIFC).
- Hizam RM, Manalo AC and Karunasena W. (2012) A review of FRP composite truss systems and its connections. In: Bijan Samali CS, Mario M. Attard (ed) *22nd*

- Australasian Conference on the Mechanics of Structures and Materials*. Sydney, New South Wales, Australia: Taylor & Francis Ltd.
- Hizam RM, Manalo AC, Karunasena W, et al. (2018) Effect of bolt threads on the double lap joint strength of pultruded fibre reinforced polymer composite materials. *Construction and Building Materials* 181: 185-198.
- Hollaway LC. (2003) The evolution of and the way forward for advanced polymer composites in the civil infrastructure. *Construction and Building Materials* 17: 365-378.
- Hollaway LC. (2010) A review of the present and future utilisation of FRP composites in the civil infrastructure with reference to their important in-service properties. *Construction and Building Materials* 24: 2419-2445.
- Humphreys MF. (2003) Development and structural investigation of monocoque fibre composite trusses. *School of Civil Engineering*. Queensland University of Technology.
- Humphreys MF, Erp GV and Tranberg CH. (1999) The structural behavior of monocoque FRP truss joints. *Advanced Composite Letters* 8: 173-180.
- Hunter-Alarcon R, Leyrer J, Leal E, et al. (2018) Influence of dissimilar composite adherends on the mechanical adhesion of bonded joints for small blade wind turbine applications. *International Journal of Adhesion and Adhesives*.
- Ibrahim RA and Pettit CL. (2005) Uncertainties and dynamic problems of bolted joints and other fasteners. *Journal of Sound and Vibration* 279: 857-936.
- Ireman T, Ranvik T and Eriksson I. (2000) On damage development in mechanically fastened composite laminates. *Composite Structures* 49: 151-171.
- ISO75-1. (2004) Plastics - Determination of temperature of deflection under load International Organization for Standardization (ISO).
- ISO527-2. (1996) Plastics: Determination of tensile properties. International Organization for Standardization (ISO).
- ISO1172. (1996) Textile-glass-reinforced plastics, prepegs, moulding compounds and laminates: Determination of the textile-glass and mineral-filler content- Calcination methods. International Organization for Standardization (ISO).
- Jones D and Ellis JW. (1986) *Polymer Products Design, Materials and Processing*, London New York: Chapman and Hall.
- K.Hassan N, A.Mohamedien M and H.Rizkalla S. (1996) Finite element analysis of bolted connections for PFRP composites. *Composites Part B: Engineering* 27B: 339-349.
- Karbhari VM, Stachowski C and Wu L. (2007) Durability of Pultruded E-Glass/Vinylester under Combined Hygrothermal Exposure and Sustained Bending. *Journal of Materials in Civil Engineering* 19: 665-673.
- Keller T. (2001) Recent all-composite and hybrid fibre-reinforced polymer bridges and buildings. *Progress in Structural Engineering and Materials* 3: 132-140.
- Keller T, Bai Y and Vallée T. (2007a) Long-Term Performance of a Glass Fiber-Reinforced Polymer Truss Bridge. *Journal of Composites for Construction* 11.
- Keller T, Bai Y and Vallée T. (2007b) Long-Term Performance of Glass Fiber-Reinforced Polymer Truss Bridge. *Journal of Composites for Construction* 11: 99-108.
- Keller T and de Castro J. (2005) System ductility and redundancy of FRP beam structures with ductile adhesive joints. *Composites Part B: Engineering* 36: 586-596.

- Keller T, Theodorou N, Vassilopoulos A, et al. (2015) Effect of Natural Weathering on Durability of Pultruded Glass Fiber-Reinforced Bridge and Building Structures. *Journal of Composites for Construction* 20: 04015025.
- Keller T and Vallée T. (2005) Adhesively bonded lap joints from pultruded GFRP profiles. Part I: stress-strain analysis and failure modes. *Composites Part B: Engineering* 36: 331-340.
- Khashaba UA, Sallam HEM, Al-Shorbagy AE, et al. (2006) Effect of washer size and tightening torque on the performance of bolted joints in composite structures. *Composite Structures* 73: 310-317.
- Korol R. (1986) Double Chords as an Alternative in Tubular Trusses. *Journal of Structural Engineering* 112: 2665-2678.
- Kumar P, Chandrashekhara K and Nanni A. (2001) Testing and Evaluation of Components for a Composite Bridge Deck. *Journal of Reinforced Plastics and Composites*.
- Kumar TV, Shankar GS and Shankar BL. (2017) Experimental Study on Effect of Stacking Sequence, Clearance and Clamping Torque on Strength of FRP Composite Bolted Joints. *Materials Today: Proceedings* 4: 10746-10750.
- Lane A and Mottram JT. (2002) The influence of modal coupling upon the buckling of concentrically pultruded fibre-reinforced plastic columns. *Proc. Inst. of Mechanical Engineers Part L: Journal of Materials - Design and Applications* 216: 133-144.
- Lau STW, Said MR and Yaakob MY. (2012) On the effect of geometrical designs and failure modes in composite axial crushing: A literature review. *Composite Structures* 94: 803-812.
- Lee HK, Pyo SH and Kim BR. (2009) On joint strengths, peel stresses and failure modes in adhesively bonded double-strap and supported single-lap GFRP joints. *Composite Structures* 87: 44-54.
- Lee Y-G, Choi E and Yoon S-J. (2015) Effect of geometric parameters on the mechanical behavior of PFRP single bolted connection. *Composites Part B: Engineering* 75: 1-10.
- Liao K, Schultheisz CR and Hunston DL. (1999) Effects of environmental aging on the properties of pultruded GFRP. *Composite Part B: Engineering* 30: 485-493.
- Luo FJ, Bai Y, Yang X, et al. (2016a) Bolted sleeve joints for connecting pultruded FRP tubular components. *Composites for Construction* 20: 04015024.
- Luo FJ, Yang X and Bai Y. (2016b) Member capacity of pultruded GFRP tubular profile with bolted sleeve joints for assembly of latticed structures. *Journal of Composites for Construction* 20: 1-12.
- Machado J, Marques E and da Silva LF. (2018) Adhesives and adhesive joints under impact loadings: An overview. *The Journal of Adhesion* 94: 421-452.
- Maji AK, Acree R, Satpathi D, et al. (1997) Evaluation of Pultruded FRP Composites for Structural Applications. *Journal of Materials in Civil Engineering* 9: 154-158.
- Manalo A, Aravinthan T, Fam A, et al. (2017a) State-of-the-Art Review on FRP Sandwich Systems for Lightweight Civil Infrastructure. *Journal of Composites for Construction* 21.
- Manalo A, Maranan G, Sharma S, et al. (2017b) Temperature-sensitive mechanical properties of GFRP composites in longitudinal and transverse directions: A comparative study. *Composite Structures* 173: 255-267.

- Manalo A, Surendar S, Van Erp G, et al. (2016) Flexural behavior of an FRP sandwich system with glass-fiber skins and a phenolic core at elevated in-service temperature. *Composite Structures* 152: 96-105.
- Manalo AC and Mutsuyoshi H. (2011) Behavior of fiber-reinforced composite beams with mechanical joints. *Journal of composite materials*: 1-14.
- Mara V, Haghani R and Al-Emrani M. (2016) Improving the performance of bolted joints in composite structures using metal inserts. *Journal of composite materials* 50: 3001-3018.
- Matharu NS and Mottram JT. Laterally unrestrained bolt bearing strength: Plain pin and threaded values. 1-8.
- Matharu NS and Mottram JT. (2012) Laterally unrestrained bolt bearing strength: Plain pin and threaded values. *6th International Conference on FRP Composites in Civil Engineering*. Rome, Italy.
- Mathieu R, Peng W, Patrice C, et al. (2010) Temperature as an Accelerating Factor for Long-Term Durability Testing of FRPs: Should There Be Any Limitations? *Journal of Composites for Construction* 14: 361-367.
- McCormick L. (1999) The Static Load Response of Fibre Composite Trusses. Toowoomba, Australia: University of Southern Queensland.
- Meiarashi S, Nishizaki I and Kishima T. (2002) Life-Cycle Cost of All-Composite Suspension Bridge. *Journal of Composites for Construction* 6: 206-214.
- Min W. (2008) The finite element value simulation of composite bolt threaded nut contact and experimental study. *School of Material Science and Engineering*. China: Taiyuan University of Science and Technology.
- Mirza FA, Shehata AA and Korol RM. (1982) Modelling of double chord rectangular hollow section T-joints by finite element method. *Computers & Structures* 15: 123-129.
- Mosallam AS. (2011) *Design Guide for FRP Composite Connections*: American Society of Civil Engineers (ASCE).
- Mottram J. (1992) Lateral-torsional buckling of a pultruded I-beam. *Composites* 23: 81-92.
- Mottram JT. (2009) Design Guidance for Bolted Connections in Structures of Pultruded Shapes: Gaps in Knowledge. *17th International Conference on Composite Materials* A1.
- Mottram JT, Brown ND and Anderson D. (2003) Buckling characteristics of pultruded glass fibre reinforced plastic columns under moment gradient. *Thin-Walled Structures* 41: 619-638.
- Mottram JT and Turvey GJ. (2003) Physical test data for the appraisal of design procedures for bolted joints in pultruded FRP structural shapes and systems. *Progress in Structural Engineering and Materials* 5: 195-222.
- Mottram JT and Zafari B. (2011a) Pin-bearing strengths for bolted connection in FRP structures. *Structures and Buildings*.
- Mottram JT and Zafari B. (2011b) Pin-bearing Strengths for Bolted Connections in FRP Structures. *Structures and Buildings*.
- Mouritz AP and Gibson AG. (2010) *Fire properties of polymer composite material*, Netherlands: Springer.
- Muttashar M, Manalo A, Karunasena W, et al. (2017) Flexural behaviour of multi-celled GFRP composite beams with concrete infill: Experiment and theoretical analysis. *Composite Structures* 159: 21-33.

- Nahla KH, A.Mohamedien M and H.Rizkalla S. (1996) Finite element analysis of bolted connections for PFRP composites. *Composites Part B: Engineering* 27B: 339-349.
- Nerilli F and Vairo G. (2017) Progressive damage in composite bolted joints via a computational micromechanical approach. *Composites Part B: Engineering* 111: 357-371.
- Nunes F, Correia M, Correia JR, et al. (2013) Experimental and numerical study on the structural behavior of eccentrically loaded GFRP columns. *Thin-Walled Structures* 72: 175-187.
- Omar T, Erp GV, Aravinthan T, et al. (2008) Truss fibre deployable shelter. *Faculty of Engineering and Surveying*. Australia: University of Southern Queensland.
- Omar T, Van Erp G, Aravinthan T, et al. (2007) Innovative all composite multi pultrusion truss system for stressed-arch deployable shelters. *Sixth Alexandria International Conference on Structural and Geotechnical Engineering*.
- Park HJ. (2001) Effects of stacking sequence and clamping force on the bearing strengths of mechanically fastened joints in composite laminates. *Composite Structures* 53: 213-221.
- Persson E, Eriksson I and zackrisson L. (1997) Effects of hole machining defects on strength & fatigue life of composite. *Composites Part A: Applied Science and Manufacturing* 28A: 141-151.
- Pfeil MS, Teixeira AMAJ and Battista RC. (2009) Experimental tests on GFRP truss modules for dismountable bridges. *Composite Structures* 89: 70-76.
- Pisano A and Fuschi P. (2011) Mechanically fastened joints in composite laminates: Evaluation of load bearing capacity. *Composites Part B: Engineering* 42: 949-961.
- Plastics R. (2002) Pultrusion industry grows steadily in US. *Reinforced Plastics*.
- Qiu C, Ding C, He X, et al. (2018) Axial performance of steel splice connection for tubular FRP column members. *Composite Structures* 189: 498-509.
- Qureshi J and Mottram JT. (2015) Moment-rotation response of nominally pinned beam-to-column joints for frames of pultruded fibre reinforced polymer. *Construction and Building Materials* 77: 396-403.
- Ragheb WF. (2010) Local buckling analysis of pultruded FRP structural shapes subjected to eccentric compression. *Thin-Walled Structures* 48: 709-717.
- Righman J, Barth K and Davalos J. (2004) Development of an Efficient Connector System for Fiber Reinforced Polymer Bridge Decks to Steel Girders. *Journal of Composites for Construction* 8: 279-288.
- Rosner CN and Rizkalla SH. (1995) Bolted connections for fiber-reinforced composite structural members: analytical model and design recommendations. *Journal of Materials in Civil Engineering* 7: 232-238.
- Roylance D. (2000) Trusses. *Department of Materials Science and Engineering*. 8th June 2000: Massachusetts Institute of Technology.
- Russo S. (2012) Experimental and finite element analysis of a very large pultruded FRP structure subjected to free vibration. *Composite Structures* 94: 1097-1105.
- Russo S. (2016) First investigation on mixed cracks and failure modes in multi-bolted FRP plates. *Composite Structures* 154: 17-30.
- S.Ramakrishna, H.Hamada and M.Nishiwaki. (1995) Bolted joints of pultruded sandwich composite laminates. *Composite Structures* 32: 227-235.
- Satavisam S, Feng P, Bai Y, et al. (2017) Composite actions within steel-FRP composite beam systems with novel blind bolt shear connections. *engineering Structures* 138: 63-73.

- Schmidt JW, Bennitz A, Täljsten B, et al. (2012) Mechanical anchorage of FRP tendons – A literature review. *Construction and Building Materials* 32: 110-121.
- SCI and BCSA. (2002) Joints in Steel Construction: Simple connections. Steel Construction Institute/British Constructional Steelwork Association.
- Shahverdi M, Vassilopoulos AP and Keller T. (2011) Experimental investigation of R-ratio effects on fatigue crack growth of adhesively-bonded pultruded GFRP DCB joints under CA loading. *Composites Part A: Applied Science and Manufacturing*.
- Shehata AA, Korol R and Mirza FA. (1987) Joint flexibility effects on rectangular hollow section vierendeel trusses. *Mechanics of Structures and Machines* 15: 89-107.
- Singamsethi SK, LaFave JM and Hjelmstad KD. (2005) Fabrication and Testing of Cuff Connection for GFRP Box Sections. *Journal of Composites for Construction* 9: 536-544.
- Smith SJ, Parsons ID and Hjelmstad KD. (1998) An experimental study of the behaviour of connection for pultruded GFRP- I beams and rectangular tubes. *Composites Structures*: 281 - 290.
- Stazi F, Giampaoli M, Rossi M, et al. (2015) Environmental ageing on GFRP pultruded joints: Comparison between different adhesives. *Composite Structures* 133: 404-414.
- Strand7. (2015) Strand7 Release 2.4.6. Sydney, Australia.
- Teixeira AMAJ, Pfeil MS and Battista RC. (2014) Structural evaluation of a GFRP truss girder for deployable bridge. *Composites Structures* 110: 29-38.
- Terrasi GP, Affolter C and Barbezat M. (2011) Numerical Optimization of a Compact and Reusable Pretensioning Anchorage System for CFRP Tendons. *Journal of Composites for Construction* 15: 126.
- TMR. (2014) Design criteria for bridges and other structures. In: (TMR) QTaMR (ed). Queensland, Australia.
- Turi EA. (1997) Thermal characterization of polymer materials. *Academic* 2.
- Turvey and Wang P. (2008) An FE analysis of the stresses in pultruded GRP single-bolt tension joints and their implications for joint design. *Computers & Structures* 86: 1014-1021.
- Turvey GJ. (1998a) Single-bolt tension joint tests on pultruded GRP plate: effects of the orientation of the tension direction relative to pultrusion direction. *Composite Structures* 42: 341-351.
- Turvey GJ. (1998b) Torsion tests on pultruded GRP sheet. *Composite Science and Technology* 58: 1343-1351.
- Turvey GJ. (2000) Bolted connections in PFRP structures. *Progress in Structural Engineering and Materials* 2: 146-156.
- Turvey GJ and Sana A. (2016) Pultruded GFRP double-lap single-bolt tension joints – Temperature effects on mean and characteristic failure stresses and knock-down factors. *Composite Structures* 153: 624-631.
- Turvey GJ and Wang P. (2007) Failure of pultruded GRP single-bolt tension joints under hot–wet conditions. *Composite Structures* 77: 514-520.
- Turvey GJ and Wang P. (2009) Failure of pultruded GFRP bolted joints: a Taguchi analysis. *Engineering and Computational Mechanics*. Institution of Civil Engineers (ICE), 155-166.
- Turvey GJ and Zhang Y. (2006) Shear failure strength of web–flange junctions in pultruded GRP WF profiles. *Construction and Building Materials* 20: 81-89.

- Uddin N and Abro AM. (2008) Design and manufacturing of low cost thermoplastic composite bridge superstructures. *engineering Structures* 30.
- Ungkurapinan N. (2000) A study of joint slip in galvanised bolted angle connections. *Civil and Geological Engineering*. Canada: University of Manitoba.
- van Rijswijk K and Bersee HEN. (2007) Reactive processing of textile fiber-reinforced thermoplastic composites – An overview. *Composites Part A: Applied Science and Manufacturing* 38: 666-681.
- Vangrimde B and Boukhili R. (2003) Descriptive relationships between bearing response and macroscopic damage in GRP bolted joints. *Composites Part B: Engineering* 34: 593-605.
- Wang Y. (2002) Bearing behaviour of joints in pultruded composites. *Journal of composite materials* 36: 2199-2216.
- Wardenier J, Packer JA, Zhao XL, et al. (2010) *Hollow Sections in Structural Applications*, Geneva, Switzerland: CIDECT.
- WCFT. (2016) Wagners Composite Fibre Technologies: Product Guide. Toowoomba, Australia: Wagners CFT Manufacturing Pty Ltd.
- Wu C and Bai Y. (2014) Web crippling behaviour of pultruded glass fibre reinforced polymer sections. *Composite Structures* 108: 789-800.
- Wu C, Bai Y and Mottram JT. (2015a) Effect of Elevated Temperatures on the Mechanical Performance of Pultruded FRP Joints with a Single Ordinary or Blind Bolt. *Journal of Composites for Construction* 20: 04015045.
- Wu C, Bai Y and Zhao XL. (2015b) Improved bearing capacities of pultruded glass fibre reinforced polymer square hollow sections strengthened by thin-walled steel or CFRP. *Thin-Walled Structures* 89: 67-75.
- Xiao Y and Ishikawa T. (2005a) Bearing strength and failure behavior of bolted composite joints (part I: Experimental investigation). *Composites Science and Technology* 65: 1022-1031.
- Xiao Y and Ishikawa T. (2005b) Bearing strength and failure behavior of bolted composite joints (part II: modeling and simulation). *Composites Science and Technology* 65: 1032-1043.
- Yang X, Bai Y and Ding F. (2015) Structural performance of a large-scale space frame assembled using pultruded GFRP composites. *Composite Structures* 133: 986-996.
- Yang X, Bai Y, Luo FJ, et al. (2016) Dynamic and fatigue performances of a large-scale space frame assembled using pultruded GFRP composites. *Composite Structures* 138: 227-236.
- Zaharia R and Dubina D. (2006) Stiffness of joints in bolted connected cold-formed steel trusses. *Constructional Steel Research* 62: 240-249.
- Zhang Y and Keller T. (2008) Progressive failure process of adhesively bonded joints composed of pultruded GFRP. *Composites Science and Technology* 68: 461-470.
- Zhang Z, Bai Y, He X, et al. (2018a) Cyclic performance of bonded sleeve beam-column connections for FRP tubular sections. *Composites Part B: Engineering*.
- Zhang Z, Bai Y and Xiao X. (2018b) Bonded sleeve connections for joining tubular glass fiber reinforced polymer beams and columns: an experimental and numerical study. *Composites for Construction*.
- Zhou A and Keller T. (2006) Joining techniques for fiber reinforced polymer composite bridge deck systems. *Composites Structures* 69: 336-345.

Appendix A: Additional study

A.1 Material characterisation

The characterisation of the mechanical properties of square hollow section (SHS) and rectangular hollow section (RHS) pultruded FRP used throughout the study are presented. Mainly the characterisation tests to determine the mechanical properties were undertaken on the coupon size specimens in longitudinal and transverse direction of the tubes. In particular, constituent material contents (percentage volume of fibres and matrix), tensile, compressive, in-plane shear, and pin bearing properties are examined. Pultruded E-glass/vinyl ester fibre reinforced polymer (FRP) tested in this study are manufactured and supplied by Wagners Composite Fibre Technologies (WCFT) based in Queensland, Australia. There are two (2) tubular sections of different dimension were used throughout the study which is 125 mm x 125 mm x 6.5 mm and 100 mm x 75 mm x 5mm. For pultruded square hollow section (SHS), the materials supplied can be set into 2 groups, namely group A1 and group A2. The group A2 was created due to additional material required which was supplied from a different batch, in order to further analyse the joint parameters involved. Meanwhile, for pultruded rectangular hollow section (RHS), the materials were supplied only from one batch and were placed as group B. Table A.1 briefly summarises the materials used for each experimental works throughout this study.

Table A.1. Summary of materials used in each experimental works

No	Experimental Program	Type of materials used
1	Tensile, compressive, in-plane shear and flexural testing Double lap single-bolt joint (DLSJ) experimental work <i>*Test coupons were cut from the listed tubular sections (Figure A.1)</i>	A1. 125 mm x 125 mm x 6.5 mm A2. 125 mm x 125 mm x 6.5 mm B. 100 mm x 75 mm x 5 mm
4	Tubular pultruded FRP (under tensile loading) under elevated temperature	A2. 125 mm x 125 mm x 6.5 mm

3	T-joint component testing (under eccentric loading)	B. 100 mm x 75 mm x 5 mm
5	Large scale pultruded FRP truss structure under static loading	B. 100 mm x 75 mm x 5 mm

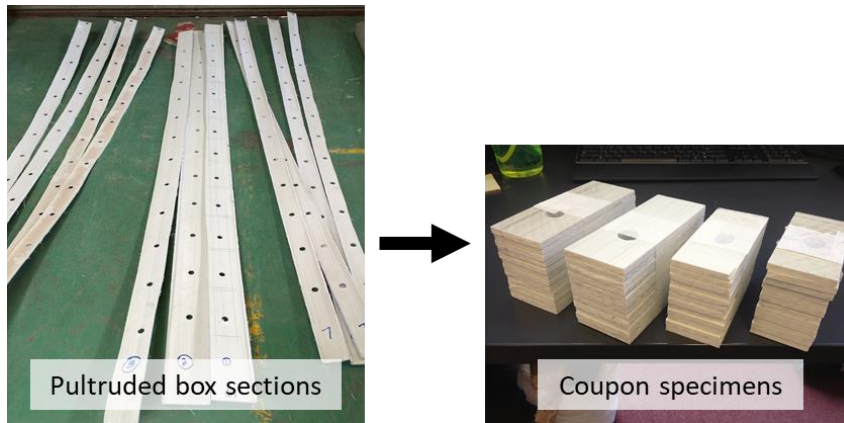


Figure A.1. Preparation of coupon specimens

Table A.2 presents the relevant test methods used and the number of tests carried out as recommended in Pre-Standard for Load and Resistance Factor Design (LRFD) of Pultruded FRP structures by ASCE. Table A.3 presents the mechanical properties of pultruded glass FRP profiles involved through-out this study.

Table A.2. Characteristic mechanical properties for FRP composite plates

Mechanical property	ASTM test method	Number of tests
Tensile	D638	10
Compressive	D6641	10
In-plane shear	D5379	10
Pin-bearing strength	D953	10

Table A.3. Mechanical properties of pultruded FRP profiles

Properties ^a	6.5 mm plate	5 mm plate
Tensile Long ^b , Peak stress (MPa)	741.53 (44.91) ^d	686.43 (44.21)
Tensile Long, Elastic modulus (MPa)	42,983 (1257)	42,922 (2281)
Tensile Trans ^c , Peak stress (MPa)	66.41 (3.78)	46.84 (3.91)
Tensile Trans, Elastic modulus (MPa)	13,350 (2,131.06)	12,198 (1,110)

Properties ^a	6.5 mm plate	5 mm plate
Compressive Long, Peak stress (MPa)	514.86 (15.27)	543.83 (43.95)
Compressive Trans, Peak stress (MPa)	161.66 (6.76)	147.70 (15.23)
In-plane shear Long, Peak stress (MPa)	113.60 (6.85)	88.95 (14.64)
In-plane shear Trans, Peak stress (MPa)	95.30 (4.72)	NA ^f
Pin-bearing (Plain), Peak stress (MPa)	291.44 (7.72)	260.12 (55.66)
Pin-bearing (Thread), Peak stress (MPa)	207.68 (11.08)	185 (7.21)
Fibre mass fraction, W_f	78.6%	81.4%
Matrix mass fraction, W_m	21.4%	18.6%
Fibre volume fraction, V_f	61%	65%
Mass volume fraction, V_m	38%	34%
Density ^e (kg/m ³)	2030	

^aTesting were conducted based on relevant standards ^bLongitudinal ^cTransverse
^dStandard deviation ^eWCFT product specification ^fNot available

Constituent fibre content and stacking sequence

From burn-out testing at 600°C, the material revealed its stacking sequence (Figure 2 and 3) which consists of symmetrical fibre layers of 0° / 45° / 0° / -45° / 0° / -45° / 0° / 45° / 0° for pultruded FRP group A1 and A2 and 0° / 45° / 0° / -45° / 0° for pultruded FRP group B. Apart from that, there are thin protective veils noticeable on the outermost surface of pultruded FRP. The constituent content of composite material was determined according to ASTM 3171, whereby the fibre weight fraction and matrix weight fraction in 125 mm x 125 mm x 6.5 mm for both groups is 78% and 22% respectively. Meanwhile, the fibre weight fraction in 100 mm x 75 mm x 6.5 mm is slightly increased compared to the former tubular section which is about 81%. The presence of high content long continuous fibres in unidirectional (0°) has increased the material tensile strength and elastic modulus. The reinforcement from stitch fabrics ($\pm 45^\circ$) has improved its transverse strength. Due to commercial confidentiality, detail discussions on the chemical composition of the glass fibre and the matrix of the said materials are not included.

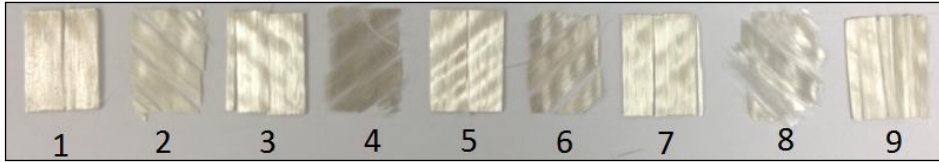


Figure A.2. Pultruded glass FRP stacking sequence of 125 mm x 125 mm x 6.5 mm (A1 and A2)

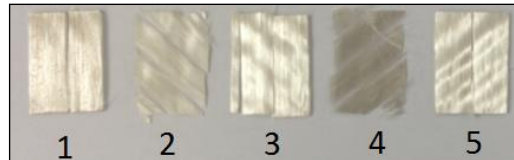


Figure A.3. Pultruded glass FRP stacking sequence of 100 mm x 75 mm x 5 mm

Pin-bearing

Pin-bearing capacity is important when designing bolted connection for pultruded FRP. It is useful for bearing resistance evaluation. Pin-bearing strength of this material had been tested in the similar way done by Mottram and Zafari (2011b). The test setup was based on WU (Warwick University) setup with a nominal bolt diameter of 20 mm and an end distance to bolt diameter up to 4 (Figure A.4). In this case, unusual threaded bolt was also included and its pin-bearing strength and mode of failure were recorded (Figure A.5).

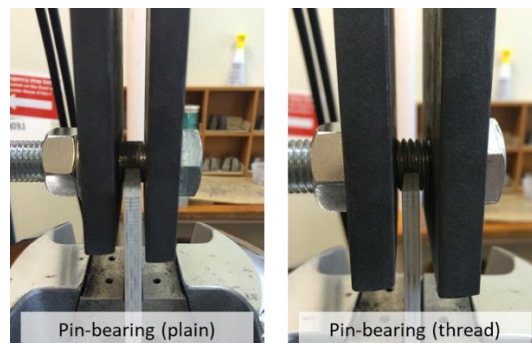


Figure A.4. Pin-bearing test set-up for both bolts plain and thread

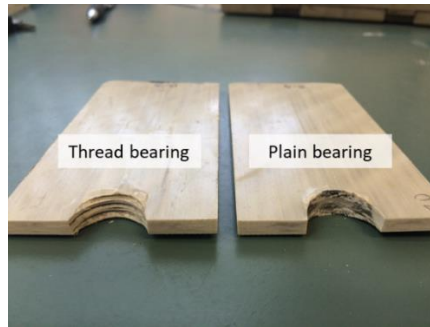


Figure A.5. Bearing mode of failure

A.2 Preliminary study on double lap single-bolted (DSLJ) coupon testing

The bolted pultruded laminates were tested up to failure in the tensile direction using 810 Material Test System (MTS) machine. The cross-head speed was 1.0mm/min. Figure A.6 shows the strain gauges arrangement on one side of test the specimens. For the specimen loaded in pin manner, the strain gauges were placed around the bolted area. Strain 1 was installed to evaluate the stress within bearing vicinity whereas strain 3 is introduced to analyse the stress endured by net-tension failure which is expected to occur in the transverse specimen. Strain 2 is important for observing the far field stress computed outside the washer and to compare it with the specimen loaded in pin manner. The load applied and hole elongation of the tested specimens were recorded with Teststar IIs while strain data were recorded using System 5000 (Model 5100B Scanner). Then, the finite element (FE) model was constructed using Strand7, and the numerical outcome were compared with the experimental results (Figure A.7).

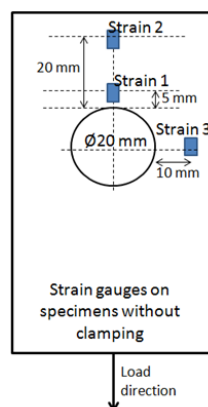


Figure A.6. Strain gauges arrangement

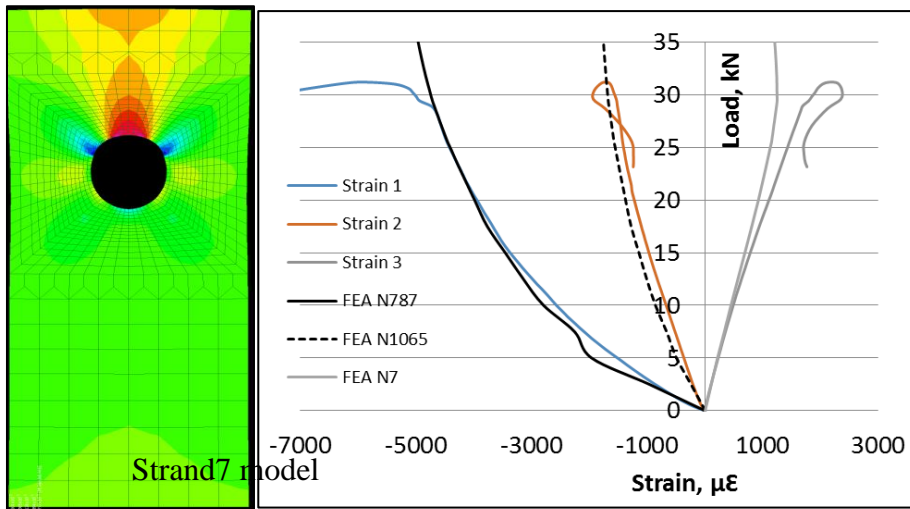


Figure A.7. Longitudinal plain experimental joint strength and Strand7 modelling

The horizontal axis represents the axial strain in micro ($\mu\epsilon$), where negative value indicates compressive strain and positive value indicates tensile strain. As can be seen, the strain 3 was in tension and the strains located in the edge distance and parallel to the loading direction were in compression side. It can be observed that, the strain data computed from the Strand7 numerical non-linear analysis are in close proximity to the experimental data.

Appendix B: Supporting Information

B.1 Article I

Construction and Building Materials 181 (2018) 185–198



Contents lists available at ScienceDirect

Construction and Building Materials

journal homepage: www.elsevier.com/locate/conbuildmat



Effect of bolt threads on the double lap joint strength of pultruded fibre reinforced polymer composite materials



R.M. Hizam^a, Allan C. Manalo^{a,*}, Warna Karunasena^a, Yu Bai^b

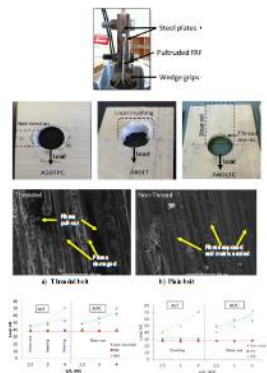
^aCentre for Future Materials, Faculty of Health, Engineering and Sciences, University Southern Queensland, QLD 4350, Australia

^bDepartment of Civil Engineering, Monash University, Clayton, VIC 3800, Australia

HIGHLIGHTS

- Investigation on the effects of threaded bolt and clamping pressure on the strength of bolted FRP joints.
- Strength of bolted joint with different edge-to-distance ratios and fibre orientation.
- Testing and analysis of 150 double lap joints.
- Joint strength behaviour, failure mechanisms and joint efficiency.
- Determination of reduction factor for the design of FRP connections using threaded bolts.

GRAPHICAL ABSTRACT



ARTICLE INFO

Article history:
Received 24 February 2018
Received in revised form 17 May 2018
Accepted 7 June 2018

Keywords:
Pultruded FRP
Bolt threads
Clamping
Connection
Joint
Failure modes

ABSTRACT

The ability to provide effective and adaptable joints for pultruded fibre reinforced polymer (PFRP) is crucial for its widespread application in civil infrastructure. This experimental based study on 150 double lap joints specimens investigated the effects of threaded bolt and clamping pressure on the joint strength behaviour, failure mechanisms and joint efficiency of bolted joints in PFRP. Double lap joints in both longitudinal and transverse directions of the laminates and with different edge distance-to-bolt diameter (e/d_b) were prepared and tested in accordance with ASTM D5961 standards. The joint strength in the longitudinal laminates with plain bolt increased for e/d_b ratio for up to 4 and with no appreciable strength gain after exceeding this ratio. On the other hand, about 30%–40% reduction in joint strength was observed in the longitudinal direction due to the bolt thread tearing through the laminates. This leads to a recommendation of 0.6 reduction factor in preliminary design of PFRP bolted connections with bolt thread present. Meanwhile, only a marginal difference of 7% was observed in transverse direction. Furthermore, the introduction of lateral clamping pressure had increased the joint strength by 60%–90% and this has lessened the thread casualty effect on the pultruded composite joints.

© 2018 Elsevier Ltd. All rights reserved.

* Corresponding author.
E-mail address: manalo@usq.edu.au (A.C. Manalo).

1. Introduction

The interest in using fibre reinforced polymer (FRP) composites in civil engineering and construction applications has increased significantly in recent years. This advanced material was initially introduced in structural applications as strengthening material for beams and columns of bridges and buildings [1–3]. With advanced manufacturing process such as pultrusion, standard structural shapes for instance box section, I-beam, etc., which resemble closely that of structural steel sections, are now readily available for the construction industry. The attractive attributes such as high strength-to-weight ratios, high resistance to corrosive environment, and low life cycle cost have made FRP composites as material of choice in structures built in aggressive environment. In spite of these attractive features, the limitation in providing effective and reliable joining method has impeded the widespread use of pultruded FRP (PFRP) sections, especially in frame structures [4–8].

The ability to provide joint versatility for PFRP in civil structures industry is crucial for its application demands. Although there are many types of connection system available, the conventional steel bolt is mostly used to join the structural components due to low cost, ease of assembly, ease of performing maintenance and inspection checks, and familiarity to the practitioners. Extensive research on bolted connections in FRP has been conducted by many researchers, focusing on the evaluation of joint performance as well as its failure modes and failure mechanism [9–21]. This also has been well recognised in the recent design guidelines, i.e. 'Pre-Standard for Load Resistance Factor Design (LRFD) of Pultruded FRP structures' and 'Guide for the Design and Construction of Structures made of FRP Pultruded Elements (CNR-DT 205/2007)' wherein the detailed parameters and design requirements for joining composite materials are presented in Chapter 8 [22] and Chapter 5 [23], respectively. As recommended by the both guidelines, fastening parameters such as joint geometry (width, spacing, end distance and bolt diameter), material thickness, clamping pressure, bolt hole tolerance, and loading conditions need to be carefully considered when designing FRP bolted connections. These parameters significantly influence the failure modes (Fig. 1) for instance bearing, shear-out, net tension and combinations of these which eventually dictate the strength of the joint connection. Meanwhile, recent review papers by Coelho and Mottram (2015) [24] and Correia et al. (2015) [25] provide a comprehensive list of published contributions covering bolted FRP joint behaviour and its mechanical response against various range of joint parameters and environment exposure conditions. Other than metallic fasteners, FRP fasteners (solid rod or bar) are adopted in rocks and soil engineering application as anchorage or strengthening strips [26]. These FRP fasteners have the potential to be used in a variety of

applications whereby its strength and stiffness properties are engineered according to different connection modes. It is ideal for applications that require fasteners to be non-corrosive, low in conductivity or no electromagnetic waves [27]. FRP threaded rods are made by machining a thread on an FRP solid rod which can be used with metal hex nuts if the threads formed are a direct match and fit. Generally, however, the forming of thread has caused defects on the screw connections which resulted in a lower connection strength, about 20%–40% of the strength of the FRP solid bar itself [28]. Moreover, unlike steel fasteners, FRP threaded rods possess linear elasticity and brittleness with anisotropic properties, making them ineffective as a joining component for advanced composites.

Currently, the use of fully-threaded steel bolts (technically known as screws or all threaded rods) for connection cannot be eliminated in large construction where full FRP sections with thick walls are involved, as it speeds up the construction process while minimizing installation errors. Moreover, it can also reduce the number of different bolts on site, allowing better stock holding and improve construction efficiency. This material combination can be found in large scale constructions involving structural truss system such as industrial cooling towers, electric transmission towers and bridges. The use of FRP composite materials for these structures are expected to show rapid growth in the near future [29]. It effectively exploits the FRP's high unidirectional strength as truss members are subjected only to axial forces. Studies on the effect of threaded bolts on the behaviour of bolted joints for PFRP, however, are very limited and the design guidelines considering the use of threaded bolts in PFRP construction is still not available. In the American pre-standard, ASCE [22], it is recommended that, for bolted joint, smooth bolt shank must be in bearing into the FRP material. For assembly purposes, the thread length should not exceed one third of plate thickness. Matharu and Mottram (2012) [30] also mentioned that the presence of bolt thread in the contact zone of composite material is detrimental to the strength of connections in long term exposure, especially in an aggressive environment. Since the bolt threads may cause tearing through the pultruded layers creating narrow gaps between the bolts and the FRP, the connection system becomes more susceptible to moisture entry.

Application of threaded bolts in joining PFRP components to produce advanced composite structures are currently restricted in design and its performance in service is limited. Instead of looking to a new modern joining method, the latter case can be resolved through experimental investigations which results in adaptability and awareness of the issues among a wider group of practitioners. It is the aim of this paper to provide a better level of understanding associated to the influence of bolt threads with the recognised joining parameters and to advice a factor that account the bolt threads effect in the preliminary FRP bolted design. This paper also reveals the joint behaviour of bolt threads on FRP materials in microscopic scale to refine the understanding on the finding mode of failures and its mechanism.

This paper presents the results of an extensive experimental work, including the scanning electron microscope (SEM) imaging which investigates the effects of bolt threads on the joint strength and failure mechanisms of a double lap joint for composite laminates cut in the longitudinal and transverse directions of PFRP. Bolted FRP joints subjected to compression are less sensitive to joint geometry and are generally stronger than joints subjected to tensile forces [31]. For this reason, FRP bolted connections in this paper were tested under axial force (tensile) to assess its strength and reliability. Assessment of bolt threads reduction factor in FRP bolted design, as well as the comparison of pultruded FRP joint strength and efficiency between plain bolts, threaded bolts, and clamped specimens were also presented.

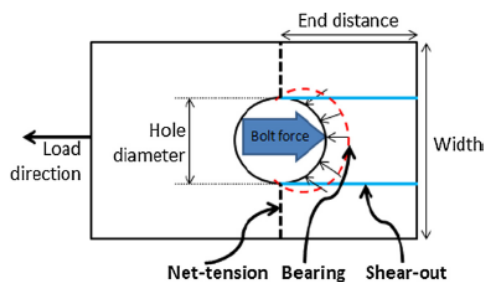


Fig. 1. Type of failure modes in composite bolted joint.

2. Experimental program

2.1. Pultruded FRP composites

The materials used in this study are 6.5 mm and 5 mm thick laminates, extracted from hollow glass FRP composite sections, manufactured and supplied by Wagners Composite Fibre Technologies (WCFT). The coupon testing for both longitudinal and transverse directions have been carried out as recommended in Pre-Standard (LRFD) of pultruded FRP to assess its mechanical properties. The results are presented in Table 1. The conducted burn-out test at 600 °C following ASTM D3171 (2011) [32] revealed that the stacking sequence of 6.5 mm and 5 mm thick FRP specimens (Fig. 2) are [0°/45°/0°/-45°/0°]_s, and 0°/45°/0°/-45°/0°, respectively. Additionally, there are thin protective veils present on the outermost surface of the FRP. The fibre weight fractions were 61% and 65% for 6.5 mm and 5 mm thick pultruded samples, respectively.

2.2. High strength structural bolt

The bolts used in the double lap joint configuration are high strength structural bolts in accordance to Australian standards AS 1252:1996 [34] and AS 1110-1995 [35]. The Steel Construction Institute (2002) [9] indicated that M20 × 60 mm long grade 8.8 all threaded bolts are used for 90% of the connections in a typical multi-storey steel frame. Thus, this type of bolt was used in this study. The M20 stainless steel (SS) 316 bolts were from commercially available sources and with properties presented in the next section. Table 2 shows the mechanical properties of class 8.8 SS bolts. The mechanical fasteners ultimate strength can be evaluated through simplification of internal forces redistribution based on designed experimental results. For this experimental program, the load transfer across the joint are classified as bearing type-bolts and pre-loaded friction-grip. Generally, in bolted connection, there are three ways the joint could break or fail which is by bolt failure, plate tearing (net-tension), and high extension of bolt hole or material tearing at the vicinity of the joint. Generally, the latter is more likely to occur when there is a difference in hardness between the materials. This phenomenon is widely observed when steel bolt is used to connect FRP materials, where the prominence failure modes of shear-out, bearing or cleavage are commonly identified. Based on the given bolt capacity and hardness differences, it is expected that the joint failure to occur on the jointed material instead of the connector.

2.3. Specimen design and preparation

A total of 150 double lap, single bolt joint (DLSJ) specimens were produced from hollow pultruded glass FRP sections with different thicknesses, i.e. 6.5 mm and 5 mm. The tests were carried out in order to determine the influence of joint geometry, presence of bolt thread and the use of clamping pressure on the joint strength and efficiency. In this experiment, the joint was designed to promote bearing failure and this type of failure is preferable in composite joint due to its progressive nature and post-failure behaviour beyond its ultimate load [13,16,36]. In the calculation of the bearing resistance of pultruded FRP, the pin-bearing capacity on the composite laminates is an important design parameter. According to Matharu and Mottram (2012) [30], the pin-bearing strength used in Eq. (1) must be the 'lowest' characteristic strength which accounts for all detrimental effects,

$$R_{br} = t d_b F_p^b \tag{1}$$

Table 1
Mechanical properties of PFRP profiles.

Properties ^a	6.5 mm plate	5 mm plate
Tensile Long ^b , Peak stress (MPa)	741.53 (44.91) ^d	686.43 (44.21)
Tensile Long, Elastic modulus (MPa)	42,983 (1257)	42,922 (2281)
Tensile Trans ^c , Peak stress (MPa)	66.41 (3.78)	46.84 (3.91)
Tensile Trans, Elastic modulus (MPa)	13,350 (2131.06)	12,198 (1110)
Compressive Long, Peak stress (MPa)	514.86 (15.27)	543.83 (43.95)
Compressive Trans, Peak stress (MPa)	161.66 (6.76)	147.70 (15.23)
In-plane shear Long, Peak stress (MPa)	113.60 (6.85)	88.95 (14.64)
In-plane shear Trans, Peak stress (MPa)	95.30 (4.72)	NA ^f
Pin-bearing (Plain), Peak stress (MPa)	291.44 (7.72)	260.12 (55.66)
Pin-bearing (Thread), Peak stress (MPa)	207.68 (11.08)	185 (7.21)
Fibre mass fraction, W _f	78.6%	81.4%
Fibre volume fraction, V _f	61%	65%
Density ^e (kg/m ³)	2030	

^a Testing were conducted based on relevant standards.
^b Longitudinal.
^c Transverse.
^d Standard deviation.
^e WCFT product specification.
^f Not available.

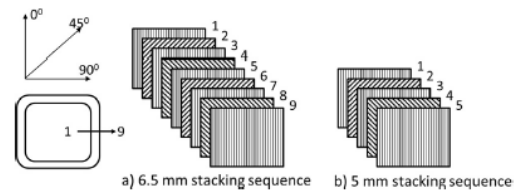


Fig. 2. Stacking sequence of 6.5 mm and 5 mm PFRP specimens.

Table 2
Bolt types and its mechanical properties (AS 1110-1995).

Item	Specification
Property class	8.8
Material type	Stainless steel 5316
Diameter of bolt, D	20 mm (M20)
Nominal shank area	314 mm ²
Area of root of thread	225 mm ²
Minor diameter, Dc	19.67 mm
Pitch, P	2.50 mm
Minimum tensile strength	830 MPa
Proof strength	600 MPa
Minimum yield strength	660 MPa
Minimum shear stress ^a	514.6 MPa
Min. breaking load in single shear (Shank)	163 kN
Min. breaking load in single shear (Thread)	117 kN
Minimum bolt tension ^b	145 kN

^a Ultimate shear stress equals 62% of ultimate tensile strength.
^b Full tightening.

where *t* = thickness of FRP material (mm); *d_b* = nominal diameter of bolt (mm); *F_p^b* = characteristic pin-bearing strength of FRP material, as stated in Table 1. The pin-bearing strength of the pultruded FRP used in this study was evaluated following the test procedure suggested by Keller et al. (2015) [37]. Their paper has addressed a few limitations with existing standards ASTM D953-02 (2010) [38] and EN 13706-2:2002 [39] and has called for an alternative test arrangement. Thus, the pin-bearing test was executed adopting the set-up used by the Warwick University (2011) [40] test setup, with a few adjustments on the bolt configuration and the test specimen's dimension. The test setup used steel bolts with a nominal diameter of 20 mm and a ratio of end distance to bolt diameter (*e/d_b*) up to 4. In this case, thread bolt was also included and its pin-bearing strength is presented in Table 3.

The results show that, the use of 20 mm diameter steel bolt with thread, has resulted in approximately 30% strength reduction compared to the bolt shank. The pin-bearing strength is also affected by about 11% reduction when the *d_b/t* increases from 3.07 to 4. It is comparable with the 15% reduction attained by Mottram and Zafari (2011) [40]. These data are used in the theoretical analyses of the bearing failure load for FRP sections with double lap joints in Section 4.

Table 4 shows the joint geometry of the specimens designed as per minimum geometric configurations as suggested by Bank (2006) [2]. Due to material dimensional constraints of the used closed section (125 mm × 125 mm × 6.5 mm and 100 mm × 75 mm × 5 mm), the minimum plate width to bolt diameter (*w/d_b* = 3) ratio was chosen. The bolt hole was carefully drilled using diamond coated drill to ensure the accuracy of bolt holes and to avoid fibre damage as suggested by Persson et al. (1997) [41].

Fig. 3 shows the nominal dimensions of the tested pultruded FRP longitudinal and transverse specimens with an *e/d_b* of 2.5. The end distance, *e*, is varied as 50 mm, 60 mm, 80 mm and 100 mm in order to increase the ratio of *e/d_b* to 2.5, 3, 4, and 5, respectively.

Table 5 outlines the experimental material groups, namely A and B which represent the 6.5 mm and 5 mm specimen thickness, respectively. The experimental program covers both longitudinal and transverse directions with different *e/d_b* ratios. Based on other research works, pultruded base material requires high *e/d_b* ratio to achieve bearing failure mode due to high orthotropic nature. In some related literatures, it is recommended that the said ratio to be at least 4 and it was also mentioned that, when the *e/d_b* ratio is 5 or higher, no appreciable gain in the joint strength will be observed [30,42]. It is important to note that, these findings are dependent on the specific type of pultruded composite materials used by the researchers. Due to this reason, the current experimental work was designed to accommodate a certain range of *e/d_b* to observe its effect on the presence of threaded bolt and clamping pressure. Initially, the *e/d_b* ratio up to 5 was introduced for bolted joint using plain bolts for both A and B material groups. Based on the preliminary outcome, the applicable range of *e/d_b* was established for the remaining

Table 3
Pin-bearing strength.

Specimens	d_b/t^1	Plain bolt, $F_{br,plain}$	Threaded bolt, $F_{br,thread}$	$\frac{F_{br,thread}^2}{F_{br,plain}^2}$
6.5 mm	3.07	291.44 (7.72) ²	207.68 (11.08)	0.71
5 mm	4.00	260.12 (55.66)	185.00 (7.21)	0.71

¹ Bolt diameter to thickness ratio.

² Standard deviation.

³ Thread to plain pin-bearing stress ratio.

Table 4
Geometric parameters for lap joint connections.

Parameters	Bank (2006)	Test specimen geometry (longitudinal & transverse)	
		6.5 mm	5 mm
End Distance to bolt diameter, e/d_b	2	2.5, 3, 4, 5	2.5, 3, 4, 5
Plate width to bolt diameter, w/d_b	3	3	3
Bolt diameter to plate thickness, d_b/t_{pl}	0.5	3	4
Washer diameter to bolt diameter, d_w/d_b	2	2	2
Hole size clearance	1.6 mm ^a	0.50–0.55 mm	

^a Maximum clearance.

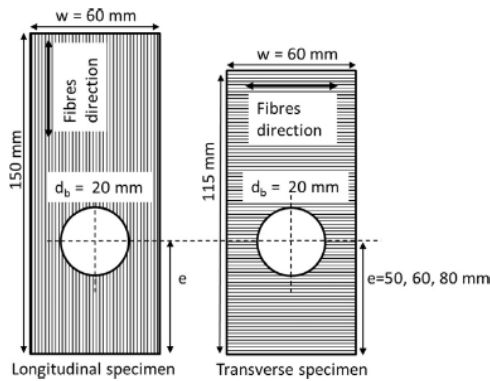


Fig. 3. Nominal dimensions of $e/d_b = 2.5$ and $w/d_b = 3$.

parameters. Conversely, for specimens in transverse direction, only e/d_b ratio of 2.5 was considered due to the width limitation of the pultruded FRP section. Similarly, by providing grips on one end of the specimen has resulted in omission of more ratios of e/d_b for transverse specimens. The test specimens were divided into four main groups, namely plain pin (P), thread (T), plain pin with clamp (PC) and thread with clamp (TC). Fig. 4 shows the illustrative diagrams of plain bolt and threaded bolt when in contact with pultruded FRP laminate. The detailed description of the groups formed and numbers of specimens allocated for testing are presented in Table 5. For instance, A60LTC means that the specimen was prepared from the 6.5 mm thick laminates (Group A) in longitudinal direction (L) with 60 mm end distance (60) and connected using threaded bolt and was subjected to clamping pressure (TC).

2.4. Test configuration and instrumentation

Pultruded glass FRP specimens were tested to failure according to ASTM D5961 (2006) [43] to investigate the behaviour of bolted laminates in longitudinal and transverse directions. Fig. 5 shows the schematic layout and photograph of double lap joint single-bolted pultruded FRP test specimens ready for testing. The pultruded FRP specimen was positioned between 12 mm machined steel plates and the other end was clamped by the hydraulic wedge with a grip pressure of approximately 8.5 MPa as per recommended by Guades (2013) [44]. Two types of stainless steel (SS) of 20 mm nominal bolt diameter or M20 were used, i.e. all threaded bolt and plain bolt shank with thread. Joints were tested in tension for two clamping conditions; the pin bearing condition (zero fastener torque) and the fully clamped condition. Fig. 5a shows how the mechanical fastener was deployed in pin-bearing

manner without any lateral restraint. However, loose SS nuts were placed for safety purposes. This DLS experimental test setup is similar to those reported by Hai and Mutsuyoshi [6] and Turvey and Sana [45]. Fig. 5b shows the joint configuration of test specimen with a recommended tightening torque of 25 Nm [46]. Steel washers with an outside diameter, d_w , of 40 mm were inserted under the head bolt and at the gaps between the steel plates and laminates to ensure that the clamping pressure was uniformly applied.

The bolted pultruded laminates and its steel fixtures were mounted at both ends in a 100 kN capacity servo-hydraulic 810 Material Test System (MTS) machine and were tested under tensile direction. The tests were conducted under the displacement control at a constant head-loading rate of 1.0 mm/min up to failure. The load and the system displacement were automatically measured and recorded for every 0.5 s by the MTS Teststar IIs data logging. The failure modes of each specimen were observed throughout the testing and a detailed assessment was carried out after the test.

3. Results and discussion

A summary of the experimental results for all tested specimens is presented in Table 6. The table lists the average maximum load, average displacement, and joint efficiency for all test parameters. In this study, the ultimate failure load (Fig. 6) is defined as the maximum load just prior to unstable, nonlinear behaviour. In some cases, however, after the load undergoes reduction, it may start to increase again beyond the original failure load but at the expense of large displacement. From this data, it is apparent that the specimens with threaded bolt resulted in lower failure load compared to the specimens with plain bolt. An average of 30–40% strength reduction was obtained when compared with longitudinal plain specimens for both A and B groups. This level of strength reduction is comparable to the reduction in the pin-bearing characteristic of pultruded FRP using threaded bolt from that of plain bolt. Detailed examination of thread effect under scanning electron microscope (SEM) is presented in Section 3.6. The tests also revealed that the clamped specimens with threaded bolts attained 60%–90% higher joint strength than that of without the clamping pressure. Concisely, by providing a sufficient lateral restraint to the joint configuration, it has significantly improved the joint capacity of glass PFRP irrespective of bolting conditions (with or without threads).

3.1. Joint efficiency

Eq. (2) is used to calculate the joint efficiency of a composite bolted joint which is based on net-strength. The joint efficiency, η , of the double lap joints, is defined as the ratio of the ultimate

Table 5
Summary of pultruded FRP specimens.

Specimen designation		e/d _b ratio	Direction	Bolt type	Clamp	No. of specimens
6.5 mm	5 mm					
A50LP	B50LP	2.5	Longitudinal	Plain	No	10
A60LP	B60LP	3	Longitudinal	Plain	No	10
A80LP	B80LP	4	Longitudinal	Plain	No	10
A100LP	B100LP	5	Longitudinal	Plain	No	10
A50LT	B50LT	2.5	Longitudinal	Thread	No	10
A60LT	B60LT	3	Longitudinal	Thread	No	10
A80LT	B80LT	4	Longitudinal	Thread	No	10
A50LPC	B50LPC	2.5	Longitudinal	Plain	Yes	10
A60LPC	B50LPC	3	Longitudinal	Plain	Yes	10
A80LPC	B50LPC	4	Longitudinal	Plain	Yes	10
A50LTC	B50LTC	2.5	Longitudinal	Thread	Yes	10
A60LTC	B60LTC	3	Longitudinal	Thread	Yes	10
A80LTC	B80LTC	4	Longitudinal	Thread	Yes	10
A50TP		2.5	Transverse	Plain	No	5
A50TT			Transverse	Thread	No	5
A50TPC			Transverse	Plain	Yes	5
A50TTC			Transverse	Thread	Yes	5

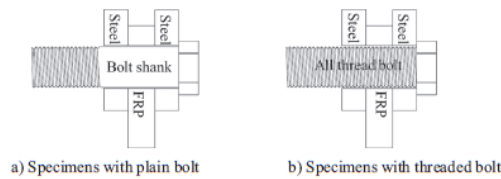


Fig. 4. Illustrative diagrams of the steel bolt in contact with FRP laminate.

joint strength to the ultimate strength of the unjointed material. It also presents the design effectiveness of bolted joint compared to unjointed continuous member of the same size [31]. S_j represents the ultimate joint strength (kN) of each parameter based on the experimental results. S_m is the ultimate load capacity of unnotched (unjointed) continuous member which can be determined by multiplying the pultruded FRP tensile strength with the affected sectional area. The affected section area is defined as the contact area between the bolt and pultruded FRP, whereby this area is likely to be the location where joint failure will occur.

$$\eta = \frac{S_j}{S_m} \tag{2}$$

In general, when comparing the results of the joint efficiency for the LP, LT, LPC and LTC groups, the LT group recorded the lowest joint efficiency. Groups LPC and LTC which obtained almost identical results for both A and B materials, recorded the highest joint efficiency, with more than half compared to unjointed members. In detail, B80LPC obtained the most joint efficiency at 69% when compared to unjointed 5 mm thickness specimen. It is worth to note that, specimens A80LPC, A60LTC, A80LTC and B80LTC achieved joint efficiency of at least 60%.

3.2. Failure mode

After the completion of each test, the specimens were disassembled from the test set-up to examine the damage on the FRP laminates. Table 6 presents the overall failure modes of each specimen. Fig. 7 presents the common failure modes identified throughout the experimental programme which are shear-out, bearing, net-tension and local crushing. Shear out failure was visible for the specimens with e/d_b = 2.5, which can be found in specimens A50LP and B50LP as shown in Fig. 7a). As the e/d_b increases, the failure mode changes from shear-out failure to bearing failure (Fig. 7b). Some of the previous studies reported that, the bearing failure of a single-bolt pultruded joint will likely occur for large

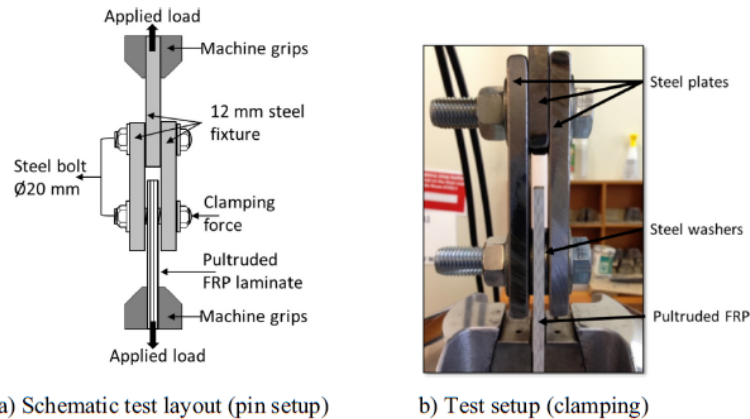


Fig. 5. Double lap joint, single-bolted pultruded FRP test fixture.

Table 6
Summary of results (Longitudinal and Transverse direction).

Specimens	Average Max. load (kN)	Standard deviation (kN)	Average Displacement (mm)	Standard deviation (mm)	Joint efficiency (%)	Mode of failure
A50LP	45.29	2.80	1.58	0.17	46.98	Shear-out
A60LP	47.25	3.64	1.92	0.42	49.01	Bearing
A80LP	52.37	1.64	1.58	0.02	54.32	Bearing
A100LP	51.97	2.69	1.97	0.21	53.91	Bearing
A50LT	30.17	2.82	2.04	0.17	31.29	Crushing
A60LT	30.66	2.38	2.06	0.12	31.81	Crushing
A80LT	29.54	1.85	1.96	0.10	31.64	Crushing
A50LPC	48.34	0.24	1.83	0.23	50.14	Shear-out
A60LPC	56.19	2.76	2.27	0.10	58.29	Shear-out
A80LPC	61.95	1.07	2.27	0.27	64.26	Shear-out
A50LTC	49.58	3.10	2.82	0.09	51.43	Shear-out
A60LTC	58.57	2.26	3.36	0.26	60.76	Shear-out
A80LTC	57.73	2.27	3.45	0.02	59.88	Shear-out
B50LP	25.65	2.61	1.15	0.18	37.36	Shear-out
B60LP	28.66	0.50	1.13	0.03	41.75	Bearing
B80LP	36.58	3.73	1.34	0.09	49.45	Bearing
B100LP	26.33	2.88	0.96	0.03	38.35	Bearing
B50LT	17.80	1.50	2.38	0.60	25.93	Crushing
B60LT	21.51	1.31	1.91	0.13	31.34	Crushing
B80LT	22.33	1.04	1.65	0.02	32.53	Crushing
B50LPC	29.31	1.49	1.36	0.05	42.70	Shear-out
B60LPC	39.88	1.78	1.71	0.20	58.11	Shear-out
B80LPC	47.47	2.87	1.94	0.18	69.16	Shear-out
B50LTC	28.30	2.28	2.24	0.18	41.22	Shear-out
B60LTC	40.28	1.25	3.15	0.21	58.68	Shear-out
B80LTC	43.62	4.66	3.62	0.68	63.55	Shear-out
A50TP	12.98	2.23	0.92	0.12	50.11	Net-tension
A50TT	12.00	0.74	1.35	0.24	46.33	Net-tension
A50TPC	13.74	1.34	1.05	0.21	53.05	Net-tension
A50TTC	13.36	0.85	1.57	0.09	51.58	Net-tension

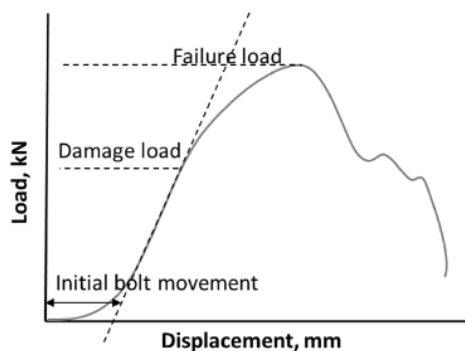


Fig. 6. Typical load vs. displacement of double lap single bolted FRP connection.

widths and larger end distances [30,47,48]. A good agreement was obtained with regard to the larger end distance condition, whereby, as the e/d_b increases, the mode of failure has changed from shear out to bearing failure. This can be seen clearly from the specimens at the e/d_b ratios of 3, 4, and 5. However, it is important to note that, if the pultruded FRP consists of highly orthotropic composite laminates, even at a very large end distance, the shear-out failure should be taken into consideration. Conversely, detailed observation has shown that the longitudinal specimen with threaded bolt were heavily crushed or broomed beneath the contact surface (Fig. 7e). Similar mode of failure was observed for all ALT and BLT specimens across the critical end distance range. This shows that, e/d_b ratio does not have any influence on the threaded specimen's failure mode. Specimens with threads in the composite joints exhibited deterioration and delamination of both fibres and

the resin matrix around the bolt hole, or what is known as the softened zone. This may have occurred due to the combined effect of the thread and the excessive compressive stress at the contact zone. When clamping pressure was introduced to longitudinal plain and longitudinal thread specimens, the shear-out failure mode was examined (Fig. 7c and f). Similar failure mode was observed at different critical end distances. In different circumstances, all transverse specimens failed in net-tension mode (Fig. 7d). This was observed in specimen A50TP, A50TT, A50TPC and A50TTC. This indistinguishable mode of failure might have occurred predominantly due to very low ultimate tensile strength in transverse direction which caused the cracks to propagate perpendicular to the load direction.

3.3. Influence of laminate orientations

Fig. 8 shows the comparison of experimental results between 6.5 mm longitudinal and transverse specimens with similar joint configurations. It is seen that the longitudinal specimens exhibit higher connection resistance than that of transverse specimens and similar findings were made by other researchers [49,50]. When fibre-to-load orientation changed from 0° to 90° , there was a massive reduction in joint resistance of about 70% for all parameters except for the joint tested with threaded bolt. On average, the threaded bolt specimens recorded about 60% lower joint capacity in the longitudinal direction than the one achieved by the transverse specimens. Significant differences of material strength between longitudinal and transverse direction of the specimens, as well as high stress concentration at the fibre-matrix interphases, especially at the hole edge region, may have contributed to the substantial decrease of joint capacity. The joint strength of transverse specimens exhibited only marginal differences and bounded in the range of 12 kN–14 kN, before rapidly declined as shown in Fig. 9. The threaded bolt specimen, A50TT, experienced minor

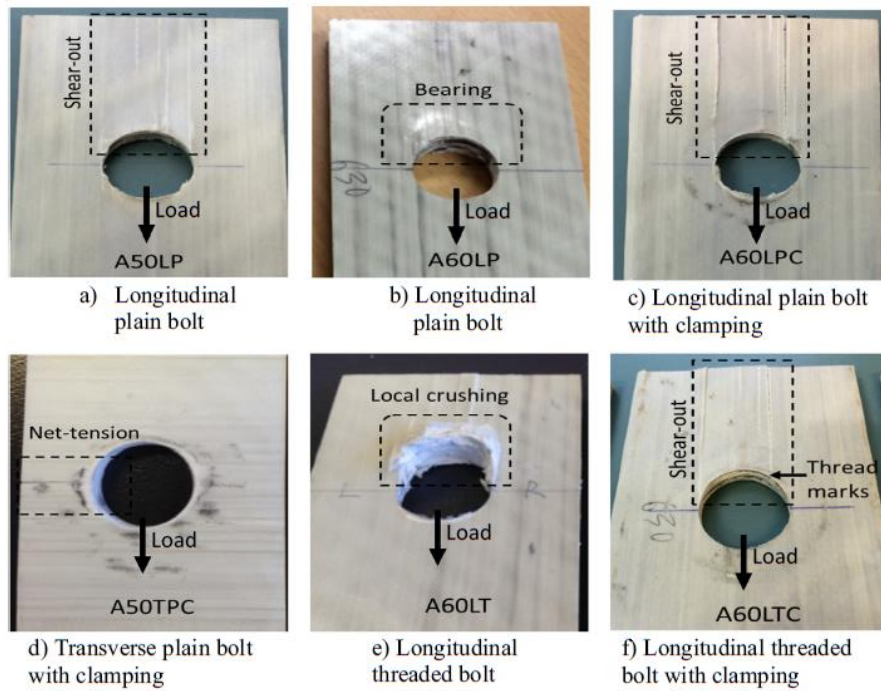


Fig. 7. Common failure modes observed after the testing.

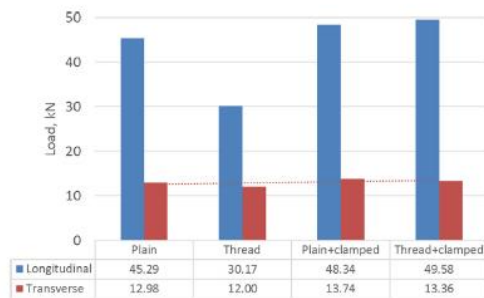


Fig. 8. Comparison between longitudinal and transverse specimens for each parameter.

decrease in its joint capacity, by 7.5% of that of A50TP. On the contrary, with the tightening torque, the average maximum load of A50TPC was slightly increased by 5.9% of that of A50TP. Meanwhile, slight improvement of 11.3% is attained by A50TTC when compared with A50TT. Nearly constant results were obtained for clamped specimens A50TPC and A50TTC, with only a 0.3% difference between them.

Fig. 9 shows that improvement of joint strength is gained with the introduction of clamping pressure but with the expense of higher joint displacement especially for specimen A50TTC. All transverse specimens prematurely failed by net-tension, meanwhile shear-out failure mode was largely observed in longitudinal specimens. The former may have occurred predominantly due to

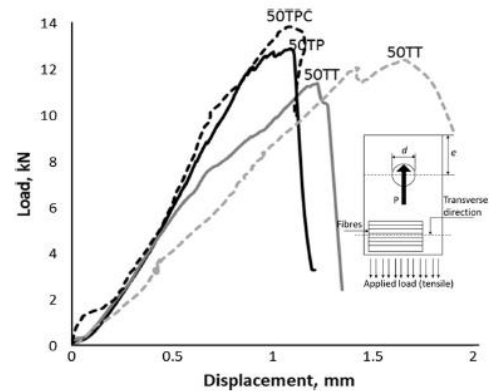


Fig. 9. Load-displacement relationship of FRP bolted joints (transverse specimens).

very low tensile strength in transverse direction and lower w/d_b ratio. This is expected as only the $\pm 45^\circ$ fibres are resisting the load. In term of w/d_b ratio, no adjustment can be made due to dimension limitation in preparing the transverse specimens from the structural shape. Similar outcome is expected for 5 mm thickness specimen as it shows a comparable tensile strength in the transverse direction to the 6.5 mm thickness specimen. Thus, the authors decided to discontinue any further testing on transverse direction and conclude the findings on threaded and clamping pressure effects.

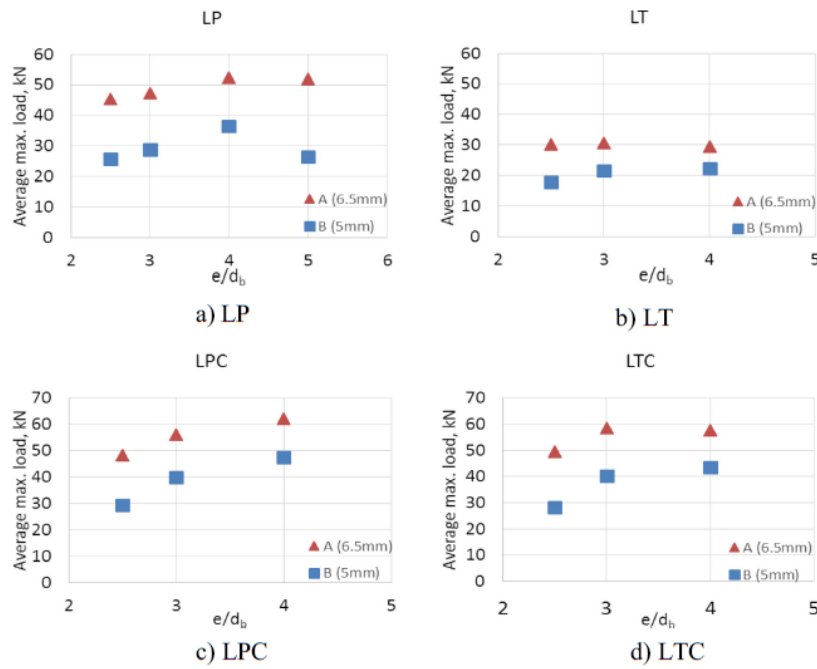


Fig. 10. Comparison between group A (5 mm) and B (6.5 mm) for each parameter as e/d_b varies.

3.4. Influence of e/d ratio on LP, LT, LPC and LTC

Fig. 10a shows that the average maximum load attained by longitudinal specimens, LP in both group A and B increased with larger ratio of e/d_b up to 4. In group A, an increment of 4% and 14% was attained by specimen LP when the e/d_b ratio was increased from 2.5 to 3 and 4, respectively. For the same comparison, specimen BLP considerably increased its joint capacity by 12% and 43%, respectively. On the other hand, specimens A100LP and B100LP experienced a slight drop or can be considered as a constant joint strength when compared to A80LP and B80LP, respectively. A reduction of 0.8% and 28% were observed for both A100LP and B100LP, respectively. Hence, most likely the joint strength remained constant after e/d_b ratio exceeded 4. This is in agreement with some of the findings in the literatures [2,42] that limits the e/d_b ratio in between 4 and 5 to characterise the bearing strength for a specific type of unidirectional pultruded composite. Similarly, for this specific pultruded FRP, when $e/d_b = 4$, the likely mode of failure is bearing and there is no appreciable gain in the joint strength after the ratio exceeded 4. Thus, $e/d_b = 5$ is intentionally excluded from further analysis in LT, LPC and LTC groups.

As shown in Fig. 10b, the joint capacity of specimens ALT and BLT with various end distances failed at average 30 kN and 20 kN, respectively. It may be observed that the e/d_b ratio has insignificant effect on the threaded joint, as the joint strength of LT group is virtually constant across the e/d_b range. Furthermore, the average maximum load attained by specimens ALPC, BLPC, ALTC and BLTC was increasing with increased e/d_b ratio. In this case, higher e/d_b ratio means that more continuous fibres are available at the end distance to provide better load carrying ability. Fig. 10c shows that specimen B50LPC attained substantial improvements, almost 36% and 62% increment of joint strength when compared to

specimens with $e/d_b = 3$ and 4, respectively. Meanwhile, A60LPC and A80LPC gained 16% and 28% increment of joint capacity. In Fig. 10d, surprisingly, longitudinal clamping specimens with threaded bolt exhibited a promising improvement of joint capacity at higher critical end distance. However, it is important to note that, between e/d_b ratio of 3 and 4, marginal differences of joint capacity were found, whereby, only 8% increment of joint capacity was gained by BLTC. Meanwhile, the joint capacity of ALPC remained constant.

3.5. Influence of laminate thickness

Fig. 11 further demonstrates the comparison of different thickness for each parameter. It can be seen clearly that, the average maximum load of 6.5 mm thickness laminates (specimen A) was higher than 5 mm thickness laminates (specimen B) in all tested parameters. Specimen A, tested with plain bolt, exhibited an average difference of roughly 38% joint strength between e/d_b ratio of

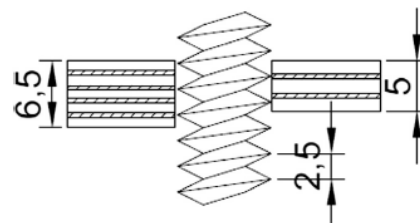


Fig. 11. Bolt threads against different plate thicknesses.

2.5 and 4, when compared with specimen B. Meanwhile, when the joints tested with threaded bolt, thicker material provides more possibilities for bolt threads to entrench into pultruded layers. For M20 bolt with 2.5 mm pitch, it was observed that 2 and 3 threads cut through the 5 mm and 6.5 mm laminates, respectively as shown in Fig. 11.

Despite having more threads in contact at vicinity of the joint, Fig. 10b shows that the joint strength of specimen exhibited average 30% higher than that of specimen B. Eventually, by adding more laminas, which in turn increased the thickness of the laminate, the specimens are capable to accommodate further stresses and distribute them evenly. This outcome agrees with the research reported by Rosner and Rizkalla (1995) [51], whereby, connection capacity increases linearly with the laminate thickness. This is consistent even with the presence of more threads at the joint contact area. Fig. 10a and b presents the comparison of joint capacity between LT and LP for both specimen group A and B, respectively. Since the presence of the threaded bolt seems to be irrelevant on the critical end distances, the 6.5 mm specimen experienced more damage due to higher strength reduction when compared to the specimen tested with plain bolt. Due to the threaded bolts, specimen ALP and specimen BLP experienced decrease in joint resistance at an average of 40% and 32%, respectively. It may be seen that, the additional 1.5 mm thickness of the specimens, to some extent decreased the joint capacity by 8%.

3.6. Influence of bolt threads

Fig. 12 presents the experimental data of 70 tested specimens in the form of comparison ratio of joint strength between the longitudinal bolt thread and longitudinal bolt plain specimens (LT/LP) across the e/d_b range of 2.5–4. The ratio explains the load-carrying capacity performance of different thickness of pultruded FRP bolted joint under undesirable 20 mm bolt thread effect. The higher ratio value interprets that the pultruded FRP bolted joint is less susceptible to the thread effect and vice versa. All the corresponding LT/LP ratio for specimen B were recorded higher than that of specimen A. At lower e/d_b , the corresponding LT/LP ratio is consistent at approximately 0.7. As e/d_b increases, the LT/LP for both specimens showed noticeable difference before declining at $e/d_b = 4$. Following this, the LT/LP ratio for specimen A is constricted at 0.6, which represents the lower bound of this overall observation. Therefore, it can be concluded that a ratio of 0.6 may serve as a reduction factor for FRP bolted connection design. This value is important in representing the effect of threads on bolts that causes an equivalent of 40% reduction in joint capacity of the FRP connection system.

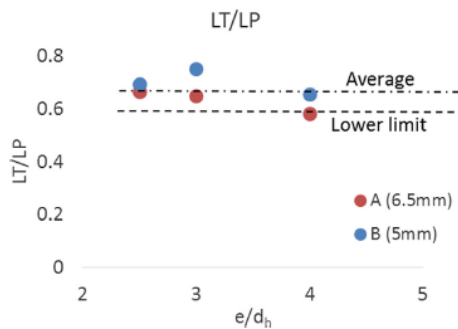


Fig. 12. Corresponding LT/LP ratio.

The reduction in joint capacity as discussed above may be caused by the unevenness of contact surface between the thread and pultruded material [52]. When the surfaces between the threaded bolt and pultruded material are subjected to a compressive load, it may initiate the separation of laminate layers due to thread embedment. Then, sufficient contact area was formed to continue to support the load applied. However, this process may cause the thread to continuously damage the through-thickness of pultruded material and severely disrupt the stress dispersion between fibres. In addition, the thread cutting through the 45° angled fibre layers could critically damage the joint resistance more than that of unidirectional layers. On the other hand, Matharu and Mottram (2012) [30] reported a reduction of 26% in joint strength when load is applied parallel to the pultrusion direction. It may be seen that, the key difference on the results reported is due to the pultruded stacking profile. The pultruded FRP used by Matharu and Mottram (2012) [30] consists of unidirectional layers interspersed with a three layered (90°, ±45°) cross-stitched Continuous Fabric Mat (CFM) which improves transverse stiffness and could provide better resistance in dealing with threaded bolt. Images shown in Fig. 13 were captured by scanning electron microscope (SEM) to observe the micro-failures of the contact surface area of softened zone, with and without the presence of the threaded bolt. In Fig. 13a, it can be seen that, fibres were severely damaged and delaminated by the threads. A few void areas were observed which was caused by the threads indenting through the laminates. This could explain the failure development of softened zone at micro-level which resulted in a lower connection strength due to the presence of thread embedment. In comparison, Fig. 13b indicates only the exposed fibres and eroded matrix after experiencing compressive stress from the bolt shank and no fibre damage is observed. Moreover, the presence of threads largely affects the hardness of contact surfaces which induced the deteriorating process on pultruded material.

In the ASCE pre-standard [22], it is noted that the bolt shank with thread should not exceed 1/3 of the thickness of pultruded plate to avoid undesirable thread effect. However, in some limitations, especially when using all threaded bolt, for this specific pultruded material under applied load in longitudinal direction, a reduction factor of 0.6 can be applied in preliminary joint design to anticipate the thread effect on the joint strength.

3.7. Influence of clamping pressure

All connections with lateral restraints showed improvement of joint capacity and had altered the final failure mode to behave in a brittle manner. Based on Eq. (3), the desirable axial bolt clamp force, F_p can be estimated by dividing the applied clamping torque, T , with coefficient of friction, μ , and fastener bolt major diameter, d_b .

$$T = \mu d_b F_p \tag{3}$$

The clamping force of 8.3 kN was calculated using Eq. (3) and it interacts well with the experimental results shown in Fig. 14a. At the initial applied loading between 8 kN and 10 kN, LPCs attained less steeper slopes compared to that of LPs, and this could be due to the combined effects of pre-tensioned bolts reduction and initial slip load. At this point, the bolt may have settled on the material, together with the presence of static friction forces induced by clamping pressure. It was noticeable that, the joined laminates deform only elastically and no relative displacement between the laminates occurs. These local contacts between the fastener and pultruded material continue to induce large deformation and delamination failure near the contact edge of the hole. After reaching the peak load, sudden drop of applied load was

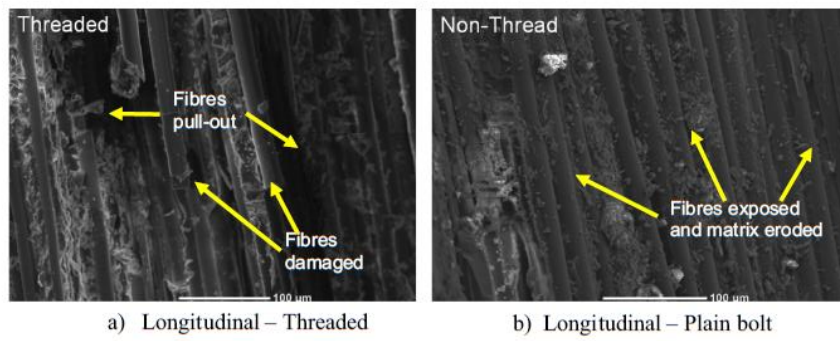


Fig. 13. Failure modes observation of testing specimens using SEM.

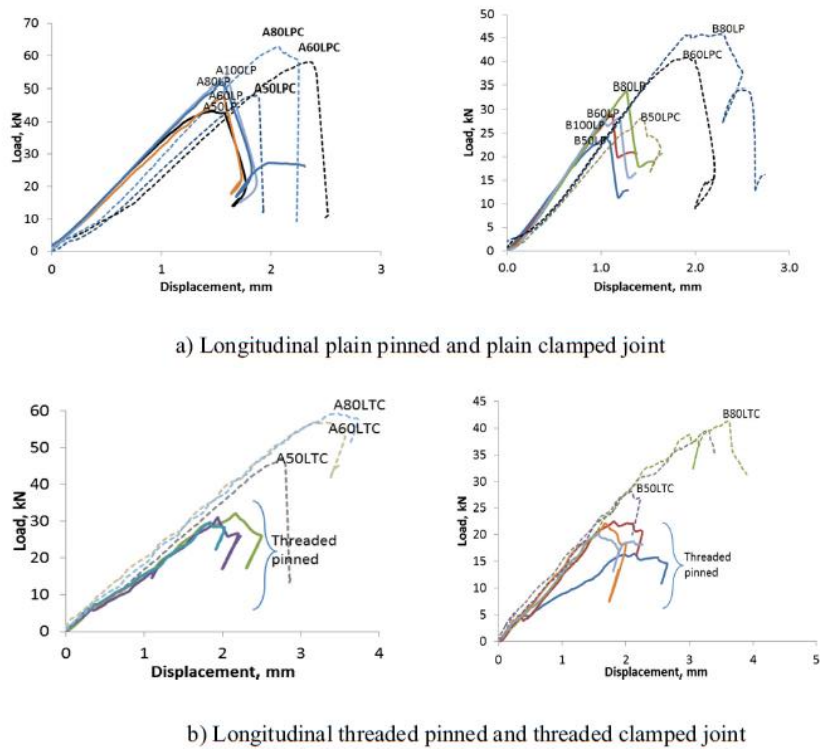


Fig. 14. Load-displacement relationship of FRP bolted joint (longitudinal specimens).

observed as the pultruded laminates experienced final delamination failure in the direction parallel to the applied loading. Similar observation was made for LTC specimens (Fig. 14b), whereby, the applied load is directly proportional to the joint displacement until rapid failure occurred. Some identical nonlinearities or bumps across the slope were observed, which could indicate the development of threaded contact on the pultruded material. However, the 6.5 MPa clamping pressure produced by tightening torque (Fig. 15) is important to retain the joint assembly. As the laminate is being pressed, this has suppressed the delamination defect progression.

At the same time, it restrains the out-of-plane deformation and when the internal damage under the washer reached a critical state, a sudden incline in load response can be observed. For long-term service life issues relating to clamping pressure such as creep relaxation, a thread-locking sealant or locking nut could be used as an alternative to overcome possible nut loosening [22].

Overall, the mechanically fastened joints in longitudinal specimens A and B that carry friction forces from the pre-tension of the bolt, attained almost 18%–95% improvement in joint capacity. It eventually produced more than 50% of joint efficiency for all

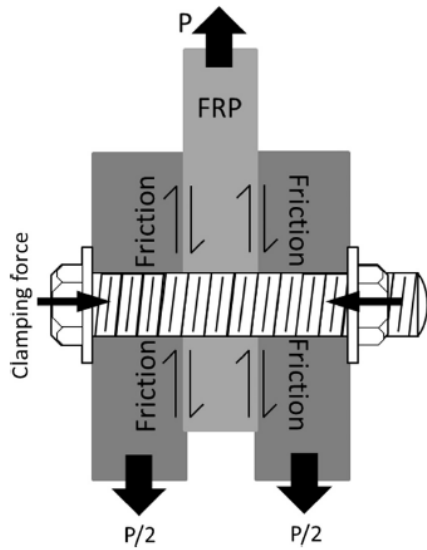


Fig. 15. Clamping pressure and friction force distribution in double lap single bolted joint.

specimens with the addition of applied torque. When comparing LTC to LT as shown in Fig. 16a, the joint capacity of both materials showed an increment almost directly proportional to e/d_b , irrespective of threaded condition. At higher e/d_b , the LTC gained average 95% joint improvement to that of LT. The comparison between LTC and LPC in Fig. 16b shows that, both parameters obtained comparable joint strength as e/d_b increases, with the average corresponding LTC/LPC ratio of 1.0. It seems that, with clamping force acting on the jointing material, it lessens the thread casualty effect on the pultruded composite joint. Thus, this 1.0 factor can be adopted in the preliminary joint design whereby both threaded bolt and lateral restraint are featured in the FRP bolted connection.

4. Theoretical evaluation of bolted joint strength

This section presents theoretical evaluation of the bolted joint strength and comparison with the experimental outcomes. This analytical approach focuses on both laminate orientations. For the longitudinal specimens, deliberate assessment especially at lower e/d_b ratio is required, where shear-out joint failure is

frequently observed as a result of a bearing failure. Both longitudinal plain and longitudinal thread were analysed and its strength limit was validated based on the failure behaviour observed. Eqs. (4) and (5) are evaluated to assess the bolted joint capacity under shear-out strength corresponding to the limit values suggested in the ASCE pre-standard [22] and Italian CNR design guidelines [23].

$$R_{sh} = 1.4 \left(e_1 - \frac{d}{2} \right) t F_{sh} \tag{4}$$

$$V_{sd} = F_{sh} (2e_1 - d) t \tag{5}$$

where t = thickness of FRP material (mm); d = bolt hole diameter (mm); e_1 = end distance (mm); and F_{sh} = shear strength of FRP. This theoretical mechanics-based equation is a function of both joint geometry and composite material strength.

The load capacity due to pin-bearing strength, R_{br} , was calculated using Eq. (1) (similar equation also included in the Italian CNR design guidelines [23]). According to Matharu and Mottram (2012) [30], the pin-bearing strength used must be the 'lowest' characteristic strength which accounts for all detrimental effects. Fig. 17 shows the mode of failure between the theoretical evaluations and experimental results for the 6.5 mm and 5 mm thickness specimens as the e/d_b ratio increases. Overall, the comparisons are in agreement with the visual inspection findings reported in Table 6, except for the computed values from Eq. (5). This equation predicts a lesser conservative estimate of the shear-out strength limit compared to Eq. (4) which accommodates a reduction factor of 0.7. Apart from this, it is interesting to note that, with clamping pressure, it significantly alleviates the damage done by the threads by changing the mode of failure from local compression crushing to shear-out failure.

For transverse specimens, net-tension failure was observed to occur along the net section, predominantly due to very low tensile strength and unfavourable joint geometry such as low w/d_b ratios. When the strength properties of the material are exceeded, failure will occur initially at the stress concentration located at midpoint on the hole edge and will propagate towards the free edge along the net section. The ultimate load for net-tension failure, P_u , can be obtained by the simple formulation as below:

$$P_u = F_T t (w - d) \tag{6}$$

where F_T is the tensile strength in the transverse direction (MPa), t is the specimen thickness (mm), w is the plate width (mm) and d is the nominal bolt hole diameter (mm). Meanwhile, in Italian CNR design guidelines [23], the following equation (Eq. (7)) is used to assess the bolted joint capacity under net-tension failure, V_{sd} .

$$V_{sd} = \frac{1}{\gamma_{nd}} F_T (w - nd) t \tag{7}$$

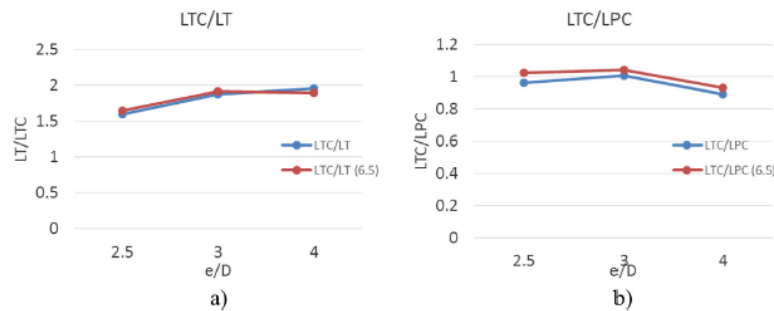


Fig. 16. Comparison of LTC/LT and LTC/LPC as e/d_b varies.

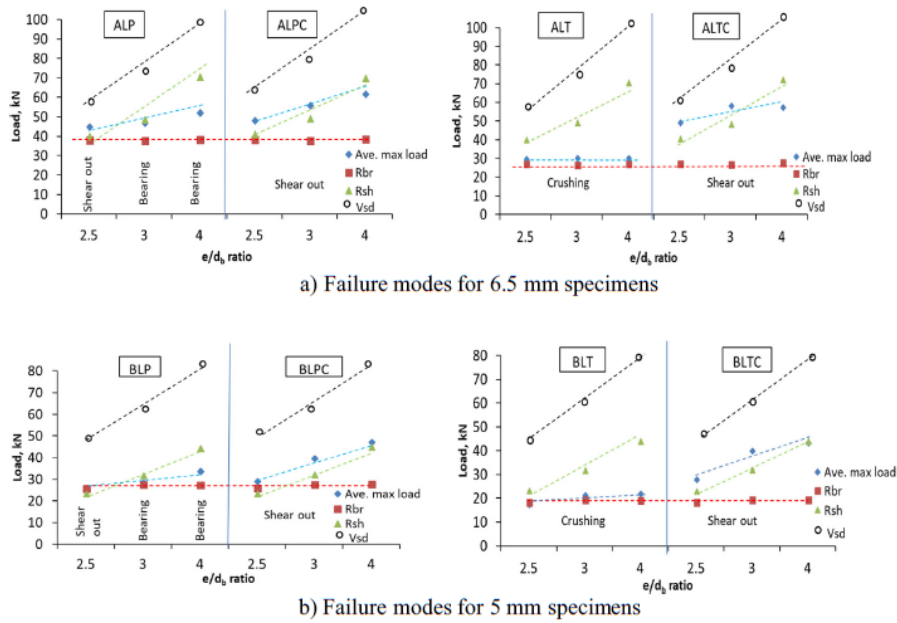


Fig. 17. Failure modes comparison of longitudinal specimens using the theoretical approach.

This equation is almost similar to Eq. (6), with the inclusion of n , the number of holes and γ_{rd} , partial model coefficient, whereby for perforated section, it is assumed to be equal to 1.11. According to the ASCE pre-standard [22], for single bolt connections, a correction factor must be used to calculate the stress concentration at the hole edge to allow for the various joint geometry. The nominal net tension strength, R_{nt} and, the stress concentration factor for a filled hole, K_{nt} shall be given by Eq. (6):

$$R_{nt} = \frac{1}{K_{nt}} (w - nd) t F_t \quad (8)$$

$$K_{nt} = C_L \left(S_{pr} - 1.5 \frac{(S_{pr} - 1)}{(S_{pr} + 1)} \varphi \right) + 1 \quad (9)$$

With $\varphi = 1.5 - 0.5 \frac{w}{e_1}$ for $\frac{e_1}{w} \leq 1$, and $\varphi = 1$ for $\frac{e_1}{w} \geq 1$
Where;

- t = minimum thickness of the connected component and/or member (mm)
- d = nominal hole diameter (mm)
- d_b = nominal bolt diameter (mm)
- n = number of bolts across the effective width (n = 1 a single bolt connection)
- w = plate width (mm)
- e_1 = plate end distance (mm)
- $S_{pr} = w/d_b$, and
- F_t = characteristic tensile strength in the transverse direction (MPa).

All Eqs. (6)–(8) are used when comparing with the experimental results of transverse specimens. Fig. 18 shows that, overall, the experimental results exceeded both theoretical values except for specimen A50TT, which could be due to the presence of threaded bolt. It can be observed that, the calculated P_u and V_{sd} are in close

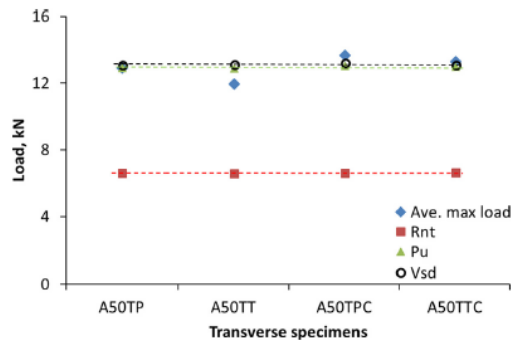


Fig. 18. Net-tension failure mode comparison of transverse specimens using the theoretical approach.

proximity to the experimental data with an average difference of 3.8% and 3.9%, respectively. On the other hand, with K_{nt} factor introduced in the net-tension formula [22], the R_{nt} values obtained are about half the values from the experimental results and the calculated P_u and V_{sd} . The average calculated value of the stress concentration factor, K_{nt} is approximately 1.95. Based on theoretical values computed, the governing mode of failure is net-tension which agrees with the visual inspection of the transverse specimens after the testing.

5. Conclusion

An experimental investigation on the influence of M20 all threaded bolt and clamping pressure on double lap, single bolted joints of pultruded FRP materials prepared from 6.5 mm and 5

mm thick hollow section structural shapes has been described. All the 150 pultruded specimens with varied geometric ratio of e/d_b were loaded parallel to the direction of pultrusion axis and a tight fitting 20 mm diameter mechanical fastener was used. Based on the results, the following conclusions are made:

- 1) The joint strength in the longitudinal laminates with plain bolt increased for e/d_b ratio for up to 4. There is no appreciable gain in the joint strength after exceeding this ratio due to the failure mode changing from shear-out to bearing.
- 2) In contrast, as the e/d_b increases from 2.5 to 4, it has insignificant effect on the longitudinal laminate with threaded bolt and all the transverse bolted specimens as the joint strengths obtained are virtually constant.
- 3) In general, transverse bolted specimens exhibit much lower joint strength than that of longitudinal bolted specimens predominantly due to very low ultimate tensile strength in transverse direction and unfavourable joint geometry of lower w/d_b ratio. These had influenced the cracks to propagate perpendicular to the load direction and failed in net-tension mode. Moreover, transverse bolted specimens with threaded bolt endured a significant drop in joint resistance of about 60% when compared to that of similar configuration in longitudinal direction.
- 4) The increase in laminate thickness from 5 mm to 6.5 mm increased the bolt strength by 38%. However, when dealing with threaded bolts, the thicker material provides more possibilities for bolt threads to entrench into the pultruded layers and consequently increased the damage impact on the joint capacity by 8%.
- 5) Based on the comparison ratio of joint strength between the longitudinal bolt thread and longitudinal bolt plain specimens (LT/LP), a reduction factor of 0.6 is proposed in preliminary FRP bolted connection design, where all threaded bolt is anticipated in pultruded joints. This value is important in representing the effect of threads on bolts that causes an equivalent of 40% reduction in joint capacity of the FRP connection system.
- 6) The combined effects of both the bolt threads and compressive stress at the contact zone in composite joints resulted in the deterioration and delamination of both fibres and the resin matrix. Under scanning electron microscope (SEM) observation, a few void areas were observed which was caused by the threads indenting through the laminates. This could explain the failure development of softened zone at micro-level which resulted in a lower connection strength due to the presence of thread embedment.
- 7) However, the bolted strength of pultruded composite joints with lateral restraint are less susceptible to thread effect. The damage done by the threads had changed from vigorous fibre-matrix crushing to shear-out failure. Consequently, the lateral clamping pressure increases the strength of bolted joints for both threaded and unthreaded bolts in longitudinal specimens and exhibited more than 50% of joint efficiency when compared to unjointed specimens.
- 8) The derived mode of failures obtained from the theoretical assessment using the nominal strength approaches for both longitudinal and transverse specimens, show very good agreement when compared to the experimental outcomes.

It is noted that the conclusions derived from this study are based on a specific type of pultruded composites and diameter of bolts considered. Further investigations on the thickness effects on threaded reduction factor, bolt diameters and its long-term outcome within an aggressive environment may be further explored.

Conflict of interest

None declared.

Acknowledgements

The authors gratefully acknowledge Wagner Composite Fibre Technologies (WCFT) for the testing materials supplied. Special thanks to Mr. Mohan Trada for his kind support and technical expertise during the experimental work.

References

- [1] L.C. Bank, J. Yin, M. Nadipelli, Local buckling of pultruded beams – nonlinearity, anisotropy and inhomogeneity, *Constr. Build. Mater.* 9 (6) (1995) 325–331.
- [2] L.C. Bank, *Composites for Construction: Structural Design with FRP Materials*, John Wiley & Sons Inc, New Jersey, 2006.
- [3] L.C. Hollaway, A review of the present and future utilisation of FRP composites in the civil infrastructure with reference to their important in-service properties, *Constr. Build. Mater.* 24 (12) (2010) 2419–2445.
- [4] R.M. Hizam, A.C. Manalo, W. Karunasena, A review of FRP composite truss systems and its connections, in: C.S. Bijan Samali, Mario M. Attard (Eds.), 22nd Australasian Conference on the Mechanics of Structures and Materials, Taylor & Francis Ltd, Sydney, New South Wales, Australia, 2012.
- [5] J.T. Mottram, Design guidance for bolted connections in structures of pultruded shapes: gaps in knowledge, 17th International Conference on Composite Materials A1(6), 2009.
- [6] N.D. Hai, H. Mutsuyoshi, Structural behavior of double-lap joints of steel splice plates bolted/bonded to pultruded hybrid CFRP/GFRP laminates, *Constr. Build. Mater.* 30 (2012) 347–359.
- [7] L. Blaga, J.F. Dos Santos, R. Bancila, S.T. Amancio-Filho, Friction riveting (PricRiveting) as a new joining technique in GFRP lightweight bridge construction, *Constr. Build. Mater.* 80 (2015) 167–179.
- [8] S. Russo, Experimental and finite element analysis of a very large pultruded FRP structure subjected to free vibration, *Compos. Struct.* 94 (2012) 1097–1105.
- [9] SCL, BCSA, *Joints in Steel Construction: Simple Connections*, Steel Construction Institute/British Constructional Steelwork Association, 2002.
- [10] C. Cooper, G.J. Turvey, Effects of joint geometry and bolt torque on the structural performance of single bolt tension joints in pultruded GRP sheet material, *Compos. Struct.* 32 (1995) 217–226.
- [11] N.K. Hassan, M.A. Mohamedien, S.H. Rizkalla, Finite element analysis of bolted connections for PFRP composites, *Compos. Part B: Eng.* 27B (1996) 339–349.
- [12] L.C. Bank, A.S. Mosallam, G.T. McCoy, Design and performance of connections for pultruded frame structures, *J. Reinf. Plast. Compos.* 13 (1994) 199–212.
- [13] Y. Xiao, T. Ishikawa, Bearing strength and failure behavior of bolted composite joints (Part I: Experimental investigation), *Compos. Sci. Technol.* 65 (7–8) (2005) 1022–1031.
- [14] U.A. Khashaba, H.E.M. Sallam, A.E. Al-Shorbagy, M.A. Seif, Effect of washer size and tightening torque on the performance of bolted joints in composite structures, *Compos. Struct.* 73 (2006) 310–317.
- [15] T. Keller, Y. Bai, T. Vallée, Long-term performance of a glass fiber-reinforced polymer truss bridge, *J. Compos. Constr.* 11 (1) (2007).
- [16] F. Ascione, L. Feo, F. Maceri, On the pin-bearing failure load of GFRP bolted laminates: an experimental analysis on the influence of bolt diameter, *Compos. B: Eng.* 41 (6) (2010) 482–490.
- [17] Y. Bai, X. Yang, Novel joint for assembly of all-composite space truss structures: conceptual design and preliminary study, *Compos. Constr.* 17 (1) (2013) 130–138.
- [18] S.T.W. Lau, M.R. Said, M.Y. Yaakob, On the effect of geometrical designs and failure modes in composite axial crushing: a literature review, *Compos. Struct.* 94 (3) (2012) 803–812.
- [19] F.J. Luo, X. Yang, Y. Bai, Member capacity of pultruded GFRP tubular profile with bolted sleeve joints for assembly of latticed structures, *J. Compos. Constr.* 20 (2016) 1–12.
- [20] S. Russo, First investigation on mixed cracks and failure modes in multi-bolted FRP plates, *Compos. Struct.* 154 (2016) 17–30.
- [21] J.T. Mottram, G.J. Turvey, Physical test data for the appraisal of design procedures for bolted joints in pultruded FRP structural shapes and systems, *Prog. Struct. Mater. Eng.* 5 (4) (2003) 195–222.
- [22] ASCE, *Pre-Standard for Load and Resistance Factor Design (LRFD) of Pultruded Fibre Reinforced Polymer (FRP) Structures*, 2010.
- [23] CNR, *Guide for the Design and Construction of Structures made of FRP Pultruded Elements*, National Research Council of Italy, Rome, 2008.
- [24] A.M.G. Coelho, J.T. Mottram, A review of the behaviour and analysis of bolted connections and joints in pultruded fibre reinforced polymers, *Mater. Des.* 74 (2015) 86–107.
- [25] J.R. Comeia, Y. Bai, T. Keller, A review of the fire behaviour of pultruded GFRP structural profiles for civil engineering applications, *Compos. Struct.* 127 (2015) 267–287.

- [26] G.P. Terrasi, C. Affolter, M. Barbezat, Numerical optimization of a compact and reusable pretensioning anchorage system for CFRP tendons, *J. Compos. Constr.* 15 (2) (2011) 126.
- [27] J.W. Schmidt, A. Bennitz, B. Täljsten, P. Goltermann, H. Pedersen, Mechanical anchorage of FRP tendons – a literature review, *Constr. Build. Mater.* 32 (2012) 110–121.
- [28] W. Min, The Finite Element Value Simulation of Composite Bolt Threaded Nut Contact and Experimental Study, School of Material Science and Engineering, Taiyuan University of Science and Technology, China, 2008.
- [29] R. Plastics, Pultrusion industry grows steadily in US, *Reinf. Plast.* (2002).
- [30] N.S. Matharu, J.T. Mottram, Laterally unrestrained bolt bearing strength: plain pin and threaded values, in: 6th International Conference on FRP Composites in Civil Engineering, Rome, Italy, 2012.
- [31] A.S. Mosallam, Design Guide for FRP Composite Connections, American Society of Civil Engineers (ASCE), 2011.
- [32] ASTM D3171, Standard Test Methods for Constituent Content of Composite Materials, American Society for Testing and Materials (ASTM) Standard, 2011.
- [34] AS/NZS 1252:1996, High-strength Steel Bolts with Associated Nuts and Washers for Structural Engineering, Standards Australia and Standards New Zealand, Australia and New Zealand, 1996.
- [35] AS/NZS 1110:1995, ISO Metric Precision Hexagon Bolts and Screws, Standards Australia and Standards New Zealand, Australia and New Zealand, 1995.
- [36] B. Vangrimde, R. Boukhili, Analysis of the bearing response test for polymer matrix composite laminates bearing stiffness measurement and simulation, *Compos. Struct.* 56 (2002) 359–374.
- [37] T. Keller, N. Theodorou, A. Vassilopoulos, J. de Castro, Effect of natural weathering on durability of pultruded glass fiber-reinforced bridge and building structures, *J. Compos. Constr.* 20 (1) (2015) 04015025.
- [38] ASTM D953, Standard Test Method for Bearing Strength of Plastics, American Society for Testing and Materials (ASTM) Standard, 2010.
- [39] EN 13706-2, Reinforced Plastics Composites. Specifications for Pultruded profiles. Method of Test and General Requirements, British Standards Institution, 2002.
- [40] J.T. Mottram, B. Zafari, Pin-bearing strengths for bolted connection in FRP structures, *Struct. Build.* (2011).
- [41] E. Persson, I. Eriksson, L. Zackrisson, Effects of hole machining defects on strength & fatigue life of composite, *Compos. A: Appl. Sci. Manuf.* 28A (1997) 141–151.
- [42] Eurocomp, Structural Design of Polymer Composites, E & FN Spon, London, 1996.
- [43] ASTM D5961, Standard Test Method for Bearing Response of Polymer Matrix Composite Laminates, American Society for Testing and Materials (ASTM) Standard, 2006.
- [44] E.J. Guades, Behaviour of Glass FRP Composite Tubes Under Repeated Impact for Piling Application, Centre of Excellence in Engineered Fibre Composites, University of Southern Queensland, Queensland, Australia, 2013.
- [45] G.J. Turvey, A. Sana, Pultruded GFRP double-lap single-bolt tension joints – temperature effects on mean and characteristic failure stresses and knock-down factors, *Compos. Struct.* 153 (2016) 624–631.
- [46] A.C. Manalo, H. Mutsuyoshi, Behavior of fiber-reinforced composite beams with mechanical joints, *J. Compos. Mater.* (2011) 1–14.
- [47] B. Vangrimde, R. Boukhili, Descriptive relationships between bearing response and macroscopic damage in GRP bolted joints, *Compos. B: Eng.* 34 (7) (2003) 593–605.
- [48] N.S. Matharu, J.T. Mottram, Laterally unrestrained bolt bearing strength: plain pin and threaded values, 1–8.
- [49] G.J. Turvey, Single-bolt tension joint tests on pultruded GRP plate: effects of the orientation of the tension direction relative to pultrusion direction, *Compos. Struct.* 42 (4) (1998) 341–351.
- [50] Y. Wang, Bearing behaviour of joints in pultruded composites, *J. Compos. Mater.* 36 (18) (2002) 2199–2216.
- [51] C.N. Rosner, S.H. Rizkalla, Bolted connections for fiber-reinforced composite structural members: analytical model and design recommendations, *J. Mater. Civ. Eng.* 7 (4) (1995) 232–238.
- [52] R.A. Ibrahim, C.L. Pettit, Uncertainties and dynamic problems of bolted joints and other fasteners, *J. Sound Vib.* 279 (3–5) (2005) 857–936.

B.2 Article II

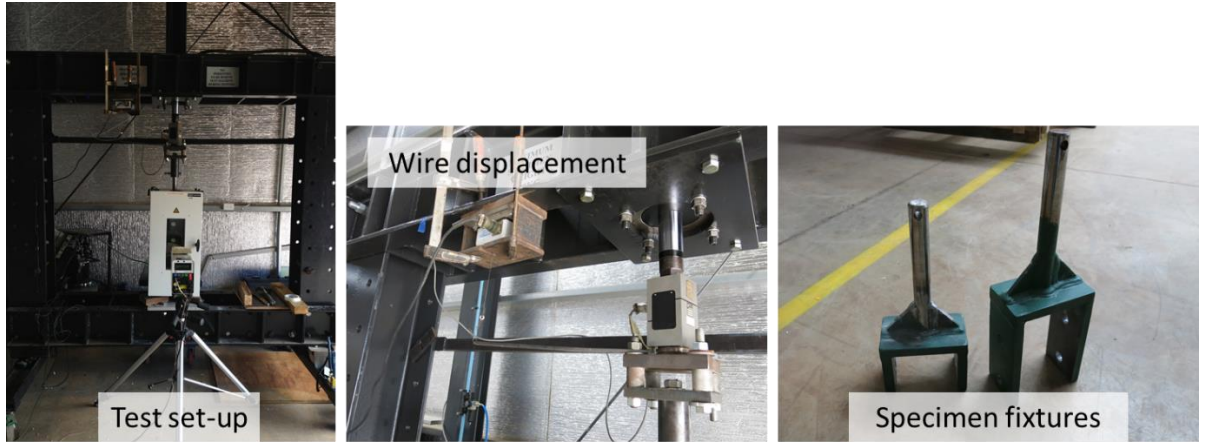


Figure B.1. Detailed of Figure 5 in Article II



Figure B.2. Detailed of Figure 11 in Article II

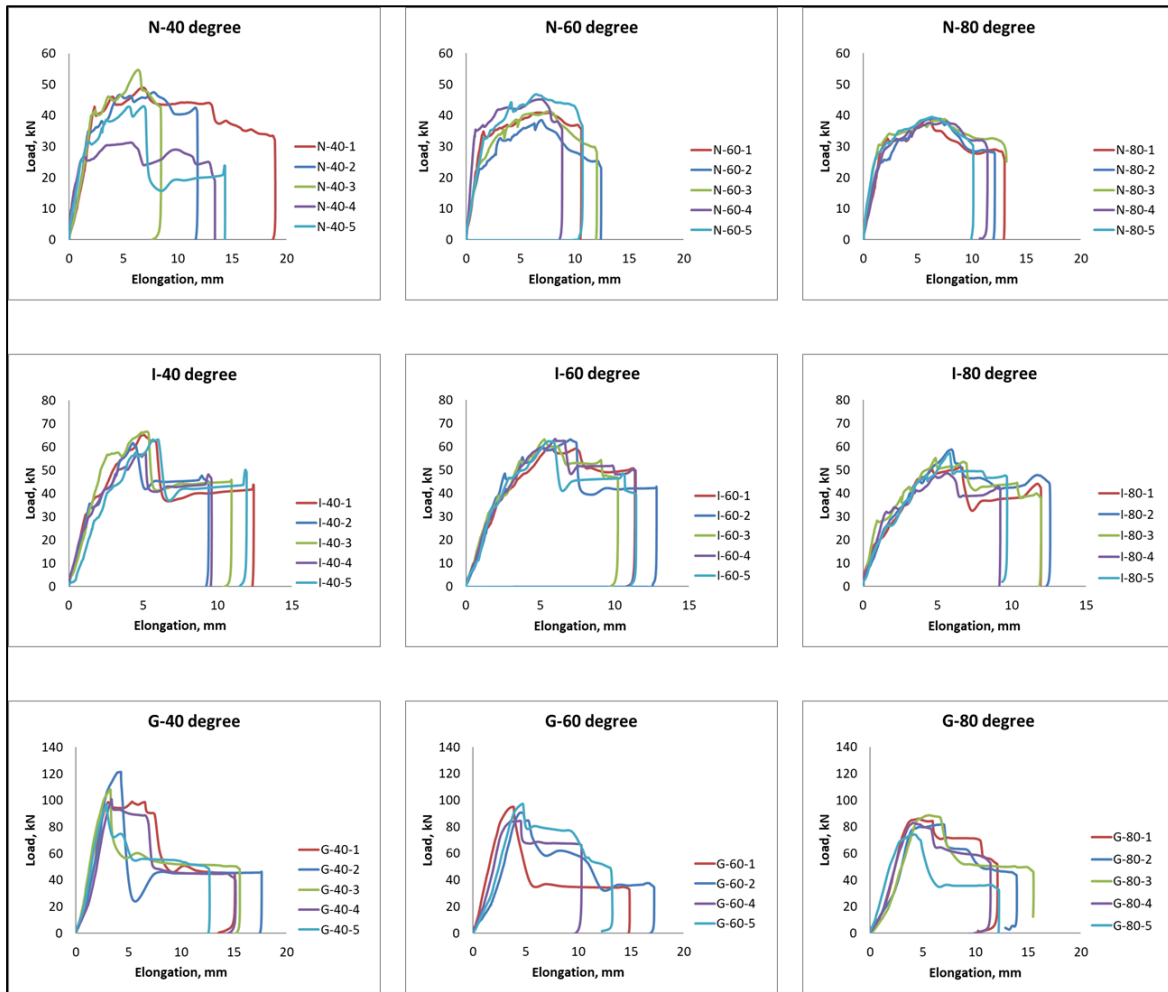


Figure B.3. Details of Figure 6 in Article II

Table B.1. Comparison ratio of Figure 15 in Article II

Specimens	Prediction (kN)	Experimental (kN)	Ratio
N-RT	50.70	56.47	0.90
N-40	46.07	45.09	1.02
N-60	40.62	42.56	0.95
N-80	35.18	38.86	0.91
G-RT	108.45	108.52	0.99
G-40	100.47	105.23	0.95
G-60	91.07	91.96	0.99
G-80	81.68	82.88	0.98

B.3 Article III

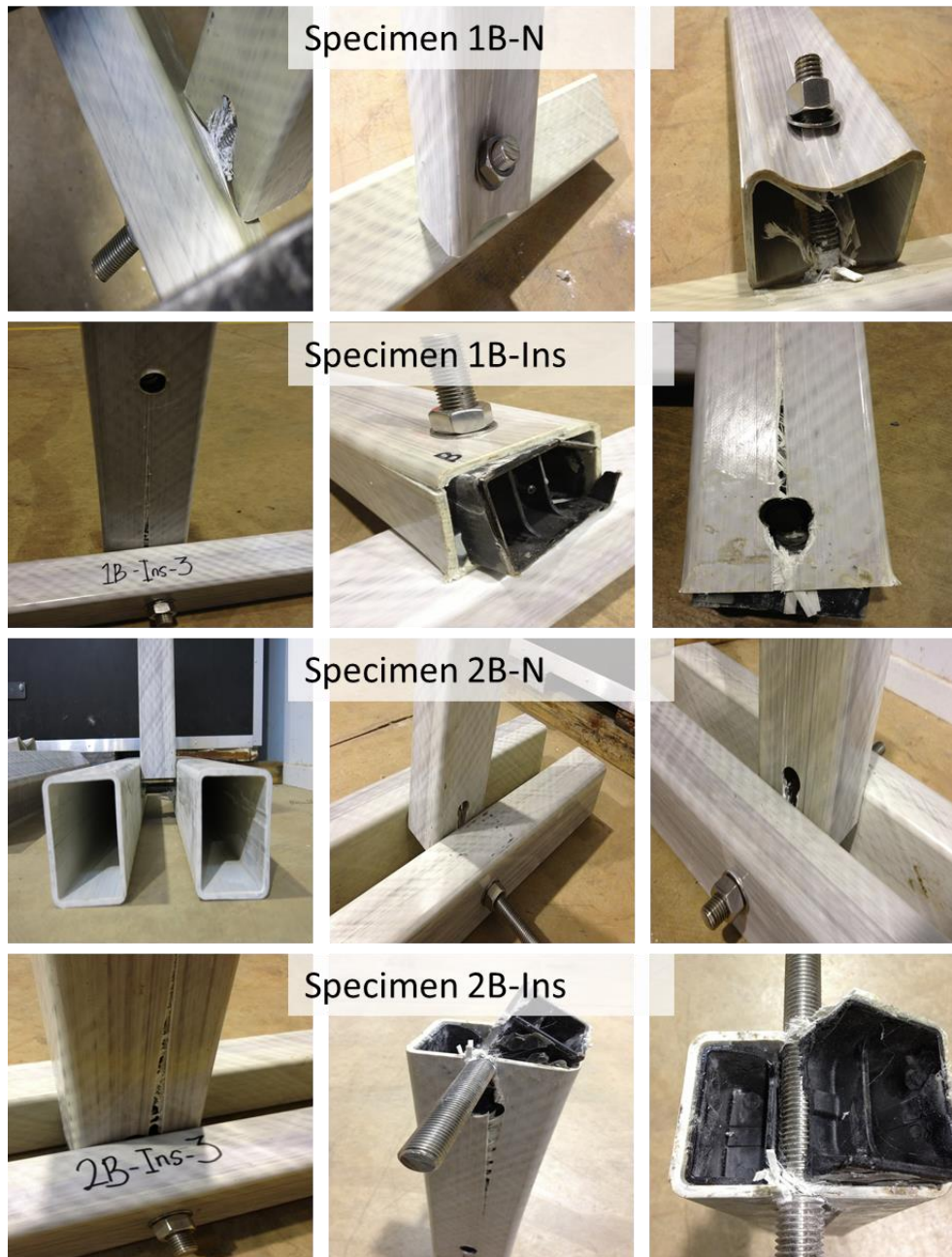


Figure B.4. Details of Figure 9 in Article III

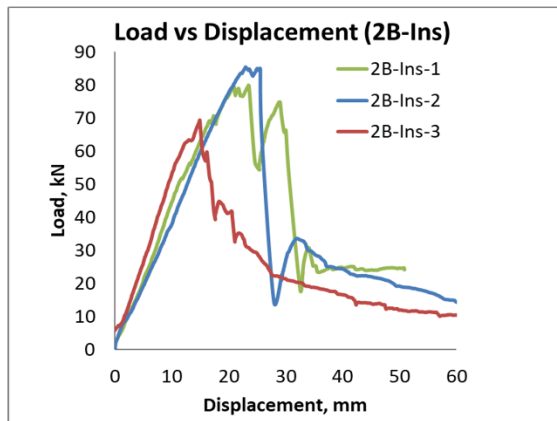
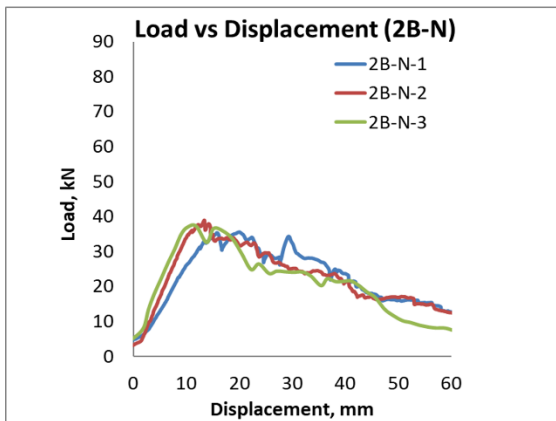
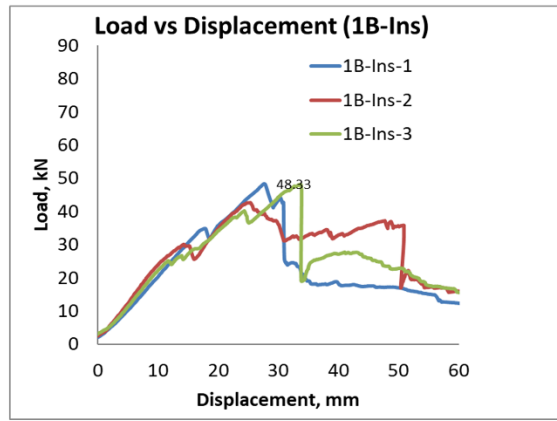
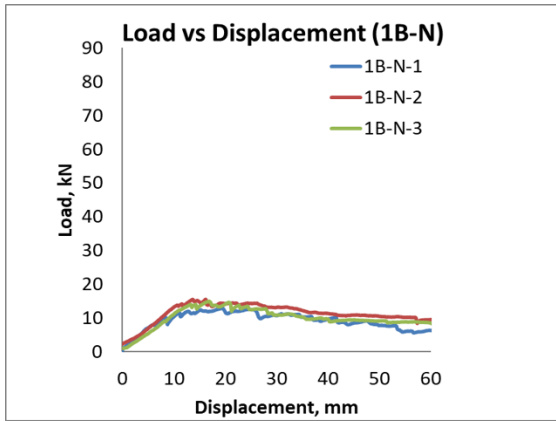


Figure B.5. Details of Figure 7 in Article III

B.4 Article IV

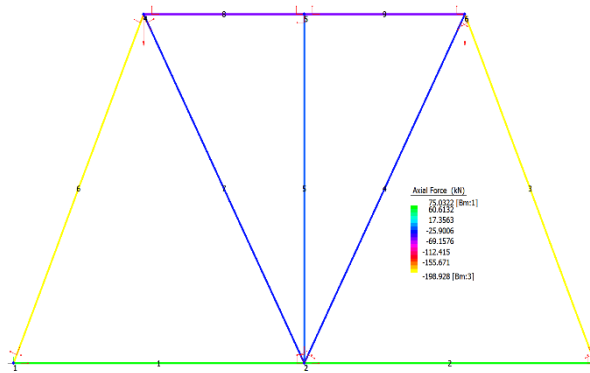


a) Load Case 1

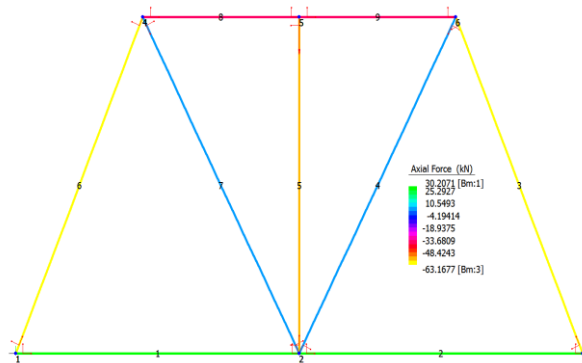


b) Load Case 2

Figure B.6. Details of Figure 4 in Article IV



a) Axial forces for Load Case 1



b) Axial forces for Load Case 2

Figure B.7. Internal member forces using Strand7 analysis

Appendix C: Conferences

C.1 Conference I

A review of FRP composite truss systems and its connections

R.M Hizam, A.C. Manalo & W. Karunasena (2012). A review of FRP composite truss systems and its connections. *Proceedings of the 22nd Australasian Conference on the Mechanics of Structures and Materials (ACMSM22)*, 11-14 December, Sydney, New South Wales, Australia, pp.85-90

ABSTRACT

This paper presents an overview of the recent developments and initiatives on FRP trusses, which has been evolving and has become a viable construction system in civil infrastructure. The paper also discusses the different jointing systems used to assemble FRP components with the aim of determining the appropriate and reliable jointing connections for fibre composites trusses. The different parameters that affect the integrity of connections such as loading condition, material preparation (stacking sequence, volume fraction, etc.), joint configuration, joint geometry, and fastening method will be evaluated. It is anticipated that by addressing these connection issues, it will minimise some ambiguities and provide an understanding to designers and engineers on the potential of fibre composites trusses and advance its application in civil engineering infrastructures.

C.2 Conference II

Effect of mechanical insert on the behaviour of pultruded fibre reinforced polymer (FRP) bolted joint

R.M Hizam, Warno Karunasena & Allan C. Manalo (2013). Effect of mechanical insert on the behaviour of pultruded fibre reinforced polymer (FRP) bolted joint. *The Fourth Asia-Pacific Conference on FRP in Structures (APFIS 2013)*, 11-13 December, Melbourne, Australia.

ABSTRACT

The performance of joints has been regarded as the main factor that limits the growth of pultruded fibre reinforced polymer in civil engineering applications. This paper investigates the effect of mechanical insert on the joint strength and failure mechanism of pultruded glass FRP (GFRP). Three (3) types of specimens were used namely joint without mechanical insert, joint with mechanical insert but without adhesive and joint with mechanical insert and adhesive. This corresponds to the specimens N, I and G, respectively. A total of fifteen specimens were tested up to failure in ambient temperature. The experimental results showed that the presence of mechanical insert has improved the joint strength by 24% and the joint stiffness by 26% of pultruded GFRP bolted joint. Meanwhile, adhesively bonded mechanical insert used in specimen G is capable to contribute almost 92% improvement of joint strength. Most of the test specimens failed in shear-out mode. Specimens I and G exhibited brittle-type failures after the maximum load. This preliminary study shows good performance of mechanical insert in improving the bolted joint connection of square hollow section (SHS) pultruded GFRP profile.

C.3 Conference III

Effect of eccentricity on the behaviour of pultruded FRP bolted joint

R.M Hizam, A. C. Manalo & W.Karunasena (2013). Effect of mechanical insert on the behaviour of pultruded fibre reinforced polymer (FRP) bolted joint. *3rd Malaysia Postgraduate Conference (MPC 2013)*, 3-4 July, Sydney, Australia.

ABSTRACT

Fibre reinforced polymer (FRP) composites are becoming an alternative choice for the development of structural truss system. It takes advantage of the unidirectional properties of fibre composites as truss members are subjected mostly to axial forces. The typical connection used for this type of structure is a bolted joint. This paper presents the behavior of closed section (100 mm x 75 mm x 5.25 mm) of pultruded glass FRP (GFRP) composite with bolted joint under eccentric loading. The T-joint component of the truss was designed with 1-bottom chord (1B) to simulate the eccentric condition and compared with a T-joint with 2-bottom chords (2B) for concentric loading. Stainless steel bolts (all-threaded) were used and tightened with a torque of 25N.m. The joint failed due to local punching shear at one side of the connection area due to eccentric effect and a load less than half that of the joint with concentric loading. It was found that the testing specimen with eccentricity experienced local damaged which had reduced its joint capability almost twice than that specimen without eccentricity.

C.4 Conference IV

An experimental investigation on the effect of threaded bolt on the double lap joint strength of pultruded fibre reinforced polymer

R.M Hizam, Warna Karunasena & Allan C. Manalo (2014). An experimental investigation on the effect of threaded bolt on the double lap joint strength of pultruded fibre reinforced polymer. *Composites Australia and the CRC for Advanced Composite Structures (2014 Australasian Composites Conference)*, 7-9 April, Newcastle, Australia.

ABSTRACT

The ability to provide the joint versatility for pultruded fibre reinforced polymer (PFRP) in civil structures industry is crucial for its application demands. Bolted joint is extensively used due to its low cost and ease of assembly. However, this jointing method can compromise the PFRP strength at the joint due to poor quality of drilling techniques, accuracy of hole size and threaded bolt. In this study, the main objective is to investigate the effect of threaded bolt on the strength of bolted joints in pultruded fibre reinforced polymer. Double lap joint configuration was prepared using longitudinal and transverse laminates and tested to failure (in tension) in accordance with ASTM D5961. The test specimens using longitudinal and transverse laminates failed in shear-out (heavily crushed) and net-tension, respectively. A significant joint capacity reduction was observed on the threaded samples due to the indentation of the thread in the fibre composite laminates. The load-elongation curve shows the slope with several knees after the first drop, which may indicate some damping effects and unstable development of internal damage.

C.5 Conference V

Behaviour of a composite truss with bolted joints

R.M Hizam, Warna Karunasena & Allan C. Manalo (2015). Behaviour of a composite truss with bolted joints. *Composites Australia and the CRC for Advanced Composite Structures (2015 Australasian Composites Conference)*, 21-23 April, Gold Coast, Australia.

ABSTRACT

Trusses are structural frames formed from one or more triangles and are commonly used to stiffen structures, for instance, in bridges and towers. Due to its dimensional simplicity and material to weight ratio, trusses have become one of the prominent structural forms in the 19th century. More recently, fibre composite truss is becoming a viable structural system in areas with adverse environment conditions. The different structural components of a composite truss are generally joined together and the joints are considered as a critical area as it governs the overall behaviour of a truss system. In this paper, a truss is constructed by assembling pultruded fibre reinforced polymer (FRP) tubular profiles using stainless steel bolted joints. Mechanical inserts were introduced at the vicinity of jointing area. The overall system behaviour of a 1 m span composite truss and the local behaviour of its connections are experimentally investigated and the results are presented in this paper. The presence of mechanical inserts resulted in the composite truss joint to fail in the desired bearing mode. After several loading and unloading cycles, it shows that the stiffness of composite truss structure is improved mainly due to contact traction at the jointing parts.

C.6 Conference VI

Effect of threaded bolts with variable edge distance-to-bolt diameter on the bolted joint strength of pultruded FRP

R.M Hizam, Warna Karunasena & Allan C. Manalo (2018). Effect of threaded bolts with variable edge distance-to-bolt diameter on the bolted joint strength of pultruded FRP. *11th Asian-Australasian Conference on Composite Materials*, 29th July – 1st August, Cairns, Australia.

ABSTRACT

The ability to provide adequate and effective connection assembly will enhance the performance of pultruded FRP (PFRP) structures and fully exploit the material's attributes such as high strength to weight ratios and high resistance to corrosive environment. Conventional metallic fastener is still a preferable way to join the PFRP structural members due to ease of assembly and design familiarity¹. There are a number of fastening parameters associated with designing FRP bolted connections (Table 1), such as bolt-hole clearance, joint geometries and clamping pressure. However, the effect of bolt threads on the PFRP joint performance has received very little attention so far². This paper investigated the effect of steel threaded bolts with different end distance-to-bolt diameter ratio (e/d_b) (maximum $e/d_b = 4$) against two different PFRP thickness, 6.5 mm and 5 mm (Figure 1). Due to the threaded bolts, specimen 6.5 mm and 5 mm experienced decrease in joint resistance at an average of 40% and 32%, respectively. The thicker PFRP material may have experienced higher thread embedment across the pultruded lamina, therefore decreasing the joint capacity further by 8%. Additionally, specimens with threaded bolts, attained consistent joint strength and has insignificant outcome across the e/d_b range.